Investigation of T cell based therapeutic strategies to target Acute Myeloid Leukaemia

Nisansala Dilrukshi Wisidagamage Don

University College London

A thesis submitted to University College London (UCL) for the

Degree of Doctor of Philosophy

I, Nisansala Dilrukshi Wisidagamage Don confirm that the work presented in this thesis is my own. Where information has been derived from other sources, I confirm that this has been indicated in the thesis.

_____

Nisansala Dilrukshi Wisidagamage Don

ABSTRACT

Acute myeloid leukaemia (AML) is a highly heterogeneous clonal disease of the myeloid line of blood cells. It is characterized by an abnormal accumulation of immature leukemic cells in the bone marrow and blood, thus, interfering with normal haematopoiesis and leading to bone marrow insufficiency. One of the main limitations of current strategies is the potential on-target off-tumour toxicity due to the expression profile of currently targeted tumour antigens.

The aim of this work was exploring different approaches to overcome this limitation. We investigated the antitumour activity of second-generation CAR targeting CD33 and a novel antigen with a more restricted expression profile, B7-H3. We found that TE9-CD8-28ζ CAR T cells targeting B7H3, were able to drive a potent antitumor response in an antigen-dependent manner, in vitro. Importantly we also demonstrated lack of hematopoietic toxicity mediated by TE9-CD8-28ζ CAR T cells, addressing one of the main limitations of current strategies targeting AML.

Another approach consisting of αβ T cells engineered to co-express a γδTCR and an B7-H3-targeting chimeric costimulatory receptor (TE9-CCR), was also explored. This system aims to drive potent anti-tumour responses through co-stimulation as well as avoid on target on tumour toxicity by separating signal 1 (TCR) and signal 2 (CCR). We demonstrated that γδ TCR-TE9-28 transduced αβ T cells were able to mount a robust anti-tumour response in vitro in an antigen-dependent manner, with full activation only when the CCR engaged the cognate antigen. In addition, preliminary evidence also showed the potential of γδ TCR-TE9-28 transduced αβ T cells to avoid on target of tumour toxicity in vitro.

IMPACT STATEMENT

Standard treatment for AML consists of rounds of combination chemotherapy with or without allogenic hematopoietic stem cell transplantation (HSCT).Unfortunately current strategies have a high relapse rate (Willemze et al., 2014). The better understanding of the AML cytogenetic and molecular landscape during the recent years, led to the development of more targeted approaches and many alternative strategies are currently under investigation including approaches to enhance T-cell immune responses to AML with Chimeric antigen receptor (CAR)-T-cells. However, developing a safe CAR-T cell-based immunotherapy targeting AML is limited by the potential on-target off-tumour toxicity due to the expression profile of currently targeted tumour antigens.

While these antigens are overexpressed on AML blasts, the healthy myeloid compartment including normal myeloid progenitors also expresses them, leading to the disruption of normal haematopoiesis and intolerable myeloablation by the current treatment strategies.

The aim of this work was exploring different approaches to overcome this on-target off-tumour toxicity. We explored CD33–specific CAR T cells as a possible therapy, as well as B7-H3–specific CAR T cell (TE9-CD8-28ζ) targeting a novel antigen with a more restricted expression profile. We found that TE9-CD8-28ζ CAR T cells targeting B7H3, were able to drive an antitumor response in terms of cytotoxicity, ability to produce cytokines and proliferate in an antigen dependent manner, in vitro. Importantly we also addressed potential hematopoietic toxicity of this construct, as this is one of the main limitations of current strategies targeting AML, and we demonstrated that TE9-CD8-28ζ CAR T cells lacked toxicity towards

healthy monocytes and normal hematopoietic progenitors present in cord blood in a colony formation assay.

Another approach consisting of αβ T cells engineered to co-express a γδTCR and an B7-H3-targeting chimeric costimulatory receptor (TE9-CCR), was also explored. This system aims to offer another degree of safety by separating signal 1 (TCR) and signal 2 (CCR). We demonstrated that γδ TCR-TE9-28 transduced αβ T cells were able to mount a robust anti-tumour response in vitro in an antigen dependent manner, with full activation only when the CCR engage the cognate antigen. In addition, preliminary evidence pointed to γδ TCR-TE9 CCR system having the capacity to avoid on target of tumour toxicity, as no significant activity was detected by the γδ TCR-TE9-28 transduced αβ T cells in in presence of their cognate antigen when the TCR was not engaged.

ACKNOWLEDGEMENTS

First and foremost, I want to thank John Anderson and Jon Fisher for supervising this project and for their guidance throughout the PhD. John, I will be forever grateful for welcoming me in your lab almost 6 years ago as a very inexperienced master's student. These years have been a roller-coaster of achievements and failures but your unbreakable positivity in the face of hardship is something that I will always look up to.

Secondly, I want to thank all the people that I crossed path with, in the Anderson, Straathof, Fisher and Donovan lab, I will always have fond memories of our time together. We shared laughs and tears but at the end of the day there was nothing that a cookie or a glass of wine could not solve, apart from magically making some viral production work. A special thank you to my fellow PhD colleagues, this journey would not have been the same without you.

Thirdly I would like to deeply thank Artemis and Paola, 6 years ago when I started this journey, I didn't know that this lab would have also given me my best friends. Thank you for believing in me and supporting me throughout it all, I'm looking forward to finally start the next chapter together.

Thank you to my amazing friends back home and now scattered around the world for being the best support system, I feel blessed to have you in my life.

To my mum and dad, I know how much you sacrificed to get me and Nu where we are today, thank you for always pushing us, this achievement is for you.

Last but not least, thank you Prasy, you have been my rock throughout it all and I could not have done this without you, I don’t think that any words could ever express my gratitude for having you in my life.

TABLE OF CONTENT

LIST OF FIGURES

LIST OF TABLES

ABBREVIATIONS

ACT	Adoptive cell therapy
ADCC	Antibody-dependent cell-mediated cytotoxicity
ALL	Acute lymphoblastic leukaemia
AML	Acute Myeloid leukaemia
ANOVA	Analysis of variance
APC	Antigen-presenting cells
BD	Binding domain
BFU-E	Burst-forming unit-erythroid
BIKE	Bispecific Killer cell Engager
BITE	Bispecific T cell engager
BTN	Butyrophilin
BTN2A1	Butyrophilin 2A1
BTN3A	Butyrophilin 3A
BTN3A1	Butyrophilin 3A1
CAR	CAR Chimeric antigen receptor
CB	Cord Blood
CCR	Chimeric co-stimulatory receptor
CDR	complementarity determining region
CFC	Colony forming cell assay
CFU	Colony forming unit assay
CFU-E	Erythroid progenitor cells
CFU-GM	Macrophage progenitor cells
CFU-GEMM	Multi-potential progenitor cell

CLIP	Class II associated Ii peptide
CRISPR	Clustered regularly interspaced short palindromic repeats
CRUK	Cancer research UK
CTL	Cytotoxic T lymphocyte
CTLA- 4	Cytotoxic T-lymphocyte antigen 4
DAG	Diacylglycerol
DC	Dendritic cell
DLBCL	Diffuse large B-cell lymphoma
DMEM	Dulbecco's Modified Eagle Medium
DMSO	Dimethyl sulfoxide
DN	Double negative
DNA	Deoxyribonucleic acid
DP	Double-positive
E:T	Effector: Target
EDTA	Ethylenediaminetetraacetic acid
EGFR	Epidermal growth factor receptor
ELISA	Enzyme-linked immunosorbent assay
ER	endoplasmic reticulum
ERK	Extracellular Signal-Regulated Kinase
FBS	Fetal Bovine serum
FC	Crystallisable fraction
FCS	Fetal calf serum
FDA	Food and Drug Administration
FITC	Fluorescein isothiocyanate

FMO	Fluorescence minus one
FSC	Forward scatter
GFP	Green fluorescent protein
GM-CSF	Granulocyte macrophage colony-stimulating facto
GVHD	Graft versus host disease
HLA	Human leukocyte antigen
HSCT	Hematopoietic stem cell transplantation
HSPC	Normal Hematopoietic Progenitors
ICAM	Intercellular adhesion molecule
ICOS	Inducible co-stimulator
IFN-γ	Interferon γ
IL	Interleukin
IL2	Interleukin-2
IMDM	Iscove's Modified Dulbecco's Medium
IP3	Inositol triphosphate
IPP	Isopentenyl-pyrophosphate
LB	Luria Bertani
LFA	leukocyte function associated antigen
LTR	Long terminal repeat
mAb	Monoclonal antibody
MAGE-3	Melanoma associated antigen 3
MAPK	Mitogen activated protein kinase
MART-1	Melanoma antigen recognised by T cells 1
MDSC	Myeloid derived suppressor cells
MFI	Mean fluorescent intensity

MHC	Major histocompatibility complex
MIIC	MHC class II compartment
NF-KB	Nuclear factor kappa-light-chain-enhancer of activated B cells
NFAT	Nuclear factors of activated T cells
NGS	Next Generation Sequencing
NIR	Near Infrared
NK cell	Natural killer cell
ORF	Open reading frame
PBMC	Peripheral blood mononuclear cell
PBS	Phosphate buffered saline
PCR	Polymerase chain reaction
PD-1	Programmed death-1
PD-L1	Anti-programmed death-ligand 1
PE	Phycoerythrin
PI3K	Phosphatidylinositol 4,5 bisphosphate 3 kinase
PIP	Phosphatidylinositol 4,5 biphosphate
RAG2	Recombination activating gene 2
ROS	Reactive oxygen species
RPMI	Roswell Park Memorial Institute Medium
SMAC	Supramolecular activation cluster
SP	Single positive
SSC	Side scatter
TAA	Tumour associated antigen
TAM	Tumour-associated macrophage

TAP	transporter associated with antigen processing
TCM	Central Memory T cells
TCR	T cell receptor
TEM	Effector memory T cells
Th	T helper cell
TIL	Tumour-infiltrating lymphocyte
TME	Tumour microenvironment
TNF-α	Tumour necrosis factor-α
TRAC	T-cell receptor α constant
UT	Untransduced
UV	Ultraviolet
WHO	World Health Organization
WT	Wild type
ZAP70	Zeta-chain-associated protein
ZOL	Zoledronate

1 INTRODUCTION

The intent of the following introduction is to explore in more details Acute Myeloid Leukaemia as well as T cell biology and tumour immunology to understand the unmet needs and approaches to tackle the disease.

1.1 Acute Myeloid Leukaemia

1.2 Epidemiology and genetics

Epidemiology

Cancer is the second leading cause of death globally, accounting for an estimated 9.6 million deaths all over the world in 2018 (WHO stats). There are around 375,000 new cancer cases in the UK every year (2016-2018) (CRUK stats)(Figure 1.1).

Acute myeloid leukaemia (AML) accounts for approximately 25% of all leukaemias, making it the most frequent type of myeloid leukaemia. AML accounted for less than 1% of all new cancer cases in the UK in 2016-2018, an estimated 3,100 new cases were diagnosed every year and an estimate of 2,600 people died of the disease (2% of all cancer deaths in the UK in 2018) (CRUK stats).

Since the early 1990s, acute myeloid leukaemia incidence rates have increased by a fifth (20%) in the UK, however it has remained stable over the last decade (CRUK stats). AML is the second most common form of leukaemia in children, however, is mainly a disease of later adulthood, with median age of presentation around 70 years (Forman et al., 2003).

The incidence rates escalate gradually from age 40-44, more steeply from age 60-64, with the highest incidence in the age group 85-89 in males, and ≥90 in females

(Ries et al., 2006), in fact the prevalence is 3.8 cases per 100,000 in adults ≤65 years while it rises to 17.9 cases per 100,000 in adults over 65 years (De Kouchkovsky & Abdul-Hay, 2016).

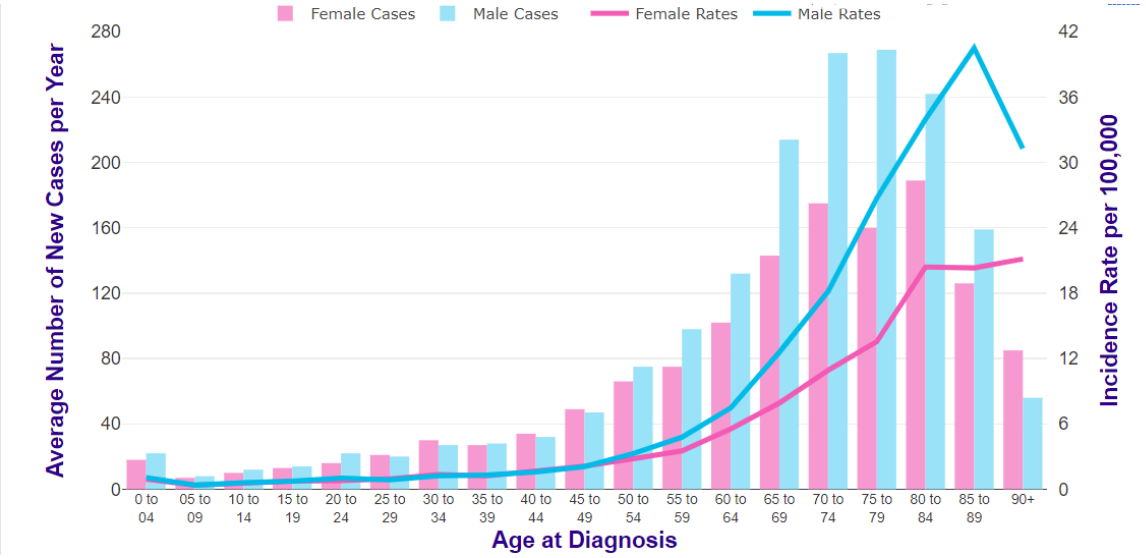

Figure 1.1 Incidence of AML is found to increase with age. Average number of new cases per year and age-specific incidence rates per 100,000 Population, UK, 2016-2018. Image adapted from Cancer Research UK statistics.

AML is a highly heterogeneous clonal disease of the myeloid line of blood cells. It is characterized by an abnormal accumulation of immature leukemic cells known as blasts in the bone marrow and blood, thus, interfering with normal haematopoiesis and leading to bone marrow insufficiency (Deschler & Lübbert, 2006). Histologically, AML is characterized by the presence of ≥20% blasts in bone marrow or peripheral blood (Estey & Döhner, 2006), however, the blood sample or the bone marrow biopsy which are used for the diagnosis are further processed for immunophenotyping, cytogenetic analysis and molecular testing to confirm the diagnosis of AML as well as the risk stratification (Arber et al., 2016b).

AML is subdivided in de novo AML, therapy-related AML and secondary AML based on if it originates respectively in individuals that were previously healthy, in individuals that have previously received a treatment with cytotoxic agents (Sill et al., 2011) or individuals that previously had a different clonal illness (Szotkowski et al., 2010).

Although exact causes for AML occurrence are not known, studies have shown that congenital abnormalities and environmental factors play a role in predisposition. Inherited diseases such as Klinefelter syndrome, Li-Fraumeni syndrome and Fanconi anaemia are associated with AML (Pötzsch et al., 2002) and moreover, studies have shown that children with Down syndrome have up to 20-fold increased likelihood of developing acute leukaemia(Fong & Brodeur, 1987). Exposure to ionizing radiation or chronic exposure to certain chemicals such as Benzene have been also associated to AML(Preston et al., 1994)(Savitz & Andrews, 1997).

Cytogenetics and Genetics

Chromosomal abnormalities are among the most important mutational drivers of AML development, almost 50% of AML cases carry either chromosomal deletions, duplications, or translocation.

Deletions of chromosomal arms 5q and 7q or loss of whole chromosomes, such as chromosome 7, 5, 9 and Y followed by monosomies 17, 18, 16, 5, and 3 are among the most common deletions in AML (Anelli et al., 2017; Mrózek et al., 2001; Papaioannou et al., 2013).

Moreover, cytogenetic abnormalities t(8;21)(q22;q22), t(15;17)(q22;q12), inv(16)(p13.1;q22) and alterations of 11q23 are the four most common

translocations occurring each in 3% to 10% of AML cases (Martens & Stunnenberg, 2010; Stasi et al., 1993). Chromosomal abnormalities also carry significant prognostic information concerning disease outcome, for example studies have shown that any type of monosomy in AML was associated with a poor outcome (Medeiros et al., 2010; Papaioannou et al., 2013). Gene mutations as well as chromosomal alterations play a key role in the development of AML. Advances in next generation sequencing (NGS) allowed to better define AML genetic landscape and nearly 30 recurrently mutated genes have been identified. AML-associated mutations can affect stem and progenitor cell population and promote disease development via multiple strategies such as hyper-activation of signalling cascades which then can lead to unregulated cell proliferation and confer resistance to apoptosis or directly affect transcription factors involved in cell proliferation and differentiation. Furthermore, mutations can induce aberrant gene expression by changing DNA structure and accessibility or the subcellular location of transcription factors.

According to Cancer Genome Atlas Research Network (TCGA), AML-associated mutations can be divided in 9 main categories:

1) transcription-factor fusions (PML-RARA, AML1-ETO)
2) gene encoding nucleophosmin (NPM1)
3) tumour-suppressor genes (TP53, WT1)
4) DNA-methylation-related genes (DNTM3A, IDH1, IDH2, TET2)
5) signalling genes (FLT3, KIT, KRAS/NAS)
6) chromatin-modifying genes (ASXL1, EZH2, MLL-fusion proteins)
7) myeloid transcription factor genes (RUNX1, C/EBPα)
8) cohesin-complex genes (STAG2)

9) spliceosome-complex genes6.

TCGA evaluated the genomes of 200 AML patients and found that an AML genome on an average harbours 13 mutations but of these only an average of 5 are driver mutation and can be found in genes recurrently mutated in AML (Network 2013). The other mutations, however, despite playing a role in the malignant cell behaviour are not shown to be directly involved in the malignant transformation.

It is hypothesised that early mutations occur in the stem cell population and often effect epigenetic regulators such as DNMT3A, ASXL1, IDH2 and TET2, resulting in the rise of “pre-leukemic” stem cells with altered self-renewal properties, but still capable of multilineage differentiation.

Later mutations, on the other hand, seems to occur in genes related to proliferation and signalling activation such as FLT3, KRAS/NRAS, PTPN11 leading to the rise of leukemic blasts.

1.2.1 Classification

The most recent classification system for AML was introduced by the World Health Organization (WHO) in 2001 and last reviewed in 2016. The aim was to combine genetic information with morphology, immunophenotyping and clinical presentation (Arber et al., 2016a; Vardiman et al., 2002).

In this classification AML is subdivided in 6 different groups: AML with recurrent genetic abnormalities; AML with myelodysplasia-related features; therapy-related AML; AML not otherwise specified; myeloid sarcoma; and myeloid proliferation related to Down syndrome(Arber et al., 2016a)(Table 1).

Due to the complexity of AML, the prognosis and risk stratification are influenced by a combination of factors such as age, cytogenetic and genetic abnormalities. However, age of patients at diagnosis, independently from the genetic risk, is a prognostic factor associated with inferior outcomes (Büchner et al., 2009; Krug et al., 2011). Studies have shown that patients ≥65 years have a poor prognosis even after intensive chemotherapy (Appelbaum et al., 2006).

Based on prognosis of known cytogenetic and molecular abnormalities, the European LeukaemiaNet (ENL) stratified AML in three main risk group: favourable, intermediate, and adverse (Döhner et al., 2017). (Table 2)

Types	Genetic abnormalities
AML with recurrent genetic abnormalities	AML with t(8:21)(q22;q22); RUNX1-RUNX1T1
	AML with inv(16)(p13.1q22) or t(16;16)(p13.1;q22); CBFB-MYH11
	APL with PML-RARA
	AML with t(9;11)(p21.3;q23.3); MLLT3-KMT2A
	ML with t(6;9)(p23;q34.1); DEK-NUP214
	AML with inv(3)(q21.3q26.2) or t(3;3)(q21.3;q26.2); GATA2, MECOM
	AML (megakaryoblastic) with t(1;22)(p13.3;q13.3); RBM15-MKL1
	AML with BCR-ABL1 (provisional entity)
	AML with mutated NPM1
	AML with biallelic mutations of CEBPA
	AML with mutated RUNX1 (provisional entity)
AML with myelodysplasia-related changes	
Therapy-related myeloid neoplasms	
AML not otherwise specified	AML with minimal differentiation
	AML without maturation
	AML with maturation
	Acute myelomonocytic leukemia
	Acute monoblastic/monocytic leukemia
	Acute erythroid leukemia
	Pure erythroid leukemia

	Acute megakaryoblastic leukemia
	Acute basophilic leukemia
	Acute panmyelosis with myelofibrosis
Myeloid sarcoma	
Myeloid proliferations related to Down syndrome	Transient abnormal myelopoiesis
	ML associated with Down syndrome

Table 1.1 WHO classification of AML and related neoplasm. Table adapted from 'Acute myeloid leukaemia: a comprehensive review and 2016 update'(De Kouchkovsky & Abdul-Hay, 2016).

Favourable	t(8;21)(q22;q22); RUNX1-RUNX1T1;
	inv(16)(p13.1q22) or t(16;16)(p13.1;q22); CBFB-MYH11
	Mutated NPM1 without FLT3-ITD/low FLT3-ITD
	Biallelic mutated CEBPA
Intermediate	Mutated NPM1 and FLT3-ITD(high)
	Wild-type NPM1 without FLT3-ITD/ low FLT3-ITD (normal
	t(9;11)(p21.3;q23.3)MLLT3-KMT2A
	Cytogenetic abnormalities not classified as favourable or
Adverse	t(6;9)(p23;q34.1); DEK-NUP214
	t(v;11q23.3); KMT2A rearranged
	t(9;22)(q34.1;q11.2); BCR-ABL1
	inv(3)(q21.3q26.2) or t(3;3)(q21.3;q26.2);
	-5 or del(5q); -7; -17/abn(17p)
	Complex karyotype
	Monosomal karyotype
	Wild-type NPM1 and high FLT3-ITD
	Mutated RUNX1
	Mutated ASXL1
	Mutated TP53

Table 1.2 AML risk stratification by ELN. Table adapted from 'Diagnosis and management of AML in adults: 2017 ELN recommendations from an international expert panel'(Döhner et al., 2017).

1.2.2 Treatment strategies

Standard treatment for AML consists of a combination of induction therapy using anthracycline and cytarabine and consolidation therapy with either chemotherapy or allogenic hematopoietic stem cell transplantation (HSCT) depending on the patient's risk group.

Induction therapy ("3+7" regimen) consists in three days of an anthracycline such as daunorubicin (≥60 mg/m2) and seven days of intravenous administration of cytarabine (100-200 mg/m2). The aim is to achieve complete remission (CR) which is defined as the presence of ≤5% blasts in the bone marrow, recovery of absolute platelet and neutrophil counts with no sign of extramedullary AML (Cheson et al., 2003). CR is achieved in 60-85% of patients ≤60 years and in 45-60% of patients ≥60, however, half of these patients eventually relapse and die without HSCT (Gerstung et al., 2017).

Consolidation therapy is required to eliminate residual leukemic blasts. High-dose cytarabine or 2-4 cycles of intermediate dose is used in patients who belong in the favourable -risk group (Döhner et al., 2017), however, relapse risk still remains high.

Instead, allogenic hematopoietic stem cell transplantation (HSCT) is recommended for patients in the high and intermediate-risk groups and in general for patients responding poorly to chemotherapy alone, if a suitable matched donor is available. Unfortunately, HSCT too, has high relapse rate and can lead up to 10-25% treatment-related mortality due to graft versus- host disease and cause adverse effects on quality of life (Cornelissen et al., 2007).

To summarize, current treatment strategies for AML result in 5-year survival rates of 40–45% among patients up to the age of 50–55 years, 30–35% among patients

up to the age of 60 and 10–15% among older patients (Willemze et al., 2014)(Figure 2- Survival curve of de novo AML at MD Anderson between 1970 and 2017), therefore, novel strategies to tackle the disease are necessary.

The better understanding of the AML cytogenetic and molecular landscape in recent years, led to the development of more targeted approaches and many alternative strategies are currently under investigation. Some examples of new approaches that led to better outcome include the use of hypomethylating agents or chemotherapy in combination with Venetoclax which is a highly selective inhibitor of the anti-apoptotic protein BCL-2 (BCL2 is thought to mediate resistance to standard therapy in patients with adverse risk AML) (Lachowiez et al., 2020).

FLT3 inhibitors and Isocitrate dehydrogenase (IDH) 1 and 2 inhibitors have also been tested in clinical trials and are now the standard of care in patients who harbour these mutations (Stein et al., 2021; Stone et al., 2017). Moreover, approaches to enhance T-cell immune responses to AML with T-cell engagers (BiTEs), checkpoint inhibitors, and chimeric antigen receptor (CAR)-T-cell approaches are currently in early clinical trial studies.

1.3 Adaptive immunity: T cells

The immune system can mount an innate or adaptive response against a variety of pathogens. The innate response is quicker and non-specific and key players are cells such as macrophages, neutrophils, and NK cells. On the contrary, T and B lymphocytes mount the adaptive response.

Adaptive immunity is generally slower, and it’s defined by two important characteristics: specificity and memory. Specificity refers to the ability of the

adaptive immune system to target specific pathogens, while memory refers to its ability to quickly respond to pathogens to which it has previously been exposed. In particular, T cells specificity is determined by a unique T cell receptor which mediates cellular immune response upon antigen recognition. While most peripheral T cells contain the αβ T cell receptor (TCR) and are defined as conventional T cells, a small fraction contains the γδ TCR. They are subpopulation with unique characteristics that serve as a bridge between innate and adaptive immune response.

1.3.1 T cells development

As mentioned above, the biggest population of peripheral T lymphocytes are αβ T cells. They comprise of two different subsets of cells which express either the CD4 or CD8 co-receptor (Bach et al., 1976). The two co-receptors are mutually exclusive, and the two different subsets have distinct functions.

CD4+ cells are called helper T lymphocytes and can be classified in Th1, Th2, Th17,Tfh, Th9 and Th22 subsets: their main roles include supporting B cells in antibodies production (Cantor & Boyse, 1977) and inducing increase in macrophages microbial activity. On the other hand, CD8+ cells are called cytotoxic lymphocytes and they cause direct cytotoxicity of infected target cells (Contor & Boyse, 1975).

T cells derive from haematopoietic stem cells, committed lymphoid progenitors arise in the bone marrow and migrate to the thymus (Scimone et al., 2006). There, the developing progenitors named thymocytes, undergo a series of maturation steps, each identified by the expression of different cell surface markers (Figure

1.2). The majority of cells in the thymus give rise to αβ T cells, however approximately 5% bear the γδ TCR. The earliest developing thymocytes are called double negative (DN) thymocytes as they lack the expression of co-receptors CD4 and CD8. This population goes through 4 stages (D1-D4) identified by the differential expression of the CD44 adhesion molecule and the CD25 interleukin-2 receptor chain (Aifantis et al., 2008; T. Naito et al., 2011). As cells progress through these stages, they go through a process called beta-selection and cells that have successfully rearranged their TCR-β chain locus are selected. The β chain then pairs with the non-rearranging pre-Tα chain to form a pre-TCR (von Boehmer & Fehling, 1997). Successful pre-TCR expression promote cell proliferation and further differentiation with the transition to a double positive (DP) stage where cells express both CD4 and CD8 co-receptors. DP cells rearrange their TCR-α chain loci, to produce a αβ-TCR. These cells then undergo positive and negative selection by interacting with epithelial cells in the cortex and with antigen presenting cells (APCs) such as dendritic cells and macrophages in the medulla. They express a high density of MHC class I or class II molecules associated with self-peptides: cells that engage self-peptide/MHC complex with the appropriate affinity survive while the rest go through apoptosis (von Boehmer et al., 1989).

This process is fundamental for mature T cells to discriminate between self and non-self-peptides. All peripheral T cells express TCRs that can recognize “self” with low affinity and naïve, resting T cells continuously receive tonic signals from self-pMHC (peptide-loaded major histocompatibility complexes) molecules in the periphery, essential for their survival (Tanchot et al., 1997).The majority of developing thymocytes die during this process and following thymocytes selection, they down-regulate either CD4 or CD8 respectively upon recognition of self-

peptide-MHC class I or self-peptide-MHC class II complexes and become single positive (SP). SP thymocytes then exit the thymus and migrate to peripheral lymphoid organs.

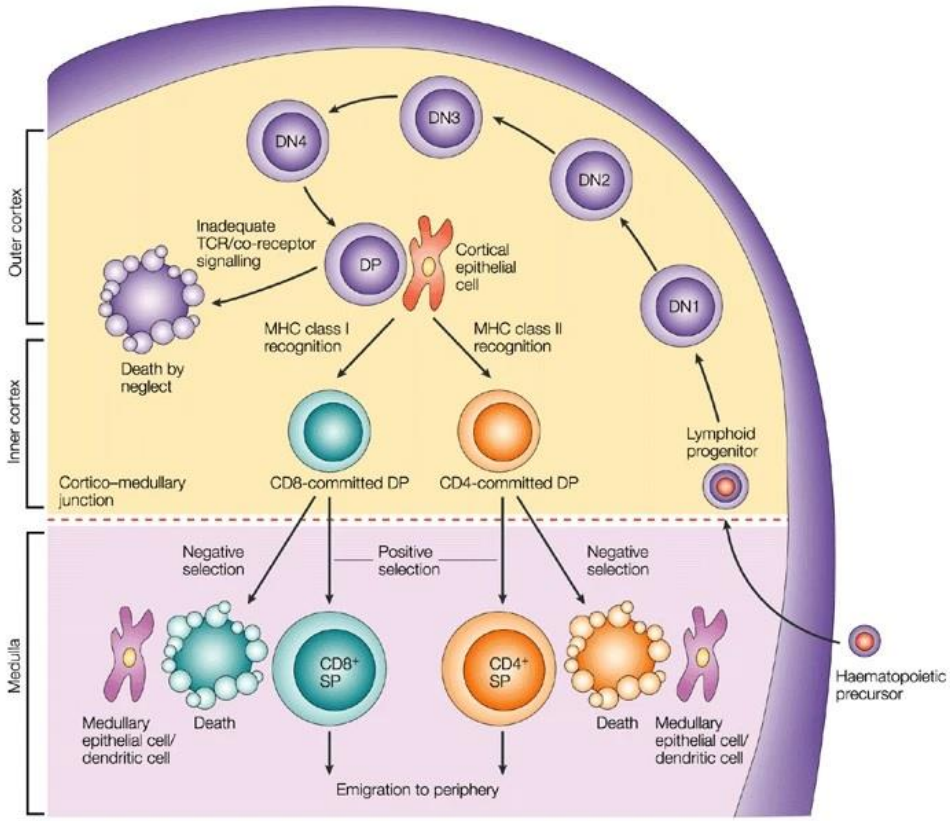

Figure 1.2 T cell development in the thymus. Adapted from (Germain, 2002).

1.3.2 T cell receptor (TCR)

The T cell receptor (TCR) is a membrane anchored heterodimeric protein composed of a disulphide linked α and β chain. It is expressed on the T cell surface and determines T cells specificity which means that it dictates what antigen that T cell will be able to recognize and respond to.

Both α and β chains consist of two immunoglobulin like domains: a constant region (C) domain that spans the cell membrane, and a variable (V) amino-terminal region

that projects outwards. The variable domain is responsible for antigen binding and can bind short antigen fragments or peptides with relatively low affinity (~1-100 μM), when they are presented by major histocompatibility complex (MHC) molecules (M. M. Davis & Bjorkman, 1988). The organization of the TCRα and TCRβ loci is broadly homologous to that of the immunoglobulin gene segments. The TCRα locus, contains V (variable) and J (joining) gene segments (V_α and J_α) while TCRβ locus, contains D (diversity) gene segments in addition to V_β and J_β gene segments.

T cell receptor gene segments go through a somatic recombination process called V(D)J recombination during T cell development and that, alongside with the insertion or deletion of additional nucleotides during this process (Schatz et al., 1992), is how variation in TCR specificity is generated. The complementarity determining region (CDR) of the TCR variable chain reflects the variability generated during the V(D)J recombination. Each variable chain contains CDR1, CDR2 and CDR3 of which CDR1 and CDR2 bind the α-helix of the MHC molecule, while CDR3 (hypervariable region) binds the peptide (Rudolph et al., 2006). Random V(D)J recombination generate a large pool of TCR with different specificities and one single antigen can be recognised by a variety of TCRs (Sewell, 2012).

TCR functionality is dependent upon association with the CD3 complex as it does not contain any signalling domains within its structure. Moreover, CD3 co-expression is necessary for the cell surface expression of the TCR.

The CD3 complex comprises 4 different chains: zeta (ζ), gamma (γ), epsilon (ε) and delta (δ). The CD3 chains γ, ε and δ have significant sequence and structural

homology between each other and are part of the same immunoglobulin-like superfamily encoded by genes on chromosome 11, while the CD3 chain ζ does not have homology to the other chains and is encoded by genes on chromosome 1 (Baniyash, 2004). The cytoplasmic domains of each chain contain immunoreceptor tyrosine-based activation motifs (ITAMs) which are involved in the signal propagation inside the cell. The γ, ε and δ chains contain one ITAM each while each ζ chain contains three.

The TCR-CD3 complex assembly happens in the endoplasmic reticulum (ER) and then a fully functional complex composed of one TCRαβ heterodimer, one CD3γε heterodimer, one CD3δε heterodimer and one CD3ζ homodimer, can be expressed on T cell surface.

1.3.3 T cell-mediated antigen recognition

αβ TCRs primarily recognize antigen presented on cell surface by an MHC molecule in a process defined as antigen presentation. MHC molecules are encoded by a cluster of genes on chromosome 6 known as major histocompatibility complex and are divided in MHC class I and MHC class II.

They both present small peptides derived from antigen processing of naïve proteins, but they have structural and functional differences. Generally, antigens of extracellular origin are presented to CD4+ cells by MHC-II molecules while intracellular peptides are presented to CD8+ T cells by MHC-I molecules (Doyle & Strominger, 1987; Norment et al., 1988).

MHC class I molecules are heterodimers composed of one heavy α chain formed of 3 different domains (α1-α3) and one light β2-microglobulin chain and they are expressed by all nucleated cells. Generally MHC class I molecule present antigens of intracellular origin, however in some cases they can also present peptides of extracellular origin via a process known as cross-presentation (Bevan, 1976) which is fundamental for CD8+ T cell cross-priming in response to viral infections (Sigal et al., 1999) and tumours (Huang et al., 1994), and it is essential for many effective vaccination responses (Yewdell & Haeryfar, 2005). Proteins can be conjugated with ubiquitin and directed to a cytoplasmic catalytic complexes called proteasomes for degradation (Pickart & Eddins, 2004). Peptides generated from this process can be either eliminated by peptidases or can be transported to the endothelium reticulum (ER) lumen by a transporter associated with antigen processing (TAP). Inside the ER, chaperone proteins such as tapasin, calreticulin and ERp57 stabilise MHC-I molecules and the assembly of these chaperones, the MHC-I molecule and TAP form the peptide loading complex (PLC). Once inside the ER, depending on their length, peptides can be further cut by ER aminopeptidases as MCH-I complexes can only bind peptides of 8-10 residues in length and only once suitable for loading can they finally bind the MHC-I. This allows the release of the chaperones and the migration of the peptide:MHC-I complex to the cell's surface for antigen presentation.

MHC class II molecules are structurally similar to MHC-I molecules: they comprise of one α and one β transmembrane chain each formed of two domains. This class of molecules are expressed by professional antigen presenting cells (APCs) including dendritic cells (DCs) and B cells but can also be expressed on mesenchymal stromal cells (Romieu-Mourez et al., 2007) or fibroblasts and

endothelial cells (Geppert & Lipsky, 1985) upon induction by stimuli such as IFN-γ. MHC-II molecules present peptides of extracellular origin derived from protein degradation via the endosomal pathway. The assembly of the α and β chains of the MHC-II molecules happens in the ER where they form a complex with the invariant chain (Ii) to avoid premature binding of peptides and to be directed to the endosomal compartments known as MHC class II compartment (MIIC) (Landsverk et al., 2009). Then, Ii is digested and a small peptide known as class II associated Ii peptide (CLIP) is left inside the peptide-binding groove of the MHC-II molecule. Exchange of CLIP with a specific peptide of endosomal origin is dependent upon activity of human leukocyte antigen DM (HLA-DM). MHC-II molecules can bind peptides of 13-24 amino acids of length (Mohan et al., 2012) and upon loading with a suitable peptide, pMHC-II complex can translocate to the cell's surface for antigen presentation (Neefjes et al., 2011).

Although many TCRs with somatic V-D-J gene rearrangements recognize peptide antigens associated to MHC molecules, this is not the only type of antigen that can be recognized. T cells can also utilize near-germline V-J TCR rearrangements to recognize vitamin metabolites, small phosphoantigens, and lipid antigens presented within various highly conserved and non-polymorphic MHC-I like molecules (Kronenberg, 2014). One of the best characterized innate-like T cell subsets are the invariant Natural Killer T (iNKT) cells, which recognize lipid antigens bound within the antigen presentation molecule CD1d (Brennan et al., 2013).

1.3.4 T cell signalling

When a T cell encounters its cognate antigen presented by MCH molecules on APCs, TCR signalling is initiated. The interaction between the TCR and the pMHC promote a cascade of events in the T cell, including cytoskeletal rearrangements and activation of transcription factors, which lead to T cell activation, proliferation, and differentiation. TCR signalling cascade starts with the phosphorylation of tyrosine residues in the ITAMs of the CD3ζ chain by Lck which is constitutively associated to the cytoplasmic regions of CD4/CD8 co-receptors.

ZAP70 is then recruited to the receptor complex and is itself activated by Lck. ZAP70 phosphorylates the linker for activation of T cells (LAT) and the SRC homology 2 (SH2)-domain-containing leukocyte protein of 76 kDa (SLP76). Their activations lead to phospholipase C-γ 1 (PLC-γ1) activation which then convert phosphatidylinositol 4,5-biphosphate (PIP-2) in inositol triphosphate (IP3) and diacylglycerol (DAG).

IP3 is responsible for calcium (Ca2+) release from the ER increasing Ca2+ concentration in the cytosol and consequent activation of calcineurin, which dephosphorylates and activates the transcription factor nuclear factor of activated T cells (NFAT).

On the other hand, DAG is responsible for activation of the mitogen-activated protein kinase (MAPK) cascade, which then activates the transcription factor activator protein 1 (AP-1). DAG also activates the scaffold protein CARMA leading to de-inhibition of the transcription factor nuclear factor kappa-light-chain-enhancer of activated B cells (NFκB). These transcription factors then translocate to the nucleus and induce transcription of genes involved in T cell differentiation,

proliferation and effector function (Malissen & Bongrand, 2015; Smith-Garvin & Koretzky, 2009)

While there is a deep understanding of the molecular mechanisms behind T cell activation, there are several hypotheses on the initial event that triggers TCR signalling following TCR engagement, and it is likely that the actual trigger is a combination of all the mechanisms proposed. These hypothesis include the aggregation model where TCR-CD3 complexes are believed to aggregate in clusters enhancing phosphorylation (Van Der Merwe & Dushek, 2011), the conformational change model, which hypothesises TCR conformational change upon p:MHC association, triggering signalling cascade (Xu et al., 2008) and the segregation model in which the trigger is thought to be the TCR clustered in areas of the plasma membrane that are enriched in molecules such as Src tyrosine kinases which promote TCR triggering and deficient of molecules such as tyrosine phosphatases which inhibit triggering instead. (S. J. Davis & van der Merwe, 2006) (Figure 1.3).

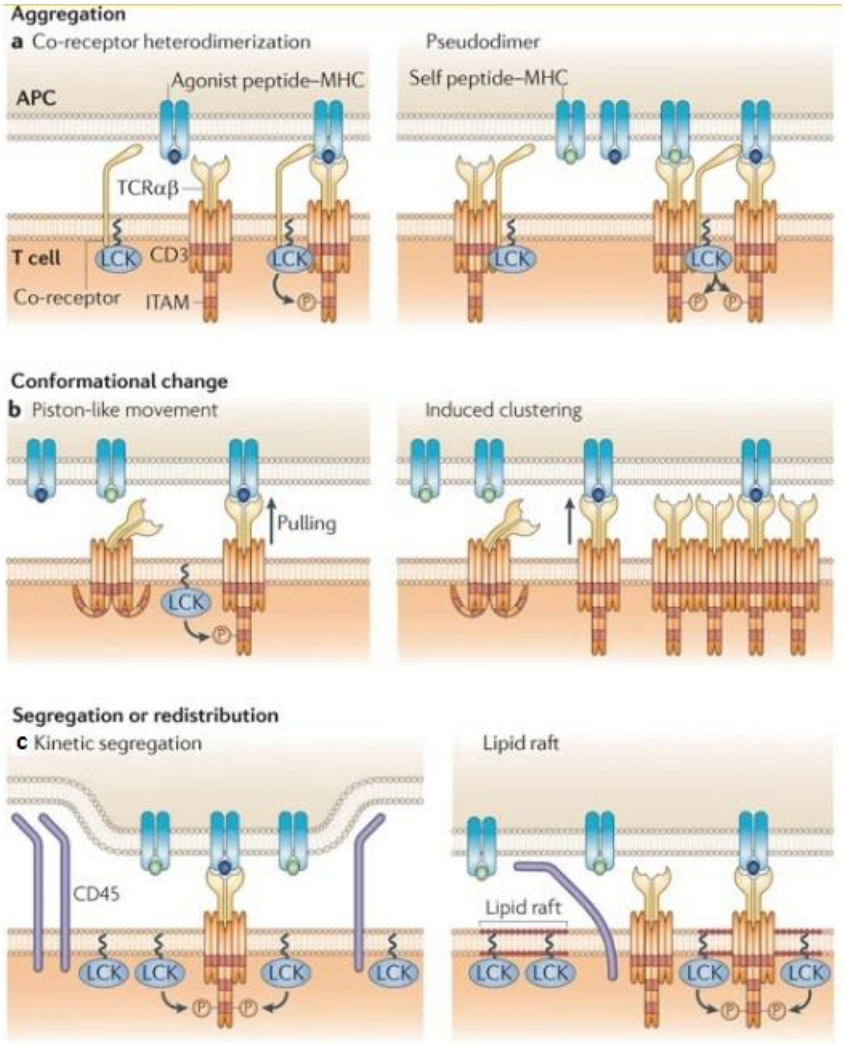

Figure 1.3 TCR triggering mechanisms. a) In the aggregation model, at higher surface densities of agonist pMHC, co-receptor binding to the same pMHC complex as the TCR, brings co-receptor-associated LCK into proximity with TCR–CD3 ITAMs (co-receptor heterodimerization). However, with low levels of agonist pMHC, two TCRs are brought together by binding low-affinity self or high-affinity agonist pMHC ligand and that the co-receptor associated with one TCR engages the agonist pMHC complex, thereby forming a dimer (pseudodimer). b) The conformational change involves either a conformational change or a piston-like displacement of the TCR-CD3 complex induced by the mechanical effects of pMHC binding to the TCR, leading to conformational changes in the cytoplasmic tails of the CD3 subunits. c) Segregation leads to triggering by placing the TCR–CD3 complex in an environment enriched in molecules that promote TCR triggering, such as Src tyrosine kinases and their substrates, and deficient in molecules that inhibit triggering, such as membrane tyrosine phosphatases (e.g., CD45). Lipid rafts are enriched in tyrosine kinases and depleted of CD45. In the kinetic segregation model pMHC engagement holds the TCR–CD3 complex in a close contact zone from which CD45 and CD148 are excluded because of the large size of their ectodomains, leading to stable phosphorylation of TCR–CD3 ITAMs by LCK. Figure has been adapted from (Van Der Merwe & Dushek, 2010).

After TCR engagement, the initial signalling cascade with phosphorylation of proximal signalling molecules happens within seconds and minutes but full activation of T cells requires more than one signal threshold, as several hours of holding without disruption of the p:MHC:TCR complex is crucial for full commitment (Acuto et al., 2008).

1.3.5 Regulation of T cell activation

T cell activation is regulated in the first place by the affinity by which the TCR bind to the p:MHC molecules, in fact engagement to a high-affinity p:MHC molecule with a lower dissociation rate results in a higher degree of TCR signalling, in contrast to engagement to a low affinity p:MHC molecule with higher dissociation rates (Mckeithan, 1995; Rabinowitz et al., 1996). This is also how T cells are able to discriminate between self and non-self-peptides as mentioned previously, considering that self-peptides are presented at higher concentrations compared to the relatively smaller amount of foreign p:MHCs.

T cell regulation is achieved by a balance of stimulatory and inhibitory signals. Full activation requires three signals. The first signal is provided by TCR signalling described in the previous section; the second signal comes from co-stimulatory receptors expressed on APCs. CD28 and B7-H2/TNF are the main receptor families involved in co-stimulatory events. CD28 and ICOS are part of the CD28 family, and they interact with CD80/CD86 and B7-H2 (ICOSL) ligands on APCs whilst 41BB, OX40 and CD27 are part of the B7-H2/TNF superfamily and engage

respectively 4-1BBL, OX40L and CD70 ligands on APCs. Studies show that upon TCR engagement, CD28 forms micro-clusters with the TCR recruiting signalling molecules (Saito et al., 2010; Chen et al., 2013) and CD28 interaction with its cognate ligands activates the PI3K pathway (Smith-Garvin & Koretzky, 2009). The third signal derives from secretion of inflammatory cytokines such as IL-2, IL-7, IL-15 which are involved in proliferation or differentiation of T cells.

The co-operative action of these signals activates T cells and promote T cell differentiation, proliferation, effector function and memory formation. It is important to highlight that this cascade of events is not achieved in the absence of co-stimulatory signal, in which scenario the outcome is a non-responsive state known as T cell anergy.

As well as co-stimulatory signals, T cell receive inhibitory signals by co- inhibitory molecules such as cytotoxic T lymphocyte antigen 4 (CTLA-4) receptor which competes with CD28 for the binding of CD80 and CD86 (Qureshi et al., 2011) and leads to dephosphorylating the CD3ζ chain decreasing proximal TCR signalling. As mentioned previously T cell activation is highly regulated and both stimulatory and inhibitory signals have a key role in it.

1.3.6 T cell effector function

Upon activation, T cell proliferate (Blattman et al., 2002) and differentiate acquiring different effector functions based on the type of T cell.

CD8+ T cells rapidly proliferate and differentiate into cytotoxic T lymphocytes (CTLs) while CD4+ T cells have a slightly delayed proliferation (Foulds et al., 2002)

and have a broader differentiation repertoire which includes type 1 T helper (Th1), Th2, Th9, Th17, Th22, regulatory T cells (Treg) and follicular T helper cells (Tfh) (Raphael et al., 2015; Wan & Flavell, 2009).

The different subtypes of CD4+ T have different cytokine profile and transcription factor expression, but their common goal is to stimulate innate and T cell responses by producing pro-inflammatory cytokines such as IFNγ, TNFα and TNFβ and different type of Interleukins. In particular, Tregs are a specialised subset of helper T cells with regulatory functions: they are crucial for the maintenance of self-tolerance and immune homeostasis. In fact, studies show that Treg depletion or dysfunction can lead to a variety of inflammatory and autoimmune diseases (Sakaguchi et al., 1995).

CD8+ T cells or cytotoxic T lymphocytes are able to directly kill target cells through the formation of the immunological synapse or supramolecular activation cluster (SMAC), by transient interactions (2-10 minutes) between the TCR and pMHC complex.

Upon TCR and p-MHC engagement, TCRs, co-stimulatory receptors, tyrosine kinases (Lck and ZAP70), serine kinases (PKC-θ) and adaptor molecules (LAT, SLP76) cluster around the site of contact to form the central-SMAC (cSMAC) (Monks et al., 1998; Varma et al., 2006). Subsequently, the integrin leukocyte function associated antigen (LFA-1) interaction with the intercellular adhesion molecule 1 (ICAM-1) on APCs form a second ring called peripheral SMAC (pSMAC), surrounding the TCR and its co-receptor. This create a seal which prevent cytolytic molecules secreted by the T cell to escape in the surrounding environment and direct the cytotoxic activity towards the target cell (Dustin et al.,

2010). The pSMAC is surrounded by a more distal ring (dSMAC), containing phosphatases CD45 and CD148 which are believed to be involved in signalling termination by facilitating TCR ubiquitination and degradation (Lee et al., 2003).

The clustering of TCRs induce microtubule reorganisation within the CTL's cytoplasm, polarising the Golgi complex and lytic granules towards the target. Lytic granules contain cytolytic proteins such as granzymes and perforin. Perforin causes the formation of pores in the target cell's membrane and allows entry of granzyme B which triggers the mitochondrial apoptotic pathway leading to DNA fragmentation and apoptosis of the target cells; the apoptotic cells are then ingested by phagocytic cells (Heusel et al., 1994; Jenkins & Griffiths, 2010; Sutton et al., 2000).

1.3.7 T cell memory formation

As described above, upon antigen recognition, naïve T cells go through a rapid expansion increasing up to 50.000-fold in number, acquiring effector function and migrate to the site of infection to 'clear' the pathogen. This process reaches its peak at day 7 post infection and is followed by death by apoptosis of the majority of expanded T cells. The remaining cells will form the long-lived memory T cell repertoire maintained throughout life. They are activated upon secondary infection by the same pathogen and are able to mount a rapid response, providing better protection compared to that generated by antigen-inexperienced T cells (Williams & Bevan, 2007).

The memory T cell repertoire is formed by central memory (TCM) and effector memory T cells (TEM). TCM has limited effector function compared to TEM but is able to differentiate rapidly to effector function upon TCR engagement. On the contrary, TEM has lower proliferative capacity but acquire effector function rapidly. Moreover, TCM express constitutively receptors CD62L and CCR7, which are involved in extravasion, facilitating the cells to reach secondary lymphoid organs. However, CD62L expression on TEM is heterogeneous and CCR7 is no longer expressed (Campbell et al., 2001). Cytokine secretion profile post activation is also different between the two subsets: TCM mainly produce IL-2, IFNγ or IL-4 while TEM produce greater amounts of IFNγ, IL-4 and IL-5, in particular CD8+ TEM also contain large amounts of intracellular perforin (Sallusto et al., 2004). The majority TCM are usually enriched in the lymph nodes and tonsils, while TEM are primarily found in the lung, liver, and gut.

The mechanisms that lead to memory formation are not well understood and two different hypotheses are proposed. One suggests that memory T cells arise from a subpopulation of effector T cells during an immune response. In support of this, a study shows genetically marked cytokine producing cells that were generated during the effector phase, were subsequently found in the memory pool (Löhning et al., 2008; Youngblood et al., 2013). On the contrary, other studies suggest that fully activated T cells can only generate more effector cells while the memory pool derive from naïve T cells, without transitioning through an effector stage (Restifo & Gattinoni, 2013).

1.4 Cancer immunology

1.4.1 Cancer immune surveillance and immunoediting

The concept of immune surveillance as the ability of immune system to recognise and eliminate tumour cells was officially proposed by MacFarlane Burnet and Lewis Thomas in 1957.

Several studies demonstrated the importance of T cells in immune surveillance: Naito et al. analysed the distribution of CD8+ T cells in colorectal cancer and observed that the presence of tumour infiltrating lymphocytes was correlated to better survival of patients (Y. Naito et al., 1998).

To date, many studies highlighted the importance of lymphocytes in tumour surveillance and control of tumour growth. One study used recombinase-activating-gene 2 (RAG2) deficient mice which lack mature lymphocytes due to their inability to initiate V(D)J rearrangement (Shinkai et al., 1992). Carcinogen methylcholanthrene (MCA) was injected in the mice and it induced tumour formation at a higher frequency in the RAG2 knockout group compared to the wild type control group. In addition, RAG2 deficient mice showed an increase in the development of spontaneous neoplastic disease which interestingly was shown to be more immunogenic when transplanted into immunocompetent hosts compared to tumours that developed in the absence of an intact immune system.

This data highlights the dual role of the immune response: T cells are fundamental in immune surveillance but at the same time the immune system is responsible for ‘shaping’ the growing tumour, eliminating the more immunogenic cells and favouring the selection of less immunogenic clones (Shankaran et al., 2001). This

mechanism, originally proposed by Schreiber, is called immunoediting and it consist of three different stages: elimination, equilibrium and escape (Schreiber et al., 2011).

In the elimination phase the innate and adaptive immune systems co-operate to detect and eliminate developing tumours to prevent them becoming clinically apparent, however, this response alone is not always sufficient to maintain a control over it.

The equilibrium phase is the longest stage, it can last many years and consist of a dynamic equilibrium between the host immune system and any malignant cell clone that has survived the elimination phase. While the selection pressure on the tumour cells in this phase is strong enough to maintain an equilibrium, it is not enough to eradicate the tumour.

Eventually for reasons that are still not well understood new variants carrying advantageous mutations arise, shifting the balance towards the last phase of immunoediting which is called escape and consists in uncontrolled growth and clinical presentation of a malignant disease. (Greaves & Maley, 2012).

1.4.2 Cancer immunotherapy and adoptive cell therapy

As mentioned earlier, over the past years there has been a focus on finding alternative approaches to traditional cancer treatment as these have demonstrated extremely limited efficacy for patients with late-stage disease in addition to their considerable side effects due to off-tumour toxicity.

Cancer immunotherapy has emerged both as an innovative alternative or potential addition to the traditional treatments, based on the concept of exploiting components of patient's immune system to target specific cancer cells and enhancing the immune response. Cancer immunotherapies include a wide range of therapies that can be classified in active and passive approaches. Passive immunotherapies include adoptive T cell therapy (ACT) and tumour specific antibodies, while active therapies include immunomodulatory monoclonal antibodies (mAb), cancer vaccines and checkpoint inhibitors.

Amongst these strategies ACT holds great potential having demonstrated promising results in recent cancer clinical trials (Dudley et al., 2008; Ruella & Kalos, 2014). ACT consists in the isolation of immune cells, their manipulation and/or expansion *ex vivo*, and re-injection back into the patient's blood stream. Usually, patients receive lymphodepleting chemotherapy prior to T cell treatment (Dobosz & Dzieciątkowski, 2019). ACT includes a number of distinct types of immunotherapy treatments: some approaches involve directly isolating tumour-specific immune cells and simply expanding their numbers, while other involve genetically engineering our immune cells to recognise a specific target.

Due to the crucial involvement of T cells in the anti-tumour immune response and their biological characteristics, T cell-based ACT is the most common application. Indeed, T cells can recognise tumour antigens and directly eliminate malignant cells. Moreover, this recognition can occur systemically, potentially allowing T cells to cure metastatic diseases. Finally, initial recognition of malignant cells leads to the formation of immunological memory, generating long lived protection.

T cells capable of recognising cancer cells have been identified in several types of malignancies and are referred to as tumour-infiltrating lymphocytes (TILs). Autologous TILs can be isolated from the patient, expanded ex vivo using tumour specific peptides and/or cytokines, and re-infused back into the patient where they can carry out their effector functions and mediate tumour control. ACT using autologous TILs is currently the most effective treatment for patients with metastatic melanoma and can mediate objective tumour regressions in 50% - 70% of the patients (Dudley et al., 2002, 2008). As mentioned earlier, these therapies are effective only when administered in combination with lymphodepleting chemotherapy to favour homeostatic proliferation and expansion of the transferred cells by avoiding endogenous Treg-mediated immune suppression and providing greater access to cytokines such as IL-15 and IL-2, which when co-administered, have proven to improve the anti-tumour response and (Antony & Restifo, 2005; Dummer et al., 2002; Gattinoni et al., 2005). However, TILs therapy is not always possible. It is indeed limited by TILs availability depending on the location of the tumour, isolation in sufficient numbers and the immunosuppressive tumour microenvironment.

Therefore, alternative approaches to develop tumour specific T cells have been developed: two of most promising area in T cell engineering include T cell receptor (TCR) gene transfer and Chimeric Antigen Receptor (CAR) based technology.

1.4.3 T Cell Receptor (TCR) gene transfer

Most of the cellular engineering approaches have been applied to αβ T cells, which are relatively easy to purify and expand from peripheral blood.

In the TCR gene transfer technology, peripheral blood T lymphocytes are ex vivo engineered with a recombinant T-cell receptor (TCR) of known specificity which recognizes a cognate peptide-loaded major histocompatibility complexes (pMHC) of a tumour-associated antigen (TAA). The TCR is typically derived from a tumour infiltrating lymphocyte (TIL) or from in vitro antigen-stimulated blood.

Proof that the T-cell receptor αβ - chain genes can transmit a functional specificity from one cytotoxic T cell to another was first seen in targeting the hapten molecule, fluorescein (Dembic et al., 1986).

The ability to transfer T-cell receptor specificities by gene transfer opened up new ways for in vitro manipulation and subsequently it has been used to target a wide range of viral and tumour antigens. Adoptive transfer of T cells genetically modified to express a cancer-specific T-cell receptor (TCR) has shown significant therapeutic potential for both haematological and solid tumours and has already resulted in impressive clinical responses in a number of human malignancies, such as metastatic synovial sarcoma, melanoma, and multiple myeloma (R. A. Morgan et al., 2006).

However, some restrictions limit the broad application of TCR engineered T cells: the vast majority of TCR engineering studies has been conducted on αβ T cells, in which antigen recognition is dependent on presentation by MHC molecule, therefore TCR transfer technology is limited by the number of peptide-MHC complexes identified so far which can be used for screening.

Other limitations include tumour immune evasion strategies such as down-regulation of MHC (Garrido et al., 2016) or loss of redundant neo-antigens (Beatty & Gladney, 2015), and the potential mispairing with the endogenous TCR,

producing novel and unforeseen specificities which might induce severe auto-immunity after adoptive transfer (Jorritsma et al., 2007). Moreover, toxicity can be caused in particular when non-immunogenic tumour-associated self-antigens are targeted (de Witte et al., 2008). For example targeting melanoma antigen recognized by T cells (MART-1) or melanoma-associated antigen 3 (MAGE-3A) has led to severe toxicities caused by recognition of cognate T cell epitopes or highly similar antigens outside tumour tissues (Cameron et al., 2013). One study targeting MAGE-3A using a TCR redirected to HLA-A*01 led to cardiotoxicity due to cross reactivity with epitopes derived from the striate-muscle protein, titin (Linette et al., 2013).

In addition to side-effects, multiple clinical trials demonstrated variable therapeutic efficacy, which, in the case of solid tumours, has been largely attributed to the suppressive nature of the tumour microenvironment (TME).

As mentioned above, the use of a transgenic αβ TCR in αβ T cells is limited by the presence of pre-existing, endogenous TCRs within these cells. Expression of TCRs at the cell surface requires the formation of a ternary complex with the CD3 components of this receptor that constitute a limiting factor for surface expression of the antigen-binding chains of the TCR. Successful expression of a transgenic αβ TCR therefore requires competition with the endogenous TCR chains for CD3 association (Ahmadi et al., 2011). In addition, and most importantly, there is also potential for the formation of hybrid TCRs due to mispairing of endogenous and transduced TCR chains (so-called mixed TCR dimers). Mispairing of transgenic and endogenous chains can lead to unpredictable, and potentially dangerous, target specificities. It has been demonstrated in vitro, that mixed TCR dimers

harbour not only alloreactivity but also autoreactivity towards normal human subsets (van Loenen et al., 2010).

Several methodologies have been explored to overcome this issue:

1) Using murine constant regions or altering rearrangement of cysteines in the transferred TCRs to avoid mispairing. While there is a risk of the host mounting an anti-murine immune response, studies demonstrated that these had no effect on the clinical outcome (J. L. Davis et al., 2010)(Cohen et al., 2006).

2) Adopting alternative cells type as substrate for TCR transfer. Using γδ T cells can be another way to overcome these limitations as alpha and beta chains do not mis-pair with γδ TCRs. Several studies show the possibility to transfer a transgenic αβ TCR in γδ T cells with enhanced antitumor activity (Dörrie et al., 2014a; Harrer et al., 2017). Furthermore, it is also possible to overcome HLA restriction derived from αβ TCR transfer, expressing instead a γδ TCR in αβ T cells. This alternative approach will be discussed in more detail in the next section.

3) Using of gene editing technology (for example, CRISPR/Cas9) to introduce a transgenic αβ TCR or γδ TCR, with simultaneous knock out of the endogenous TCR during the TCR transfer. This did lead to enhanced reactivity to primary haematological malignancies compared with T cells expressing both endogenous and transgenic TCRs (Legut et al., 2018).

1.4.4 Chimeric Antigen Receptor (CAR) technology

CAR-T cell-based technology is an alternative way to redirect T cell specificity against tumour antigens, by expressing on their surface a synthetic molecule called

Chimeric Antigen Receptor (CAR). The CAR structure comprises of an extracellular binding domain, a spacer-linker domain, a transmembrane domain, and an intracellular signalling domain.

Specificity is provided usually by a single-chain variable fragment (scFv) derived from a monoclonal antibody against a specific antigen epitope. The linker/spacer region called hinge or stalk depending on the length, is responsible of projecting the scFv into the extracellular cytoplasmic space and should provide both sufficient flexibility to mediate an immune synapse and length to facilitate access to the target antigen. The location of the epitope recognized by the scFv and the length and flexibility of the spacer are important factors to consider as they are involved in antigen engagement and formation of the synapse (Guest et al., 2005; Hombach et al., 2000; Moritz & Groner, 1995).

The transmembrane domain is normally derived from the linker or membrane-proximal endodomain and is responsible of anchoring the CAR to the membrane and for stable CAR expression(Bridgeman et al., 2010).

CARs have undergone fine tuning since they have been first developed and can be divided in 3 generations based on the structure of their intracellular domain.

The first generation CARs, contained a single CD3 ζ- chain or FcεRIγ intracellular signalling domain; however T cells transduced with such constructs proliferated poorly and failed to exhibit a robust cytokine response, due to poor T cell activation (Brocker & Karjalainen, 1995), therefore the intracellular domain was modified to overcome these limitations.

Second generation CARs contained both CD3ζ and the cytoplasmic domain of a co-stimulatory receptor, such as CD28, 4-1BB, OX40 or ICOS. This addition

improved T cell function by conferring greater strength of signalling and persistence to the transduced lymphocytes (Finney et al., 2004; Sadelain et al., 2013). This translated into better persistence in patients (Savoldo et al., 2011).

Third generation CARs incorporate two co-stimulatory domains to the CD3ζ signalling domain. Preclinical studies of third generation CARs have produced mixed results: while in some mouse models these receptors seem to confer yet greater potency to transduced T cells, in other models these CARs showed no in vivo treatment benefits and failed to outperform second generation CARs in their respective models (Tammana et al., 2010; Zhong et al., 2010).

The advantage of CAR gene therapy over TCR gene therapy is that CAR recognition of antigen is not dependent on presentation by MHC, meaning they are not restricted by a particular HLA molecule and can be used in patients of different HLA types. Moreover, they are not associated with mispairing risk, inherent in TCR gene therapy.

In addition, in CAR-based therapy there is less limitation of targetable antigens since it does not require processing and existence in an MHC restricted peptide complex . indeed, any cell surface molecule can potentially be targeted; not limited to proteins.

Due to the MCH unrestricted nature of the CAR, however, one of the disadvantages of derives from the potential of the CAR-T cells to target both healthy and tumour cells expressing their cognate antigen with the risk of causing on-target off-tumour toxicity. As mentioned before, most of cellular engineering approaches have been applied to αβT cells. In haematological malignancies, CAR T cells targeting CD19 in acute lymphoblastic leukaemia (ALL) have achieved one

of the most promising responses in CAR T cell-based therapy and it has received approval for sale in the United States for the treatment of diffuse large B-cell lymphoma (DLBCL) and acute lymphoblastic leukaemia (ALL). CD19 CART cell is toxic to CD19+ ALL as well as healthy CD19+ B-cells due to the MHC unrestricted nature of the CAR. This results in B cell aplasia which is considered to be an acceptable toxicity; in other cases though, such as AML, off tumour toxicity can be fatal (Lamers et al., 2006; Richard A. Morgan et al., 2010) and new strategies are necessary to overcome this limitation.

Using other cell types as substrate in cancer immunotherapy have the potential to overcome it. There are several ongoing studies using NK cells and γδT cells which demonstrates the feasibility of using effector cells with an innate immune phenotype, possessing broader tumour recognition potential (Boissel et al., 2009; Cheng et al., 2013; Gammaitoni et al., 2017).

1.4.5 γδ T cells relevance

Among the other cell types that are being studied in cancer immunotherapy, γδ T cells can be used as alternative cell substrate to overcome certain αβ T cells limitations in both TCR and CAR technologies as their features include non-MHC restricted antigen recognition and potent anti-tumour responses suggesting natural roles in tumour control (J. P. H. Fisher, Heuijerjans, et al., 2014), making them an attractive candidate for therapeutic exploitation.

γδ T cells display a combination of innate and adaptive immunity functions. In fact, they receive signals from a multitude of co-receptors, some of which are usually

associated with NK cells, conferring them NK-like properties of potent antibody-dependent and independent cytotoxicity (J. P. H. Fisher et al., 2016; Himoudi et al., 2012). Among these receptors are NKG2D (Nedellec et al., 2010), DNAM-1 (J. Gertner-Dardenne et al., 2012) and FcγRIII (J. P. H. Fisher et al., 2016; Julie Gertner-Dardenne et al., 2009). Moreover, several studies highlighted a correlation between the presence of infiltrating γδ T cells in the tumour microenvironment and therapy outcome. In a recent study about the prognostic landscape of genes and infiltrating immune cells across human cancers, investigating almost 6,000 patient-derive tumour samples, authors found the presence of infiltrating γδ T cells to be the strongest predictor of positive outcome(Gentles et al., 2015).

As mentioned in the T cell development section, T cells differentiate in the thymus generating functionally distinct subpopulations of mature T cells (Fahl et al., 2014): γδ T cells are a subgroup of T cells with distinct T cell receptors γ and δ chains on their surface and they comprise only 1-10% of circulating T cells (J. P. H. Fisher, Yan, et al., 2014a) in contrast to αβ T cells which comprise 65–70% of circulating lymphocytes.

γδ T cells diverge from αβ T cells in the thymus with lineage commitment by the DN3 stage of the thymic development (Fahl et al., 2014). Advances in next generation sequencing have produced more insights on their distribution. Their repertoire changes during fetal development, with Vγ9Vδ2+ predominance in the second trimester of fetal development while Vγ9−Vδ1+ subsets predominate towards full gestation (Dimova et al., 2015). In adult life, there is a age-related extra thymic increase in circulating Vγ9Vδ2+ proportions (Parker et al., 1990; Pauza & Cairo, 2015) while γδT cells expressing Vγ2–5, 8–9, and Vδ1–8 chains (Lefranc, 2001) can also be detected in peripheral blood.

The Vδ1+ subset is a minor population in the blood but is the predominant tissue-resident population of γδ T cells. They can be mainly found at mucosal sites such as the dermis and intestinal epithelia where they can comprise 20–50% of the tissue-resident lymphoid compartment (Silva-Santos et al., 2015). Unlike the Vδ2+ subset, Vδ1+ γδ T cells often don't pair with a specific Vγ chain, although clonal expansion can be seen in some organs, which can be different among individuals. Vδ1+ γδ T cells can display an NK-like phenotype in their expression of natural cytotoxicity receptors such as NKp30, NKp44 and NKp46 (Silva-Santos & Strid, 2018). A unique ligand for the Vδ1+ TCR has not been identified yet, however, recent studies have identified MHC class I homologue MICA and lipid antigen α-galactosylceramide (α-GalCer) presented by CD1d, as possible cognate antigen for Vδ1+ TCR (Russano et al., 2006; Spada et al., 2000).

In contrast, Vγ9Vδ2+ T cells subset is the most abundant in circulation, therefore, it is the one most publications have focused on: despite being widely studied, much less is known about γδTCR-mediated recognition mechanisms, compared to αβ T cells.

Studies show that Vγ9Vδ2 T cells respond in an MHC unrestricted manner to targets with high phosphoantigen burden, associated with malignant transformation and disordered EGFR signalling (Asslan et al., 1999; Poupot & Fournié, 2004). Vγ9Vδ2 T cells respond to phosphoantigens such as isopentenyl-pyrophosphate (IPP), metabolites accumulated as results of dysregulation of the mevalonate pathway of cholesterol biosynthesis (Benzaïd et al., 2012). However, they can also be activated in the presence of target cells that are incubated with lysates from certain microbial species that produce phosphoantigens such as

hydroxymethyl-butyl-pyrophosphate (HDMAPP/HMBPP) through the MEP (2-C-methyl-D-erythritol 4-phosphate) isoprenoid pathway (Belmant et al., 2006).

Studies show that aminobisphosphonates (NBP) can be used to inhibit the enzyme farnesyl pyrophosphate synthase of the mevalonate pathway leading to accumulation of intracellular IPP. (Cabillic et al., 2010), which translate in the possibility of using commercially available aminobisphosphonates such as Zoledronate to expand Vγ9Vδ2 T cells from donors.

Furthermore, while no direct contact between the Vγ9Vδ2 TCR and phosphoantigens (pAgs) have been reported, cell-to-cell contact is necessary to achieve Vγ9Vδ2 T cell activation (Morita et al., 1995), suggestive of a cell-surface ligand on the target cell.

Homology in parts of the CDR3 sequences between Vγ9Vδ2T cells derived from different type of expansion and different donors, suggest that they recognize a ligand held in common. While previous studies pointed to butyrophilin 3A1 (BTN3A1) (Vavassori et al., 2013) of the butyrophilin (BTN) family as the sole ligand involved, recent findings point to a synergic action between butyrophilin 3A1 (BTN3A1) and butyrophilin 2A1 (BTN2A1) (Karunakaran et al., 2020; Rigau et al., 2020).

Vγ9Vδ2 TCR recognition models until the recent findings suggested two main possible mechanism of action. The first suggested that the Ig-like extracellular domain of BTN3A1 can directly bind pAgs and that there is specific and direct interaction of soluble Vγ9Vδ2 TCR with the BTN3A1–pAg complex) (Vavassori et al., 2013). In contrast other studies suggested the important role of the intracellular B30.2 domain, which might sense increased levels of intracellular pAgs and directly

interact with them inducing a conformational change in the BTN3A1 molecule, which could then be recognized by the Vγ9Vδ2 TCR (Sandstrom et al., 2014).

Recent findings, supporting the synergic action between BTN3A1 and BTN2A1 instead, show BTN2A1 direct binding to the IgV domain of the Vγ9 chain and direct association of BTN2A1 to BTN3A1 even when there was no activation by phosphoantigens (Karunakaran et al., 2020). As support to these findings, another group found BTN2A1 as a critical mediator of pAg sensing and a direct ligand for Vγ9+ TCRs using a TCR-tetramer staining and CRISPR-screen approach (Rigau et al., 2020).

The revised model suggests alongside Vg9 interaction with BTN2A1, BTN3A1 association with BTN2A1 could serve to spatially orientate BTN3A homo- or heterodimers and, following pAgs exposure, could recruit another ligand to the complex for TCR CDR3-mediated recognition. In this context, pAgs binding to BTN3A1 B30.2 domain, could regulate the strength of BTN3 association with such a ligand, and/or trafficking of such complexes to the cell surface.

Despite these findings, Vγ9Vδ2 TCR mediated recognition is a complex mechanism and there is still a lack of knowledge on the totality of factors that are involved in it and further studies are required to clarify such mechanistic models.

1.4.6 γδ TCR gene transfer

Several studies investigated the potential of TCR transfer to and from γδ T cells as an alternative substrate to the traditional αβ TCR transfer approaches in order to overcome its limitations.

It has indeed been demonstrated that it is possible to introduce a tumour reactive αβ TCR in γδ T cells, without the risk of mispairing (van der Veken et al., 2009; Van Der Veken et al., 2006). Additionally, αβ TCR-transduced γδ T cells have been shown to retain the functionality of their original TCR and were able to respond to stimuli transferred via either TCR with rapid, γδ-like kinetics (Hiasa et al., 2009). Another study has shown that a γδ T cells transduced to express an HLA-A*0101 restricted αβTCR targeting a peptide derived from an adenovirus hexon protein, were able to mount an antigen specific cytokine response and produced more IFN-γ and TNF-α compared to CD8+ αβ T cells against the same target (Dörrie et al., 2014b).

In order to overcome the limitations such as the restriction to specific HLA type and the possibility of antigen negative escape variants, transfer of invariant natural killer (iNKT) TCR to γδ T cells or γδTCR to αβ T cells were proposed, yielded exciting results.

The structure of a prototypic Vγ9Vδ2 TCR clone (G115) was described for the first time by Allison et al in 2001 (Allison et al., 2001). This clone was subsequently expressed in αβ T cells (Marcu-Malina et al., 2011) and authors showed that mis-pairing with endogenous γ or δ chains was not occurring.

αβ T cells expressing the γδTCR showed lack of alloreactivity and enhanced cytotoxicity and cytokines release against a γδ sensitive target -Daudi, displaying similar functional properties to “native” Vγ9Vδ2 cells. Vγ9Vδ2 TCRs derived from different T cell clones were studied for anti-tumour activity and alanine scanning of the TCR sequences demonstrated that small differences in the γ9 and δ2 CDR3 regions, which are critical for ligand interaction, were responsible for the variation

in responses (Gründer et al., 2012). Combinatorial-γδTCR-chain exchange has been shown as an efficient method for designing high-affinity γ9δ2TCRs that mediate improved antitumor responses when expressed in αβT cells both in vitro and in vivo in a humanized mouse model.

These findings suggest that it is possible to tune a αβ T cells with an appropriate Vγ9Vδ2 TCR so that it has enhanced reactivity against a specific target of interest.

1.4.7 Chimeric antigen receptors in γδ T cells

As well as for the TCR transfer studies, the majority of work with CARs has been done in αβ T cells. γδ T cells expressing a first-generation CAR was firstly described by Rischer et al in 2004. The authors showed enhanced antigen-specific tumour reactivity by γδ T cells expressing a CAR-targeting GD2 compared to non-transduced γδ T cells. When antigen was present, γδ T cells expressing anti GD2-CAR upregulated activation markers such as CD69 and increased production of cytokines such as IFN-γ. Similar results were seen using γδ T cells expressing anti CD19-CAR (Rischer et al., 2004). In addition to this engineering strategy, different studies focused on harnessing the innate properties of the Vγ9Vδ2 T cells in the context of CAR T cell-based immunotherapy.

The basic structure of CARs used in αβT cell engineering comprised of a CD3-ζ signalling endodomain and an antibody based ectodomain which allows CAR-T cells to simultaneously bypass MHC-restriction and to specifically target a tumour antigen through their ScFv. As mentioned previously, this can lead to on-target off-

tumour toxicity due to the CAR reacting to their cognate antigen present on healthy cells.

Using γδ T cells has the potential to overcome this limitation; as γδ TCRs are not MHC-restricted and detect moieties associated with cellular stress, it is possible to design a CAR that only comprises of one or multiple co-stimulatory endodomain (Chimeric Costimulatory Receptor or CCR) allowing to discriminate between an antigen positive healthy cell and an antigen positive tumour cell.

This approach has been described by Fisher et al. in the context of neuroblastoma (J. Fisher et al., 2017). NKG2D blocking is a well-studied immune escape mechanisms involved in neuroblastoma (Raffaghello et al., 2005) partially responsible for Vγ9Vδ2 T cells having minimal innate cytotoxicity towards the tumour (J. P. H. Fisher, Yan, et al., 2014b). In order to restore the cytotoxicity, the authors used a CCR targeting GD2, containing a DAP10 (endodomain motif from the NKG2D adaptor) endodomain but no CD3-ζ signalling domain as TCR signalling was mediated by the γδ TCR. Using this strategy, GD2-DAP10 CCR showed enhanced cytotoxicity and IL-2, IFN-γ, and TNF-α cytokines production towards GD2+ neuroblastoma while GD2+ cells that did not engage the Vγ9Vδ2 TCR were spared (J. Fisher et al., 2017). Moreover, it is has been demonstrated that CAR-expressing γδ T cells retain their cross-presentation ability (Capsomidis et al., 2018) making this system even more attractive. This system suggests the possibility of avoiding on-target off-tumour toxicity and could be translated to different cell types for optimization.

1.5 AML immunotherapy

1.5.1 Current strategies and challenges

Many immunotherapy approaches are currently under investigation in order to overcome the limitations of conventional AML treatment strategies. Thanks to numerous studies we now have not only more understanding about the molecular heterogenicity of AML , but also about the interplay between AML blasts, the hematopoietic niche, and the cells of the immune system for AML development and growth (Isidori et al., 2014; Ladikou et al., 2020), as well as tumour microenvironment, systemic tolerance and tumour escape mechanisms in AML (Austin et al., 2016; Isidori et al., 2014).

The main mechanisms involved in AML immune evasion (Figure 1.3) consist in:

1) Over-expression on AML blasts of inhibitory T-cell ligands such as PD-L1, Gal-9, CD155, CD112 and CD86, impairing T and NK- cell effector function.

2) Alter the cytokine milieu by producing of immunosuppressive cytokines and release within the bone marrow niche other soluble factors such as reactive oxygen species (ROS), indoleamine 2,3-dioxygenase-1 (IDO1), arginase II (ArgII). These mechanisms promote T-cell exhaustion and apoptosis, drive the expansion of Tregs and myeloid-derived suppressor cells (MDSCs), and induce the switch of macrophages to tumour-associated macrophages (TAMs).

3) AML blasts reduce their expression of antigen presentation molecules, thus hiding themselves from immune cells such as dendritic cells (DCs) and macrophages.

These insights in the tumour induced immune tolerance have open the doors to new effective way to counteract on those mechanism and approaches to enhance-cell immune response to AML. Examples of these therapies include blocking inhibitory pathways such as PD-1/PD-L1 or CTLA-4, CTLA4, TIM3, blocking functional enzymes such as IDO, cancer vaccines and adoptive NK and CAR-T cell immunotherapy and Bispecific antibodies (BITEs and BIKEs).

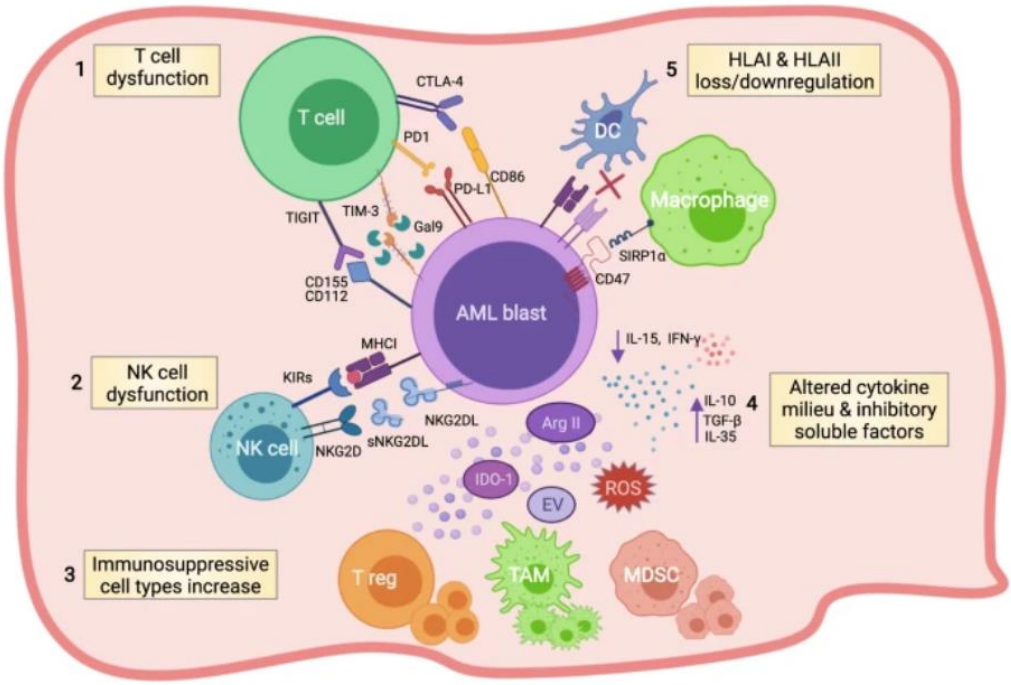

Figure 1.3 Immune evasion mechanism AML. The figure illustrates the main mechanisms involved in AML immune evasion. Figure adapted from (Ruella & Maus, 2016)

Current immunotherapy strategies to target AML include antibody and CAR-T cell-based approaches targeting antigens such as CD33 and CD123, which are overexpressed on leukemic blasts.

One of the biggest challenges of these strategies derives from the expression profile of the antigens that are targeted: while they are overexpressed on leukemic blast, these antigens are also expressed on healthy cells such as normal

hematopoietic stem and progenitor cells; CD123 is also expressed on endothelial cells (Ehninger et al., 2014). Targeting these antigens would lead to ablation of the myeloid cell pool and bone marrow failure, therefore, different strategies to overcome these limitations are currently under investigation. This also include testing different antigens as target.

A CAR-T cell-based approach targeting CD33 and B7H3 is explored in the first result chapter of this thesis, therefore, a background on these two antigens as potential target antigens for AML, as well as current strategies and limitations regarding their use, is provided below.

CD33

CD33 is expressed in approximately 90% of myeloblasts in patients bearing AML, and for this reason it is widely studied as potential target in the AML immunotherapy field. CD33 is a 67 kDa transmembrane glycoprotein, part of the sialic acid-binding immunoglobulin (Ig)-like Lectins (Siglec; Siglec-3) superfamily involved in cell-cell interactions. It is overexpressed on AML Blasts and leukemic stem cells, and it is not associated to a specific karyotype which makes it an attractive candidate for AML targeted therapies, however, its expression profile is a cause of concern for potential toxicity as it is also expressed on myeloid-committed cells in the bone marrow and on circulating monocytes and constitutively expressed on dendritic cells (DC). It is also expressed on neutrophils, NK cells, B-cells subset, and Kupffer cells in the liver, while it is downregulated on peripheral granulocytes and resident macrophages.

CD33 has been the target of multiple immunotherapy strategies from antibody strategies to CAR-T based immunotherapies. Among other antibody strategies, CD33 was targeted by gemtuzumab ozogamicin, an immunoconjugate combining anti-CD33 antibody with the toxin calicheamicin. It received FDA approval based on a reported 30% response rate in a phase II clinical study (Sievers et al., 2001). However, gemtuzumab ozogamicin was temporarily discontinued given safety concerns and disappointing efficacy results seen in phase III clinical trial: a study showed development of hepatic sinusoidal liver injury after the antibody-conjugate was infused. Cause for hepatic toxicity was elucidated by histological analysis, which showed striking deposition of sinusoidal collagen, suggesting that gemtuzumab ozogamicin targeted CD33+ cells residing in hepatic sinusoids (Rajvanshi et al., 2002; Rowe & Löwenberg, 2013).

More recent studies though, showed high efficacy of gemtuzumab ozogamicin in Acute Promyelocytic Leukaemia (APL) and in AML the addition of gemtuzumab ozogamicin to induction/consolidation chemotherapy, improved event-free survival and overall survival in newly diagnosed AML patients, with a safe toxicity profile (Castaigne et al., 2012; Lo-Coco et al., 2004; Taksin et al., 2007). Therefore, US FDA, followed by the European Medicines Agency, reapproved the use of gemtuzumab ozogamicin combined with daunorubicin and cytarabine for patients with newly diagnosed CD33 positive AML in 2017. The FDA has also approved gemtuzumab ozogamicin for use as a single agent in relapsed or refractory AML and in children (Niktoreh et al., 2019).

A different antibody based therapy consists in the use of bispecific antibody as mean to eliminate cancer cells without genetic alteration of the T cells or need for ex vivo expansion/manipulation, providing an off-the-shelf immunotherapy (Huehls

et al., 2015). In the BiTe and BiKe molecules, binding domains are two single chain variable fragment (scFv) regions, derived from mAbs, joined by a flexible peptide linker with affinities for both a selected leukaemia associated antigen such as CD33 or CD19 as well as a selected target on an effector immune cell, like CD3 expressed on T-cells (in BiTes) or CD16 expressed on NK-cells (in BiKes) (Gramer et al., 2013). In a study using AMG330, a human BiTe with binding specificity for CD33 (N-terminal) and CD3Ɛ (C-terminal) authors showed that when co-cultured with primary AML blasts, AMG330 induced T cell activation, PDL1 over-expression on T-cells, IFN-γ, TNF-α, IL-2, IL-10 and IL-6 cytokines release and reduced bone marrow immune-suppressive CD14+ HLA-DRlow monocytic-like myeloid derived suppressor cells (Friedrich et al., 2014; Krupka et al., 2014).

Additional antibody-based therapies include unconjugated monoclonal antibodies that can enhance antibody dependent, cell mediated cytotoxicity mediated by natural killer cells and radioimmunoconjugates with a radionuclide attached to a monoclonal antibody.

Several CAR T-cell therapies against CD33 have also made it to clinical trial phases 1 and 2 and different strategies such as the use of CAR T-cell, CAR γδT-cell, and CAR NK-cell, have been investigated . In a clinical trial study run at M.D. Anderson Cancer Center, ten adult r/r AML patients were recruited, three of which received anti-CD33 CAR T-cells at a dose level (0.3 x 10^6 cells/kg) (Wang et al., 2015)(Tambaro et al., 2021). Two of the three patients developed toxicities including CRS, tumour lysis syndrome and acute kidney injury and all three patients ultimately died from AML disease progression, despite CAR T-cell detection in peripheral blood.

Another group reported potent in vitro activity against AML cell lines by their CD33-specific CART with ScFv derived from gemtuzumab ozogamicin. However, reported anti-tumour effects were associated with profound cytopenia. In order to avoid long-term myelosuppression, the authors induced transient expression of anti-CD33 CAR by electroporating the CD33-specific CAR mRNA into human T cells (Kenderian et al., 2015).

Immunotherapies directed against CD33 have demonstrated on-target off-tumour due its expression profile. A recent study attempt to overcome this limitation and enable immunotherapy against AML using anti-CD33 CAR-T or antibody therapy, by genetically ablating CD33 in human stem/progenitor cells, using Cas9/guide RNA mediated gene editing. In this study the authors model a post remission human marrow with minimal residual leukemic disease in mice and show effective clearance of acute myeloid leukaemia and the reconstitution of the CD33-deleted human graft.

Other ongoing efforts to overcome hematologic toxicity include the identification of novel target antigens such as CLL-1, Lewis Y, FLT3, and CD44v6 and dual targeting approaches such as compound CAR-T targeting both CD33/CD123 or CD123/CLL1, which could also bypass the problem of loss of target antigen seen on leukaemia cells at the time of relapse.

B7-H3

In contrast, B7-homolog 3 (B7-H3) has only recently been considered as potential target for AML-directed CAR T-cell therapy. B7-H3 (or CD276) is a 110-kDa type I transmembrane protein, a coreceptor belonging to the B7 family of immune

checkpoint molecules. The nature of its signalling it is still not fully understood and while the exact receptors through which it signals remain unknown, three candidates have been identified so far as potential cognate target: TLT-2, IL20RA, and PLA2R1 (Picarda et al., 2016).

When first identified, B7-H3 was characterized as a T-lymphocyte stimulating protein. However, current evidence in the literature points towards a predominantly immunoinhibitory role for B7-H3, particularly in the context of the tumour microenvironment. Physiological expression of B7H3 is thought to be relatively restricted with low levels of expression on the liver, testes and placenta, gastric tissues, salivary glands and adrenal glands (Wang et al., 2014). Expression can also be induced on DCs, monocytes, macrophages and lymphocytes by inflammatory cytokines (Chapoval et al., 2001). Importantly, B7-H3 has been found to be overexpressed in multiple childhood and adult human cancers including being overexpressed on leukemic blasts in patients with AML. B7-H3 expression in AML appears to be higher in AML with a monocytic immunophenotype(Guery et al., 2015), which is often associated with aggressive clinical features (Dobrowolska et al., 2013).

The expression pattern of B7-H3 makes it a promising target for immunotherapy and its role in T cell modulation offers a potential means of checkpoint inhibition.

Anti-B7-H3 CAR T-cells have shown promising results in preclinical in vitro and in vivo models (Lichtman et al., 2021; Liu et al., 2021; Zhang et al., 2020). In a study by Lichtman et al., anti-B7-H3 CAR T-cells showed cytotoxicity and IFN-γ and IL-2 release against AML cell lines OCI-AML2, OCI-AML3, THP1, and U937 as well as against primary AML patient samples with E:T ratio of 1:5 after 48 hours (Lichtman

et al., 2021). Another study uses anti-B7-H3 and anti-CD70 CARs in tandem against NHI-460 and A375 AML cell lines. At an E:T ratio of 8:1; the tandem CAR T-cells had approximately 50% and 60% specific cell killing respectively, compared to single CD70 CAR T-cell which only showed 35% and 40% killing efficiency (Yang et al., 2020).

B7-H3 seems to be homogeneously overexpressed only in a small percentage sample of liver, breast, cervical, and bladder cancers, while its expression is highly heterogeneous in other cancer types. Recently, two posters presented at the American Society of Haematology (ASH) Conference, reported that B7-H3-targeted CAR immunotherapy could be an effective treatment for AML patients with B7-H3 overexpression, as B7-H3 was highly expressed in a substantial fraction of AML patients. However, due to the heterogenicity of its expression, the authors suggested that it may be necessary to develop a dual-targeting approach, such as combining B7-H3 with a second AML surface antigen, in order for the therapy to be effective (Guéry et al., 2013; Lichtman et al., 2021).

While B7H3 expression is restricted in normal tissues, its mRNA expression was ubiquitous in almost all of the normal tumour-adjacent tissues (TATs) from TCGA database that were analysed in one study(Zhang et al., 2020). Moreover, previous studies have shown B7-H3 expression can be induced in normal tissue in response to inflammation (Veenstra et al., 2015). This upregulation mechanism needs to be taken into consideration in order to develop a safe immunotherapy strategy.

Given the molecular heterogeneity of AML and the natural diversity of AML blasts, the best strategy to overcome AML lies upon the discovery of novel techniques for monitoring of the minimal residual disease (MRD), to identify possible recurring

clones at an early timepoint, together with biomarkers of early response and genomic profiling, as well as treatment approaches that can combine chemotherapy, immunotherapy, and molecular therapy.

1.6 Research aims and hypothesis

Developing a safe a CAR-T cell-based immunotherapy targeting AML is limited by the potential on-target off-tumour toxicity due to the expression profile of currently targeted tumour antigens such as CD33, CD123 and CLL-1. While these antigens are overexpressed on AML blasts, the healthy myeloid compartment including normal myeloid progenitors also expresses them, leading to the disruption of normal haematopoiesis and intolerable myeloablation by the current treatment strategies.

The overall aim of this project is focused on overcoming this limitation by exploring different approaches:

- Explore CD33–specific CAR T cells as a possible therapy, with the possibility of further engineering in order to reduce potential toxicity.
- Explore a new AML associated target with a more restricted expression profile, B7-H3, by assessing B7-H3–specific CAR T cells functionality in vitro as well as the potential hematopoietic toxicity of this approach.
- Explore a safer way of targeting AML-associated antigens by co-expressing a γδTCR and an AML-targeting chimeric costimulatory receptor (CCR) on αβ T cells. The aim is to separate the signal deriving from the TCR and the one deriving upon antigen recognition by the CCR, thus avoiding the potential on-target off-tumour toxicity caused by current strategies using second generation CARs.

The following research questions were investigated:

RESULT CHAPTER I:

1. Is a second generation anti-CD33 CAR effective towards CD33 expressing AML targets?
2. Is a second generation anti-B7H3 CAR effective towards B7H3-expressing AML targets?
3. Could a second generation anti-B7H3 CAR prevent potential hematopoietic toxicity?

RESULT CHAPTER II:

4. Could αβ T cells serve as better chassis for TCR and CAR transfer compared to γδ T cells?
5. Can the G115 tumour reactive γδTCR be expressed on αβ T and is it functional?
6. is the G115 tumour reactive γδTCR able to redirect the anti-tumour activity of αβ T cells towards a γδTCR sensitive target?

RESULT CHAPTER III:

7. Is it possible to co-express the anti-B7H3 CCR and the G115 tumour reactive γδTCR on αβ T cells?
8. Does the CCR confer increase functionality in presence of the antigen when the gdTCR is engaged?
9. Does separating the signal 1 (TCR) and signal 2 (CCR) in this specific system, prevent on-target off-tumour toxicity?

2 Material and Methods.

2.1 Molecular biology methods.

2.1.1 Plasmids

All plasmids used in this project were cloned into the backbone of SFG γ-retroviral vectors.

The SFG γ-retroviral vector contains a Moloney murine leukaemia virus (MMLV Ψ) signal peptide which directs the cell to package the gene of interest (GOI) into viral particles and long terminal repeats (LTR) regions, which consist of transcriptional enhancer and promotor sequences. They are both necessary for the insertion of the viral genome into the host DNA, through driving transcription and encapsulation of the inserted genome into viral particles, respectively (Vargas et al., 2016). Along with this is an ampicillin resistance gene, which enabled the positive selection of successfully transduced clones.

2.1.2 Cloning products

DNA gene fragments (gBlock), primers and all cloning strategies were designed using SnapGene software (version 4.2.11). All products were purchased from Integrated DNA Technologies (IDT).

2.1.3 Polymerase chain reaction (PCR)

To amplify selected DNA, Phusion DNA Polymerase from New England Biolabs (NEB) was used in a Polymerase Chain Reaction (PCR). Annealing temperature of the primers used was determined by the T_m calculator tool provided by NEB. The amplification reaction was carried out in a PTC-200 DNA Engine thermocycler with heated lids (MJ Research).

Components of the reaction and cycle of a standard PCR are as follow:

Reagent	Amount
5x Phusion HF Buffer	10 µL
10mM dNTPs	1 µL
10µM Forward Primer	2.5 µL
10µM Reverse Primer	2.5 µL
Templated DNA	0.1-1 ng
Phusion DNA Polymerase	0.5 µL
Nuclease Free Water	to 50 µL

Table 2.1 Standard 50 µL PCR reaction

PCR Step	Cycles	Temperature	Time
Initial Denaturation	1	98°C	30 seconds
Denaturation	15-25	98°C	5-10 seconds
Annealing		45-72°C	10-30 seconds
Extension		72°C	15-30 seconds/ kb
Final Extension	1	72°C	5-10 minutes
Hold	1	4°C	Forever

Table 2.2 Standard PCR cycle

2.1.4 Agarose gel electrophoresis, DNA gel extraction and purification.

Agarose gel consisting of 1% agarose dissolved in 1x TBE buffer and diluted SybrSAFE (1:10.000) was used to separate DNA fragments based on their molecular weight. DNA products were mixed with Purple loading dye 6x (NEB) and loaded on the gel. To identify the correct product, 1Kb or 100 bp ladder (NEB) depending on the size expected, were also loaded on the gel. Electrophoresis was run at 100-150V for 40min-1h and the band of interest was then cut under a blue light transilluminator, and DNA was extracted using the Wizard SV Gel & PCR Clean-Up kit (Promega) as per manufacturer's instructions.

2.1.5 Restriction digest and double digestion

Restriction digest using one or a combination of restriction enzymes was performed either for ensuring the identity of the plasmid/DNA of interest or before ligating a DNA fragment (insert) into a DNA vector. DNA was incubated with the appropriate restriction enzymes at 37 °C for 30 min.

Components of a 50 µL restriction digest reaction re as follow:

Reagent	**Amount**
DNA	1µg
10x Buffer	5µL
Restriction Enzyme	1µL each (10 units)
Nuclease Free Water	up to 50µL

Table 2.3 Standard 50 µL restriction digest

Restriction digest products were then run on a 1% agarose gel and DNA extracted as described in the previous section. The digested DNA fragments (insert and vector) were ligated at 1:1, 2:1, 3:1, and 5:1 ratio usually. The amounts of DNA needed was calculated using NEB's online tool NEBioCalculator. An extra reaction with vector DNA and no insert was included as control for self-ligation.

Component of a ligation reaction are as follow:

Reagent	**Amount**
Quick Ligase Reaction Buffer (2x)	10 µL
Vector DNA	100 ng
Insert DNA	calculated with NEB tool
Quick Ligase	1 µL
Nuclease Free Water	up to 20 µL

Table 2.4 Standard 20 µL ligation reaction

Ligation reactions were incubated on ice for 5 minutes at room temperature. Then, 2 µL of the reaction was used for bacterial transformation.

2.1.6 Bacterial transformation

Plasmid DNA was amplified in NEB® 5-alpha Competent *E. coli* -High Efficiency (New England Biolabs, UK)**.** For a single transformation**,** a 25 µl aliquot of *E. coli* was thawed on ice and 1 µl of plasmid or 2 µl of a ligation reaction were mixed with it. The mix was incubated on ice for 30 min and then heath-shocked at 42°C for 35 s to facilitate DNA intake. Bacterial cells were then transferred back to ice for at least 2 min and then cultivated in 250 µl of SOC outgrowth media for 40 min at

37°C, in a bacterial shaker (200 rpm). Bacterial suspension was then spread on agar plates with antibiotics (100 ug/mL ampicillin) with disposable loop spreader and left to grow colonies overnight at 37°C.

2.1.7 Mini- and Midi- DNA preparations

For a small-scale plasmid expansion (miniprep), single bacterial colonies were picked with a pipette tip and transferred into 5ml LB supplied with antibiotics (100 ug/mL ampicillin). Bacterial cells were expanded overnight in a shaker (200 rpm) at 37°C. Plasmid DNA was then extracted using QIAprep Spin Miniprep kit (Qiagen) as per manufacturer's instructions.

For a larger scale plasmid expansion (midiprep), individual bacterial colonies were picked and transferred to 120-150mL LB with antibiotics (100 ug/mL ampicillin) and cultured overnight in a bacterial shaker (200 rpm) at 37°C. Plasmid DNA in this instance, was extracted using Nucleobond Xtra Plasmid Purification Kit (Machery-Nagel) according to manufacturer's instructions. Isolated DNA was reconstituted in 20-30 µl (miniprep) or 200-300 µl (midiprep) ddH_2O and kept at -20 °C for long-term storage. Plasmid's identity was confirmed by restriction digest and sent off for sequencing.

2.1.8 DNA quantification and sequencing

DNA concentration was determined using a NanoDrop ND-100 UV/Vis spectrophotometer (Thermo Scientific) recording at a wavelength of 260/80nm.

The instrument was calibrated before every use. SourceBioscience DNA sequencing service (Nottingham, UK) was used to validate all DNA constructs and cloning products.

2.2 Cell culture methods

2.2.1 Cell culture

All cell work was carried out in a sterile environment and all the cells were cultured in humidified incubators at 37 °C with 5% CO_2. Cell lines went through a routine mycoplasma check and were used in experiments only after confirmed negative.

All the cells were cultured in complete media supplemented with 10% fetal calf serum (FCS) and 1% L-Glutamine (Sigma-Aldrich). When culturing primary cells, RPMI was also supplemented with 1% Penicillin/ Streptomycin (Sigma-Aldrich) and when culturing HEK293T, IMDM was also supplemented with 5mM HEPES. Table 2.5 include a list of cell lines used within this project and their culturing conditions.

Medium was changed when cells reached 80% confluency: growth rate is different within cell lines.

Splitting of suspension cell lines consisted in transferring adequate cell numbers to fresh medium, while for adherent cell lines extra steps to detach the cells were necessary. Cells were washed with phosphate buffered saline (PBS) and then detached with 0.05% Trypsin-EDTA for 2-3 min at 37 °C. Complete medium was then added to stop the enzymatic reaction and adequate cell numbers were resuspended in fresh media and transferred to a new tissue culture flask.

Adequate numbers were determined by cell counting. Cells were stained with 0.4% trypan blue solution (Gibco) and transferred to a Neubauer hemacytometer (Immune Systems) for cell counting under the microscope. Dying cell have impaired cell membrane and can take up the dye, therefore it's possible to count the lives cell by exclusion.

Cell line	Origin	Characteristic	Culture medium
HEK293T	Human embryonic kidney	Adherent	IMDM - 25mM Hepes
J.RT3-T3.5	Acute T cell leukaemia	Suspension	RPMI
Jurkat WT	Acute T cell leukaemia	Suspension	RPMI
Jurkat B7-H3	Acute T cell leukaemia	Suspension	RPMI
SUP-T1 WT	T-cell lymphoblastic lymphoma	Suspension	RPMI
SUP-T1 CD33	T-cell lymphoblastic lymphoma	Suspension	RPMI
Daudi	Burkitt's lymphoma	Suspension	RPMI
MV4-11	Myelomonocytic leukaemia	Suspension	IMDM
NOMO-1	Acute myeloid leukaemia	Suspension	RPMI
THP-1	Acute monocytic leukaemia	Suspension	RPMI
3T3	Embryonic fibroblast	Adherent	DMEM
3T3 B7H3	Embryonic fibroblast	Adherent	DMEM

Table 2.5 List of cell lines used within the project.

2.2.2 Freezing of cells

Cells were pelleted and resuspended in FCS + 10% Dimethyl sulfoxide (DMSO). They were then transferred to Thermo Scientific™ Mr. Frosty™ Freezing Container, which is designed to achieve a rate of cooling remarkably close to -

1°C/minute, optimal for cell preservation, and stored at -80 °C before being transferred to liquid nitrogen for long term storage.

2.2.3 PBMC isolation

Blood samples were obtained from heathy volunteers or leucocyte cones from NHS in accordance with local ethical approvals for culturing of live cells from healthy volunteers and patients. Samples from volunteers were transferred into Falcon tubes containing 0.5 ml EDTA to prevent blood coagulation. Blood samples were diluted in an equal amount of PBS and 30 ml of diluted blood was layered on 20 ml of Ficoll (Lymphopure™ - Biolegend). PBMCS were isolated by low density centrifugation for 20 min, at 300 x g, RT, with no breaks. This allow the formation of a gradient: PBMCs are in the interface between the Ficoll and the plasma.

The interface of PBMCs was collected in a new falcon and washed with PBS. Cells were then pelleted and resuspended in 5 ml of Ammonium-Chloride-Potassium (ACK) lysis buffer for 15 min. ACK Lysing Buffer was used for the lysis of red blood cells in the samples. The cells were then washed again, re-suspended in complete RPMI medium, and counted by Trypan blue exclusion.

2.2.4 Depletions – Negative selections

Depending on the experiment or the stage of it, negative selection using magnetic beads was performed either for depletion or for negative selection of a population of interest.

CD56 depletion

When expanding αβ T cells, natural killer (NK) CD56+ cells were depleted from the isolated PBMCs to avoid unspecific cell lysis of target cells. PBMCs were incubated with magnetic anti-CD56+ beads (Miltenyi) and then applied to a magnetic LD column in a MACS separator. While CD56+ cells are caught in the column, the flow through consisted in cell population depleted of CD56+ cells. Depletions to less than 3% of CD56+ cells were achieved regularly (data not shown).

αβ TCR depletion

After transducing αβ T cells to express G115 γδ TCR, αβ TCR depletion was performed in order to negatively select the population of interest: αβ TCR- γδ TCR+ αβ T cells. Cells were stained with a biotinylated anti-αβ TCR antibody following manufacturer's directions and then with anti-biotin magnetic beads. The cell suspension was then applied to a LD column in a MACS separator field and flow through of αβ TCR- cells was collected.

Monocytes isolation

Monocytes were isolated from PBMCs using the Pan-monocyte isolation kit (Miltenyi) according to the manufacturer's directions. PBMCs were incubated with a Biotin-antibody cocktail provided and then with anti-Biotin magnetic beads. Monocytes were separated by negative selection by applying the cells suspension to a LS column in a MACS separator. The monocyte-enriched flow through was washed in PBS and resuspended in complete RPMI and plated according to experimental plan. The success of all the depletions and selections were confirmed by flow cytometry (Figure 2.2).

Within this thesis, all the experiments using monocytes were conducted on allogeneic monocytes, if not stated otherwise.

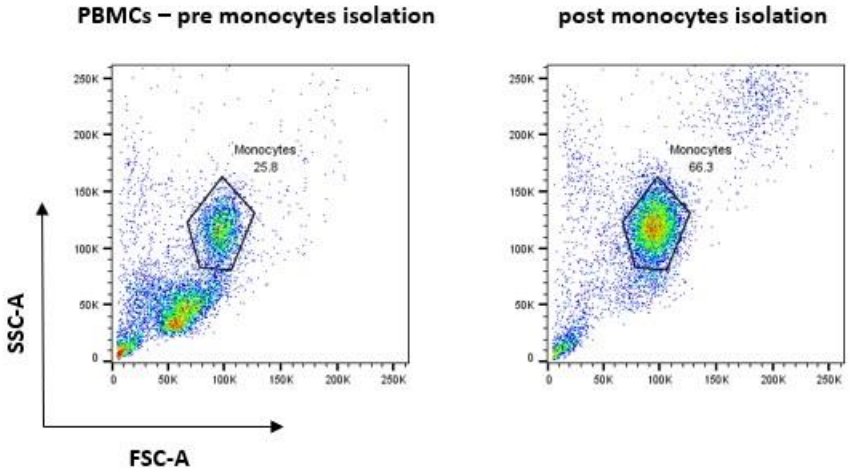

Figure 2.2 Monocytes isolation from whole blood. Monocytes were isolated from PBMCs using the Pan-monocyte isolation kit (Miltenyi) according to manufacturer's directions. PBMCs were incubated with a Biotin-antibody cocktail provided and then with anti-Biotin magnetic beads and separated by negative selection by applying the cells suspension to a LS column in a MACS separator. Representative plots show PBMCs before monocytes isolation and positively selected monocytes population post monocytes isolation. Monocytes population is identified here based on size (FSC-A) and granularity (SSC-A).

2.2.5 T cell activation and expansion

After PBMCs isolation, αβ and/or γδ T cells were activated and expanded depending on the experiment.

For αβ T cells activation, the PBMCs suspension was resuspended at 1 x 10^6 cells per ml in complete RPMI and supplemented with 0.5ug/ml anti-CD3 (OKT3) , anti-CD28 (Miltenyi Biotec) and 100 IU/ml Proleukin IL-2 (Novartis). Cells were then plated in a 24 well plate at 2 x 10^6/well.

For γδ T cells activation, the PBMCs suspension was resuspended at 2 x 10^6 cells per ml in complete RPMI and supplemented with 5 μM zoledronic acid (Actavis) and 100 IU/ml Proleukin IL-2. Cells were then plated in a T75 flask at 2 x 10^6/ml.

T cells were supplemented with 100 IU/ml Proleukin IL-2 every 2 days.

T cell expansion was assessed by flow cytometry prior to transduction or use as untransduced control in any experiment (Figure 2.3). αβ and γδ T cells were consistently expanded with 90-97% CD3+ αβTCR+ population in expanded αβ T cells and 70-90% CD3+Vδ2 population in expanded γδ T cells. . It is a normal observation to see a small remaining contaminant population following activation. In αβ expanded cells, these contaminant cells are sometimes a small population of γδ T cells (data not shown) and/or cells that have failed to expand but have not died; on previous occasions these contaminant cells have been characterised and they resulted in a small number of B cells and NK cells but very few remaining monocytes. This is also the case for expanded γδ T cells, where contaminants include also αβT cells (data not shown).

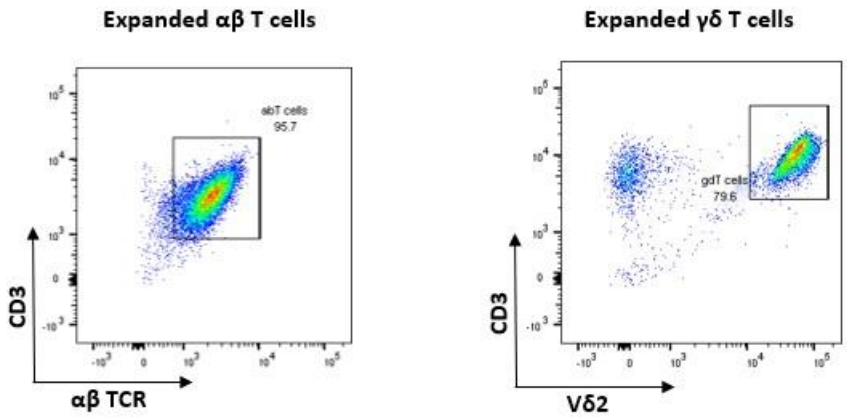

Fig 2.3 αβ and γδ T cell expansion. αβ and/or γδ T cells were activated and expanded depending on the experiment, after PBMCs isolation. αβ T cells were activated with 0.5ug/ml anti-CD3 (OKT3) and anti-CD28 (Miltenyi Biotec) while γδ T cells were activated with 5 μM zoledronic acid. Cells

were supplemented with 100 IU/ml Proleukin IL-2 and plated at a density of at 2 x 10^6 cells/well. T cell expansion was assessed by flow cytometry prior transduction. Viable CD3+ cells were gated on either αβ TCR or Vδ2.

2.2.6 γ-retrovirus production by transient transfection

SFG γ -retroviral plasmids containing a single stranded DNA GOI can be transiently expressed by transfection or stably produced in a cell line with the co-expression of packaging and envelope proteins. To ensure safety of the system, genes encoding the structural and replication proteins (Gag/Pol) and the envelope glycoproteins (Env) are delivered in separate expression vectors. The RD114 Env, which allow entry into human cells among other species, was used in this project. In fact, its target receptor, the neutral amino acid transporter (RDR), is widely expressed on human HSCs.

γ-retrovirus containing the plasmids of interest was produced by transient transfection of HEK293T cell line.

1.5x10^6 293T cells were seeded in a 100 mm^2 petri dish (Thermo Fisher) in 10 ml of complete IMDM. The following day, at 70% confluency, the cells were transiently transfected: correct confluency is important to achieve a good transfection efficiency.

For 1 reaction, 30 µl of Genejuice transfection reagent (Merk) was added to 470 µl of plain IMDM in a falcon and incubated at room temperature for 5 min. Packaging plasmids and plasmid containing the DNA of interest were then added to the mix and incubated for further 15 min. Volumes of plasmids were calculated based on the concentrations needed: see table 2.6. The total 500 µl reaction was

then added drop wise on the 293T cells after removing 4 ml of IMDM from the plate in order to produce a more concentrated γ-retrovirus and cells were cultured at 37 °C. γ-retroviral supernatant was harvested at 48 and 72h and pooled supernatant was spun down at 300 x g for 3 min to exclude any transferred HEK293T cells. The retrovirus was used on the same day for transduction of T cells. If more concentrated virus was needed only the 48h harvest was used for T cell transduction.

Plasmid	Concentration
Gag-pol	4.6875 µg
Env (RD114)	3.125 µg
γ-retroviral construct - DNA of interest	4.6875 µg

Table 2.6 Plasmid components for transfection reaction

2.2.7 T cell transduction

αβ T cell transduction was performed 48h post activation while in exponential growth phase. A day prior to it, 500 µl/well of Retronectin (Takara Bio) was plated in a non-tissue culture treated 24 well plate and stored at 4°C overnight: retronectin reagent facilitate transduction by co-localizing viral particles and target cells.

On the day of the transduction, αβ T cells were resuspended at $6x10^5$ T cells/ ml in complete RPMI and supplemented with Proleukin for a final concentration of 100 IU/ml. 500 µl of cell suspension was then plated on the pre-coated 24 well plate after removing Retronectin. αβ T cells to be transduced and αβ T cells to be

used as untransduced control, were handled the same way, therefore 1.5 ml of γ -retroviral supernatant or 1.5 ml of complete RPMI respectively, was transferred to each well for a total of 2ml/well. Spin inoculation was performed at 1000 x g for 40 min at room temperature and plates were then incubated at 37°C. Post 48h, cells were collected, washed, resuspended in fresh complete RPMI supplemented with Proleukin at 100 IU/ml and re-plated on tissue culture treated 24 well plate at $1x10^6$ T cells/ ml for a total volume of 2ml/well. Thy were rested for further 48 hours before assessing transduction efficacy by flow cytometry.

2.3 In vitro functional assays

2.3.1 Cytotoxicity assay

The cytotoxic activity of CAR T cells and γδTCR-transduced αβ T cells was assessed chromium (^{51}Cr) release assay.

Up to 1×10^6 target cells were labelled with 20 µl ^{51}Cr (PerkinElmer). After labelling, cells were washed with complete RPMI and resuspended at the desired concentration. 5,000 ^{51}Cr-labelled target cells were then cultured with increasing concentration of CAR T cells or γδTCR-transduced αβ T cells in 96 well V bottom plates (Greiner Bio-one), at 10:1, 5:1, 2.5:1 and 1.25:1 E:T ratio for 4h at 37°C.

The principle of this assay is based on the ability of cytotoxic T cells to kill their target by disrupting the integrity of the cell membrane thereby allowing the release of ^{51}Cr bound to protein from the target cells. Therefore, the amount of radioactivity

which is released in the supernatant is taken as an indicator of the amount of lysis which has occurred.

Target cells were also cultured alone and with 1% Triton-X-100 to assess respectively background and maximum killing. Post incubation, cells were spun down and 50µl of supernatant was transferred into Isoplate-96 HB plates (PerkinElmer). Then, 150 µl of scintillation liquid (Optiphase Supermix, PerkinElmer) was added to each well and plates were incubated in the dark overnight at room temperature. ^{51}Cr release counts were acquired the day after using a 1450 MicroBeta TriLux scintillation counter (PerkinElmer).

Lysis of the target cell lines was calculated based on the following formula:

$$\frac{(\text{Experimental } ^{51}\text{Cr release} - \text{Spontaneous } ^{51}\text{Cr release}) \times 100}{(\text{Maximum } ^{51}\text{Cr release} - \text{Spontaneous } ^{51}\text{Cr release})} = \% \text{ Lysis}$$

2.3.2 Quantification of cytokines by ELISA

Enzyme Linked Immunosorbent Assay (ELISA) was used to detect and quantify cytokines produced by T cells. IL-2 and IFN-γ were detected in supernatant collected from 18 hours co-culture of effector and target cells. Co-cultures were usually set up on day 6-7 post-transduction in a 48 well plate at 1:1 E:T ratio for a total of 0.5×10^6 cells/well.

ELISA was performed according to manufacturer's direction using an ELISA Max Deluxe kit (Biolegend): 96 well ELISA plates were coated with human IL-2 or human IFN-γ capture antibodies and incubated at 4°C overnight. The following day, the plates were blocked to prevent unspecific binding and then samples as well as

standards for IL-2 and IFN-γ were loaded on the plates, followed by detection antibodies and Avidin-HRP.

Plates were analysed by reading the absorbance at 450 nm on a microplate reader (Tecan) and corrected by subtraction of background control values. Cytokines concentration was determined by correlation with a standard curve.

2.3.3 Proliferation assay

2.3.3.1 7 days short-term proliferation assay

In results chapter I and II, 7 days co-cultures (unless stated otherwise) were set up usually on day 6-7 post transduction, to investigate effector cell (T cells) proliferation in response to a specific stimulus.

In order to track the proliferation, effector cells were labelled with CellTrace Violet Proliferation kit (ThermoFisher Scientific) which allowed to monitor distinct generations of proliferating cells by dye dilution: 1 µl of CellTrace stock solution was diluted in 1 ml of PBS at a working concentration of 5 µM and was used to label up to $1x10^7$ cells. Cells were incubated in the dark at room temperature for 20 min and then quenched with complete RPMI media by adding 5x the stain volume and incubated for another 5 mi. Cells were then washed, counted and ready to be used in the assay.

Effector cells were then co-cultured with target cells in tissue culture treated 48 well plates at 1:1 E:T ratio for a total of $0.5x10^6$ cells/well in 0.5 ml of complete RPMI and incubated at 37 °C for 7 days. No IL-2 was added to the co-cultures. Effectors were also culture with no target in order to detect any background activity.

Co-cultures were monitored over 7 days and media refreshed if needed by replacing half of the supernatant in each well with fresh complete RPMI, always maintaining the same volumes among each condition. On Day 7, cells were collected, and proliferation was assessed by flow cytometry.

In order to quantify the proliferation, the change in MFI, referred to as the delta MFI (ΔMFI) of CellTrace violet between the experimental condition (e.g. CAR T cell cultured with a specific target) and the untransduced T cells cultured with the same target was determined. While CellTrace dilution give a qualitative information about the proliferation, CountBright Absolute Counting Beads (ThermoFisher) were used to quantify the cell numbers of the populations of interest, when applicable. In some experiments, where it was not possible to label the effector cells with CellTrace violet dye, only CountBright Absolute Counting Beads (ThermoFisher) were used to assess the proliferation. When this was the case, this is stated in the relevant results section.

2.3.3.2 7 days proliferation + 18h restimulation assay

In results chapter III, untransduced αβ T cells and γδ TCR, γδ TCR-TE9-28 and γδ TCR-TE9-41BB transduced αβ T cells were co-cultured with specific targets and effector cells expansion as well as their ability to produce cytokines in response to a specific stimulus was investigated. Effector cells were not labelled with CellTrace Violet in this instance.

Target cells were treated with the monoclonal anti- BTN3A antibody (mAb) 20.1 antibody (untreated cells were used as control). Following manufacturer's direction, 1ug was used to stain up to 10^8 cells in 100ul volume; cells were

incubated at 37 °C for 1h and then wash twice. Desired number of target cells were counted, pelleted, and resuspended in 3-5 ml of complete RPMI, and cells were irradiated at 40 grays (Gy) with irradiator IBL 437C (94-468) in order to prevent target cell growth which can be a confounding factor when studying effector cells expansion and/or proliferation. Post irradiation, target cells were washed and resuspended at required concentrations for plating.

Effector cells were then co-cultured with target cells in tissue culture treated 48 well plates at 1:1 E:T ratio for a total of $0.5x10^6$ cells/well in 0.5 ml of complete RPMI and incubated at 37 °C for 18h. No IL-2 was added to the co-cultures. Again, Effectors were also cultured with no target in order to detect any background activity. Post 18 hours, 200ul of supernatant was collected without disturbing effector and target cells in the co-culture and cytokine quantification was performed by ELISA as explained in section 2.3.2. The supernatant volume that was collected from each well, was replaced by the same volume of fresh complete RPMI and co-cultures were incubated again at 37 °C for 7 days. Again, no IL-2 supplement was provided to the cells.

After 7 days, supernatant from the co-culture was replaced with fresh complete RPMI containing the same stimulus (antigen +/- target cells untreated or treaded with 20.1 monoclonal antibody) that was provided when the co-cultures were set up. While the same stimulus in terms of antigen and 20.1 treatment, was provided, targets cells were not irradiated in this instance, as they were labelled with CellTrace violet for detection in flow cytometry. In order to achieve this, 250µl of supernatant was discarded from each well in the co-culture, without disturbing the effector and target cell at the bottom of the well, and it was replaced by the same volume of fresh complete RPMI containing CellTrace violet labelled untreated and

20.1 treated targets. The same number as the initial seeding density of target cells were added to the co-cultures ($1.25x10^5$ targets/well). The co-cultures were then incubated for further 18 hours at 37°C. After 18 hours incubation post re-stimulation, 300ul supernatant was collected to quantify IL-2 and IFN-γ by ELISA, while the remaining volume containing effector and target cells were collected for flow cytometry analysis. Count Bright Absolute Counting Beads were used to detect T cells numbers and loss of Cell Trace- labelled live target cells.

2.3.4 Clonogenic assay

Clonogenic assay, also known as colony forming cell (CFC) assay, colony forming unit (CFU) assay and methylcellulose assay] is an in vitro assay used in the study of hematopoietic stem cells. The assay is based on the ability of individual hematopoietic progenitor cells called colony-forming units (CFU) to proliferate and differentiate into colonies in a semi-solid media in response to cytokine stimulation. The colonies formed can be enumerated and characterized according to their unique morphology. This assay was used in this project to investigate colony formation from cord blood (CB) and NOMO-1 leukemic cells after they were treated with the TE9-CD8-28ζ CAR T cells. Untransduced T cells were used as control.

H4434 Classic Methocult media (STEMCELL Technologies) was used in this assay as semi-solid matrix: it contains rh SCF (stem cell factor) , rh GM-CSF (Granulocyte macrophage colony-stimulating factor), rh IL-3, rh EPO and allows the growth of CFU-E (Erythroid progenitor cells), BFU-E (burst-forming unit-erythroid), CFU-GM (Granulocyte and/or macrophage progenitor cells) and CFU-GEMM (multi-potential progenitor cells) in CB as well as leukemic colonies.

Prior to the experiment, Methocult media was aliquoted in Sterilin™ 7 ml Bijou (Thermo Scientific) with 2 ml/aliquot and stored at -20 °C. Effector cells (untransduced T cells and TE9-CD8-28ζ CAR T) and target cells (CB and NOMO-1) were co-cultured in a tissue culture treated 48 well plate at 5:1 E:T ratio for 18 hours at 37°C.

Post incubation, the cells in each co-culture condition was collected separately and washed in Iscove's MDM with 2% FBS (STEMCELL Technologies) which is the recommended media for preparing and washing samples for CFU assay. Cells were then resuspended again in Iscove's media at the desired concentration calculated estimating to have 20.000 cells of CB in 40 µl of cell suspension and 2.000 cells of NOMO-1 cells in 40 µl of the cell suspension, if any lysis did not occur. 40 µl of cell suspension was then transferred to one 2 ml Methocult aliquot and vigorously shaken in order to distribute evenly the cells in the Methocult. 1 ml of Methocult containing the desired number of cells (10.000 for CB and 1.000 for NOMO-1) were then plated in a well of a tissue culture treated 6 well plate using a 16 Gauge Blunt-End Needle (STEMCELL Technologies).

These seeding densities were chosen in order for NOMO-1 and CB conditions to be as comparable as possible, with the approximation that only 1% of cells from the CB are hemopoietic progenitors colony forming units. Other densities were tested but they either were crowding the well too much or did not produce enough colonies to be quantified properly – data not shown.

The plates were surrounded by PBS to maintain high humidity levels and prevent drying up of the Methocult and they were incubated at 37°C for 14 days. Numbers and morphology of the colonies were assessed by microscopy on day 14 and then,

in order for the colonies to show up on a photograph, the colonies were stained dark purple with p-iodonitrotetrazolium violet (Sigma).

2.4 Flow cytometry

2.4.1 Flow cytometry for detection of surface antigens

Flow cytometry uses fluorophore conjugated antibodies to detect the expression of cell surface or intracellular molecules. It rapidly analyses single cells or particles as they flow past multiple lasers inducing light scatter and multiple fluorescence emissions. The visible light scatter is measured in two different directions, forward scatter (FSC) which give indication on the cell size and side scatter (SSC) which indicates the internal complexity or granularity of the cell while fluorescence emissions provide information on the fluorescence signal intensity.

To detect surface antigens, cells were washed in PBS and incubated for 10 min at 4°C with Fc block reagent (Miltenyi Biotec) to prevent unspecific binding of Fc-γ receptors on the cell surface and with a viability dye (Zombie NIR – Biolegend) to exclude dead cell, following manufacturer's directions. Cells were then washed and incubated with a cocktail of antibodies of interest depending on the experiment following manufacturer's direction regarding optimal concentration. All antibodies that have been used previously in the laboratory have been tittered for optimal concentration, therefore results from previous titering were used for determining the right concentrations; when using new antibodies, however, they were titered prior to use in the experiments.

When staining with fluorochrome-conjugated antibodies, cells were incubated for 30 min at 4°C. When staining with un-conjugated primary antibody followed by a fluorochrome-conjugated secondary antibody, an extra step of staining was included. Cells were firstly incubated with the primary antibody for 45 min at 4°C and after washing off whatever unbound, it was stained with the secondary for 30 min at 4°C.

Cells were finally washed off of unbound antibodies and resuspended in 250 µl of PBS for flow cytometry analysis. If cells were to be analysed the day after, cells were resuspended with 100 µl Fixation buffer (Biolegend) for 10 min at 4°C and washed with PBS before. Cells were analysed on a BD LSRII flow cytometer (BD Bioscience). For absolute cell counting, in the experiments where stated, CountBright Absolute Counting Beads were added to the samples shortly before analysis.

In all the experiments OneComp eBeads compensation beads (ThermoFisher) were used for single colour controls to correct fluorescence spill over and Fluorescence-Minus-One (FMO) controls were included as needed to set accurate gatings. The acquired data were exported as FCS files and were analysed using FlowJo 10.7.1 software.

2.4.2 Phospho-Flow Cytometry

Flow cytometry also offers the possibility to investigate activation state and measure signalling at a specific time point in individual cells by staining for signalling molecules and phosphorylated proteins (Phospho-Flow Cytometry). The

staining method is slightly different from common intracellular staining as it requires for the cells to be rapidly fixed to avoid dephosphorylation and ensures the preservation of the cellular state at the time of fixation and strong permeabilization methods are required to ensure access to the intracellular compartment.

Phospho-Flow assay assess the signalling upon T cell activation by using stimulatory primary antibodies and then cross-liking with a secondary antibody to allow the formation of an immunological synapse-like structure mimicking the condition of a physiological activation. This assay was previously optimized in the lab, and it was used to assess the signalling mediated by the G115 γδTCR. The media of effectors G115 γδTCR transduced αβ T cells and untransduced T cells in culture is replaced the night prior to the assay with X-VIVO15 serum-free media (Lonza) as the FCS present in the original complete RPMI may induce non-specific stimulation of signalling routes involved in cellular activation.

The day of the assay all the steps are performed on ice and using pre-chilled reagents in order not to induce any unwanted activation and all steps were performed very quickly and precisely as the assay is time sensitive. . Effector T cells were washed in cold PBS and then incubated with Fc block reagent and viability dye for 10 min at 4°C. Cells were washed and resuspended in serum free media X-VIVO15. All samples were kept on ice.

Cells were stimulated with either anti-CD3 (OKT3) or anti-Vδ2 (B6) primary mouse anti-human antibodies following manufacturer's direction for optimal concentrations: the stimulatory antibodies were loaded to the samples on ice and incubated for 10 min. Unstimulated samples in which cells were not incubated with primary antibodies were included as controls. Cells were then washed in cold X-

VIVO15 media in a pre-chilled centrifuge at 4°C and stained with a donkey anti mouse secondary antibody to induce crosslinking, following manufacturer's direction for concentrations. This incubation step was performed on a heat block set to 37°C and the reaction was stopped by adding fixation buffer at time 0s and time 360s. Unstimulated samples in which cells were not incubated with primary antibodies were included as controls.

The cells were then incubated for at least 20 min at room temperature and then permeabilized adding 1ml of cold methanol to each sample and incubated for 20 min 4°C. The cells were washed twice and intracellular staining using anti- pZap70-PE, anti-pERK-Pacific blue, and anti-Nf-KB-Alexa Fluor488 was performed. The antibodies were added to the samples following manufacturer's direction for concentrations and the cells were incubated for 45 min at 4°C. Post incubation, cells were thoroughly washed and resuspended in PBS for flow cytometry analysis.

2.5 Statistical analysis

Analyses were performed using GraphPad Prism version 9.0 (GraphPad, San Diego, CA). Data is expressed as mean ± SD. Error bars, where displayed, indicate the standard deviation of data from replicate experiments unless stated otherwise.

Statistical tests used for the in vitro assays are stated in the figure legends. T-tests were used for comparison of two groups or conditions, while Analysis of variance (ANOVA) was used to determine statistical significance for multiple comparisons. Significance is represented by: * $p \leq 0.05$, ** $p \leq 0.01$, *** $p \leq 0.001$, **** $p \leq 0.0001$.

3 RESULTS I - Characterization of CD33 and B7-H3–specific CAR T cells targeting AML

3.1 Introduction

The purpose of this first chapter is to evaluate CD33–specific CAR T cells and B7-H3–specific CAR T cells as potential therapies to target AML.

In this results chapter we assessed the surface expression of CD33 and B7-H3 in a panel of tumour cell lines and then compared the in vitro activity of a CD33–specific CAR and a B7-H3–specific CAR, with different stalk and transmembrane domains as well as evaluated the potential hematopoietic toxicity of the CAR chosen as lead based on the results of the functional assays performed.

3.2 Cloning of CD33 and B7-H3 CAR constructs

In order to investigate the in vitro activity of a CD33–specific CAR and a B7-H3–specific CAR, four second generation CARs were compared (Figure 3.1):

- CD33-CH2CH3 stalk-28tm-CD28-ζ
- CD33-CD8 hinge-CD8tm-CD28-ζ
- TE9-CH2CH3 stalk-28tm-CD28-ζ
- TE9-CD8 hinge-CD8tm-CD28-ζ

Second generation CD33-CH2CH3 stalk-28tm-CD28-ζ CAR targeting CD33 and TE9-CD8hinge-CD8tm-CD28-ζ CAR targeting B7-H3 were previously generated by other members of our team.

The CD33-CH2CH3 stalk-28tm-CD28-ζ CAR was originally supplied by Martin Pule as part of an on-going academic collaboration. Subsequently the CAR sequence was re-derived via synthetic gene block.

The CD33-CH2CH3 stalk-28tm-CD28-ζ CAR expressing plasmid comprised of:

- RQR8 sequence preceding the CAR sequence, encoding for a RQR8 molecule, which is co-expressed with the CAR for selection and safety purposes (Philip et al., 2014). RQR8 is a suicide gene, it contains a CD20 epitope which is recognised by the anti-CD20 antibody Rituximab, the action of which is to delete the RQR8+ cells. This safety switch is important for clinical translation purposes. Moreover, RQR8 contains a 16 amino acid epitope recognised by the anti-CD34 antibody clone QBend10 and which can be used for detection and/or selection of RQR8+ cells.
- FMD-2A self-cleaving peptide separating the RQR8 from the ScFv and allow equimolar expression of both constructs on the surface of T cells.
- Anti-CD33 ScFv was derivatised from the monoclonal antibody component of the clinically employed human anti-CD33 mAb Mylotarg (Gemtuzumab ozogamicin).
- Fc stalk or Fc IgG derived CH2CH3 spacer, composed by the constant heavy chain domains CH2 and CH3 from IgG4. It is longer and more flexible compared to a CD8 hinge spacer and has better access to binding epitopes proximal to the target cell membrane. The Fc stalk contains mutations to prevent unintended binding of bystander IgG Fcγ receptors on innate immune cells (Hombach et al., 2010; Hudecek et al., 2015).
- CD28 transmembrane.

- CD28 co-stimulatory endodomain.
- CD3-ζ signalling domain.

The TE9-CD8hinge-CD8tm-CD28-ζ CAR, was originally generated by a former member of the team, Kathleen Birley, as part of her project.

The TE9-CD8hinge-CD8tm-CD28-ζ CAR expressing plasmid comprised of:

- RQR8 sequence.
- T2A self-cleaving peptide separating the RQR8 from the ScFv.
- TE9-scFv: originally, 17 unique anit-B7-H3 ScFv were identified from an existing phage display library. These were tested against recombinant and cell bound B7-H3 and five ScFv were taken forward into Chimeric antigen receptor format. Of these, TE9 showed superior cytokine production and was selected as lead.
- CD8 hinge spacer and transmembrane: the CD8 hinge derives from the human CD8α chain, and it is a shorter and less flexible non-IgG–based spacer, naturally lacking FcγR binding activity.
- CD28 co-stimulatory endodomain.
- CD3-ζ signalling domain.

Starting with these two plasmids, we then generated TE9-CH2CH3 stalk-28tm-CD28-ζ and CD33-CD8hinge-CD8tm-CD28-ζ by cloning the CH2CH3stalk-28tm into the original TE9 CAR and the CD8hinge-CD8tm into the original CD33 CAR.

Hence, the following four constructs were available for cross comparison studies:

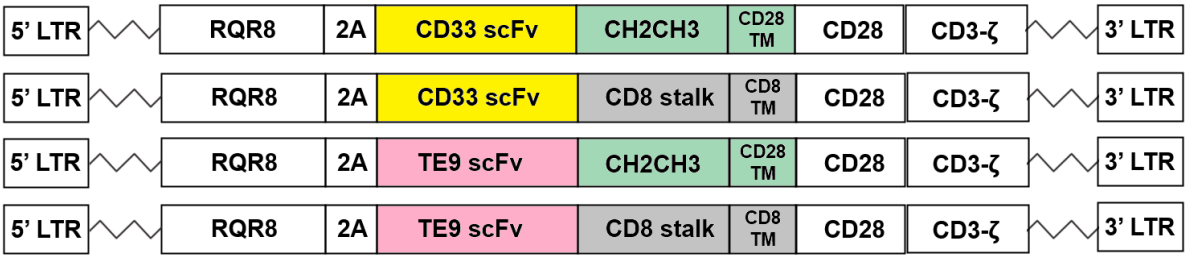

Fig 3.1 Design of second-generation CAR constructs targeting CD33 and B7-H3. SFG gamma-retroviral vectors encoding for second generation anti-CD33 and anti-B7-H3 CARs with either CH2CH3 stalk-CD28 transmembrane or CD8 stalk-CD8 transmembrane, were generated by cloning as described above. Each construct contains long terminal repeats (LTR) of the Moloney murine leukaemia virus (MoMLV), responsible for driving the transcription of the gene of interest.

3.3 AML-associated CD33 and B7H3 antigens expression on tumour cell lines.

3.3.1 Surface expression of CD33 in a panel of human cell lines.

In order to investigate the in vitro activity of the CD33–specific CAR T cells, CD33 expression on isogenic cell lines SUP-T1 WT and SUP-T1 CD33, and on AML cell lines MV4-11, NOMO-1, THP-1 was determined, in order to validate their use as potential therapeutic targets. CD33 surface expression was determined by flow cytometry through median fluorescence intensity (MFI). In order to do so, cells were stained with a commercially available anti-human CD33-APC antibody from Biolegend, following manufacturer's directions (blue histogram). Unstained cells were used as negative control (red histograms).

No surface expression of CD33 was detected on SUP-T1 WT cells (MFI=140) while SUP-T1 CD33 cells expressed high levels of CD33 on their surface (MFI=113439) (Figure 3.2A). SUP-T1 WT and SUP-T1 CD33 were used respectively as negative and positive control cell lines for the CD33–specific CAR T cells.

CD33 expression at various levels was detected on AML cell lines MV4-11, NOMO-1, and THP-1, with MFI of 21010, 16638, 3785 respectively (Figure 3.2B).

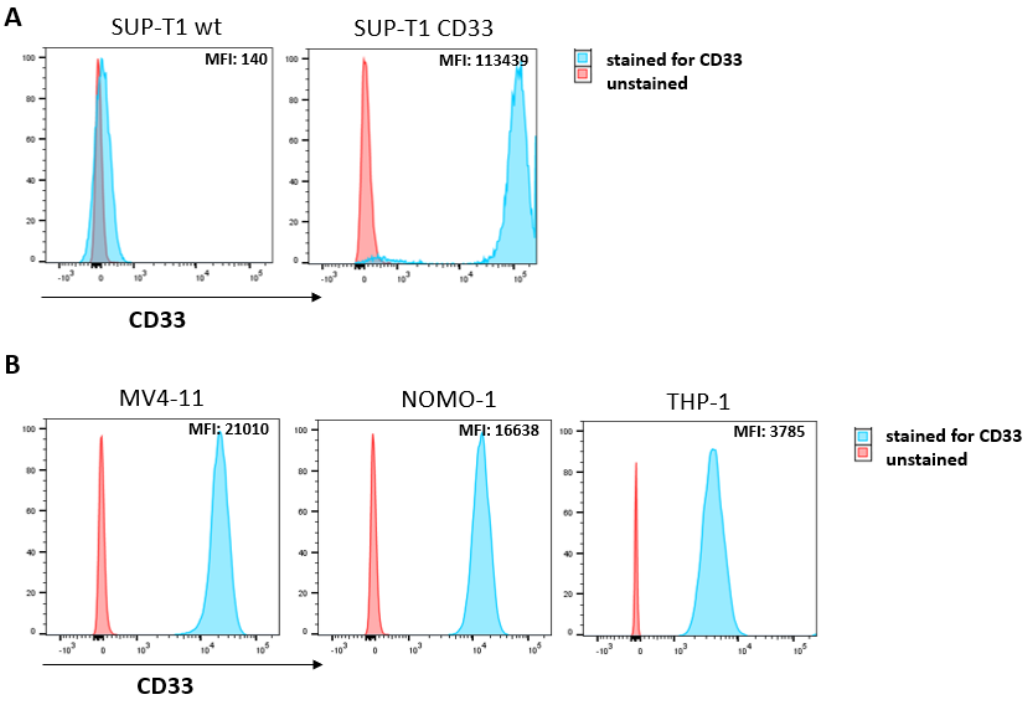

Figure 3.2 Surface expression of CD33 in a panel of human cell lines. Surface CD33 expression was assessed through median fluorescence intensity (MFI) by flow cytometry, using an anti-human CD33-APC antibody (blue histograms). Unstained cells were used as control (red histograms). Representative histograms of CD33 detection on isogenic cell lines SUP-T1 wt and SUP-T1 CD33 (A) and on MV4-11, NOMO-1, and THP-1 AML cell lines (B).

3.3.2 Surface expression of B7-H3 in a panel of human cell lines.

In order to investigate the activity of a B7-H3–specific CAR T cells, TE9 CARs, B7-H3 expression on a panel of human cell lines was also determined through median fluorescence intensity (MFI) by flow cytometry.

Isogenic cell lines Jurkat WT and Jurkat B7-H3, and AML cell lines MV4-11, NOMO-1, THP-1 were stained with a commercially available anti-human CD276

(B7-H3)-APC antibody from Biolegend, following manufacturer's directions (blue histogram). For consistency unstained cells were used as negative control (red histograms, however, isotype controls were used when testing a new antibody or to avoid any inconsistency.

Jurkat B7-H3 cells expressed higher levels of B7-H3 on their surface (MFI=14618), while no notable surface expression of B7-H3 was detected on Jurkat WT cells (MFI=391) (Figure 3.3A). Jurkat WT cells were also stained with an isotype control to investigate the slight shift in MFI that was observed between the stained sample and the unstained control: the staining with the anti-B7-H3 antibody mostly overlaps with the staining with the isotype control (Figure 3.3B) and represent either negative or very low-level staining. The staining that we observe, might be off target against another antigen or against extremely low level B7H3. However, the Jurkat WT were found to have such consistently low staining that they were used as a negative control in our experiments.

Different levels of B7-H3 were detected on AML cell line MV4-11, NOMO-1, and THP-1, with MFI of 4246, 6981, 2723 respectively (Figure 3.3C).

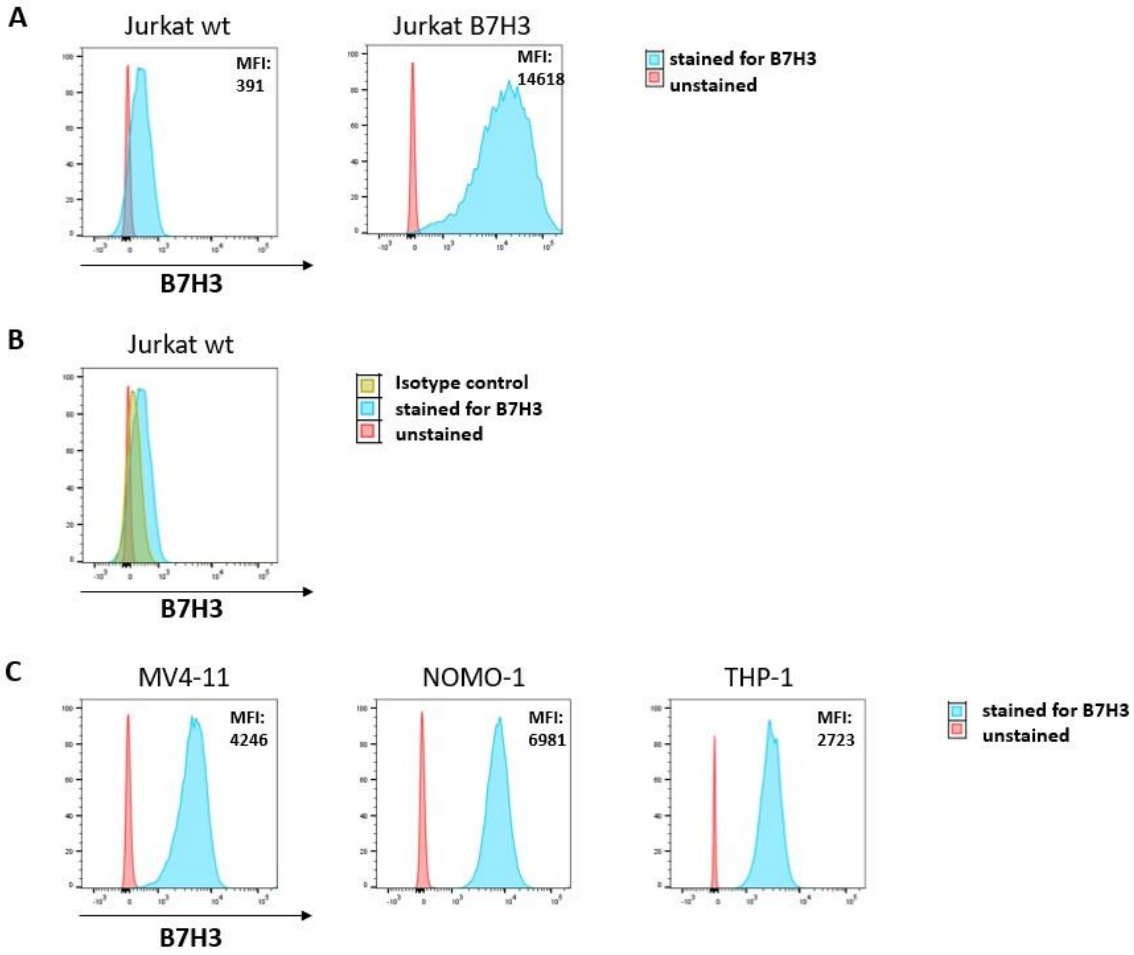

Figure 3.3 Surface expression of B7-H3 in a panel of human cell lines. Surface B7-H3 expression was assessed through median fluorescence intensity (MFI) by flow cytometry, using anti-human CD276 (B7-H3) – APC antibody (blue histograms). Unstained cells were used as control (red histograms). Representative histograms of B7-H3 detection on isogenic cell lines Jurkat wt and Jurkat B7-H3 (A) and on AML cell lines MV4-11, NOMO-1, and THP-1 (C). Isotype control (green) is shown as additional control in Jurkat wt (B).

3.4 Investigation of CD33–specific and B7-H3–specific CAR T cells activity in vitro.

After assessing the surface expression of CD33 and B7-H3 on a panel of tumour cell lines and validating their use as a potential therapeutic target, the next aim of

this research chapter was to investigate the in vitro activity of the CD33–specific CAR T cells and the and the B7-H3–specific TE9 CAR T cells.

Their activity was studied by assessing their ability to lyse targets expressing their cognate antigen, and by the ability to produce cytokines and proliferate in response to those targets. In order to do so, the following CAR constructs were used in different functional assays:

1. CD33-CH2CH3 stalk-28tm-CD28-ζ (CD33-Fc-28ζ in short)
2. CD33-CD8hinge-CD8tm-CD28-ζ (CD33-CD8-28ζ in short)
3. TE9-CH2CH3 stalk-28tm-CD28-ζ (TE9-Fc-28ζ in short)
4. TE9-CD8hinge-CD8tm-CD28-ζ (TE9-CD8-28ζ in short)

In the following experiments, untransduced (UT) T cells were used as a negative control. We are however aware that T cells transduced with an irrelevant CAR, such as an endodomain truncated version of the CARs that we are testing, or a CAR with the same backbone as the CARs under investigation but targeting an irrelevant antigen, would have been a stronger negative control compared to untransduced T cells as cells would be subjected to comparable stress. This will be considered for further investigations.

3.4.1 Expression of CD33 and TE9 CARs on primary human T lymphocytes.

In order to investigate the in vitro activity of the CD33 and TE9 CAR T cells, peripheral blood mononuclear cells (PBMCs) were isolated from healthy donors and activated αβT cells were transduced on day 3 with retroviral supernatant produced by triple transfection of 293Ts to express CD33-Fc stalk-28-ζ , CD33-CD8 stalk-28-ζ, TE9-Fc stalk-28-ζ and TE9-CD8 stalk-28-ζ CAR constructs.

Transduction efficacy was assessed by flow cytometry by directly staining the CD33 CARs with a Biotinylated Human Siglec-3 / CD33 Protein followed by Streptavidin-PE secondary staining and staining the TE9 CARs with B7-H3-Histag protein and a secondary anti-His-APC antibody. Figure 3.4A shows representative plots illustrating the gating strategy to identify CD3+CAR+ cells after exclusion of doublets and dead cells. Live cells were then gated on CD3 and αβTCR and expression of the CAR was assessed in the CD3+ αβTCR+ population. Figure 3.4B shows the transduction efficiency of T cells expressing CD33-Fc stalk-28ζ, CD33-CD8 hinge-28 ζ, TE9-Fc stalk-28ζ and TE9-CD8 hinge-28 ζ CARs, as mean of 3 independent donors. The transduction efficiency ranged from 29±6% (mean±SD, n=3) to 36±3% (mean±SD, n=3) and no significant differences were observed between the CAR expression levels in the four constructs.

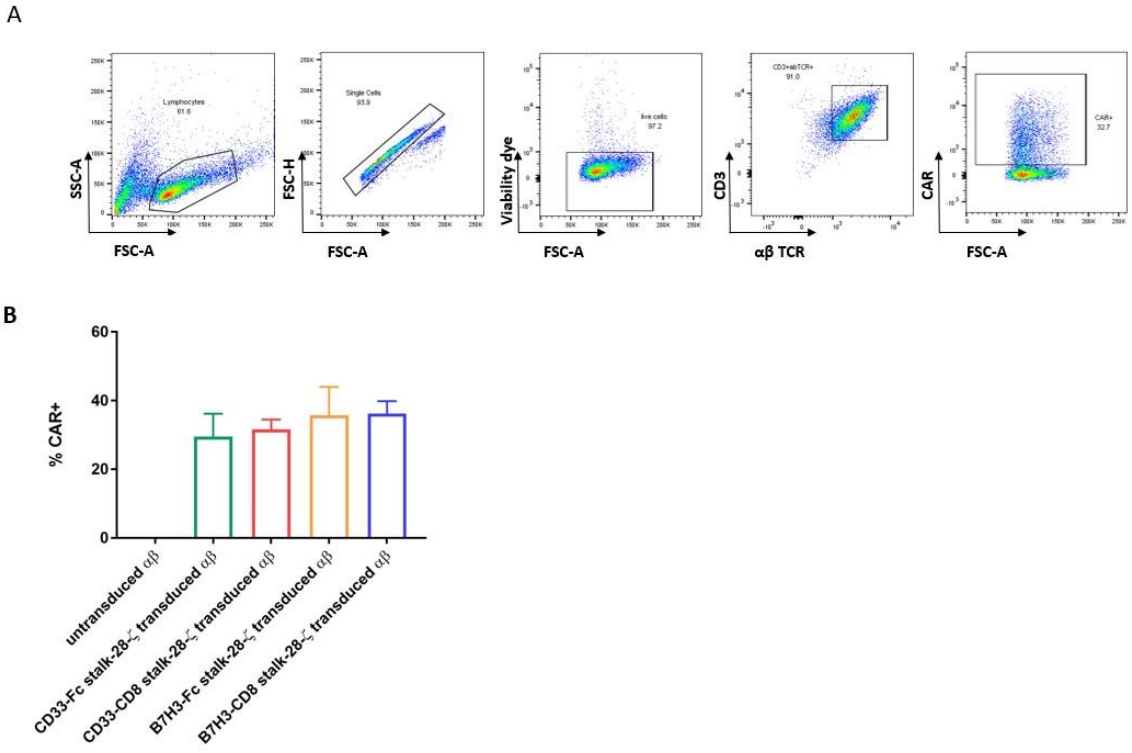

Figure 3.4 Transduction efficiency of CD33 and TE9 CAR constructs on primary αβ T cells. Activated αβ T cells were transduced with retroviral supernatant to express CD33-Fc stalk-28-ζ , CD33-CD8 stalk-28-ζ, TE9-Fc stalk-28-ζ , TE9-CD8 stalk-28-ζ CAR constructs. Transduction

efficacy was assessed by flow cytometry by directly staining the CD33 CARs with a Biotinylated Human Siglec-3 / CD33 Protein followed by Streptavidin-PE staining and the TE9 CARs with B7-H3-Histag protein and a secondary anti-His-APC antibody. (A) Representative plots showing the gating strategy to identify CD3+CAR+ cells after exclusion of doublets and dead cells. (B) Mean CAR expression ±SD (n=3 independent biological replicates). No statistically significant differences were found between CAR expression levels as determined by one-way ANOVA followed by Tukey's post-hoc analysis.

3.4.2 Cytotoxic activity of CD33 and TE9 CAR T cells towards reference cell lines.

After confirming the expression of the CARs on the T cell surface, the cytotoxic activity of CD33-Fc-28ζ, CD33-CD8-28ζ, TE9 Fc-28ζ and TE9-CD8-28ζ CAR T cells towards reference cell lines expressing their cognate antigen, was assessed by a 4h chromium (^{51}Cr) release assay as described in the material and methods section (Figure 3.5).

In this assay, target cells are pre-labelled with the radioisotope and then incubated with the effector cells. The assay relies on the ability of cytotoxic T-cells to kill their target cells by disrupting the integrity of the cell membrane thereby allowing the release of protein bound ^{51}Cr. The amount of radioactivity which is released in the supernatant is taken as an indicator of the amount of lysis which has occurred. Effector cells were incubated with target cells at ratios of 10:1, 5:1, 2.5:1 and 1.25:1 for 4 hours and killing compared to background cell death of the target cells with no effector cells and 100% cell death calculated by incubating cells with Triton X-100 to ensure 100% cell lysis.

CD33-Fc-28ζ and CD33-CD8-28ζ expressing T cells, were co-cultured with SUP-T1 wt and SUP-T1 CD33. As shown in figure 3.5A, both CD33-Fc-28ζ and CD33-CD8-28ζ expressing T cells did not lyse SUP-T1 WT as the ^{51}Cr release is minimal

and comparable to the ^{51}Cr release by the untransduced T cells co-cultured with the same target. In contrast both CD33-Fc-28ζ and CD33-CD8-28ζ expressing T cells show antigen specific and dose dependent killing of SUP-T1 CD33, as ^{51}Cr release is significantly higher at E:T ratio of 10 compared to untransduced T cells co-cultured with the same target ($p<0.0001$).

No significant differences were detected between the cytotoxic activity of CD33-Fc-28ζ and CD33-CD8-28ζ T cells at any E:T ratio. The mean % of lysis is between 46% for CD33-Fc-28ζ transduced T cells and 49% for CD33-CD8-28ζ transduced T cells, at 10:1 E:T ratio. In the same way, TE9-Fc-28ζ and TE9-CD8-28ζ expressing T cells, were co-cultured with Jurkat wt and Jurkat B7-H3. As shown in figure 3.5B, both TE9-Fc-28ζ and TE9-CD8-28ζ expressing T cells did not lyse Jurkat WT. Indeed, the ^{51}Cr release is minimal and comparable to the one of the untransduced T cells co-cultured with the same target.

When co-co-cultured with antigen positive Jurkat B7-H3, however, TE9-CD8-28ζ T cells demonstrated antigen dependent killing of Jurkat B7-H3, as ^{51}Cr release is significantly higher compared to untransduced T cells co-cultured with the same target ($p<0.0001$). At 10:1 E:T ratio, cell lysis of Jurkat B7-H3 is 40% (mean).

Interestingly, TE9-Fc-28ζ T cells does not seem to kill Jurkat B7-H3. No significant difference can be detected when compared to % of cell lysis from the untransduced control.

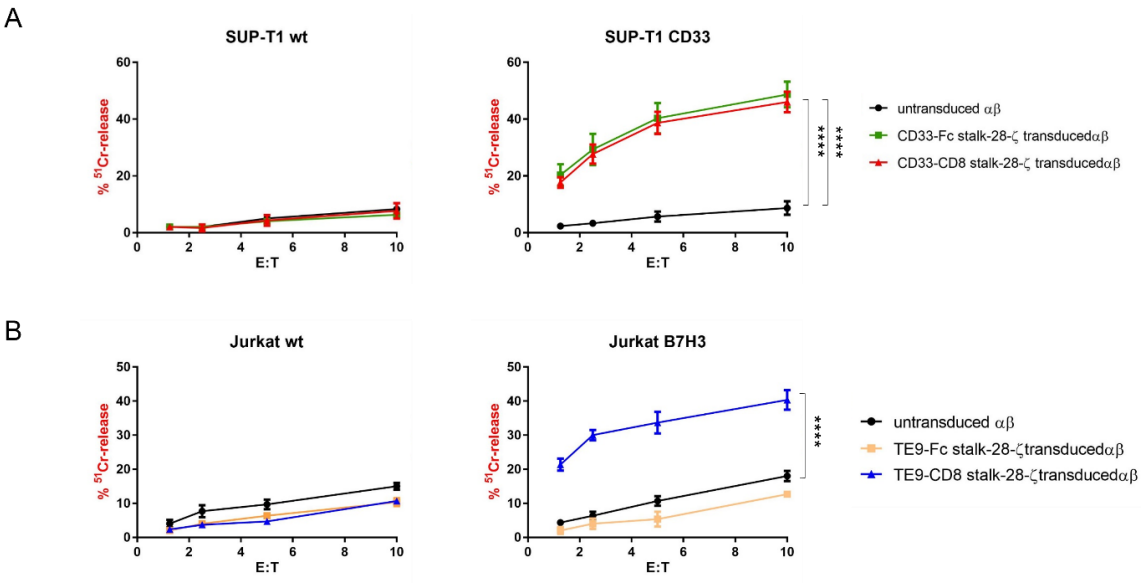

Figure 3.5 Cytotoxicity mediated by CD33 CARs against isogenic cell line SUP-T1 wt and SUP-T1 CD33 (A) and by TE9 CARs against isogenic cell line Jurkat wt Jurkat B7-H3 (B). αβ T cells transduced with CD33-Fc stalk-28-ζ , CD33-CD8 stalk-28-ζ, TE9-Fc stalk-28-ζ , TE9-CD8 stalk-28-ζ CAR were co-cultured for four hours with 51Cr-labelled target cells, at the following E:T ratios: 1.25:1, 2.5:1, 5:1 and 10:1. Untransduced αβ T cells were used as controls. Graphs show mean ± SD (n=3 independent biological replicates). Statistical analysis was performed by 2-way ANOVA, followed by Tukey post hoc analysis : **** p<0.0001.

3.4.3 Cytotoxic activity of CD33 and TE9 CAR T cells towards AML cell lines.

Cytotoxic activity of CD33-Fc-28ζ, CD33-CD8-28ζ, TE9-Fc-28ζ and TE9-CD8-28ζ T cells was then evaluated on a panel of AML targets: MV-411, NOMO-1 and TH-P1 (Figure 3.6) Effector cells were incubated with target cells at ratios of 10:1, 5:1, 2.5:1 and 1.25:1 for 4 hours and killing compared to background cell death of the target cells with no effector cells and 100% cell death calculated by incubating cells with Triton X-100 to ensure 100% cell lysis.

When co-cultured with MV4-11, CD33-Fc-28ζ and CD33-CD8-28ζ transduced T cells do not show any significant increase in cell lysis when compared to untransduced effector co-cultured with the same target. Also, no significant

difference between CD33-Fc-28ζ and CD33-CD8-28ζ transduced T cells is detected. TE9-Fc-28ζ transduced T cells show a small but significant increase in cell lysis when co-cultured with MV4-11 compared to the untransduced control ($p = 0.02350$) with mean 16% killing at 10;1 E;T ratio. In contrast, TE9-CD8-28ζ transduced T cells clearly demonstrate a significant increase in cytotoxic activity against MV4-11 compared to the untransduced control ($p<0.0001$) and the other effectors with a mean 23% killing at 10:1 E:T ratio.

The same pattern can be seen when the effectors are co-cultured with NOMO-1 and THP-1 target cells: TE9-CD8-28ζ transduced T cells show a significant increase in killing compared to the untransduced control ($p<0.0001$ in both NOMO-1 and THP-1) with a mean % killing of 20% and 38% respectively, at 10:1 E:T ratio.

On the other hand, CD33-Fc-28ζ , CD33-CD8-28ζ and TE9-Fc-28ζ transduced T cells do not show any significant increase in ^{51}Cr release when compared to the untransduced control.

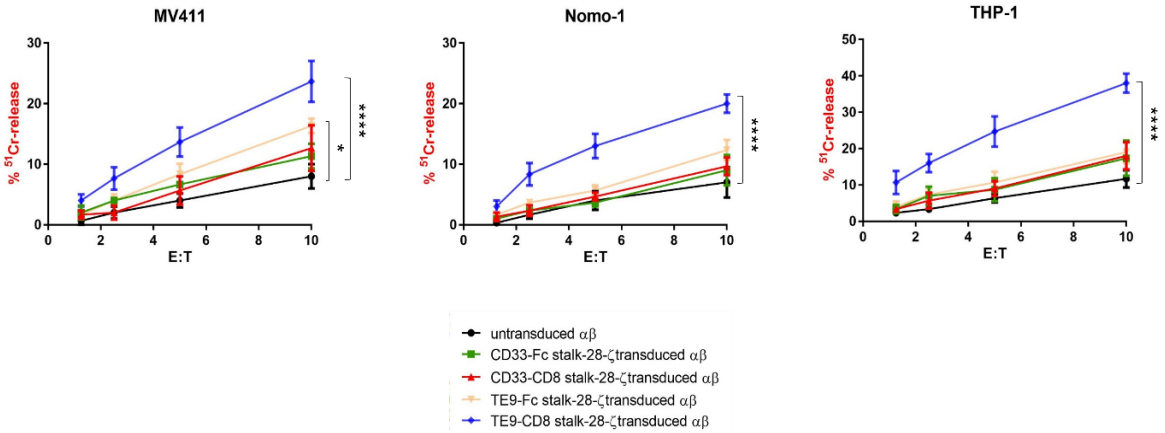

Figure 3.6 Cytotoxicity mediated by CD33 CARs and TE9 CARs against AML cell lines. αβ T cells transduced with CD33-Fc stalk-28-ζ , CD33-CD8 stalk-28-ζ, TE9-Fc stalk-28-ζ , TE9-CD8 stalk-28-ζ CAR were co-cultured for four hours with 51Cr-labelled target cells MV4-11, NOMO-1 and THP-1, at the following E:T ratios: 1.25:1, 2.5:1, 5:1 and 10:1. Untransduced αβ T cells were used as controls. Graphs show mean ± SD (n=3 independent biological replicates). Statistical analysis was performed by 2-way ANOVA, followed by Tukey post hoc analysis : * P<0.1 ****p<0.0001.

3.4.4 Quantification of IL-2 and IFN-γ production mediated by CD33 and TE9 CAR T cells against isogenic cell lines expressing their cognate antigen.

The ability of CAR T cells to produce proinflammatory cytokines is an important assessment of CAR T cell function. In order to study this, effector cells (CD33-Fc-28ζ, CD33-CD8-28ζ, TE9-Fc-28ζ and TE9-CD8-28ζ T cells) and target cells were co-cultured for 18h at a 1:1 ratio. After 18 hours, the cells were pelleted, and the supernatant was collected in order to quantify the cytokines present.

ELISA to detect IFN-γ and IL-2 was performed according to manufacturer's direction, and plates were analysed by reading the absorbance at 450 nm on a microplate reader and corrected by subtraction of background control values. Cytokines concentration was determined by correlation with a standard curve.

CD33-Fc-28ζ and CD33-CD8-28ζ transduced T cells, were co-cultured with SUP-T1 WT and SUP-T1 CD33 (Figure 3.7A). Effector only condition was analysed in order to detect any background cytokine production by the effectors, however no detectable IFN-γ or IL-2 was produced when the effectors were cultured with no targets. Both CD33-Fc-28ζ and CD33-CD8-28ζ transduced T cells produced significantly higher amount of IL-2 compared to the untransduced control when co-cultured with SUP-T1 CD33 but not when co-cultured with SUP-T1 WT, 8879±5741 (mean pg/mL cytokine release±SD, n=3) and 9798± 3612 pg/mL respectively

(p=0.0036, p= 0.0013). No significant difference in IL-2 production was observed between the two CARs when co-cultured with SUP-T1 CD33. Following the same pattern, CD33-Fc-28ζ and CD33-CD8-28ζ produced significantly higher amount of IFN-γ compared to the untransduced control when co-cultured with SUP-T1 CD33 but not when co-cultured with SUP-T1 WT, 13518±1003 and 12995±3803 pg/mL respectively (p<0.0001). Again, no significant difference in IFN-γ production was observed between the two CARs.

TE9-Fc-28ζ and TE9-CD8-28ζ transduced T cells, were co-cultured with Jurkat WT and Jurkat B7-H3 cell lines (Figure 3.7B). Both effectors did not produce any detectable amount of IFN-γ and IL-2 when they were cultured alone or with Jurkat WT. TE9-CD8-28ζ CAR T cells released significantly higher amounts of cytokines compared to the untransduced control, when co-cultured with Jurkat B7-H3, 1175±316 pg/mL IL-2 and 6626±3674 pg/mL IFN-γ respectively (p<0.0001).

In contrast, TE9-Fc-28ζ did not produce either IL-2 or IFN-γ when co-cultured with Jurkat B7-H3, reflecting what was seen in terms of cytotoxic activity against Jurkat-B7H3.

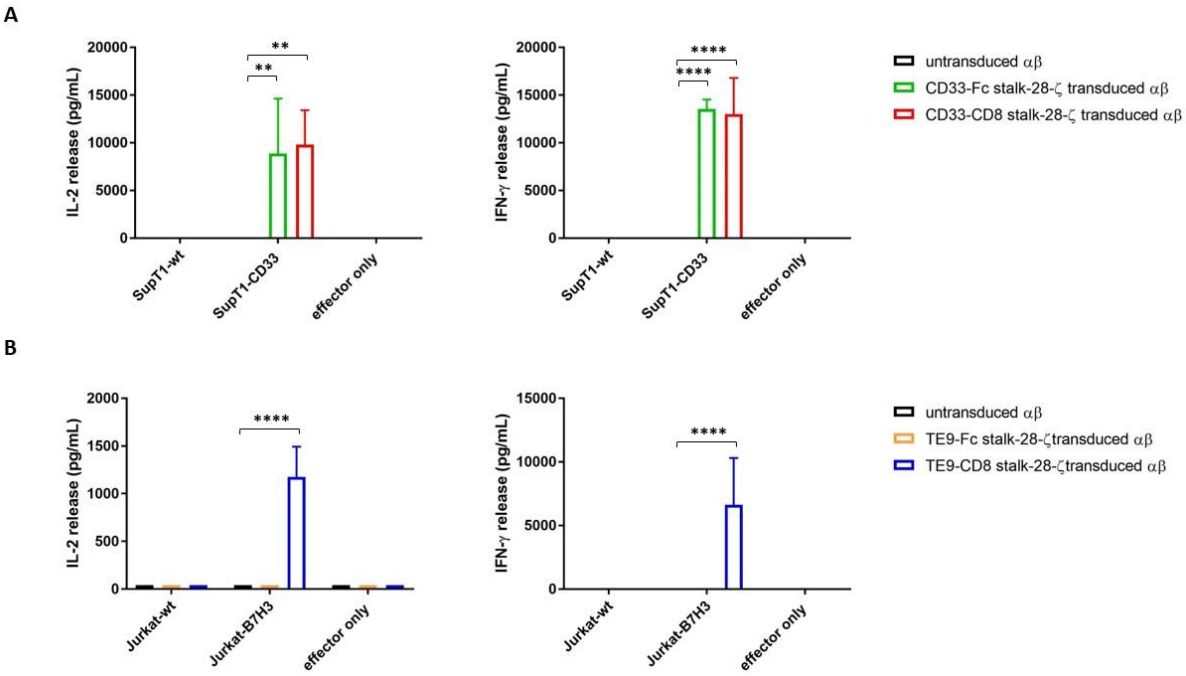

Figure 3.7. Quantification of IL-2 and IFN-γ production mediated by CD33 and TE9 CAR T cells against isogenic cell lines expressing their cognate antigen . αβ T cells transduced with CD33-Fc stalk-28-ζ and CD33-CD8 stalk-28-ζ were co-cultured for 18 hours with SUP-T1 wt and SUP-T1 CD33 (A) while TE9-Fc stalk-28-ζ and TE9-CD8 stalk-28-ζ CAR were co-cultured with Jurkat wt and Jurkat B7-H3 (B), or alone at 1:1 E:T ratio. Untransduced αβ T cells were used as controls. IL-2 and IFN-γ were measured by ELISA. Graphs show mean ± SD (n=3 independent biological replicates). Statistical analysis was performed by 2-way ANOVA, followed by Tukey post hoc analysis : ** p<0.01 ****p<0.0001.

3.4.5 Quantification of IL-2 and IFN-γ production mediated by CD33 and TE9 CAR T cells against AML cell line.

CD33-Fc-28ζ, CD33-CD8-28ζ, TE9-Fc-28ζ and TE9-CD8-28ζ transduced T cells were co-cultured with AML cell lines MV4-11, NOMO-1, THP-1, for 18h at a 1:1 ratio as described previously (Figure 3.8).

After 18 hours, the cells were pelleted, and the supernatant was collected in order to quantify IL-2 and IFN-γ produced. Effector cells were cultured alone in order to

detect any background cytokine release, however no detectable IFN-γ or IL-2 was produced when cultured with no targets.

TE9-CD8-28ζ CAR T cells released significantly higher amount of IL-2 when co-cultured with MV4-11, NOMO-1 and THP-1 compared to untransduced control (9830±2655 pg/mL, 14119±3453 pg/mL and 15735±4735 pg/mL respectively).

In contrast CD33-Fc-28ζ, CD33-CD8-28ζ and TE9-Fc-28ζ transduced T cells did not release any detectable amount of IL-2 in the supernatant. TE9-CD8-28ζ transduced T cells also produced significantly higher amount of IFN-γ when co-cultured with MV4-11, NOMO-1 and THP-1 compared to the untransduced control (19408±3900 pg/mL, 17033±1836 pg/mL, 20772±1937 pg/mL respectively).

In contrast the three other CARs were less reactive to the three AML target lines. CD33-Fc-28ζ produced smaller amount of IFN-γ in response to MV11, NOMO-1 and THP-1 (7266±2744 pg/mL, 4998±3896 pg/mL, 5657±476 pg/mL respectively) and so did CD33-CD8-28ζ (975.8248±949 pg/mL, 1130±630 pg/mL, 1858±1455 pg/mL) and TE9-Fc-28ζ (3518±4146 pg/mL, 5180±6931 pg/mL,3802±3491 pg/mL). However, no statistically significant difference was detected for these three CARs compared to the untransduced control against the same targets.

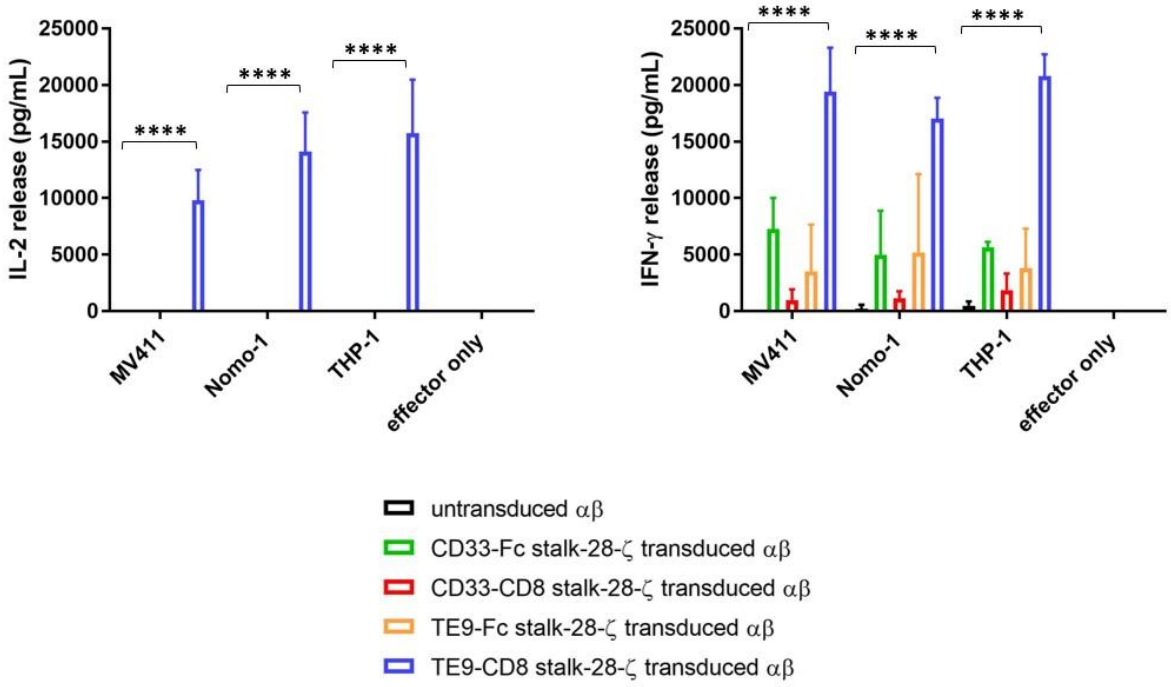

Figure 3.8 Quantification of IL-2 and IFN-γ production mediated CD33 and TE9 CAR T cells against AML cell lines . αβ T cells transduced with CD33-Fc stalk-28-ζ , CD33-CD8 stalk-28-ζ, TE9-Fc stalk-28-ζ , TE9-CD8 stalk-28-ζ CAR were co-cultured for 18 hours with AML cell line MV4-11, NOMO-1 and THP-1 cell line or alone at 1:1 E:T ratio. Untransduced αβ T cells were used as controls. IL-2 and IFN-γ were measured by ELISA. Graphs show mean ± SD (n=3 independent biological replicates). Statistical analysis was performed by 2-way ANOVA, followed by Tukey post hoc analysis : ****p<0.0001.

3.4.6 Proliferation mediated by CD33 and TE9 CAR T cells.

An important characteristic of CAR T cells is their ability to proliferate upon recognition of target antigens. It is equally important that CAR T cells do not proliferate independently or upon recognition of unspecific antigens.

In order assess the proliferation, untransduced T cells, CD33-Fc-28ζ, CD33-CD8-28ζ, TE9-Fc-28ζ and TE9-CD8-28ζ CAR T cells labelled with Cell trace violet were co-cultured with SUP-T1 WT, SUPT1 CD33, Jurkat WT, Jurkat B7-H3 and AML

cell lines MV4-11, NOMO-1 and THP-1 at 1:1 ratio for 7 days. All the effector T cells were also cultured with no target in order to subtract any background proliferation. Proliferation dyes such as cell trace violet can be used to monitor multiple generations through dye dilution, which indicates that a labelled population has undergone cell division.

Figure 3.9A shows a representative gating strategy to identify CD3+, αβTCR+ T cells that have proliferated as per dye dilution, after the exclusion of dead cells and doublets. In order to quantify this short-term proliferation, the change in MFI, referred to as the delta MFI (ΔMFI) of Cell trace violet between the CAR T cell cultured with a specific target and the untransduced T cells cultured with the same target was determined.

Figure 3.9B shows the Cell trace violet dye dilution in one representative donor. The other two donors followed the same trend (data not shown). As it can be seen on the figure, all the effector T cells cultured alone with no target, as well as the untransduced T cells cultured with the different target cell line, show minimal background proliferation which makes the data easily interpretable.

CD33-Fc-28ζ CAR T cells proliferated in an antigen dependent manner when co-cultured with SUP-T1 CD33, while they show no proliferation when cultured with antigen negative cell lines SUP-T1 WT, Jurkat WT and Jurkat B7-H3. The same trend is seen with CD33-CD8-28ζ transduced T cells.

Some degree of proliferations can be seen when CD33-Fc-28ζ and CD33-CD8-28ζ are co-cultured with AML cell lines. However, it is not comparable to the proliferation seen in response to the positive control SUP-T1 CD33. CD33-Fc-28ζ

CAR T cells seem to proliferate a slightly more than CD33-CD8-28ζ CAR T cells in response to the AML cell lines.

TE9-CD8-28ζ CAR T cells proliferated in an antigen dependent manner in response to Jurkat B7-H3, while no proliferation can be detected when they are cultured with antigen negative cell lines Jurkat WT, SUP-T1 WT and SUP-T1 CD33. In contrast TE9-Fc-28ζ CAR T cells showed no proliferation in response to any of those targets, in accordance with what seen in terms of cytotoxicity and cytokine release. When co-cultured with AML cell lines, TE9-Fc-28ζ CAR T cells show a small degree of proliferation, comparable to what seen with CD33-Fc-28ζ CAR T cells against the same target. In contrast, TE9-CD8-28ζ CAR T cells proliferated in response to the AML targets, in a higher degree compared to all the other effectors against the same targets. Its proliferation against MV4-11, NOMO-1, and THP-1 looks even greater than the proliferation in response to the positive control Jurkat B7-H3.

Again, ΔMFI of Cell trace violet between the CAR T cell cultured with a specific target and the untransduced T cells cultured with the same target, was determined in order to quantify the short-term proliferation. Statistical differences were determined by one-way ANOVA comparing the experimental condition to the control cell line SUP-T1 WT for CD33-Fc stalk-28-ζ and CD33-CD8 stalk-28-ζ CAR T cells and to the control cell line Jurkat WT for TE9-Fc stalk-28-ζ and TE9-CD8 stalk-28-ζ CAR T cell.

ΔMFI proliferation of CD33-Fc-28ζ and CD33-CD8-28ζ CAR T cells co-cultured with SUP-T1 CD33 is statistically greater than the ΔMFI proliferation of the same effectors co-cultured with SUP-T1 WT ($p<0.0001$). Even though there is a small

degree of proliferation by CD33-Fc-28ζ CART cells in response to AML targets, which is not statistically significant.

TE9-Fc-28-ζ CAR T cells demonstrate a low level of proliferation in response to the Jurkat B7-H3 and AML cell lines, however, no significant difference is seen compared to when they are co-cultured with the antigen negative cell line Jurkat WT. In contrast, ΔMFI proliferation of TE9-CD8-28-ζ CAR T in response to Jurkat B7-H3, MV4-1, NOMO-1 and THP-1 is significantly greater compared to ΔMFI proliferation with Jurkat WT condition, with $p<0.001$ for Jurkat B7-H3 and $p<000.1$ for the AML cell lines. Moreover, the response of TE9-CD8-28-ζ CAR T to MV4-11 and NOMO-1 is statically greater than the response to Jurkat B7-H3 ($p=0.0095$ and $p= 0.0377$ respectively).

A

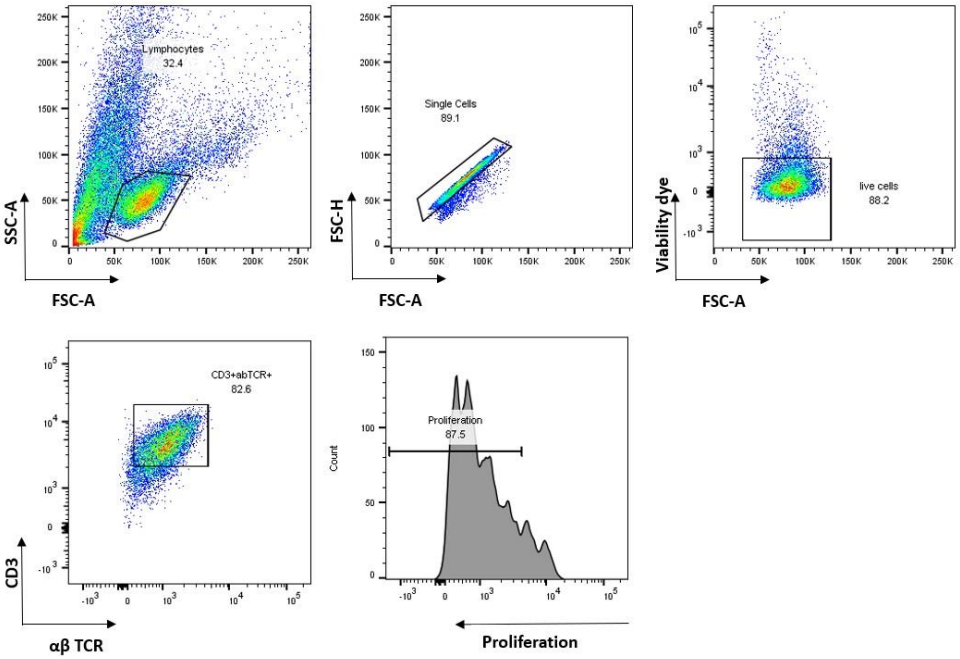

B

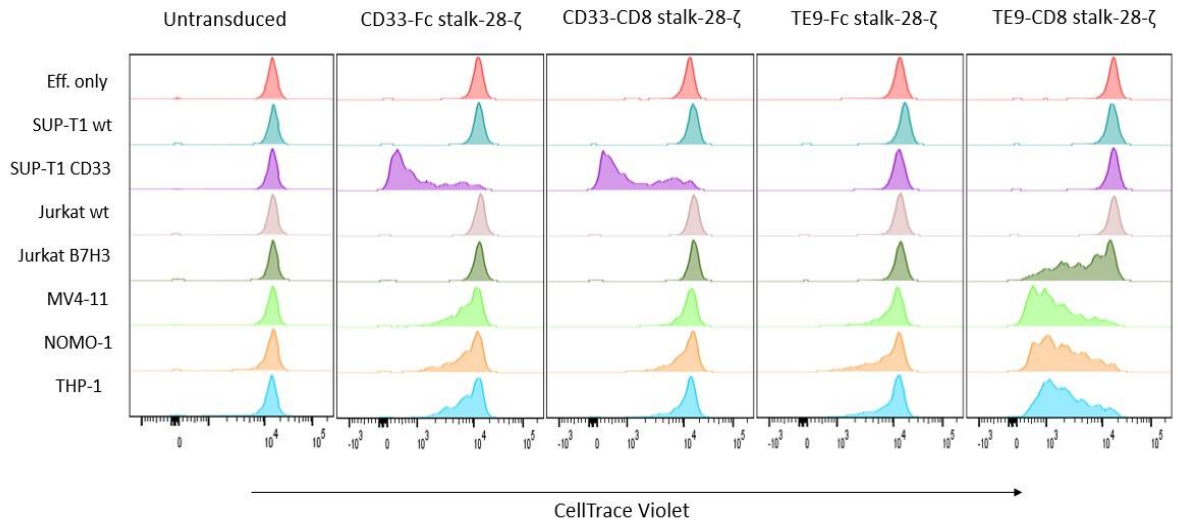
Untransduced
CD33-Fc stalk-28-ζ
CD33-CD8 stalk-28-ζ
TE9-Fc stalk-28-ζ
TE9-CD8 stalk-28-ζ
Eff. only
SUP-T1 wt
SUP-T1 CD33
Jurkat wt
Jurkat B7H3
MV4-11
NOMO-1
THP-1
CellTrace Violet

C

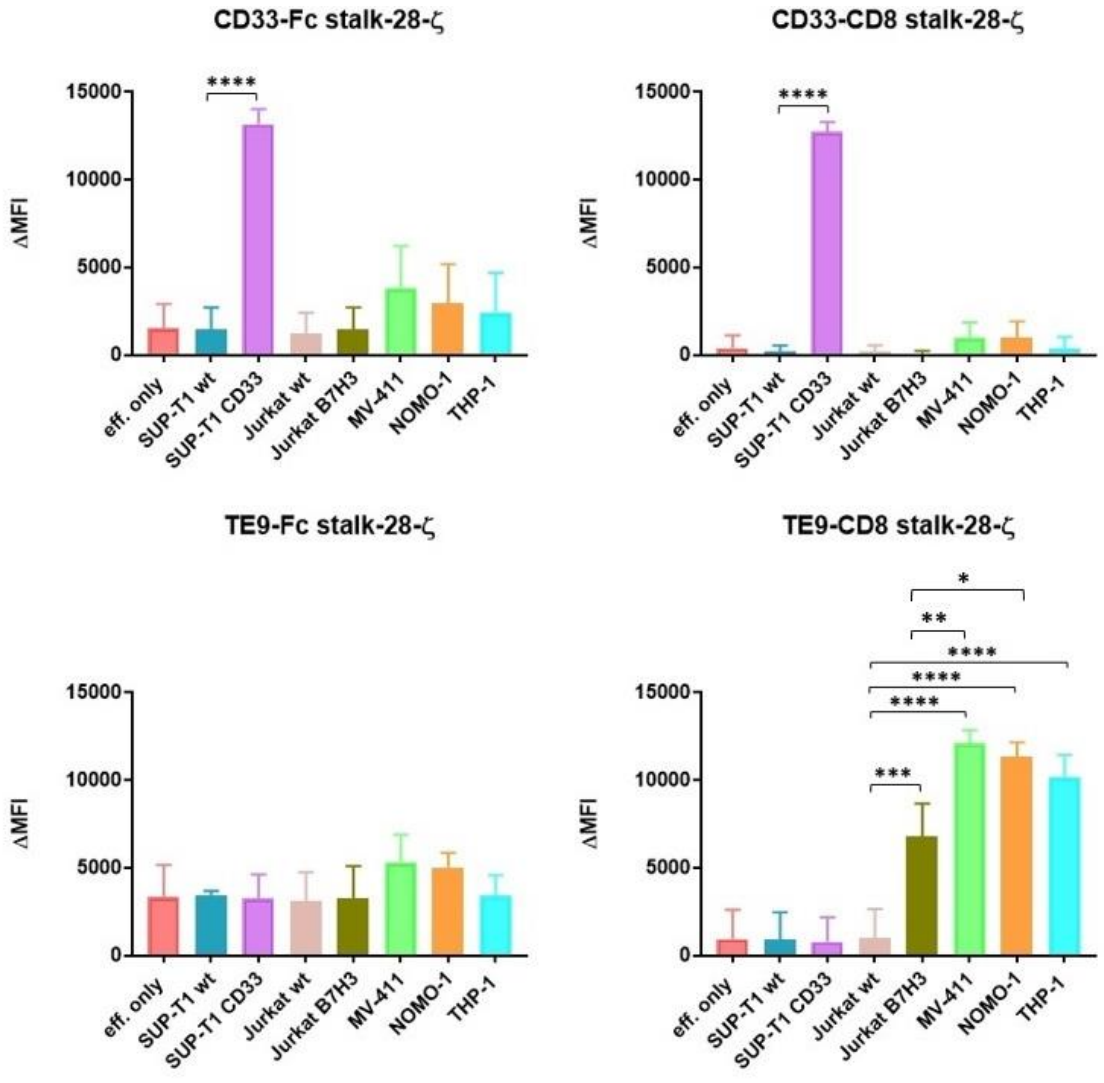
CD33-Fc stalk-28-ζ
CD33-CD8 stalk-28-ζ
TE9-Fc stalk-28-ζ
TE9-CD8 stalk-28-ζ
ΔMFI
15000
10000
5000
0
****
***
**
*
eff. only
SUP-T1 wt
SUP-T1 CD33
Jurkat wt
Jurkat B7H3
MV-411
NOMO-1
THP-1

Figure 3.9 Proliferation mediated by CD33 CARs and TE9 CARs. Untransduced αβ T cells and αβ T cells transduced with CD33-Fc stalk-28-ζ , CD33-CD8 stalk-28-ζ, TE9-Fc stalk-28-ζ and TE9-CD8 stalk-28-ζ CAR labelled with cell trace violet proliferation dye were co-cultured for 7 days with SUP-T1 wt and SUP-T1 CD33, Jurkat wt and Jurkat B7-H3 and AML cell lines MV4-11, NOMO-1 and THP-1 cell line or alone at 1:1 E:T ratio. (A) Representative gating strategy to identify CD3+, αβTCR+ cells after exclusion of dead and doublet cells. The proliferation gating is set on control untransduced T cells, and the dilution of cell trace violet indicates proliferation of a population. (B) Representative histograms showing the cell trace violet dilution in one donor. (n=3 independent biological replicates). (C) Mean ΔMFI±SD for CAR T cells (n=3 independent biological replicates). Statistical differences were determined by one-way ANOVA comparing experimental condition to control cell line, SUP-T1 WT for CD33-Fc stalk-28-ζ and CD33-CD8 stalk-28-ζ CAR T cells and Jurkat WT for TE9-Fc stalk-28-ζ and TE9-CD8 stalk-28-ζ : *** $p<0.001$, **** $p<0.0001$.

3.5 TE9-CD8-28-ζ CAR T cells potential hematopoietic toxicity

We explored in the introduction that one of the main concerns of current immunotherapy strategies targeting AML derive from the expression profile of the currently targeted antigens. Their expression on myeloid-committed cells (early progenitors) in the bone marrow and on circulating monocytes is a reason of concern for potential toxicity. Based on the results of the functional assays performed comparing the CD33-specific CARs and the B7-H3-specific CAR, TE9-CD8-28-ζ CAR was chosen as lead to bring forward to assess potential hematopoietic toxicity. Hematopoietic toxicity was firstly investigated in terms of TE9-CD8-28-ζ CAR T cells activity against allogeneic monocytes and then the toxicity towards normal Hematopoietic Progenitors (HSPCs) in the cord blood of a healthy donor was assessed by performing a Colony Forming Assay.

3.5.1 B7-H3 expression on Monocytes

In order to investigate TE9-CD8-28-ζ CAR T cells activity against allogeneic monocytes, we determined B7-H3 expression on healthy monocytes through median fluorescence intensity (MFI) by flow cytometry. Monocytes were isolated from PBMCs by negative selection using a Pan-monocyte isolation kit, as described in the material and methods section and they were stained on the same day with a commercially available anti-human CD276 (B7-H3)-APC antibody from Biolegend (blue histogram). Unstained cells were used as negative control (red histograms). No surface expression of B7-H3 was detected on selected monocytes, MFI=248 (Figure 3.10). MV-411 were tested alongside as positive control for B7-H3 staining; figure not included as we have previously shown MV4-11 B7-H3 staining.

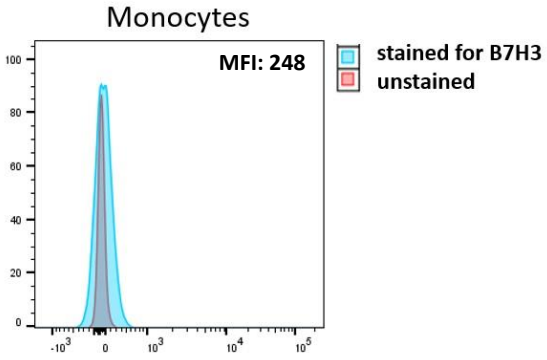

Figure 3.10 Surface expression of B7-H3 in human monocytes . Representative histograms of B7-H3 detection on human monocytes. Surface B7-H3 expression was assessed through median fluorescence intensity (MFI) by flow cytometry, using anti-human CD276 (B7-H3) – APC antibody (blue histograms). Unstained cells were used as control (red histograms).

3.5.2 Cytotoxic activity of TE9-CD8-28-ζ CAR T cells towards monocytes.

TE9-CD8 stalk-28-ζ expressing CAR T cells cytotoxic activity towards allogeneic monocytes was assessed by a 4h chromium (^{51}Cr) release assay (Figure 3.11). AML target cell line MV4-11 was used as positive control based on the previous results. Effector cells were incubated with ^{51}Cr labelled monocytes at ratios of 10:1, 5:1, 2.5:1 and 1.25:1 for 4 hours and cell lysis detected by ^{51}Cr release in the supernatant as explained previously. TE9-CD8 stalk-28-ζ CAR T cells did not lyse monocytes; indeed, no statistically significant difference was observed between the transduced T cells and the untransduced control. In contrast, statistically significant difference in cell lysis between TE9-CD8 stalk-28-ζ CAR T cells and the untransduced control was detected when the effectors were co-cultured with MV4-11 (p=0.0374).

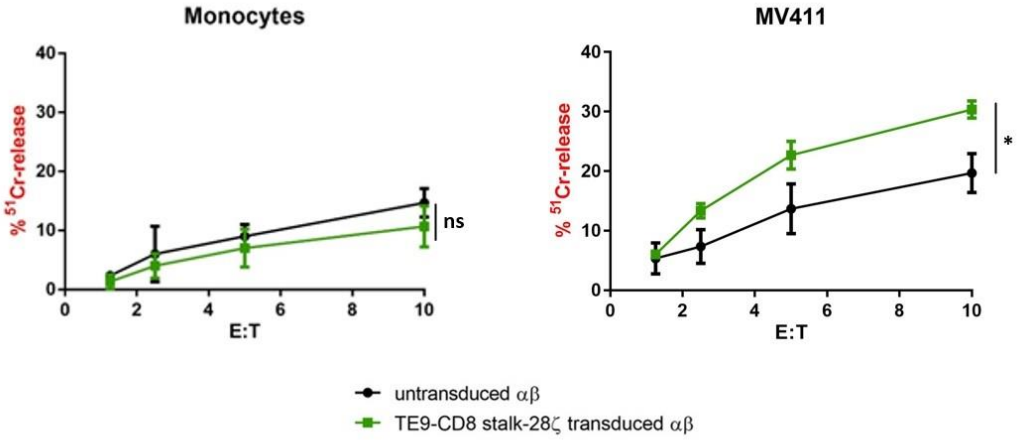

Figure 3.11 Cytotoxicity mediated by TE9-CD8 stalk-28-ζ CAR against human monocytes. αβ T cells transduced TE9-CD8 stalk-28-ζ CAR were co-cultured for four hours with 51Cr-labelled monocytes, at the following E:T ratios: 1.25:1, 2.5:1, 5:1 and 10:1. Untransduced αβ T cells were used as controls. αβ T cells transduced TE9-CD8 stalk-28-ζ CAR were also co-cultured with MV-

411 as positive control. Graphs show mean ± SD (n=3 independent biological replicates). Statistical analysis was performed by 2-way ANOVA, followed by Tukey post hoc analysis.

3.5.3 Quantification of IL-2 and IFN-γ production mediated by TE9-CD8-28-ζ CAR T cells against Monocytes.

Cytokines release by TE9-CD8 stalk-28-ζ CAR T cells when co-cultured with allogeneic monocytes or MV4-11 for 18h was investigated by ELISA as described previously (Figure 3.12). TE9-CD8 stalk-28-ζ CAR T cells produced small amounts of IFN-γ and IL-2 when co-cultured with monocytes (3589±1411 - pg/mL±SD - and 766±897 pg/mL respectively), however, no statistical difference was observed compared to the untransduced control cultured with the same target. In contrast, in accordance with what seen previously, TE9-CD8 stalk-28-ζ CAR T cells released higher levels of IFN-γ and IL-2 (13979±5709 pg/mL and 11120±1295 pg/mL) compared to the untransduced control ($p<0.0001$ and $p=0.0091$ respectively).

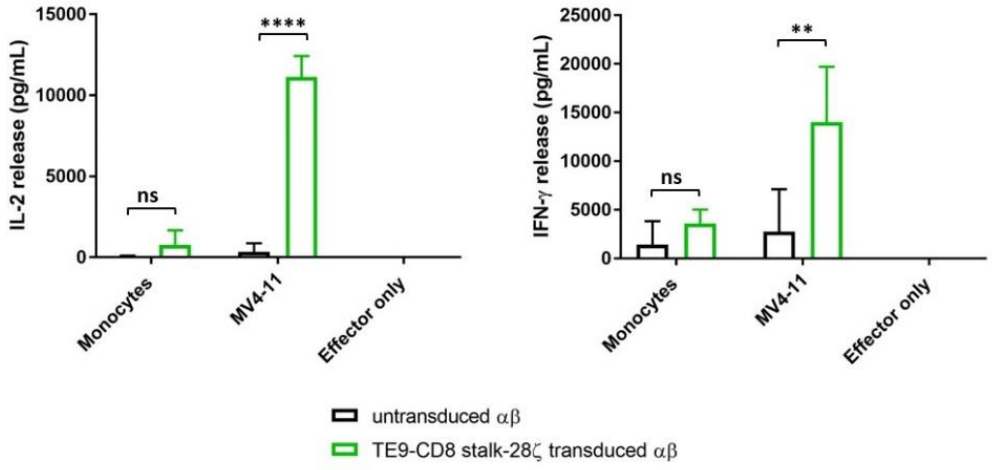

Figure 3.12 Quantification of IL-2 and IFN-γ production mediated by TE9-CD8 stalk-28-ζ CAR T cells against human monocytes. αβ T cells transduced TE9-CD8 stalk-28-ζ CAR were co-cultured for 18 hours with human monocytes or alone at 1:1 E:T ratio. TE9-CD8 stalk-28-ζ CAR T cells were also co-cultured with MV-411 as positive control. IL-2 and IFN-γ were measured by ELISA following manufacturer's direction . Graphs show mean ± SD (n=3 independent biological

replicates). Statistical analysis was performed by 2-way ANOVA, followed by Tukey post hoc analysis.

3.5.4 TE9-CD8-28-ζ CAR T cells proliferation in response to Monocytes.

To provide further evidence of lack of response against healthy monocytes, after assessing cytotoxic activity and cytokine release by TE9-CD8-28-ζ CAR T towards the target, proliferation was assessed by flow cytometry in a 7-day co-culture with allogeneic monocytes. T cells were also co-cultured with MV4-11 as control for the proliferation. TE9-CD8-28-ζ CAR T cells were labelled with Cell trace violet and dilution of the dye as well as the ΔMFI between the experimental condition and the untransduced control against the same target was calculated.

Figure 3.13A shows the Cell trace violet dilution in one representative donor post 7 days co-culture with monocytes and MV4-11 target cell lines. Untransduced T cells cultured with no target showed minimal background proliferation while TE9-CD8-28-ζ CAR T cells show proliferation when cultured with no target.TE9-CD8-28-ζ CAR T cells proliferate more in response to MV4-11 compared to the untransduced control, even though some background proliferation can be seen when the untransduced αβ T cells are co-cultured with the same target. Interestingly, the same trend was observed for monocytes. While a greater proliferation was observed when TE9-CD8-28-ζ CAR T cells were co-cultured with monocytes, a certain degree of background proliferation detected when the untransduced T cells were cultured with the same target. This reflects on the ΔMFI proliferation; indeed, no statistically significant difference can be seen in ΔMFI proliferation between TE9-CD8-28-ζ CAR T cells co-cultured with monocytes or MV4-11 (3.13B).

Hence, there appears to be a high level of background proliferation over 7 days induced by both monocytes and MV411 suggesting that this 7-day assay is non informative for antigen specific effects. These background effects might be attributable to antigen presenting properties of myeloid cells that lead to background stimulation effects in long term assays that were not seen in the short-term cytotoxicity or cytokine assays.

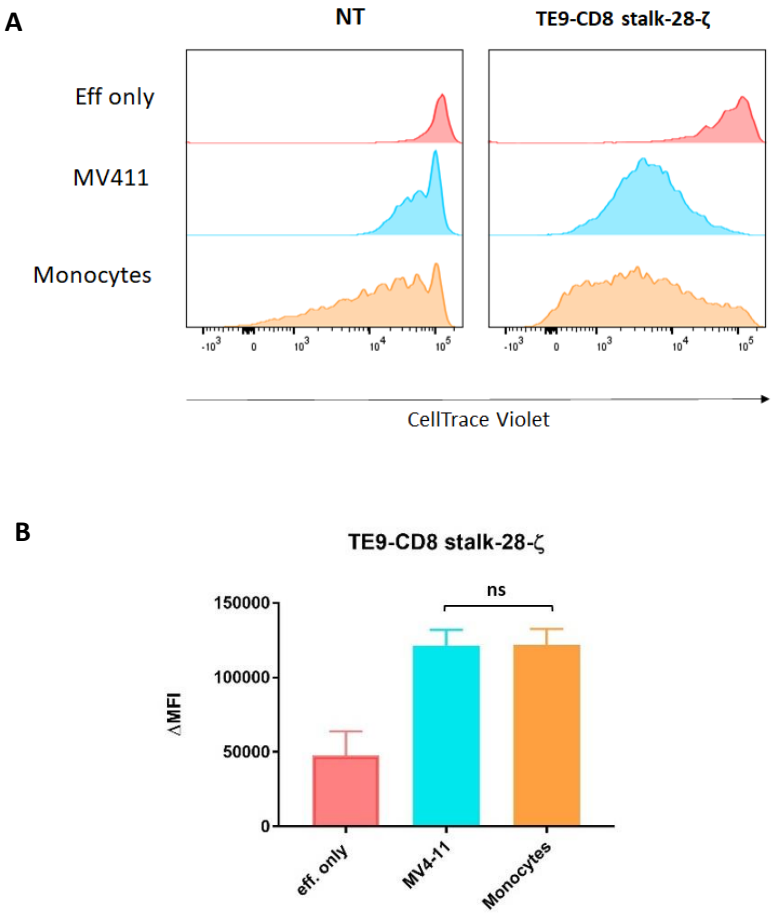

Figure 3.13 Proliferation mediated by TE9-CD8 stalk-28-ζ CAR against human monocytes. Untransduced αβ T cells and αβ T cells transduced with TE9-CD8 stalk-28-ζ CAR labelled with cell trace violet proliferation dye were co-cultured for 7 days with Monocytes and AML cell line MV4-11 or alone at 1:1 E:T ratio. (A) Representative histogram showing the cell trace violet dilution in each condition (n=3 independent biological replicates). (B) Mean ΔMFI±SD for CAR T cells (n=3 independent biological replicates). Statistical differences were determined by one-way ANOVA comparing the proliferation of TE9-CD8 stalk-28-ζ CAR T cells with monocytes and MV4-11.

3.5.5 TE9-CD8 stalk-28-ζ CAR T cells toxicity towards normal Hematopoietic Progenitors - Colony-forming unit (CFU) assay.

In order to assess TE9-CD8 stalk-28-ζ CAR T cells toxicity towards normal hematopoietic progenitors, the CAR T cells were co-cultured with Cord Blood (CB) for 18h and then the co-cultures were plated in a semi-solid matrix – methylcellulose, supplemented with appropriate cytokines and supplements to allow the growth of CFU-E (Erythroid progenitor cells), BFU-E (burst-forming unit-erythroid), CFU-GM (Granulocyte and/or macrophage progenitor cells) and CFU-GEMM (multi-potential progenitor cells). Approximately 1% of CB, contains hematopoietic progenitors. If the TE9-CD8 stalk-28-ζ CAR T cells were to be toxic towards the hematopoietic progenitors, colony formation on methylcellulose would be depleted.

TE9-CD8 stalk-28-ζ CAR T cells were also co-cultured with AML cell lines MV4-11, NOMO-1, THP-1 to assess whether the CAR T cells from the same donors are able to deplete leukemic colony formation. Untransduced T cells co-cultured with CB and AML cell lines as well as all the effectors and all the targets cultured with either no targets or no effectors were included as controls. Co-cultures were set up at 5:1 E:T ratio and two co-cultures were set up in parallel. One set was used to assess the killing of the target cell lines by TE9-CD8 stalk-28-ζ CAR T cells after the 18h co-culture through flow cytometry analysis, while the other set was used to transfer specific amount of cells from the co-culture to the semi-solid methylcellulose media and assess colony formation past 14 days of incubation.

3.5.5.1 Cytotoxicity mediated by TE9-CD8-28-ζ CAR T cell towards AML cell lines in a 18h co-culture.

It was not logistically possible to detect hematopoietic progenitors killing by TE9-CD8-28-ζ CAR T using flow cytometry due to small number of stem cells within cord blood, so only AML cell line killing by the effectors was assessed. In this set of co-cultures, target cell lines MV4-11, NOMO-1 and THP-1 were labelled with Cell trace violet for detection. Anti-human CD3 antibody was used to detect the T cells while zombie NIR viability dye, Cell trace violet and anti-human B7-H3 antibody were used to detect the loss of live target cells. Count Bright Absolute Counting Beads were used to assess the absolute cell number. Figure 3.14A illustrate the gating strategy to detect counting beads and loss of target cells in one representative donor following overnight culture at 5:1 E:T ratio. Cells are gated on SSC-A and FCS-A and gated on the live cells. CD3-neg live cells are gated as non-effector cells and then gated on Cell trace violet (which the target cells were labelled with) and B7-H3 (which the targets are positive to). It is possible to see in the figure that the live B7-H3 positive population decrease sequentially from being cultured with no effectors, to being cultured with untransduced T cells and finally with TE9-CD8-28-ζ CAR T cells. Calculation of absolute numbers of live AML cells after been cultured with untransduced T cells and TE9-CD8-28-ζ CAR T cells was based on this gating (Figure 3.14B).

Targets were cultured with no effectors as negative control. As it can be observed in the histogram cell numbers of live MV4-11 are significantly lower when co-cultured with TE9-CD8-28-ζ CAR T cells when compared to the untransduced control ($p<0.0001$). The mean absolute cell count ±SD is 855±505 versus114028±42524 for the untransduced.

The same trend was observed for the NOMO-1 cells (p=0.0003) with respectively mean cell count of 81341±9822 when co-cultured with untransduced T cells and 756±739 when co-cultured with TE9-CD8-28-ζ CAR T cells. While the same trend can also be observed for the THP-1 cells , the difference in absolute numbers between co-culture with CAR T cells and untransduced T cells is not statistically significant, with 33±25 and 32826±24061, respectively.

Interestingly, while we see decrease of live B7-H3 positive population it is possible to see in the figure that the same population retained Cell Trace Violet.

We initially hypothesized that the target cells might not have been killed but just lost the antigen, however if that was the case, when transferring part of this population to methylcellulose to evaluate colony formation we should see formation of colonies by these antigen-loss leukemic cells. As it will be described in the next section, there was no colony formation from this specific co-culture, therefore, further analysis is necessary to speculate on what this population could be.

The same data can be extrapolated in terms of percentage of killing, calculated by normalizing against target alone (Figure 3.14C). TE9-CD8-28-ζ CAR T cells were considerably more cytotoxic towards the AML cell lines compared to the untransduced control. Indeed, the increase in percentage of killing of AML cell lines MV4-11 and NOMO-1 by the TE9-CD8-28-ζ CAR T is statistically significant compared to the untransduced control. THP-1s follow the same trend but the difference of percentage in killing between the transduced and untransduced T cells is not statically significant.

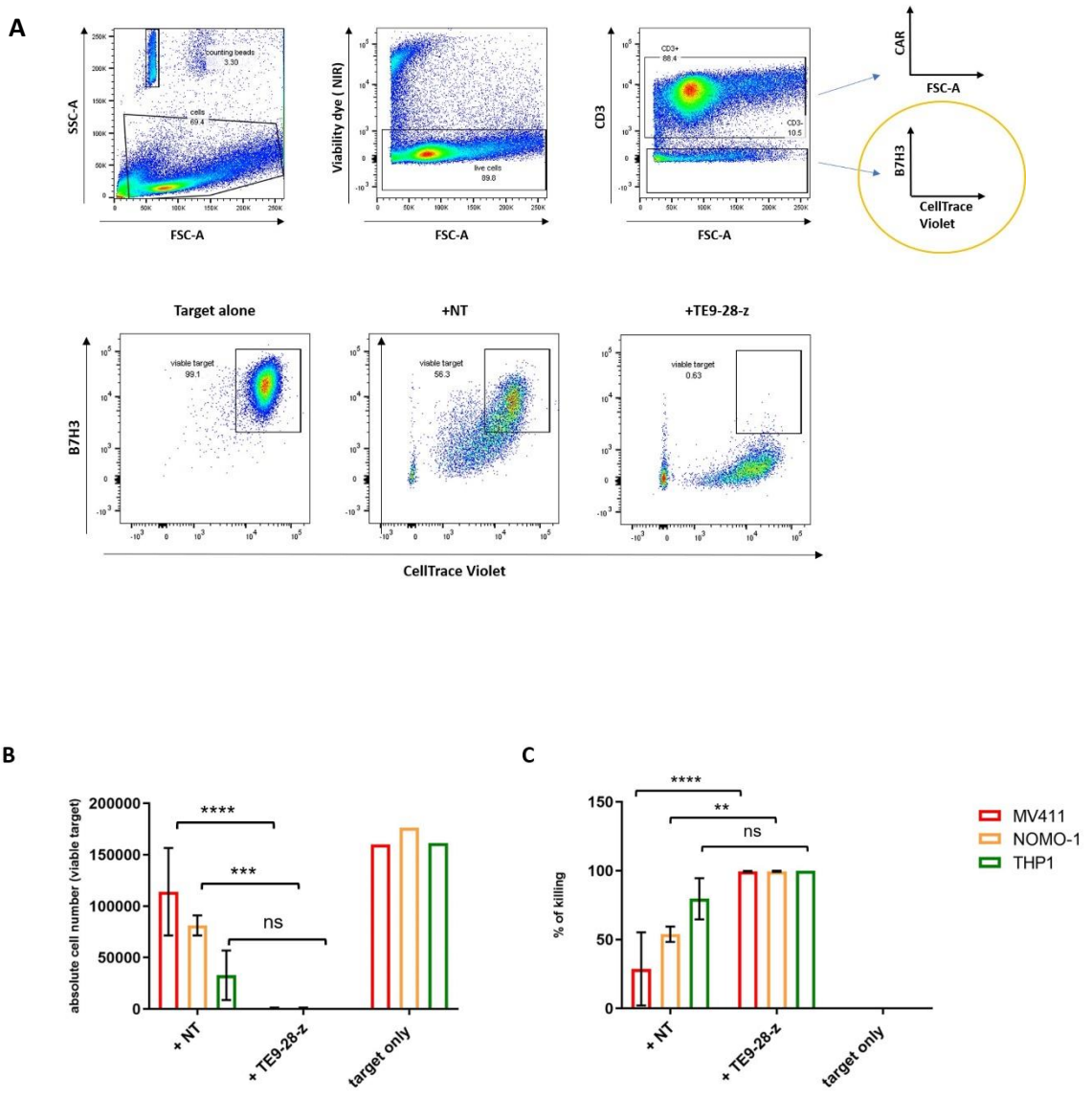

Figure 3.14 cytotoxicity mediated by TE9-CD8 stalk-28-ζ CAR T cells towards AML cell lines in a 18h co-culture at 5:1 E:T ratio. Untransduced αβ T cells and αβ T cells transduced with TE9-CD8 stalk-28-ζ CAR labelled with cell trace violet dye were co-cultured for 18h with AML cell lines MV4-11, NOMO-1 and THP-1 cell line or alone at 5:1 E:T ratio. (A) Representative gating strategy to identify CD3+ cells and Cell Trace labelled B7-H3+ target cells after exclusion of dead and doublet cells. The viable target gating is set on target cells co-cultured with no effectors. (B)Histograms showing the mean absolute target cells numbers ±SD using CountBright absolute counting beads (n=3 independent biological replicates). (C) Histograms showing the % of killing of target cells ±SD (n=3 independent biological replicates). Statistical analysis was performed by 2-way ANOVA, followed by Tukey post hoc analysis: *** p<0.001, *** p=0.0003, ** p=0.0010.

3.5.5.2 Colony-forming unit (CFU) assay

Colony formation assay was set up as described in the material and method section. Due to a shortage of material, among the co-cultures set up with the AML cell lines, only the conditions cultured with NOMO-1 were brought forward in the colony forming unit (CFU) assay.

TE9-CD8-28-ζ CAR T cells were co-cultured with NOMO-1 and Cord Blood at 5:1 E:T ratio for 18h and then 1000 NOMO-1 cells and 10.000 cord blood cells were seeded in a semi-solid matrix – methylcellulose. To clarify, what was seeded was a specific volume from the co-culture, calculated based on the numbers of effectors and targets plated the day prior and the number of cells we'd want to transfer to methylcellulose and accounting no killing has occurred.

Seeding densities were chosen for NOMO-1 and CB conditions to be as comparable as possible, based on the assumption that only one 1% of cells from the CB are hemopoietic progenitors colony forming units. H4434 Classic Methocult media was used as semi-solid matrix: it contains rh SCF (stem cell factor) , rh GM-CSF (Granulocyte macrophage colony-stimulating factor), rh IL-3, rh EPO and allows the growth of CFU-E (Erythroid progenitor cells), BFU-E (burst-forming unit-erythroid), CFU-GM (Granulocyte and/or macrophage progenitor cells) and CFU-GEMM (multi-potential progenitor cells) in CB, as well as promoting leukemic colonies from leukaemia samples or cell lines.

The success of the experiment relies on the basis that TE9-CD8-28-ζ CAR T cells are cytotoxic towards AML cell line NOMO-1, reflecting on less colony forming

units transferred to the Methocult after TE9-CD8-28-ζ CAR T cells are co-cultured with the AML cell lines compared to when they are co-cultured with untransduced T cells.

Conversely, if TE9-CD8-28-ζ CAR T cells were to be not cytotoxic towards the hematopoietic progenitors within the cord blood, no significant difference should be observed between the numbers of colony forming units when TE9-CD8-28-ζ CAR T cells were co-cultured with CB cells compared to when they were cultured with untransduced T cells.

The plates were monitored for two weeks, and the colony formation was quantified on day 14. Numbers and morphology of the colonies were assessed by microscopy. The colonies were stained dark purple with p-iodonitrotetrazolium violet (Sigma. Cat no. I8377-250MG) in order for the colonies to show up on a photograph. This step is toxic to cells and therefore was performed only at the termination of the experiment.

Figure 3.15A shows the colonies formed by NOMO-1 cells and CB after been cultured with no effectors or co-cultured with untransduced or TE9-CD8-28-ζ CAR T cells. The images were taken after the colonies were stained with p-iodonitrotetrazolium violet. Untransduced and TE9-CD8-28-ζ CAR T cells were also cultured with no target to identify any background colony formation induced by the effector cells. Both NOMO-1 cells and CB cells induced colony formation when cultured with no target. Colony formation can be observed also when the targets where co-cultured with untransduced T cells. The difference in colony formation between NOMO-1 and CB was striking when observing the effect of TE9-CD8-28-ζ CAR T cells. As it can be seen in the images, TE9-CD8-28-ζ CAR

T cells depleted the formation of leukemic colonies when co-cultured with NOMO-1, however it did not deplete the formation of colonies when co-cultured with cord blood.

The numbers of colonies were determined by microscopy (Figure 3.15B). From the numbers is evident that Donor 1 had a high background cytotoxicity towards the NOMO-1 compared to the other two donors, however this donor was included in calculating the statistical significance in the difference of colony formation when target where co-cultured with TE9-CD8-28-ζ CAR T cells compared to when they were co-cultured with untransduced T cells.

NOMO-1 leukemic colony formation decreased drastically when the targets were co-cultured with TE9-CD8-28-ζ CAR T compared to the untransduced control. In contrast, no significant difference can be seen in the number of colonies after co-culturing cord blood with TE9-CD8-28-ζ CAR or untraduced T cells (Figure 3.15C).

A

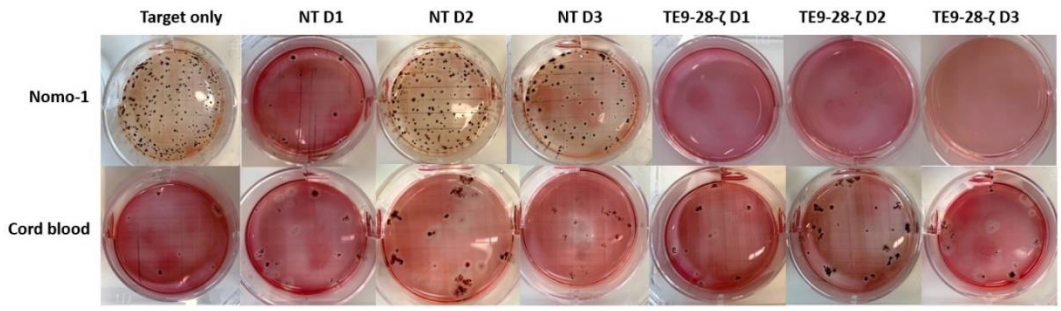

B

		Untransduced			TE9-CD8stalk-28-ζ		
	Target only	D1	D2	D3	D1	D2	D3
NOMO-1	238	15	195	114	0	0	0
Cord Blood	31	37	43	38	40	53	41
Effector only		0	0	0	0	0	0

C

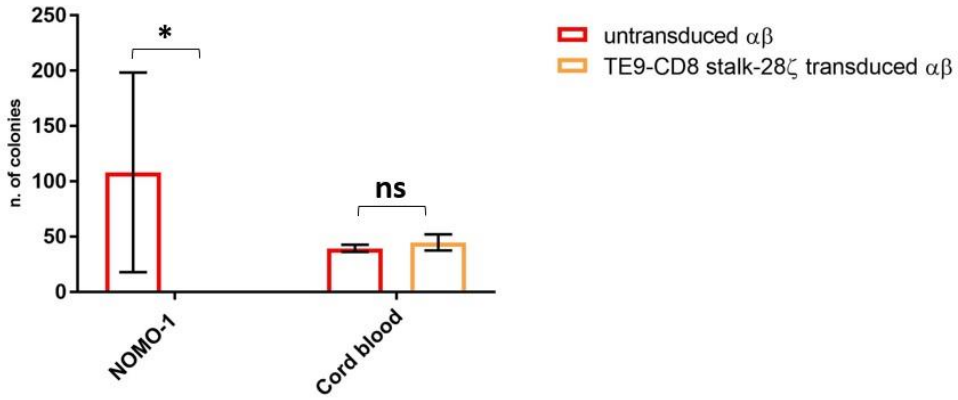

Figure 3.15 Colony forming unit assay. Untransduced αβ T cells and αβ T cells transduced with TE9-CD8 stalk-28-ζ CAR were co-cultured for 18h with AML cell line NOMO-1 or alone at 5:1 E:T ratio. Cells from the co-cultures were then transferred to a semi-solid matrix (H4434 Classic Methocult) at a density of 1000 cell/plate for NOMO-1 and 10.000 cell/plate for cord blood. Cells were incubated for 14 days and monitored throughout. (A) Leukemic colonies, granulocyte-macrophage (CFU-GM) and erythrocyte burst-forming unit erythroid (BFU) colonies were scored on day 14 by microscopy. (B) Statistical analysis was performed by 2-way ANOVA, followed by Tukey post hoc analysis: * p= 0.0380 (n=3 independent biological replicates).

It was not possible to conclude that TE9-CD8-28-ζ CAR T cells were not cytotoxic towards hematopoietic progenitors without investigating whether the CB colony formation derived from both myeloid and erythroid progenitors. Therefore, the morphology of the colonies was assessed by microscopy (Figure 3.16A) and counts for each subpopulation was taken (Figure 3.16B). Figure 3.16A show the morphology of the leukemic colonies derived from NOMO-1 cells.

Based on the morphology of the colonies, we could identify only BFU-E (burst-forming unit erythroid) and CFU-GM (granulocyte-macrophage progenitor cells) colonies. As can be seen from the microscopy images both BFU-E and CFU-GM

colonies were detected after CB was co-cultured with untransduced T cells but also after being co-cultured with TE9-CD8-28-ζ CAR T cells. No significant difference was detected in terms of number of erythroid or myeloid colonies between the untransduced and the TE9-CD8-28-ζ CAR T co-cultures (Fig 3.16C).

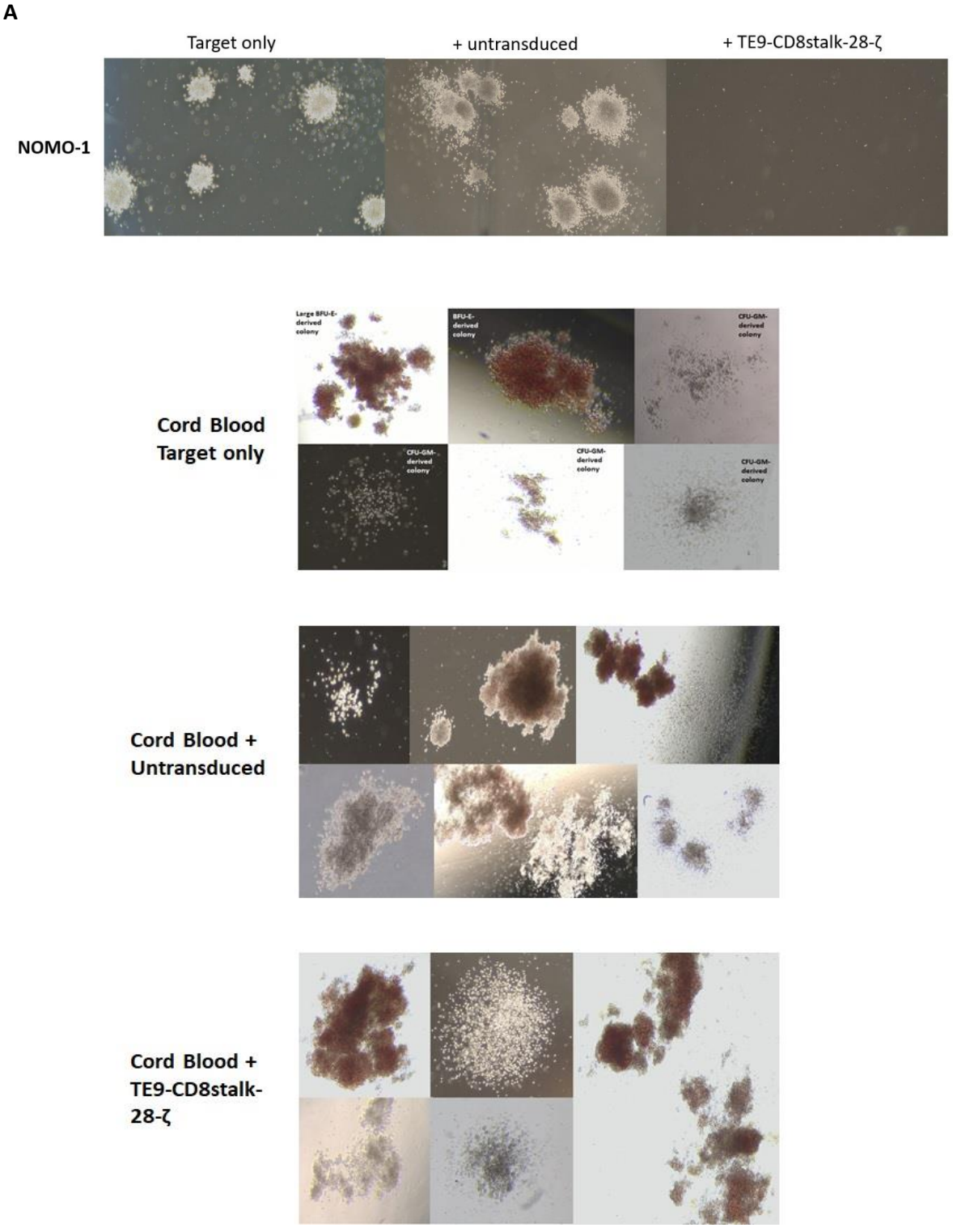

B

		Untransduced			TE9-CD8stalk-28-ζ		
	Target only	D1	D2	D3	D1	D2	D3
Cord Blood total colonies	31	37	42	38	40	53	41
Myeloid colonies	12	10	19	17	9	20	19
Erythroid colonies	19	27	24	21	31	33	22

C

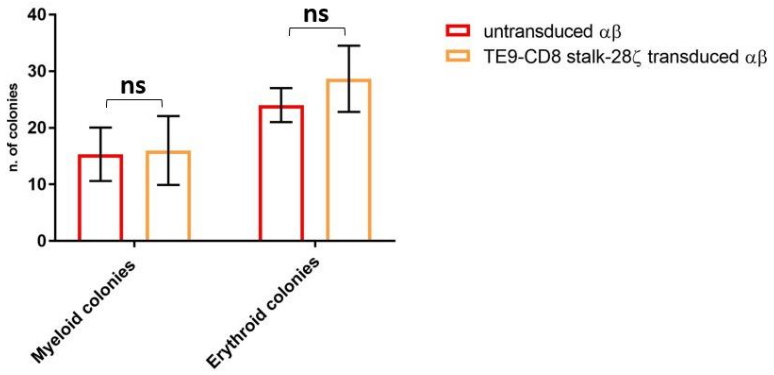

Figure 3.16 Morphology of colony forming units (CFU assay). (A) Morphology of leukemic colonies derived from NOMO-1 and hematopoietic colonies derived from cord blood(CB) was assessed by microscopy. (B) number of BFU-E (burst-forming unit erythroid) CFU-GM (granulocyte-macrophage) colonies was assessed by microscopy. (C) Statistical analysis was performed by 2-way ANOVA, followed by Tukey post hoc analysis (n=3 independent biological replicates).

3.6 Discussion

The aim of this first chapter was to characterize CD33–specific CAR T cells and B7-H3–specific CAR T cells as potential therapies to target AML as well as to identify a good binder to bring forward in a CCR format to co-express with a γδTCR in αβT cells to investigate that system. The expression profile between the two chosen antigens is quite different with each other.

CD33 is expressed in approximately 90% of myeloblast in patients bearing AML and it is not associated to a specific karyotype which makes it an attractive candidate. While CD33 is overexpressed in AML blasts and leukemic stem cells, it is also expressed in myeloid-committed cells in the bone marrow and on circulating monocytes and is constitutively expressed on dendritic cells. The potential toxicity would lead to ablation of the myeloid cell pool and bone marrow failure, which is not tolerable toxicity. CD33 as target antigen for AML has been widely studied in both antibodies and CAR based strategies. Gemtuzumab ozogamicin, which is an immunoconjugate combining anti-CD33 antibody with the toxin calicheamicin, has reported 30% response rate in a phase II clinical study (Sievers et al., 2001) and is currently used in clinical practise. Other studies have focus on targeting CD33 with CAR T cell-based strategies, and while potent in vitro activity against AML cell lines have been demonstrated, the reported anti-tumour effects were associated with profound cytopenia (Kenderian et al., 2015).

In contrast, B7-H3 has only recently been considered as potential target for AML-directed CAR T-cell therapy. B7-H3 has been found to be overexpressed in multiple human cancers including being overexpressed on the leukemic blasts in patients with AML. B7-H3 expression in AML appears to be higher in AML with a

monocytic immunophenotype (Guery et al., 2015), which is often associated with aggressive clinical features (Dobrowolska et al., 2013).

In this chapter we evaluated alongside 4 different CAR constructs: two CAR constructs targeting B7H3 and two CAR constructs targeting CD33, containing either a CH2CH3 stalk (Fc stalk) or a CD8 stalk as spacer: CD33-Fc-28ζ, CD33-CD8-28ζ, TE9-Fc-28ζ and TE9-CD8-28ζ. The rationale for investigating constructs with a different spacer is because the spacer region is responsible of projecting the scFv into the extracellular cytoplasmic space and should provide sufficient flexibility to the immune synapse size to facilitate access to the target antigen. The location of the epitope recognized by the scFv and the length and flexibility of the spacer are important factors to consider for CAR functionality, as they are involved in antigen engagement and formation of the immunological synapse between target and effector (Guest et al., 2005; Hombach et al., 2000; Moritz & Groner, 1995).

As mentioned previously, the Fc stalk is longer and more flexible compared to a CD8 hinge spacer and has better access to binding epitopes proximal to the target cell membrane. The Fc stalk included in our constructs contains mutations to prevent unintended binding of bystander IgG Fcγ receptors on innate immune cells (Hombach et al., 2010; Hudecek et al., 2015). In contrast, CD8 spacer is a shorter and less flexible non-IgG–based spacer, naturally lacking FcγR binding activity.

The generated second-generation CD33–specific and B7-H3–specific CAR constructs were then investigated in vitro to assess their anti-tumour activity. Firstly, CD33 and B7H3 expression was evaluated on a panel of cell lines through median fluorescence intensity (MFI) by flow cytometry (**Figures 3.2 - 3.3**). CD33 and B7H3 expression was confirmed on AML cell lines MV4-11, NOMO-1, and

THP-1. Isogenic cell lines SUP-T1 WT and SUP-T1 CD33 were used to test antigen dependent activity of the anti-CD33 CAR T cells. CD33 expression was confirmed on SUP-T1 CD33, while no CD33 was detected on SUP-T1 WT. In contrast, isogenic cell lines Jurkat WT and Jurkat B7H3 were used to test antigen dependent activity of the anti-B7-H3 CAR T cells. B7H3 expression was confirmed on Jurkat B7-H3 , while no B7-H3 was detected on Jurkat WT.

As we are evaluating these CAR constructs alongside each other, we are aware that it would have been more accurate to test them in the same isogenic cell line expressing either CD33 or B7-H3, however, at the time there was no availability of SUP-T1 B7-H3 or Jurkat CD33 cell lines in the lab. In order to avoid time constraint associated with the process of producing a new cell line, we decided to use the above mentioned two different isogenic cell lines to assess antigen-dependent activities of the anti-CD33 and anti-B7H3 CARs.

T cell lymphocytes were transduced with retroviral supernatant produced by triple transfection of 293Ts to express CD33-Fc stalk-28-ζ , CD33-CD8 stalk-28-ζ, TE9-Fc stalk-28-ζ and TE9-CD8 stalk-28-ζ CAR constructs. The expression of the four CAR constructs on T cell lymphocytes was then investigated by flow cytometry. All the CARs constructs, as previously described contained a RQR8 sequence preceding the CAR sequence, encoding for a RQR8 molecule, which is co-expressed with the CAR for selection and safety purposes (Philip et al., 2014). RQR8 contains a 16 amino acid epitope recognised by the anti-CD34 antibody clone QBend10 and which can be used for detection and/or selection of RQR8+ cells. The CAR and RQR8 sequence are separated by a T2A self-cleaving peptide which is used to achieve equimolar expression of two constructs expressed within

the same viral vector (Daniels et al., 2014, Wang et al., 2011, Szymczak et al., 2004).

However, we found that RQR8 staining did not give an accurate picture on the expression of CD33 CAR T cells (data not shown) therefore we decided to use proteins that would bind directly to the CARs for both anti-CD33 and anti-B7-H3 construct for better accuracy. Biotinylated Human Siglec-3 / CD33 Protein followed by Streptavidin-PE was used to detect CD33 CARs and B7-H3-Histag protein and a secondary anti-His-APC antibody was used to detect B7H3 CARs. All CAR constructs showed comparable transduction efficiency **(Figure 3.4**) with no statistically significant differences in fluorescent intensities. Therefore, based on the assumption that the different ScFv and spacers will not alter the stability or surface expression of the CAR, we hypothesised that whatever difference in activity seen in the following experiments could be attributed to the activity of the CAR, rather than the level of surface expression. However, it is important to mention that having used different detection reagents in order to check transduction efficiency of anti-CD33 CARs versus anti-B7-H3 CARs, we cannot conclude that they have the same expression levels on the cell surface, without quantifying the number of molecules expressed. This will be considered in future experiments.

Functionally effective CAR T cells are expected to lyse target cells, produce proinflammatory cytokines and proliferate in an antigen-dependant manner, therefore, functional assays were performed in order to investigate their in vitro activity.

The cytotoxic activity of anti-CD33-CAR T cells and anti-B7H3 CAR T cells was investigated by a Cr^{51} release assay and firstly assessed on the isogenic cell line positive and negative for their cognate antigen.

As mentioned in the results section, untransduced T cells were used as negative control, however, we are aware the use of an irrelevant CAR, either a truncated version targeting the same antigen of interest or a CAR with the same transmembrane/endodomain structure but targeting an irrelevant antigen, would have been a better control in this context, as all the effectors would have been subjected to similar stress. However, we tried to be as consistent as possible; transduction was performed as described in the material and methods section. All the effectors, untransduced T cells included have gone through the same process from being plated in retronectin precoated plates to being spinoculated at 300g for 40 mins with the only difference that the untransduced T cells received just complete RPMI media while the cells to be transduced received an equivalent volume of viral supernatant.

Both CD33-Fc-28ζ and CD33-CD8-28ζ CAR T cells demonstrated high cytotoxicity towards antigen positive SUP-T1 CD33 while no cell lysis was detected on SUP-T1 WT, demonstrating that the cytotoxic activity of the anti-CD33-CARs was antigen dependent (**Figure 3.5A**). The cytotoxic activity of anti-B7H3-CARs was detected on Jurkat WT and Jurkat B7H3. TE9-CD8-28ζ CAR T cells induced cell lysis in Jurkat B7H3 while no killing was detected on Jurkat WT. In contrast, TE9-Fc-28ζ CAR T cells did not demonstrate any cytotoxic activity in either Jurkat WT or Jurkat B7H3, indeed the percentage of cell lysis was comparable to the one of the untransduced control (**Figure 3.5B**).

The correct spacer is important for engagement with the target cells. While the mechanism behind the lack of killing by the Fc stalk is unknown, we think it might be related to accessibility of the binder to the recognition epitope on B7H3 for the TE9 binder. While the Fc stalk is more flexible than the CD8 spacer, that does not necessarily imply that it has a better chance of accessing a tricky binding epitope; Antigenic dimensions, stalk length, epitope location, are all factor that need to align in a specific setting in order for a functional immune synapse to be formed. Nonetheless, we still decided to bring this CAR forward to evaluate against AML cell lines.

The cytotoxic activity of the CARs was then assessed on AML cell lines MV4-11, NOMO-1, and THP-1 (**Figure 3.6**) TE9-CD8-28ζ CAR T cells demonstrated a significant increase in killing compared to the untransduced control in response to all the AML targets. TE9-Fc-28ζ CAR T cells induced cell lysis in MV4-11, which was found statistically significant when compared to the activity of the untransduced control. However, no increase in killing was seen towards NOMO-1 and THP-1 cell lines. Interestingly both CD33-Fc-28ζ and CD33-CD8-28ζ CAR T cells did not lyse any of the AML target cells, indeed no statistically significant difference was observed in their activity when compared to the untransduced control. As AML cell lines are abundant in Fc-γ receptors, we initially hypothesised that the Fc portion of the CD33-Fc-28ζ CAR might be interfering with the CAR activity by interacting with these receptors, even though this is very unlikely considering that the Fc stalk we are using has been mutated for this very reason. Moreover, even if that were the case for the CD33-Fc-28ζ CAR, this explanation could not be applied for CD33-CD8-28ζ CAR T cells as it contains a CD8 spacer. Before speculating about possible mechanism of action involved in the lack of

killing of AML cell lines by the CD33-Fc-28ζ and CD33-CD8-28ζ CAR T cells, we decided to also evaluate their ability to produce cytokine and proliferate in response to targets.

The production of IL-2 and IFN-γ is crucial for the persistence and proliferation of CAR T cells in vivo. Furthermore, the production of IFN-γ is associated with T cell activation (van der Stegen et al., 2015). We firstly quantified the IFN-γ and IL-2 production mediated by the anti-CD33 CARs and anti-B7-H3 CARs against the isogenic cell lines (**Figure 3.7**). CD33-Fc-28ζ and CD33-CD8-28ζ CAR T cells demonstrated a statically significant increase in IFN-γ, and IL-2 production compared to the untransduced control when they were co-cultured with SUP-T1 CD33, while no detectable amounts of cytokines was produced by neither of the effectors when they were co-cultured with SUP-T1 WT cells. These results provide further evidence of lack of response when the antigen is not engaged.

TE9-CD8-28ζ CAR T cells also demonstrated antigen dependent activation as they produced significant levels IL-2 and IFN-γ in response to Jurkat B7-H3, while no cytokines were detected when the effectors were co-cultured with Jurkat WT. In contrast, in accordance with what was observed in terms of cytotoxic activity, TE9-Fc-28ζ CAR T cells did not produce any cytokines in response to either Jurkat WT or Jurkat B7H3.

Cytokine release was then investigated on AML cell lines (**Figure 3.8**). TE9-CD8-28ζ CAR T cells demonstrated significant production of IL-2 in response to all the AML targets compared to the untransduced control. In contrast IL-2 production was not observed by any of the other effectors. TE9-CD8-28ζ CAR T cells also demonstrated significantly higher production of IFN-γ compared to the

untransduced control and compared to the other effectors. TE9-Fc-28ζ, CD33-Fc-28ζ and CD33-CD8-28ζ CAR T cells also appear to produce some levels of IFN-γ, however it was found not significant when compared to the untransduced control.

An important characteristic of CAR T cells is their ability to proliferate upon recognition of target antigens and it is equally important that they do not proliferate when their cognate antigen is not present. Therefore, proliferation by our CAR T cells in response to isogenic cell lines positive and negative for their cognate antigen as well as in AML targets, was investigated in a 7-day proliferation assay. Effector cells were labelled with CellTrace violet dye in order to monitor cell proliferation through dye dilution. In order to quantify this short-term proliferation, the change in MFI, referred to as the delta MFI (ΔMFI) of CellTrace violet between the CAR T cell cultured with a specific target and the untransduced T cells cultured with the same target was determined (**Figure 3.9**).

It was observed that CD33-Fc-28ζ and CD33-CD8-28ζ CAR T cells proliferated in response to SUPT1-CD33 while no significant proliferation is observed when they were co-cultured with the antigen negative SUP-T1 WT, in accordance with the cytotoxicity and cytokine data. When the effectors were co-cultured with AML cell lines, it is possible to observe a low level of proliferation of CD33-Fc-28ζ and CD33-CD8-28ζ CAR T cells, with higher ΔMFI for CD33-Fc-28ζ. However, this proliferation in not significant compared to the untransduced control and is not comparable with the high proliferation mediated by the CD33-Fc-28ζ and CD33-CD8-28ζ CAR T cells in response to SUP-T1 CD33.

No significant proliferation was detected in TE9-Fc-28ζ CAR T cells when co-cultured with any of the target compared to the effector cultured with no targets. This result just strengthens the previous cytotoxicity and cytokine release data.

In contrast, TE9-CD8-28ζ CAR T cells proliferated in an antigen-dependent manner: indeed, proliferation is detected in response to Jurkat B7H3 while no significant proliferation is detected in response to Jurkat WT. The effector also proliferated in response to AML targets and the proliferation in response to MV4-11 and NOMO-1 is statically greater than the response to the positive control Jurkat B7-H3.

Overall, these results demonstrated that TE9-CD8-28ζ CAR T cells was able to drive an antitumor response in terms of cytotoxicity, ability to produce cytokines and proliferate in an antigen dependent manner. These data also demonstrated suboptimal activity of TE9-Fc-28ζ CAR T cells against the same targets. TE9-Fc-28ζ CAR T cells demonstrated suboptimal activity towards positive control Jurkat B7H3 as well as AML targets. While we cannot be sure on the mechanism behind the lack of activity, we hypothesis as mentioned previously that it might be related to accessibility of the binder to the recognition epitope on B7H3 for the TE9 binder, due to the length and spatial orientation of the FC stalk. To date, we don't have any information on binding epitope for TE9 scFv.

CD33-Fc-28ζ and CD33-CD8-28ζ CAR T cells were able to mount a response in terms of cytotoxicity, cytokine production and proliferation in an antigen dependent manner when tested against SUP-T1 WT and SUP-T1 CD33 but were suboptimal against AML targets. While we do not know the exact mechanism behind the lack of activity towards these targets, we can speculate on possible reasons.

Majzner et al. have demonstrated that CD19 CAR activity is dependent upon antigen density and insufficient reactivity against cells with low antigen density has been shown as an important cause of CAR resistance in other studies (Majzner et al., 2020), therefore, we hypothesized that the difference in antigen density between SUP-T1 CD33 and the AML cell lines could be involved in lack of response of the anti-CD33 CARs to the latter. While antigen density was not evaluated directly in any of the target cell lines, the intensity of fluorescence when stained with anti-B7H3 antibody could be taken as an indirect indication of it, to assess differences between targets, considering that the same amount of antibody and the same number of cells were used for staining. In fact, The MFI for CD333 in SUP-T1 CD33 cells is higher than the MFI in the AML cell lines (5X, 6X, 30X respectively for MV-411, NOMO-1 and THP-1).

Another hypothesis is that the CD33 expressed on SUP-T1 CD33 might be a different isoform than the CD33 expressed on AML cell line. This could be tested by producing a soluble CD33 scFv-protein and testing binding to both SUP-T1 CD33 and AML cell lines, however, as generating an optimal CD33 CAR was beyond the scope of the thesis, we did not investigate further.

Based on these results we selected the TE9-CD8-28ζ CAR construct to be brought forward in order to investigate the potential hematopoietic toxicity, which is one on the main limitation of current strategies targeting AML. We firstly investigated the activity of TE9-CD8-28ζ CAR T cells towards allogeneic monocytes isolated from healthy donors. B7H3 expression on monocytes was assessed by flow cytometry and no detection was observed. We then demonstrated the lack of toxicity of TE9-CD8-28ζ CAR T cells towards monocytes in terms of cytotoxicity and cytokine

production (**Figure 3.11 and 3.12**), again strengthening the antigen dependent activity of this CAR.

To provide further evidence of lack of response against healthy monocytes, proliferation of TE9-CD8-28ζ CAR T cells in response to monocytes was assessed. However, high level of background proliferation over 7 days induced by monocytes was detected as also untransduced T cells proliferated (**Figure 3.13**). This suggest that this 7-day assay is non informative for antigen specific effects. Allogeneic reaction occurs when non-self-signal is sensed by alloreactive T cells in this instance; the background proliferation in this context might be attributable to antigen presenting properties of myeloid cells that lead to background stimulation effects in long term assays that were not seen in the short-term cytotoxicity or cytokine assays. Presence of DC could further increase this response, however, there are few circulating DCs in blood, so very few professional APCs are likely to be present in the monocytes population that was isolated using the Pan Monocytes isolation kit.

To investigate further the lack of toxicity towards the myeloid compartment, the activity of TE9-CD8-28ζ CAR T cells towards normal hematopoietic progenitors present in cord blood was investigated in a colony formation assay. TE9-CD8-28ζ CAR T cells were co-cultured with cord blood and AML cell line NOMO-1 for 18 hours before transferring comparable seeding densities to a methylcellulose matrix containing rh SCF (stem cell factor) , rh GM-CSF (Granulocyte macrophage colony-stimulating factor) rh IL-3, and rh EPO which allows the growth of erythroid progenitor cells (CFU-E), burst-forming unit-erythroid (BFU-E), granulocyte and/or macrophage progenitor cells (CFU-GM) and multi-potential progenitor cells (CFU-

GEMM) in cord blood, as well as promoting growth of leukemic colonies from leukaemia samples or cell lines.

After 14 days the colony formation was assessed by microscopy (**Figures 3.15 – 3.16**). TE9-CD8-28ζ CAR T cells completely depleted the colony formation of leukemic colonies derived from NOMO-1 cells; indeed, a striking difference can be observed when compared to the untransduced control. In contrast, TE9-CD8-28ζ CAR T cells did not deplete the colony formation from either myeloid or erythroid progenitors from cord blood, indeed the presence of both BFU-E (burst-forming unit erythroid) and CFU-GM (granulocyte-macrophage progenitor cells) colonies were detected after cord blood was co-cultured TE9-CD8-28-ζ CAR T cells.

Overall, these results show that B7H3 could be a suitable candidate for targeted therapies as TE9-CD8-28-ζ CAR T cells demonstrated antigen dependent anti-tumour activity and lack of toxicity in the hematopoietic compartment.

An in vivo study is essential to complete this set of data, however due to time limitation it was not possible to conduct the experiment. However, a large batch of NOMO-1-GFP luciferase cells to allow tracking in vivo and matched untransduced and TE9-CD8-28-ζ CAR T cells have been produced as an in vivo experiment to evaluate the activity of TE9-CD8-28-ζ CAR T cells in NSG engrafted with NOMO-1 is in the plan for the future.

4 RESULTS II - transfer of a tumour-reactive γδ T-cell receptor to redirect αβ T antitumour activity.

4.1 Introduction

T-cell receptor transfer by gene transfer technology widened the field of in vitro manipulation. It has been used since, to target a variety of viral and tumour antigens with significant therapeutic potential for both haematological and solid tumours (R. A. Morgan et al., 2006). The vast majority of the studies focus on αβ TCR gene transfer, however, as mentioned previously limitations such as restriction of HLA types and the presence of pre-existing endogenous TCRs with potential mispairing leading to unpredictable target specificity, incentivize towards exploring alternative cell types as substrate for TCR transfer.

An attractive candidate is γδ T cells: they have the potential to kill tumour cells of haematologic and solid tumours (Kabelitz et al., 2007) and because of their TCR which is non-reactive with classical MHC, they are able to mediate selective antitumour reactivity whilst showing relative lack of reactivity to healthy tissues.

However, while αβ T cells have been used extensively and shown their potential to mediate tumour responses and to persist long term to prevent recurrence, γδ T has no proven track record in adoptive transfer for long term disease control. Additionally, in previous work conducted by our own lab it was found that γδ T from blood failed to expand beyond 2 -3 weeks in vitro suggesting that they might lack memory cells capable of long-term disease control.

We therefore hypothesised that γδ TCR in αβ T cells could combine long term expansion and engraftment capacity of αβ T with lack of GVHD and capacity of co-expression with CCR that is associated with γδ T cells.

While the end goal is to co-express on a αβT cell, a tumour reactive γδ TCR and a CCR targeting a tumour associated antigen as an alternative approach to deliver antigen specific tumour reactivity as well as provide a safety mechanism to avoid on-target off tumour toxicity, the focus on this chapter is on characterising the γδ TCR component of the proposed system.

The aim of this chapter consists in exploring the intrinsic proliferative capacity of αβ and γδ T cells and investigating the expression of a tumour reactive γδ TCR on αβ T cells and assessing its ability to redirect αβ T cells against γδ sensitive cancer cells.

4.2 Intrinsic expansion capacity of αβ and γδ T cell populations

In order to explore the hypothesis that αβ T cells could be a better chassis to carry a broadly tumour-reactive γδ TCRs, the intrinsic expansion capacity of αβ and γδ T cells was compared. To evaluate differences in their capacity to expand, PBMCs were isolated from healthy donors and stimulated with soluble anti-CD3 antibody (OKT3). OKT3 stimulate CD3 providing the same stimulus to αβ and γδ T cell populations within the sample of PBMCs.

Cells were kept in culture for 20 days and expansion was assessed by flow cytometry every 4 days post activation with OKT3, using Count Bright Absolute Counting Beads to assess the absolute cell numbers and anti-human αβ TCR and

anti-human Vδ2 antibodies to detect the two populations. Total counts of αβ TCR+ and Vδ2+ cells and frequencies of each cell population within each donor and their fold expansion compared to day 0 baseline were analysed. To assess cell number or percentage of cells at any given time point, the gating strategy displayed in Figure 4.1A was used.

When assessing γδ T cell expansion, we focused our attention on the Vδ2 subset as they are predominant in peripheral blood, and they are the population of γδ T cells that are subject of our investigation in this chapter.

Figures 4.1B and 4.1C show the expansion of αβ and Vδ2 cell populations in three independent biological replicates, over the course of 20 days. In Figure 4.1B, the proliferation is represented as absolute cell numbers at each given timepoint, calculated based on the relative counting beads number. Figure 4.1C shows the fold expansion at each given timepoint relative to the absolute cell numbers on day 0 before stimulation. Our analysis is mainly focused on T cell expansion between day 0 and day 4 as it naturally reaches a plateau after that, given that the cells were not further restimulated and are not re-plated to allow further expansion (Figure 4.1B).αβ TCR+ absolute cell numbers at day 4 increased significantly compared to the unstimulated control on day 0, with a 3.7±0.84 mean ± SD fold T cell expansion compared to the 1.3-fold expansion in Vδ2+ T cells on the same timepoint. The difference in fold change between αβ and Vδ2 populations is statistically significant ($p= 0.0024$).

Figure 4.1D shows the frequencies of αβ TCR+ and Vd2+ cell populations gated on CD3+ lymphocytes. Despite no significant differences between the different

time points are detected, it shows that the frequency of αβ T cell subpopulation prevails on γδ T cells within the T cell population.

Therefore, we hypothesised that expressing a broadly tumour-reactive γδ TCR in αβ T cells might be a method of enhancing its functionality and provide it with a greater intrinsic capacity for cells expressing a γδ TCR to expand.

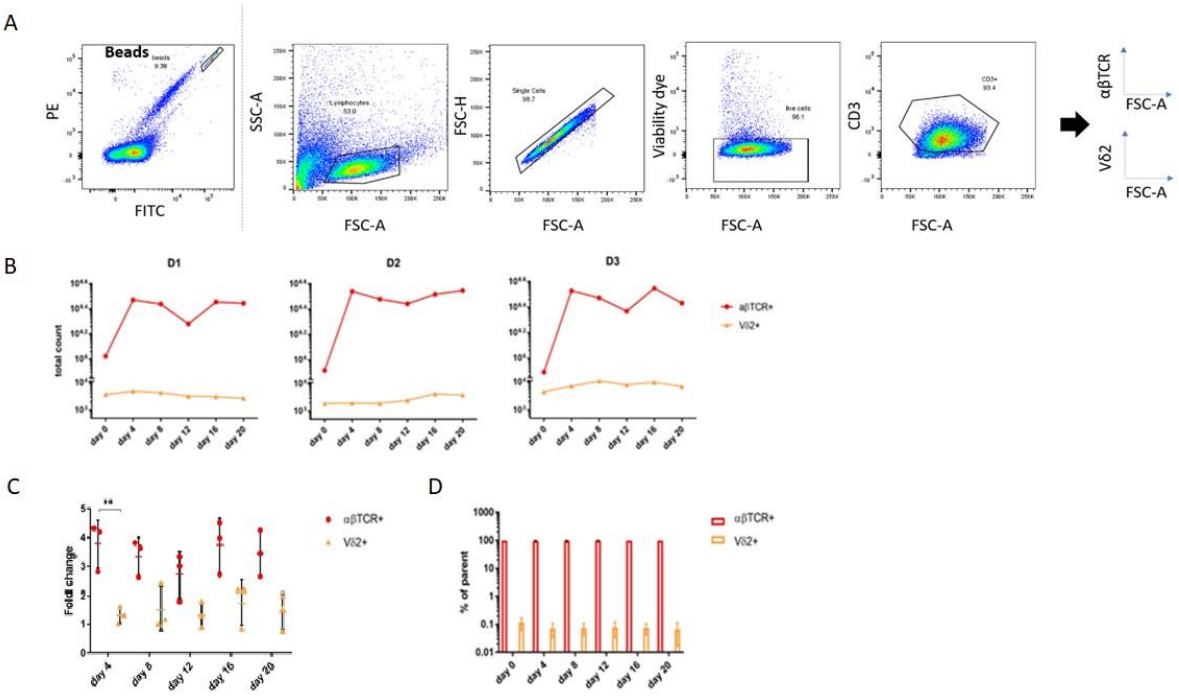

Figure 4.1 Intrinsic proliferative capacity of αβ and γδ T cell populations in response to OKT3 stimulus. Post PBMCs isolation, T cells were stimulated with OKT3 and frequencies of αβ and γδ cells were detected at day 0, 4, 8,12,16 and 20 by flow cytometry. (A) Representative plots showing the gating strategy to detect CD3+ αβTCR+ or CD3+Vδ2+ cells after exclusion of doublets and dead cells. (B) Proliferation of αβ and γδ cells was assessed by determining absolute cell numbers calculated based on relative numbers of counting beads (n=3). (C) Proliferation fold change relative to day 0 absolute counts. (D) Frequencies of αβ and γδ cell within the CD3+ population were detected by using anti-human CD3 BV785, anti- human αβ TCR-FITC and anti- human Vδ2-PE antibodies. Statistical analysis was performed by 2-way ANOVA, followed by Tukey post hoc analysis: ** $p<0.01$.

4.3 Cloning of the retroviral vector expressing G115 transgenic γδ TCR

The widely studied prototypic Vγ9Vδ2 TCR clone G115 was chosen as γδ TCR clone for our study. Its structure was described for the first time by Allison et al in 2001 (Allison et al., 2001) and the sequences of the Vγ9 and Vδ2 chains were published by the team led by Prof. Jurgen Kuball (Patent: 2868439)**.**

The SFG gamma-retroviral vector encoding for the G115 γδ TCR that was used in our study was derived from a plasmid that was originally generated by Dr. Jonathan Fisher. The original plasmid comprised of the G115 γδ TCR sequences in tandem with sequences encoding for an anti-CD33 CCR. For the purpose of our study in this chapter the sequences encoding for the anti-CD33 CCR were eliminated by restriction cloning. The resulting G115 γδ TCR expressing plasmid comprised of a SFG gamma-retroviral vector backbone and the following components between the LTR regions (Figure 4.2):

- G115 Vδ2 published sequence, encoding for the δ chain of the TCR.
- Furin-V5-SGSG-F2A linker between G115 Vγ9 and G115 Vδ2 sequences: Yang et al (Yang et al., 2008) demonstrated that the identity of the linker sequence between the α and β chains had an important role in maximising successful TCR expression and identified the above mentioned Furin cleavage site – V5 peptide – SGSG – F2A peptide linker as the most efficient for αβ TCR expression by comparing different linkers. We hypothesised that the same expression could be achieved for γ and δ chains. Additionally furin and 2A allow for expression of both chains in equimolar expression without

any additional amino acids added. The V5 peptide was originally included by the authors for western blot analysis purposes, however, surprisingly they noticed an increase in TCR expression when the furin cleavage site was followed by a V5 peptide tag. While the exact mechanism for enhanced processing is unknown, the authors speculate that the V5 peptide sequence may permit enhanced ribosomal skipping in this context.

- G115 Vγ9 published sequence encoding for the γ chain of the TCR.

Figure 4.2 Design of G115 γδ TCR expressing construct. The retroviral vector used was the splicing oncoretroviral vector SFG, pseudotyped with an RD114 envelope. The sequences between the LTR regions include G115 Vδ2, furin cleavage site,V5 tag, Ser-Gly linker, F2A peptide, G115 Vγ9.

4.4 Characterization of the transgenic G115 γδ TCR in vitro

4.4.1 Expression of the transgenic G115 γδ TCR on J.RT3-T3.5 cells

In order to validate the G115- γδ TCR construct, its expression was investigated on J.RT3-T3 cell line. J.RT3-T3.5 is a derivative mutant of the Jurkat leukaemia cell line that lacks the beta chain of the T-cell antigen receptor. This results in this cell line not being able to recruit CD3 and therefore form a fully functional TCR-CD3 complex expressed on the cell surface. Introducing the G115- γδ TCR construct in this setting allows it to not incur in TCR chain mispairing and also remove competition for the CD3 recruitment.

In order to investigate the capacity of the cell line for expressing the G115- γδ TCR, J.RT3-T3.5 cells were transduced with retroviral supernatant to express the G115-γδ TCR. Transduction efficacy was assessed by flow cytometry by staining with an anti-CD3 BV785 and anti- Vδ2-PE antibody from Biolegend. The anti- Vδ2-PE antibody is used to detect the Vδ2 chain of the γδ TCR. Untransduced J.RT3-T3.5 cells were used as negative control.

Figure 4.3 shows representative plots illustrating the gating strategy to identify CD3+ Vδ2+ cells after exclusion of doublets and dead cells. The untransduced J.RT3-T3.5 cells were double negative for CD3 and Vδ2. In contrast, J.RT3-T3.5 transduced to express the γδ TCR, are bright for both CD3 and Vδ2. This reflects the ability of the introduced transgenic γδ TCR to recruited CD3 and form a functional TCR-CD3 complex, leading to the expression of the γδ TCR on the cell surface.

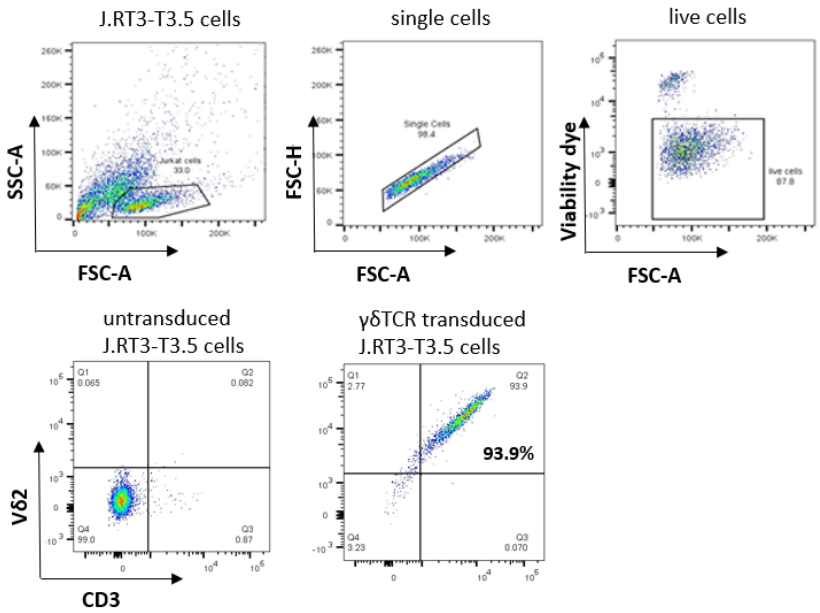

Figure 4.3. Transduction efficacy of G115 γδ TCR construct on J.RT3-T3.5 cells. J.RT3-T3.5 cells were transduced with retroviral supernatant to express G115 γδ TCR construct. Transduction efficiency on untransduced J.RT3-T3.5 and G115 γδ TCR transduced J.RT3-T3.5 cells was determined by flow cytometry. Detection of the CD3+ Vδ2+ population was achieved by using anti-CD3 BV785 and anti- Vδ2-PE antibodies. Representative plots showing the gating strategy to detect CD3 + Vδ2+ cells after exclusion of doublets and dead cells.

4.4.2 Expression of the transgenic G115 γδ TCR on primary human αβ T cells.

After confirming the expression of the G115 γδ TCR construct on J.RT3-T3.5 cell line, its expression on αβ T cells was investigated. In order to achieve this, PBMCs were isolated from healthy donors, and activated αβT cells were transduced on day 4 with retroviral supernatant to express the G115- γδ TCR construct. A fraction of the PBMCs isolated was also used to activate γδ T cells using Zoledronic Acid. These cells as well as untransduced αβT cells were used as controls.

Transduction efficacy was assessed by flow cytometry by staining with anti-CD3 BV785, anti-αβTCR-FITC and anti- Vδ2-PE antibodies from Biolegend. Figure 4.4A shows representative plots illustrating the gating strategy to identify CD3+ cells after exclusion of doublets and dead cells. The cells were then gated on αβTCR and Vδ2. Untransduced αβ T cells were positive for αβTCR and negative for γδ TCR. In contrast αβ T cells that were transduced to express the G115- γδ TCR started to acquire a different distribution as it can be observed on the representative plots.

In the G115- γδ TCR transduced αβ T cells it was possible to identify three different populations:

- A population of cells which remained positive for αβTCR and are negative for Vδ2 (αβTCR+Vδ2-).
- A population that co-expressed the endogenous αβTCR and the transgenic γδTCR (αβTCR+ Vδ2+).
- A population that did not express the endogenous αβTCR but expressed the transgenic γδTCR (αβTCR- Vδ2+).

Figure 4.4B represent the frequency of each population across multiple experiments (n=10). Control non transduced αβ T cells are 93%±3.7 (Mean ± SD) positive for αβTCR and negative for γδ TCR. It is a normal observation to see a small remaining contaminant population following activation, these are cells that have failed to expand but have not died; on previous occasions these contaminant cells have been investigated and they resulted in a small number of B cells and NK cells but very few remaining monocytes.

In contrast, G115- γδ TCR transduced αβ T cells are on average 38.4%±9 is αβTCR+ Vδ2-, 27.6%±6.7 αβTCR+ Vδ2+ and 31.5%±5.7 αβTCR- Vδ2+.

We cannot speculate on the mechanism involved in the downregulation of the endogenous TCR and upregulation of the transgenic TCR. Competition due to greater numbers of the transduced TCR components or greater affinity of γδ TCR for CD3 assembly, or combination of both, or an effect of transgenic TCR to diminish expression of one or both chains of the αβ TCR, could all be plausible mechanism of action.

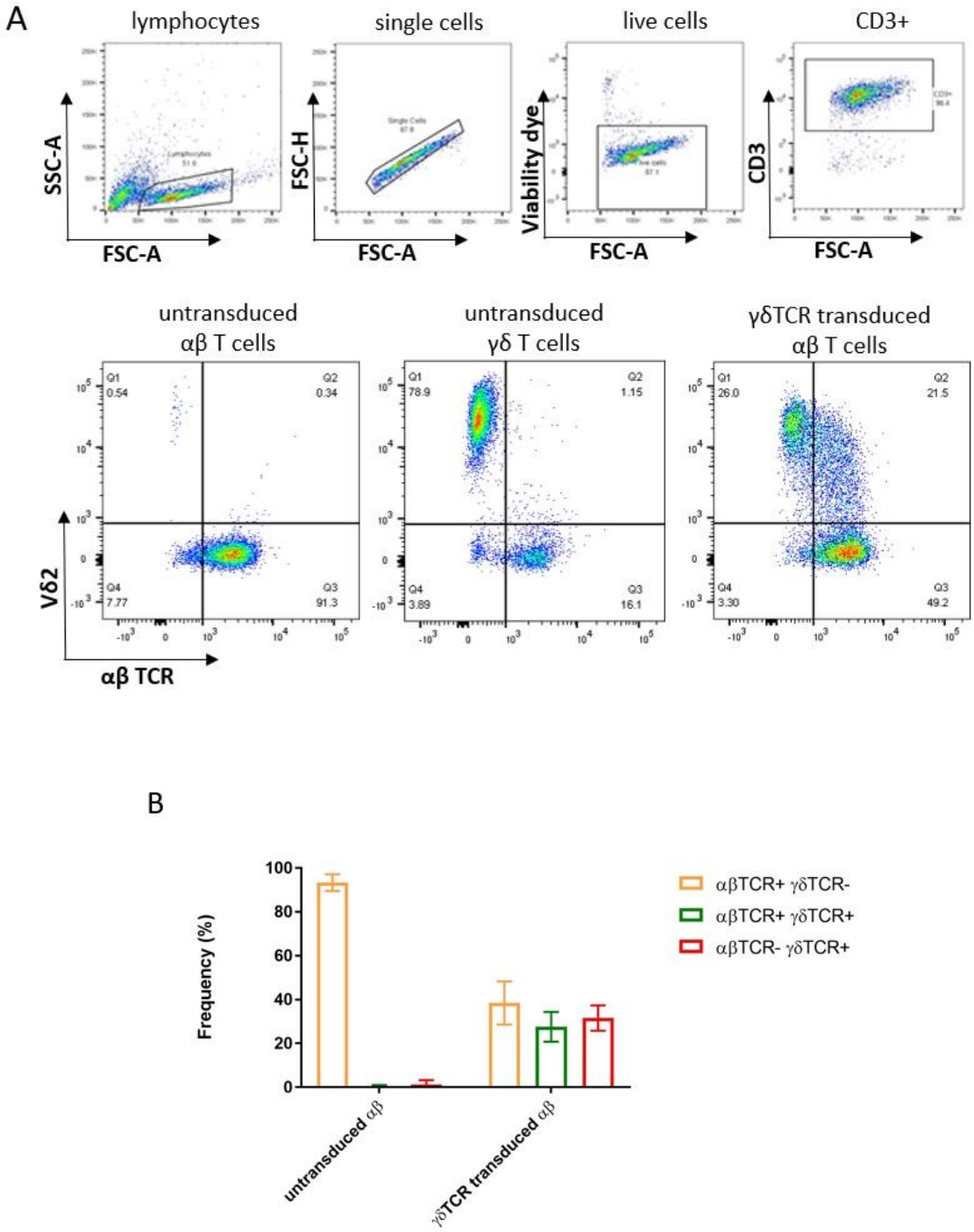

Figure 4.4. Transduction efficacy of G115 γδ TCR construct on primary human αβ T cells. Activated αβ T cells were transduced with retroviral supernatant to express G115 γδ TCR construct on day 4 post isolation. Transduction efficacy was determined by flow cytometry by using anti-CD3 BV785, anti- Vδ2-PE and anti αβ TCR-FITC antibodies. A) Representative plots showing the gating strategy to detect the transduced populations after exclusion of doublets and dead cells. Untransduced αβ T cells and naïve γδ T cells were used as controls. (B) mean expression of each population ± SD (n=10 independent biological replicates).

4.4.3 G115- γδ TCR transduced αβ T cells phenotype

4.4.3.1 CD4 and CD8 expression on G115- γδ TCR transduced αβ T cells.

In order to validate that the αβTCR- Vδ2+ population within the G115- γδ TCR transduced αβ T cells are indeed αβ T cells that have downregulated their endogenous αβ TCR, CD4 and CD8 expression on these cells was investigate by flow cytometry. The majority of naïve γδ T cells are usually CD4−CD8− (>70%) while only some are CD8+CD4− (<30%) and a very few are CD4+CD8−(<1%) (Garcillán et al., 2015). Keeping this expression profile in mind,

αβTCR+ Vδ2- and αβTCR- Vδ2+ populations within the G115- γδ TCR transduced αβ T cells, were stained using anti-human CD4 and anti-human CD8 antibodies.

Figure 4.5A shows representative plots illustrating the gating strategy to identify CD4 and CD8 populations. What was observed was that the CD4 and CD8 expression profile within the αβTCR+ Vδ2- and αβTCR- Vδ2+ populations were comparable. Figure 4.5B illustrate the mean expression of CD4 and CD8 within the αβTCR+ Vδ2- and αβTCR- Vδ2+ populations of the G115- γδ TCR transduced αβ T cells across 3 independent donors. 42±5.5% of the cells were CD4+ and 52.1±8% CD8+ within the αβTCR+ Vδ2- population and 46.6±8% were CD4+ and 47.4±8.5% were CD8+ within the αβTCR- Vδ2+ population. No statistically significant differences were found between the expression levels of CD4 and CD8 across the two populations analysed.

To avoid the possibility that the αβTCR- Vδ2+ population within the G115- γδ TCR transduced αβ T cells derived from a transduction-induced expansion of a small population of naïve γδ T cells present in the PBMCs, we originally depleted γδ T

cells using magnetic separation after PBMCs isolation and before activating the T cells. However, we observed that the depletion was putting unnecessary stress on the cells, interfering with the normal expansion of αβ T cells (data not shown). Detecting CD4 and CD8 expression on the G115- γδ TCR transduced αβ T is a valid alternative to confirm that the majority of transduced T cells are indeed αβ T cells that have downregulated their endogenous αβ TCR. Therefore, no γδ depletion was performed in any of the following experiments.

To confirm the identity of such population sequencing of the cells to demonstrate functional rearrangements of the αβ TCR and lack of rearrangements of the γδ TCR would be required. However, the cost and the complexity of this approach is beyond the scope of the thesis. Therefore, while CD4 and CD8 expression is circumstantial evidence and does not fully prove that the single positive population are αβ T cells that have downregulated their endogenous, we proceeded on the assumption that we were evaluating converted αβ T cells.

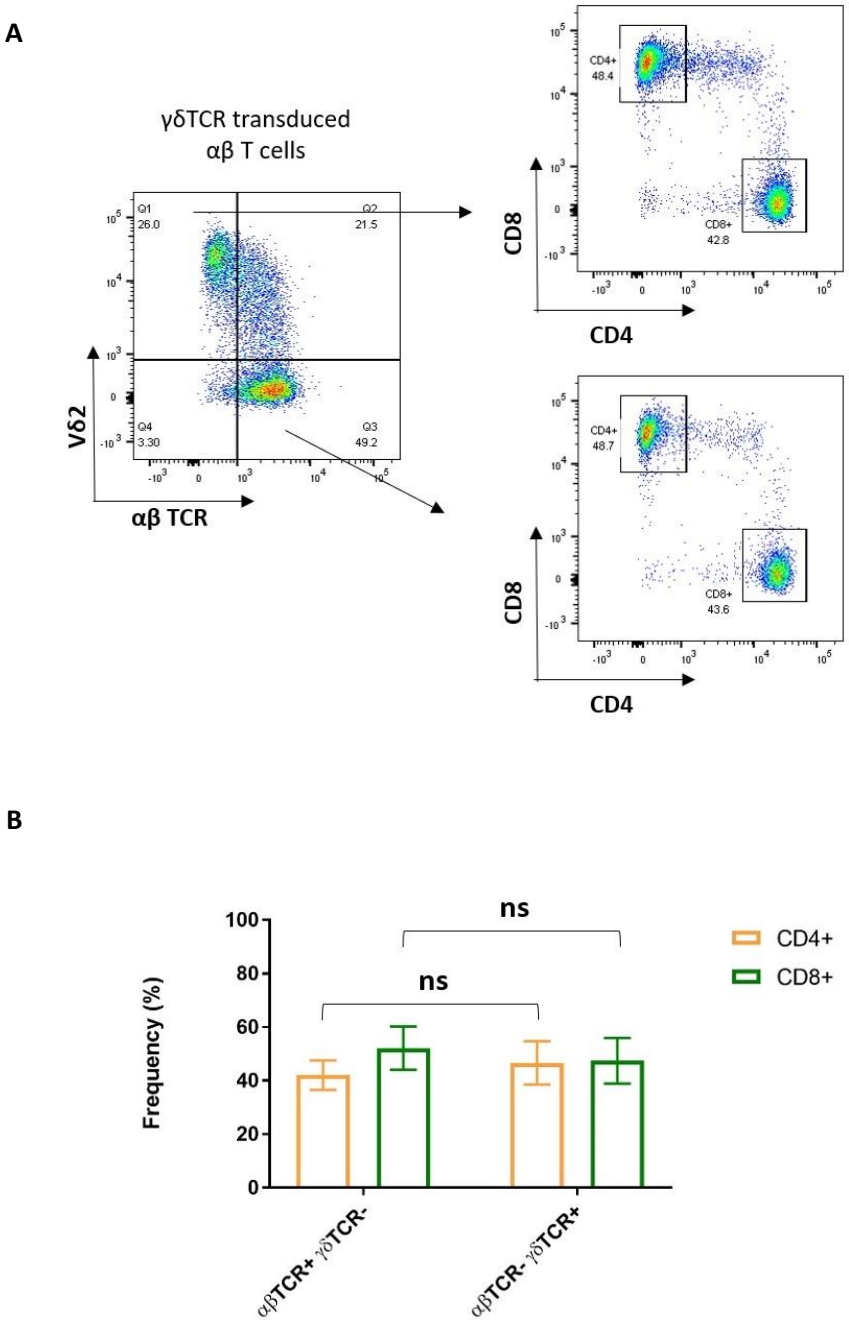

Figure 4.5 Expression on CD4 and CD8 on G115 γδ TCR transduced αβ T cells. Activated αβ T cells were transduced with retroviral supernatant to express G115 γδ TCR construct. (A) Representative plots showing the gating strategy to identify CD4 and CD8 populations. CD4 and CD8 expression in the αβTCR- γδ TCR+ and αβTCR+ γδ TCR- populations within the G115- γδ TCR transduced αβ T cells was determined by flow cytometry by using anti-human CD4 and anti-human CD8 antibodies after exclusion of doublets and dead cells and gating on CD3+ cells. (B) mean expression of CD4 and CD8 populations ± SD (n=3 independent biological replicates). Statistical analysis was performed by 2-way ANOVA, followed by Tukey post hoc analysis.

4.4.3.2 CD16 and CD56 expression on G115- γδ TCR transduced αβ T cells.

Expression of NK-like receptor such as CD16 (Fcγ receptor III) and CD56 on G115- γδ TCR transduced αβ T cells was assessed by flow cytometry in order to investigate whether the G115- γδ TCR gene transfer conferred any γδ-like phenotypical features to the αβ T cells. CD56 and CD16 are both associated with a cytotoxic phenotype, CD16 in particular facilitate antibody-dependent cellular cytotoxicity (ADCC) by binding to the Fc portion of various antibodies.

In order to investigate this, G115- γδ TCR transduced αβ T cells, untransduced αβ T cells and untransduced γδ T cells were stained with anti-CD3, anti αβ TCR, anti-Vδ2, anti CD56 and anti-CD16 antibodies. Cells were gated on CD3+ cells after exclusion of doublets and dead cell, and then gated on the αβ TCR and Vδ2 as shown previously. Untransduced αβ T cells, untransduced γδ T and all the 3 population within the γδ TCR transduced αβ T cells, were then gated on CD16 and CD56 (Figure 4.6A). Figure 4.6B shows the mean CD16 and CD56 expression ± SD across 3 independent biological replicates.

CD56 was expressed in 39±7% of naïve γδ T cells, while there was only a background level of expression on untransduced αβ T cells. All 3 populations within the G115- γδ TCR transduced αβ T cells retained the same expression profile of the latter. CD16 was expressed in 99±0.1% of naïve γδ T and in 39±1.9% of untransduced αβ T ($p<0.0001$). Interestingly in the G115- γδ TCR transduced αβ T cells, the different populations expressed different levels of CD16.

The untransduced αβ TCR+ γδ TCR- population retained the same expression levels of naïve untransduced αβ T (40±2%), indeed no statistically significant difference was detected. The αβ TCR+ γδ TCR+ population which co-express both

TCRs, started upregulating CD16 with a mean expression level of 70±10%. The single positive population αβ TCR- γδ TCR+ CD16 expression level resembled the one of naïve γδ. Indeed, while statistically significant differences in CD16 levels of expression could be detected between the αβ TCR+ γδ TCR- and the αβ TCR- γδ TCR+ populations ($p<0.0001$), no significant difference in CD16 levels between the αβ TCR- γδ TCR+ population and naïve γδ T cells was detected.

The upregulation of CD16 by itself is not proof of conversion to a γδ phenotype, as in NK cells CD16 is a well-recognised activation marker. Therefore, the αβ T cells expressing CD16 may represent activated conventional or unconventional αβ T cells; further studies would be required. However, it is possible that signalling through the transgenic TCR, for example as a result of the stress conditions following viral infection, might manifest as CD16 upregulation. Therefore, we next sought to determine whether the transgenic γδ TCR is functional in the transduced cells.

A

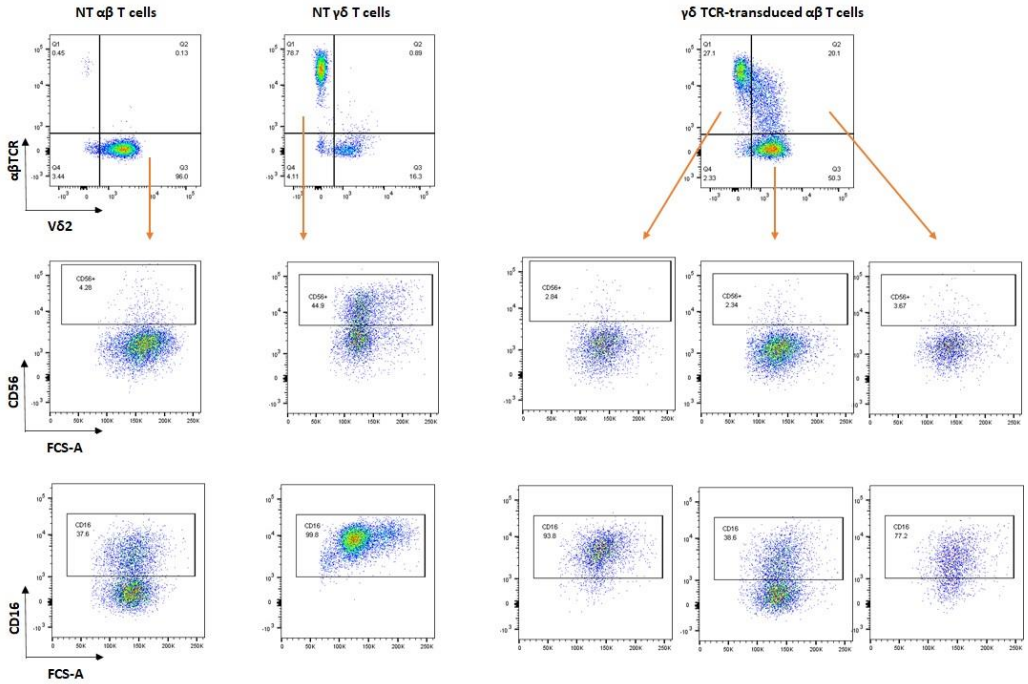

B

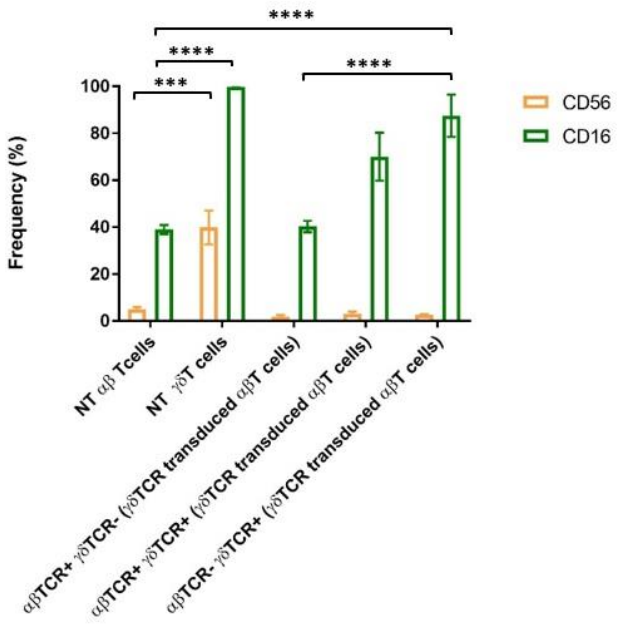

Figure 4.6 CD16 and CD56 expression on G115- γδ TCR transduced αβ T cells. Representative plots showing the gating strategy to identify CD16 and CD56 populations in untransduced αβ T cells, untransduced γδ T cells and G115- γδ TCR transduced αβ T cells. CD16 and CD56 expression was determined by flow cytometry using anti-human CD16 and anti-human CD56 antibodies after exclusion of doublets and dead cells and gating on CD3+ cells (not shown) and then gating on αβ TCR and Vδ2 . (B) mean expression of CD16 and CD56 populations ± SD (n=3 independent biological replicates). Statistical analysis was performed by 2-way ANOVA, followed by Tukey post hoc analysis : ****p<0.0001.

4.4.4 Signalling mediated by G115 transgenic γδ TCR in αβ T cells.

Once the expression of the G115 transgenic γδ TCR on αβ T cells was validated, the focus shifted to assessing the ability of the newly introduced TCR to signal. The signalling cascade consist in a combination of phosphorylation and dephosphorylation events: Phospho-Flow cytometry offers an effective way of measuring signalling at a specific time point in individual cells by assessing the phosphorylated status of proteins involved in the signalling cascade.

The Phospho-Flow assay assesses the signalling upon T cell activation downstream from the TCR. T cell activation is achieved by using anti-TCR

stimulatory primary antibodies and then cross-liking with secondary antibodies to allow the formation of an immunological synapse-like structure. The staining method for detecting signalling molecules and phosphorylated proteins is a bit different from normal intracellular staining. Cells need to be rapidly fixed to avoid dephosphorylation and sometimes stronger permeabilization methods are required to ensure permeabilization of the nuclear membrane. A detailed protocol is described in the material and methods section.

Activated untransduced αβ T cells and G115 γδ TCR transduced αβ T cells were stimulated either with anti-CD3 antibody (OKT3) or anti-Vδ2 antibody (B6) and the phosphorylation state of intracellular proteins ERK, NF-KB and ZAP-70 at 360s was detected by Phospho-Flow. ZAP-70 is immediately downstream from CD3-ζ so it would be predicted to be an early signalling event whereas ERK, NF-KB follows from second messengers including events downstream from calcium influx, so they are likely to be later events.

Post stimulation cells were crosslinked using a donkey anti-mouse secondary antibody. The cells were then fixed, permeabilized by methanol and intracellular staining was performed using pERK, pNF-KB, and pZAP-70 antibodies. Unstimulated effectors were used as control.

Histograms in Figure 4.7A show pERK, pNF-KB, and pZAP-70 signals in one representative donor, when cells were unstimulated (grey), crosslinked with CD3 (red) and crosslinked with Vδ2 (green). Unstimulated control refers to cells that were not treated with stimulatory antibodies. When CD3 was stimulated, both untransduced αβ T cells and G115 γδ TCR transduced αβ T cells showed a shift in the signal for pERK, pNF-KB, and pZAP-70, compared to the unstimulated

controls at 360s following cross linking. This condition was used as a positive control as by stimulating CD3, the activation was induced independently from the type of TCR expressed.

In order to evaluate the signalling through the transgenic G115 γδ TCR, however, untransduced αβ T cells and G115 γδ TCR transduced αβ T cells were stimulated with an anti-Vδ2 antibody. In this instance, untransduced αβ T cells were used as negative control as they do not express a γδ TCR. When Vδ2 was stimulated, pERK, pNF-KB, and pZAP-70 signals induced by untransduced αβ T cells overlap with the unstimulated controls. However, when Vδ2 was stimulated in G115 γδ TCR transduced αβ T cells, the signals of the phosphorylated proteins overlap with the ones induced from CD3 crosslinking. The mean MFI ± SD of pERK, pNF-KB, and pZAP-70 across 3 independent biological replicates are shown in figure 4.7B.

There are no statically significant differences in pERK, pNF-KB, and pZAP-70 signals between untransduced αβ T cells and G115 γδ TCR transduced αβ T cells in the unstimulated conditions and when the effectors are CD3-crosslinked. However, when Vδ2 is cross linked, G115 γδ TCR transduced αβ T cells induced an increase in phosphorylation of ERK, NF-KB, and ZAP-70 compared to the unstimulated controls and compared to the untransduced αβ T cells stimulated with the same antibodies. The shift in MFI of pERK and pNF-KB between untransduced αβ T cells and G115 γδ TCR transduced αβ T cells is statically significant ($p= 0.0367$ and $p= 0.0417$ respectively). While the shift in MFI of Zap-70 follows the same trend, the difference detected is not statistically significant.

The difference in pERK and pNF-KB MFI in the G115 γδ TCR transduced αβ T cells stimulated with Vδ2 is also statistically significant when compared to their

unstimulated controls. Again, while Zap-70 follows the same trend, the difference detected is not statistically significant.

Therefore, in γδ TCR transduced αβ T cells there is evidence that cross linking the transgenic TCR leads to signalling events as manifested by phosphorylation of ERK and Nf-KB pathways at 360s following stimulation. The reason phosphorylation of ZAP70 was not significant in the γδ TCR transduced αβ T cells might reflect the time point of evaluation since ZAP70 as mentioned earlier, is an expected early event following TCR stimulation.

For completeness, this experiment requires to be repeated in the future as a time course experiment : evaluating multiple time points, including earlier time points than 360s would be more accurate and would allow to visualize the contribution of phosphorylation and de-phosphorylation of the investigated signalling molecules over a longer period of time.

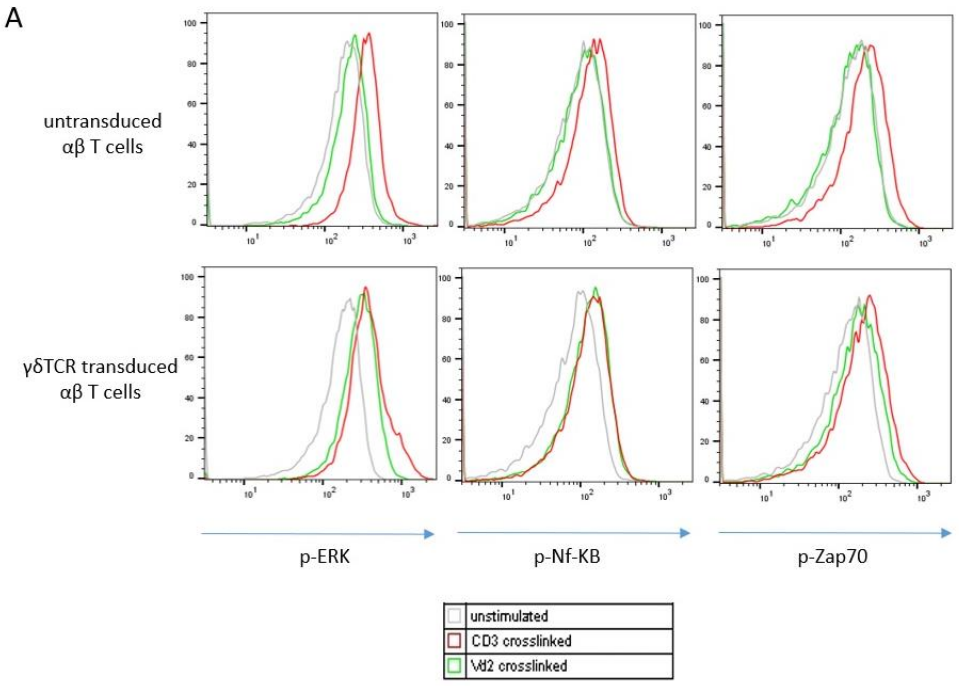

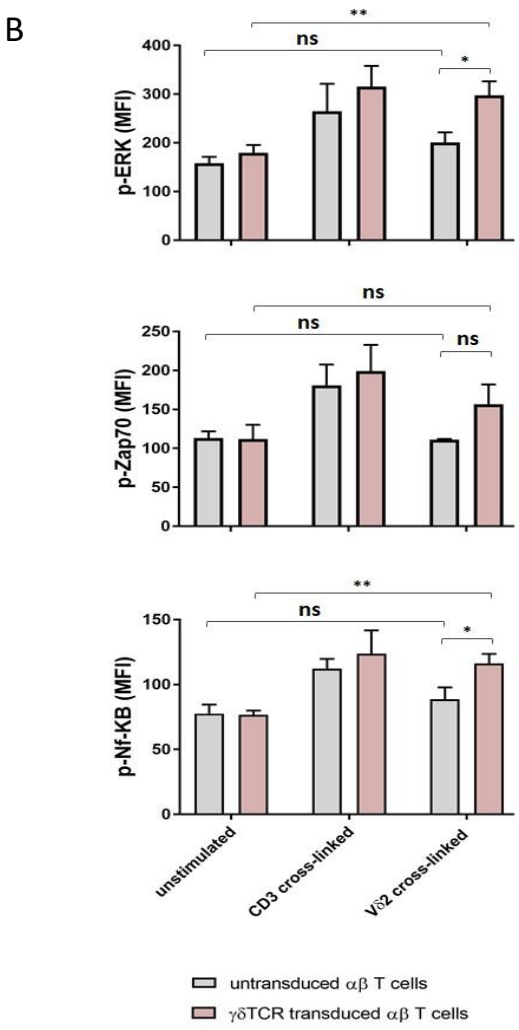

Figure 4.7. Signalling mediated by G115 transgenic γδ TCR in αβ T cells. Activated Untransduced αβ T cells and G115 γδ TCR transduced αβ T cells were stimulated either with anti-CD3 antibody (OKT3) or anti-Vδ2 antibody (B6) and phosphorylation state of intracellular proteins ERK, NF-KB and ZAP-70 was detected by Phosphoflow. Post stimulation cells were crosslinked using a donkey anti-mouse secondary antibody. 360s post crosslinking, cells were fixed, permeabilized by methanol and intracellular staining was performed using anti-pERK, anti-pNF-KB and anti-pZAP-70 antibodies. (A) Representative plots showing pERK, pNF-KB and pZAP-70 signals when cells were unstimulated (grey), crosslinked with CD3 (red) and crosslinked with Vδ2 (green). (B) mean MFI ± SD of pERK, pNF-KB, and pZAP-70 (n=3 independent biological replicates). Statistical analysis was performed by 2-way ANOVA, followed by Tukey post hoc analysis : *p<0.1 **p<0.01.

4.4.5 Cytotoxicity mediated by transgenic G115 γδ TCR in αβ T cells towards a γδ T cell sensitive target.

After confirming the expression of the transgenic G115 γδ TCR on the αβ T cell surface and assessing its ability to initiate a signalling cascade, the ability of G115 γδ TCR construct to redirect αβ T cells cytotoxicity towards a γδ T cell sensitive target, Daudi, was assessed by a 4h chromium (^{51}Cr) release assay.

In order to achieve this, PBMCs were isolated from healthy donors and activated αβT cells were transduced on day 4 with retroviral supernatant to express the G115- γδ TCR construct. Transduction efficacy was confirmed by flow cytometry as described previously. A fraction of the PBMCs isolated was also used to activate γδ T cells using Zoledronate. These untransduced naïve γδ T cells were included as positive control while untransduced αβ T cells were included as negative control. G115- γδ TCR transduced αβ T cells, untransduced αβ T cells and untransduced γδ T cells were incubated with target cells Daudi, at ratios of 10:1, 5:1, 2.5:1 and 1.25:1 for 4 hours and killing compared to background cell death of the target cells with no effector cells and 100% cell death calculated by incubating cells with Triton X-100 to ensure 100% cell lysis. The E:T ratio in this experiment were not corrected for transduction efficiency, therefore the numbers of effector G115- γδ TCR transduced αβ T cells, do not relate just to the G115- γδ TCR+ cells but include all 3 population with different level of γδ and αβTCR that were previously described in figure 4.4, .

As shown in figure 4.8, untransduced αβ T cells did not lyse the Daudi cells (3±3% Mean % ^{51}Cr release ± SD at 10:1 ratio, n= 4 independent biological replicates). In contrast, as expected untransduced γδ T cells demonstrated dose dependent

cytotoxicity towards the Daudi cells (34.5±9.4%). Interestingly, G115- γδ TCR transduced αβ T cells demonstrated overlapping cytotoxicity with untransduced γδ T cells towards the Daudi cell line, suggesting that the transgenic G115- γδ TCR is able to redirect αβ T cells cytotoxicity towards a γδ sensitive target. Indeed, no statistically significant difference in the percentage of ^{51}Cr released between untransduced γδ T cells and G115- γδ TCR transduced αβ T cells was detected. In contrast the difference in cell lysis between the untransduced αβ T cells and G115- γδ TCR transduced αβ T cells was statistically significant ($p<0.0001$).

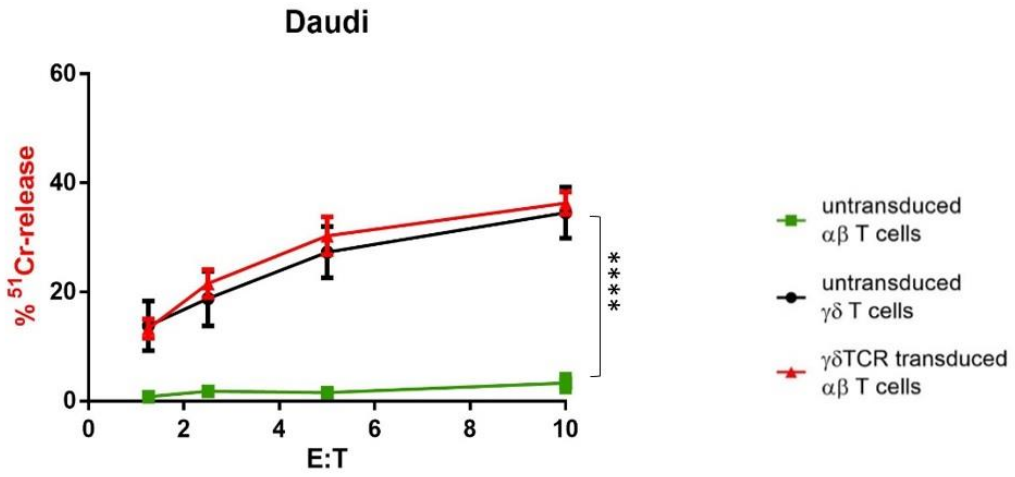

Figure 4.8. Cytotoxicity mediated by transgenic G115 γδ TCR in αβ T cells towards a γδ T cell sensitive target Daudi. G115 γδ TCR transduced αβ T cells were co-cultured for four hours with 51Cr-labelled Daudi target cells, at the following E:T ratios: 1.25:1, 2.5:1, 5:1 and 10:1. Untransduced αβ T cells and untransduced γδ T cells were used as controls. Graphs show mean ± SD (n=4 independent biological replicates). Statistical analysis was performed by 2-way ANOVA, followed by Tukey post hoc analysis : **** p<0.0001.

4.4.6 Quantification of IL-2 and IFN-γ production mediated by transgenic G115 γδ TCR in αβ T cells towards a γδ T cell sensitive target.

G115 γδ TCR transduced αβ T cells ability to produced cytokines such as IFN-γ and IL-2 in response to a γδ sensitive target was then investigated.

In order to study this, untransduced αβ T cells, untransduced γδ T cells and γδ TCR transduced αβ T cells, were co-cultured with Daudi cells for 18h at a 1:1 ratio. Effectors-only condition was included in order to detect any background cytokines production by the effectors. Post co-culture, the cells were pelleted, and the supernatant was collected in order to quantify the cytokines present. As previously described, ELISA to detect IFN-γ and IL-2 was performed according to manufacturer's direction, and plates were analysed by reading the absorbance at 450 nm on a microplate reader and corrected by subtraction of background control values. Cytokines concentration was determined by correlation with a standard curve (Figure 4.9).

Effectors cultured with no target produced very low levels of IFN-γ or IL-2. Untransduced αβ T cells and interestingly also untransduced γδ T cells did produce very low levels of cytokines when co-cultured with Daudi cells. No significant difference was observed between these levels and the one produced when the effectors where culture with no targets.

In contrast γδ TCR transduced αβ T cells co-cultured with Daudi cells produced high concentrations of IL-2 and IFN-γ, 15521±1459 (mean pg/mL cytokine release±SD, n=3) and 22453± 3342 pg/mL respectively, highlighting the role of the transgenic G115- γδ TCR construct in promoting increased cytokine production in αβ T cells ($p<0.0001$). Of interest also, there was a striking difference in cytokine production between untransduced γδ T cells and γδ TCR transduced αβ T cells ($p<0.0001$).

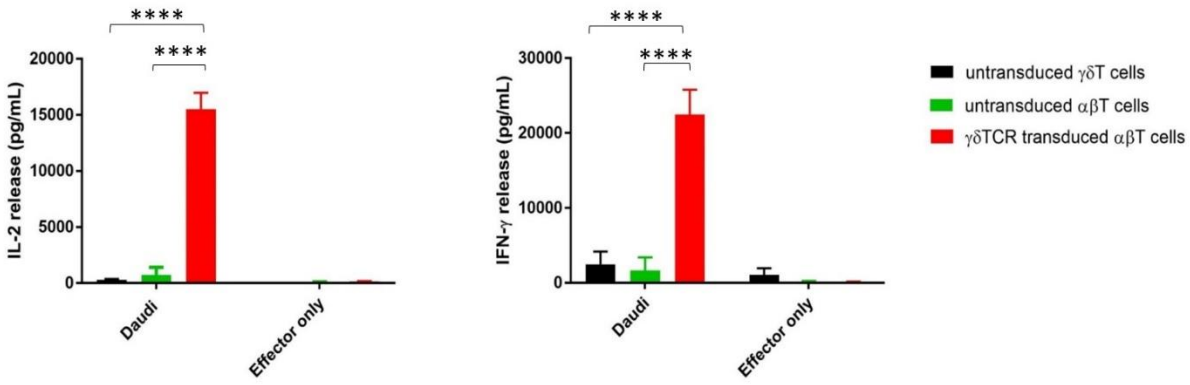

Figure 4.9. Quantification of IL-2 and IFN-γ production mediated by G115 transgenic γδ TCR in αβ T cells towards γδ T cell sensitive target Daudi. G115 γδ TCR transduced αβ T cells were co-cultured for 18 hours with Daudi cell line or alone at 1:1 E:T ratio. Untransduced αβ T cells and untransduced γδ T cells were used as controls. IL-2 and IFN-γ were measured by ELISA from supernatant from the co-culture. Graphs show mean cytokine release ± SD (n=3 independent biological replicates). Statistical analysis was performed by 2-way ANOVA, followed by Tukey post hoc analysis :**** $p<0.0001$.

4.4.7 Proliferation mediated by transgenic γδ TCR in αβ T cells towards a γδ T cell sensitive target

In order to assess the proliferation mediated by transgenic G115, γδ TCR transduced αβ T cells and untransduced αβ T were labelled with Cell trace violet and co-cultured with Daudi cells for 12 days at 1:1 at a density of $0.5x10^6$ cells/well in 0.5 ml of media. Effector T cells were also cultured with no target in order to subtract any background proliferation. Media colour was monitored overtime and media was refreshed if needed. Dilution of Cell trace violet indicating labelled populations that have undergone cell division, was detected by flow cytometry (Figure 4.10) after staining with anti-CD3, anti-αβ TCR and anti-Vδ2 antibodies to gate on the populations of interest.

All the effectors cultured with no target, retained the dye and no visible cell proliferation could be observed as it can be seen in the figure. Untransduced αβ T

cells displayed some unspecific proliferation towards Daudi cells and the same dilution profile was seen for the αβ TCR+ γδ TCR- within the γδ TCR transduced αβ T cell sample. In contrast, Cell trace violet dilution in the αβ TCR+ γδ TCR+ and αβ TCR- γδ TCR+ populations was greater compared to the untransduced controls cultured with the Daudi cells.

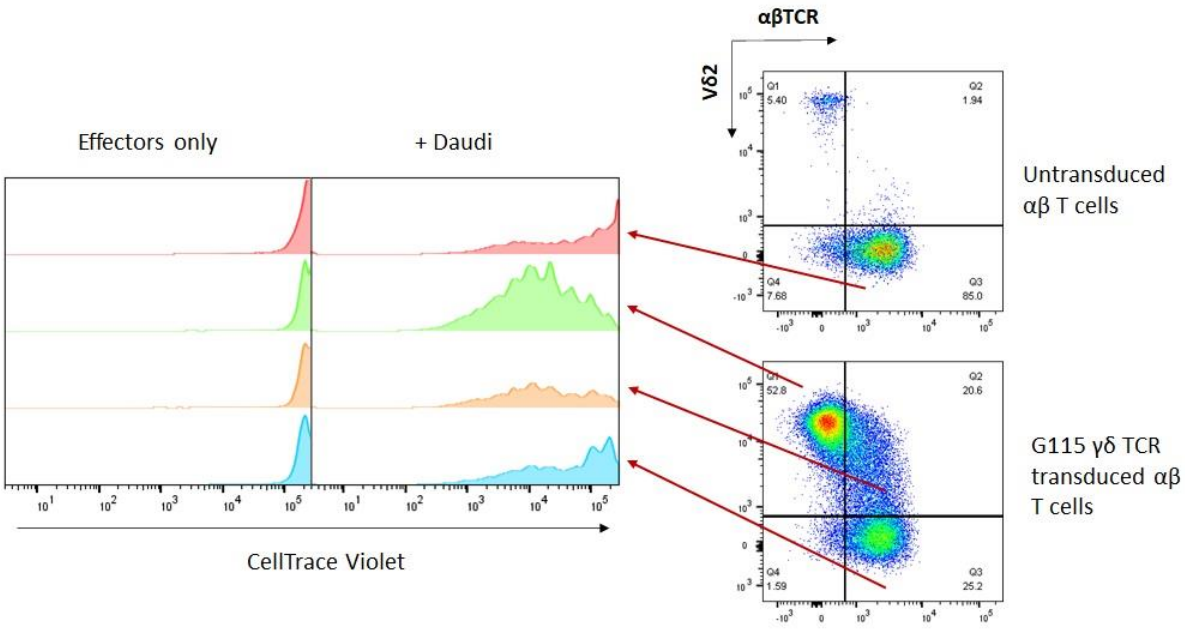

Figure 4.10 Proliferation mediated by transgenic γδ TCR in αβ T cells towards γδ T cell sensitive target Daudi. Untransduced αβ T cells and G115 γδ TCR transduced αβ T cells labelled with cell trace violet proliferation dye were co-cultured for 12 days with Daudi cell line or alone at 1:1 E:T ratio. Cells were stained with anti-CD3, anti-αβ TCR and anti-Vδ2 antibodies after exclusion of doublets and dead cells, in order to gate on the populations of interest. Representative histograms showing the cell trace violet dilution in each population (n=2 independent biological replicates).

4.4.8 Sensitivity to Zoledronate mediated by transgenic G115 γδ TCR in αβ T cells

In order to investigate whether the activity of G115 γδ TCR transduced αβ T cells could be upregulated, their cytotoxic activity as well as their ability to produce cytokines was assessed by culturing them with target cells that have been treated with Zoledronate.

As mentioned in the introduction, Zoledronate is a aminobisphosphonates (NBP) that can be used to inhibit the enzyme farnesyl pyrophosphate synthase of the mevalonate pathway leading to accumulation of intracellular IPP, a type of phosphoantigens that the γδ T cells respond to (Cabillic et al., 2010).In order to achieve this, allogeneic monocytes were used as target. These cells are not normally engaged by γδ T cells, however after being stimulated with Zoledronate they promote γδ T cell engagement by upregulating phosphoantigens (Roelofs et al., 2009). This is also the mechanism involved in ZOL-induced γδ T cells expansion in PBMCs.

Allogeneic monocytes were isolated from PBMCs using magnetic separation and were either cultured without any conditioning or treated with Zoledronate overnight. Untransduced αβ T cells, untransduced γδ T cells and γδ TCR transduced αβ T cells were then co-cultured for 4h with monocytes untreated or treated with ZOL at ratios of 10:1, 5:1, 2.5:1 and 1.25:1 and cytotoxic activity was assessed by a chromium (^{51}Cr) release assay.

As shown in figure 4.11A, untransduced αβ T cells, untransduced γδ T cells and γδ TCR transduced αβ T cells showed very low or background levels of cytotoxicity toward the allogeneic monocytes that were not treated with Zoledronate. When the

effectors were cultured with targets treated with Zoledronate, however, difference in cytotoxic activity was detected. Untransduced αβ T cells showed no change in cytotoxicity even towards the monocytes that were treated with ZOL. No significant difference was detected when compared to the same effector co-cultured with the untreated monocytes. In contrast, both untransduced γδ T cells and γδ TCR transduced αβ T cells demonstrated a statistically significant increase in ^{51}Cr release in response to ZOL-treated monocytes, compared to their response to untreated targets ($p<0.0001$). ^{51}Cr release at 10:1 ratio was 74±3% (Mean % ^{51}Cr release ± SD, n= 3 independent biological replicate) and 43±8% respectively, with the cytotoxic activity induced by γδ T cells significantly superior to the one induced by γδ TCR transduced αβ T cells ($p<0.0001$).

Of note, as previously shown, of γδ TCR transduced αβ T cells only a certain percentage were γδTCR+, hence effective E:T ratios in terms of γδTCR expressing cells is different between the naturally expressing cells and the artificially transduced cells. Therefore, it is not possible to draw inferences from this experiment on the relative cytotoxicity of the naturally expressed receptor versus the transgenic receptor. Cytokine production mediated by the same effectors in the same culturing conditions was also assessed. In order to achieve this, the effectors cells were co-cultured for 18h at a 1:1 ratio with allogeneic monocytes untreated or pre-treated with ZOL and quantification of IFN-γ and IL-2 production was assessed by ELISA (Figure 4.11B). Effectors only condition was included in order to detect any background cytokine production, however no significant background release was detected. Untransduced γδ T cells did not release any detectable amount of IL-2 when co-cultured with untreated or ZOL-treated monocytes. Untransduced αβ T cells, however, produced some level of IL-

2 when co-cultured with untreated monocytes and ZOL-treated monocytes, 2273±1278 (mean pg/mL cytokine release±SD, n=3) and 7094±4551 pg/mL respectively, although no statistically significant difference was detected between the two conditions. We hypothesized that this response can be attributed to alloreactivity, due to the target being allogeneic monocytes.

In contrast, γδ TCR transduced αβ T cells mean IL-2 production when co-cultured with ZOL-treated monocytes was significantly higher compared to the cytokine release when they were co-cultured with untreated target cells. The mean IL-2 release was 8178±1820 pg/mL versus 783±460 pg/mL (p= 0.0012).

γδ T cells produced some levels of IFN-γ, 7542±2901 pg/mL when co-cultured with untreated monocytes and 9942±676 pg/mL when cultured with ZOL-treated target cells, however, there was no statistically significant difference between the two conditions. Again, production of IFN-γ could be attributed to allogenic reaction by contaminant αβ T cells in the expanded γδ T cells samples.

Untransduced αβ T cells seems to have had an allogeneic response to monocytes as they released an even greater amount of IFN-γ when the effector cells were co-cultured with untreated and ZOL-treated target cells. The mean IFN-γ release is 26622±4562 pg/mL and 29539±1835 pg/mL respectively with no significant difference detected.

When analysing γδ TCR transduced αβ T cells activity however, while they did produce some levels of IFN-γ when co-cultured with untreated monocytes (16401±5199 pg/mL), the cytokine production was significantly increased (p=0.0025) when co-cultured with ZOL-treated target cells (27451±2410).

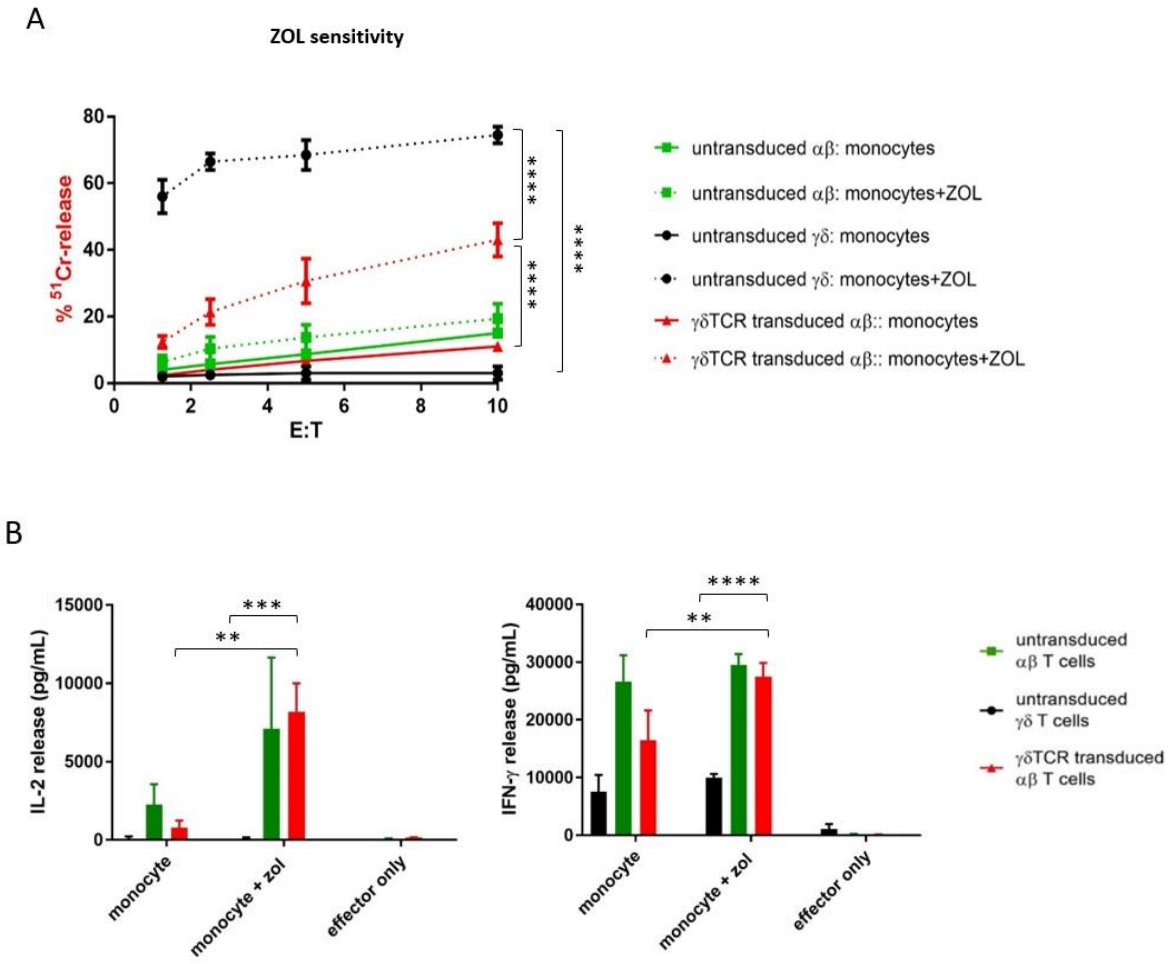

Figure 4.11 Sensitivity to Zoledronate mediated by the transgenic G115 γδ TCR in αβ T cells. (A) Untransduced αβ T cells, untransduced γδ T cells and G115 γδ TCR transduced αβ T cells were co-cultured for 4h with 51Cr-labelled allogeneic monocytes untreated or pre-treated with Zoledronate overnight , at the following E:T ratios: 1.25:1, 2.5:1, 5:1 and 10:1. Graphs show mean ^{51}Cr release ± SD (n=3 independent biological replicates). (B) Quantification of IL-2 and IFN-γ production mediated by G115 transgenic γδ TCR in αβ T cells against allogeneic monocytes untreated or pre-treated with Zoledronate overnight. G115 γδ TCR transduced αβ T cells were co-cultured for 18 hours with target or alone at 1:1 E:T ratio. Graphs show mean cytokine release ± SD (n=3 independent biological replicates). Statistical analysis was performed by 2-way ANOVA, followed by Tukey post hoc analysis : ** P<0.01, *** P<0.001**** p<0.0001.

4.4.9 Selection of γδ TCR+ αβ TCR- αβT cells to eliminate alloreactivity due to the presence of the αβTCR

4.4.9.1 Negative selection of γδ TCR+ αβ TCR- αβT cells

We hypothesised that the allogenic reaction observed in the previous experiment could be attributed to the presence of the αβ TCR. Indeed, in all the previous experiments, the γδ TCR transduced αβ T cells that were used as effectors comprised of a mixed population comprised of γδ TCR- αβ TCR+, γδ TCR+ αβ TCR+ and γδ TCR+ αβ TCR- αβ T cells sub-populations.

Moreover, while using the mixed γδ TCR transduced αβ T cells as effectors was acceptable for the purpose of this chapter, it could complicate interpretation of results in more complicated experimental setting as it will not make it possible to attribute the response seen to a specific population. Therefore, we devised a protocol to isolate our main population of interest, γδ TCR+ αβ TCR- cells within the γδ TCR transduced αβ T cells (Figure 4.12A).

PBMCs were isolated from healthy donors and activated αβT cells were transduced on day 4 with retroviral supernatant to express the G115- γδ TCR construct. Transduction efficacy was confirmed by flow cytometry on day 9. On day 10, γδ TCR+ αβ TCR- αβ T cells were isolated by negative selection using magnetic separation with anti-biotin beads and biotinylated anti- αβ TCR antibody in order to deplete the αβ TCR+ populations. The success of the selection was confirmed by flow cytometry: G115- γδ TCR transduced αβ T cells were stained with anti-CD3, anti-αβ TCR and anti-Vδ2 antibodies. Cells were gated on CD3+ cells as shown previously by excluding doublets and dead cells (gating not shown here). The cells were then gated on Vδ2 and αβ TCR.

Figure 4.12B show representative FACS plot of G115- γδ TCR transduced αβ T cells before and after the depletion of the αβ TCR+ populations. The figure display enrichment of the γδ TCR+ αβ TCR- population as the depletion eliminated the untransduced αβ T cells within the sample as well as the population that co-expressed the αβ TCR and the γδ TCR. Figure 4.12C display mean frequencies of the γδ TCR+ αβ TCR- population before and after depletion. Post depletion 96±0.8% of the CD3+ cells were γδ TCR+ αβ TCR- compared to the 31±4% in the undepleted samples ($p<0.05$).

A

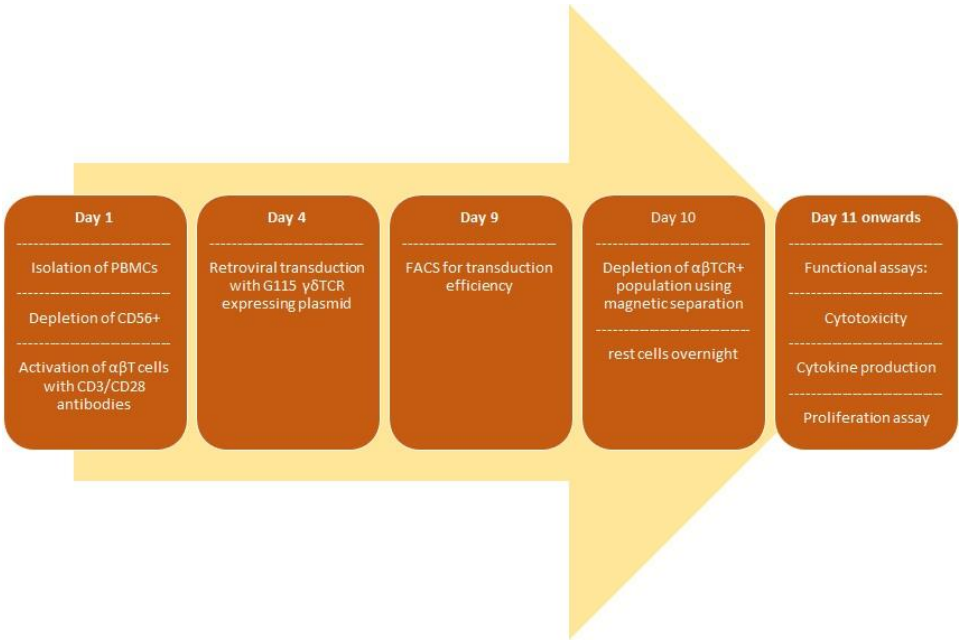

B

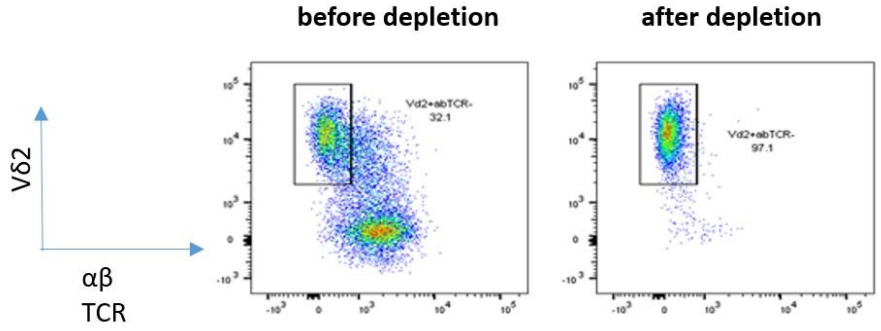

C

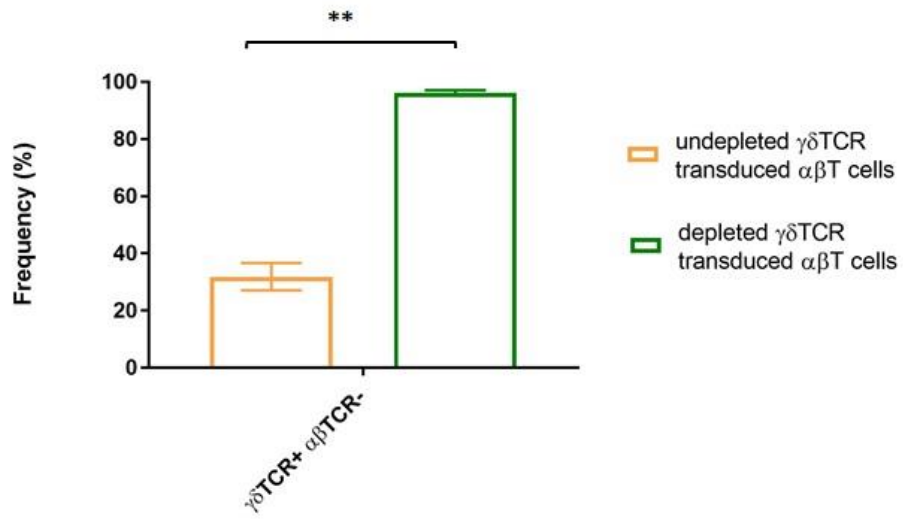

Figure 4.12 Selection of γδ TCR+αβ TCR- αβT cells. G115 γδ TCR transduced αβ T cells were depleted of the αβ TCR+ population through magnetic separation using biotinylated αβ TCR antibody and anti-Biotin Microbeads on day 6 post transduction. After depletion cell were analysed by flow cytometry by using anti- Vδ2-PE and anti αβ TCR-FITC antibodies. (A) diagram showing timeline from PBMCs isolation to functional assays set up. (B) representative FACS plot displaying αβ TCR+ and Vδ2+ populations pre- and post-depletion. (C) Mean frequency ± SD of the γδ TCR+ αβ TCR- population pre- and post-depletion (n=3 independent biological replicates). Statistical analysis was performed by a paired t test: **P<0.05.

4.4.9.2 Cytotoxicity mediated by purified γδ TCR+αβ TCR- αβT cells

In order to assess whether the selected γδ TCR+αβ TCR- αβ T cells display a reduced alloreactivity, untransduced αβ T cells, untransduced γδ T cells, γδ TCR transduced αβ T cells and selected γδ TCR+αβ TCR- αβ T cells were co-cultured for 4h with monocytes at 10:1, 5:1, 2.5:1 and 1.25:1 ratio and cytotoxic activity was assessed by a chromium (^{51}Cr) release assay (Figure 4.13).

While the overall cytotoxicity Is not really high, significant differences between the different populations can be detected. γδ TCR transduced αβ T cells demonstrate

a level of cytotoxicity towards the monocytes which is higher than naïve γδ T cells cytotoxicity ($p< 0.0001$) and close to the ^{51}Cr release profile of the untransduced αβ T cells. In contrast, selected γδ TCR+αβ TCR- αβ T cells cytotoxicity reflects the cytotoxicity profile of the than naïve γδ T cells, indeed no statistically significant difference was detected. ^{51}Cr release towards monocytes by the γδ TCR+αβ TCR- αβ T cells is lower compared to the one prompted by γδ TCR transduced αβ T cells and the difference is statistically significant ($p<0.0001$). This result demonstrated that by depleting the αβ TCR+ population it was possible to reduce alloreactivity by the effectors.

We are aware that cytokines production would have provided a more sensitive marker for alloreactivity, however, due to technical reasons it was not possible to carry out that specific experiment. Ideally, production of IL-2 and IFN-γ should be evaluated for future works.

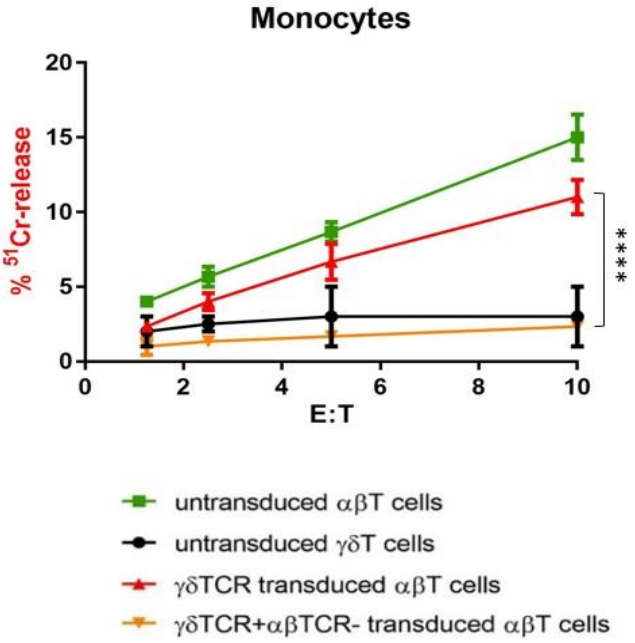

Figure 4.13 Cytotoxicity mediated by un-depleted and depleted G115 γδ TCR transduced αβ T cells against allogeneic monocytes . G115 γδ TCR transduced αβ T cells were co-cultured for

four hours with 51Cr-labelled target cells, at the following E:T ratios: 1.25:1, 2.5:1, 5:1 and 10:1. Untransduced αβ T cells and untransduced γδ T cells were used as controls. Graphs show mean^{51}Cr release ± SD (n=3 independent biological replicates). Statistical analysis was performed by 2-way ANOVA, followed by Tukey post hoc analysis : **** p<0.0001.

4.4.10 Expression of G115 γδ TCR over time.

In order to understand the time window for functional assays as well getting insights on the expression of the G115 γδ TCR over time, the expression of the transgene was assessed by flow cytometry, in both undepleted γδ TCR transduced αβ T cells and in the selected γδ TCR+ αβ TCR- cells on day 6 and 13 post-transduction.

Effector cells were kept in culture without any additional stimulus rather than 100 IU IL-2 every other day, to keep the cells healthy. Cells were stained with anti-CD3, anti-αβ TCR and anti-Vδ2 antibodies and gated on CD3+ cells as shown previously by excluding doublets and dead cells (gating not shown here). The cells were then gated on Vδ2 and αβ TCR.

Figure 4.14A show representative FACS plots gated on αβ TCR and Vδ2 in undepleted and depleted γδ TCR transduced αβ T cells at day 6 and day 13 post-transduction. In both depleted and undepleted conditions it is possible to see a decrease in the Vδ2+ population towards a more αβ TCR+ phenotype. Figure 4.14B shows the mean expression of the γδ TCR+ αβ TCR- population across 3 independent biological replicates and analysis to identify any statistical significance in this drop was performed by 2-way ANOVA, followed by Sidak's post hoc analysis.

The frequency of the population drops from a mean expression of 31±4% on day 6 post-transduction to a mean expression of 19±1% on day 13 post-transduction

in the undepleted γδ TCR transduced αβ T cells (p=0.0097). Following the same trend, the expression levels drop from a mean 96±0.8% on days 6 post-transduction to a 78±5 on day 13 post transduction for the depleted T cells (p=0.0008)

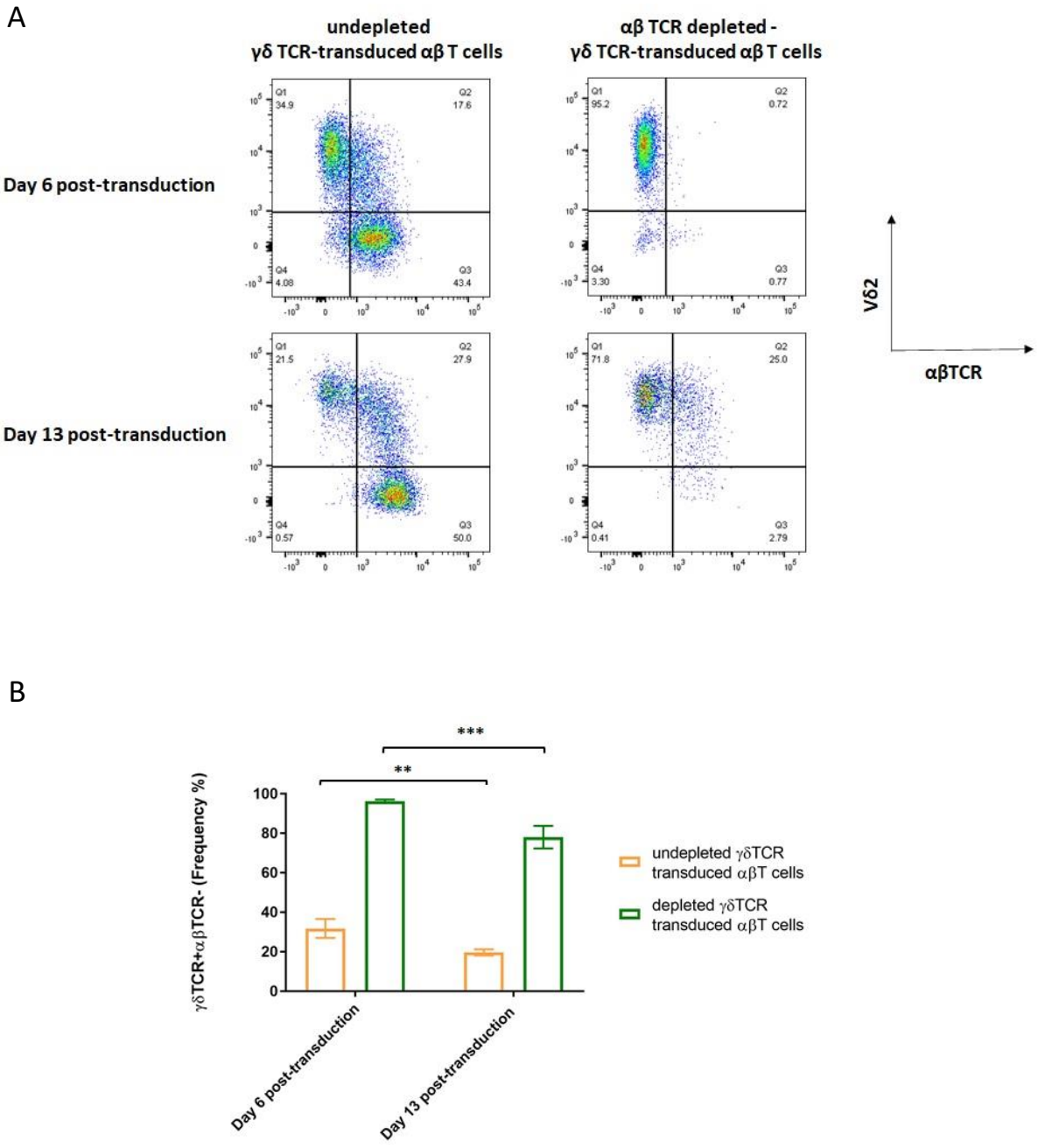

Figure 4.14 Expression of the transgenic G115 γδ TCR overtime. (A) representative FACS plots gated on αβ TCR and Vδ2 in undepleted and depleted γδ TCR transduced αβ T cells at day 6 and day 13 post-transduction. Cells were stained with anti-CD3, anti-αβ TCR and anti-Vδ2

antibodies and gated on CD3+ cells by excluding doublets and dead cells (gating not shown). The cells were then gated on Vδ2 and αβ TCR. (B) mean expression of the γδ TCR+ αβ TCR- population ± SD (n=3 independent biological replicates) in undepleted and depleted γδ TCR transduced αβ T cells. Statistical analysis was performed by 2-way ANOVA, followed by Tukey post hoc analysis : ** $p<0.01$, ***$p<0.001$.

4.5 Discussion

The majority of TCR gene transfer studies have been done in conventional αβ T cells. However, as mentioned previously, limitations such as restriction of HLA types and the presence of pre-existing endogenous TCRs which could lead to unpredictable target specificity through TCR mispairing are valid reasons to explore alternative cell types as substrate for TCR transfer.

γδ T cells represent an attractive alternative as their TCR is non-reactive with classical MHC and they are able to mediate selective antitumour reactivity whilst showing relative lack of alloreactivity. While αβ T cells have been extensively studied and have demonstrated potential in anti-tumour responses and long-term persistence, γδ T cells do not have a proven track record in adoptive transfer for long term disease control. Moreover, previous work from our lab demonstrated that γδ T cells from blood failed to expand beyond 2 -3 weeks in vitro suggesting they might lack memory cells capable of long-term disease control. We therefore hypothesised that γδ TCR in αβ T cells could combine long term expansion and engraftment capacity of αβ T cells with lack of GVHD and capacity of co-expression with a CCR that is associated with γδ T cells as our ultimate goal is to explore a safer approach of targeting AML-associated antigens.

The aim of this chapter consisted in investigating the expression of a tumour reactive γδ TCR on αβ T cells and assessing its ability to redirect αβ T cells against γδ sensitive cancer cells.

To validate our hypothesis that αβ T cells could be a better chassis to carry a broadly tumour-reactive γδ TCRs, we investigated the intrinsic expansion capacity of αβ and γδ T cells within the same samples PBMCs, given the same stimulus

(**Figure 4.1**). PBMCs were stimulated with soluble OKT3 and cultured over 20 days and absolute cell counts of αβ and γδ T cells were calculated by counting beads. Our analysis is limited in scope, focused on the expansion between day 0 and 4 as the cells were not re-stimulated or replated to allow further expansion. We demonstrated, however, that αβ T cells expanded significantly more compared to γδ T cells, as it can be observed in the fold expansion comparing absolute cell numbers to the control on day 0: αβ T cells had a mean fold expansion ± SD of 3.7 compared to the 1.3-fold expansion of γδ T.

This was a preliminary experiment to see if there is a difference in expansion in response to the same stimulus. However, because of differences in CD3 nature and expression between αβ and γδ T cells, it is not possible to conclude that γδ T cells have reduced sustained proliferative response. Nevertheless, the stronger expansion of αβ T to this response was consistent with the idea that insertion of γδ TCR into αβ T cells might have an optimal expansion for a therapeutic agent.

The rest of the chapter focused on investigating the expression of a tumour reactive γδ TCR on αβ T cells and assessing its anti-tumour activity. The prototypic Vγ9Vδ2 TCR clone G115 (Allison et al., 2001) was chosen as γδ TCR clone for our study as it has been widely studied and demonstrated to be tumour reactive. A G115 γδ TCR - SFG gamma-retroviral vector was generated and its surface expression on J.RT3-T3.5 was confirmed by flow cytometry **(Figure 4.3)**. As mentioned previously J.RT3-T3.5 is a derivative mutant of the Jurkat leukaemia cell line that lacks the beta chain of the T-cell antigen receptor, therefore it allows a clean detection of a transgenic TCR.

G115 γδ TCRs surface expression was subsequently assessed in αβ T cells (**Figure 4.4**) and 3 three different populations were detected by flow cytometry post transduction with the transgenic TCR: a population negative for αβ TCR and negative for γδ TCR, a population positive for both αβ and γδ TCRs and a population negative for αβ TCR and positive for γδ TCR.

We are not aware of the exact mechanism of action involved in the downregulation of the endogenous TCR and upregulation of the transgenic TCR. Competition due to greater numbers of the transduced TCR components or greater affinity of γδ TCR for CD3 assembly, or combination of both, or an effect of transgenic TCR to diminish expression of one or both chains of the αβ TCR, could all be plausible mechanism of action.

The expression of CD4 and CD8 molecules in the αβTCR- Vδ2+ population was assessed by flow cytometry, to validate whether this population are αβ T cells that have downregulated their endogenous αβ TCR, considering that majority of naïve γδ T cells are usually CD4−CD8− (>70%) (Garcillán et al., 2015). We demonstrated that the αβTCR- Vδ2+ population was positive for either CD4 or CD8 (**Figure 4.5**). However, this result does not fully prove that the single positive population are αβ T cells that have downregulated their endogenous αβ TCR, as CD4 and CD8 expression is circumstantial evidence. To confirm the identity of such population sequencing of the cells to demonstrate functional rearrangements of the αβ TCR and lack of rearrangements of the γδ TCR would be required. However, the cost and the complexity of this approach is beyond the scope of the thesis, therefore we proceeded on the assumption that we were evaluating converted αβ T cells.

We conducted some preliminary work in which we attempted to purify the initial αβ T cells population by depleting γδ TCR+ and CD56+ cells post PBMCs isolation (data not shown), in order to make sure that the αβTCR- Vδ2+ population post transduction of expanded αβT cells with the G115- γδTCR, did not contain any naïve γδ T cells. However, the stress T cells were subjected to by double depletion of γδ TCR+ and CD56+ cells right after PBMCs isolation, did not allow proper T cell expansion. Therefore, moving forward we only performed CD56+ depletion, as we did for any effector in all our experiments, and decided to use CD4 and CD8 expression results as evidence that the αβTCR- Vδ2+population in γδTCR- transduced αβ T cells were converted αβ.

Expression of NK-like receptor such as CD16 and CD56 on G115- γδ TCR transduced αβ T cells was also assessed by flow cytometry in order to investigate whether the G115- γδ TCR gene transfer conferred any γδ-like phenotypical features to the αβ T cells. While the αβTCR- Vδ2+ population is negative for CD56, an upregulation of CD16 comparable to what observed in naïve γδ T cells, was detected. Again, these are just circumstantial items of evidence for fundamental cell identity, as CD16 is a well-recognised activation marker in NK cell. The αβT cells positive for CD16 may just represent activated cells. Hence, Further studies would be required to define phenotypic shift following TCR expression, since the evidence of upregulation of CD16 by itself does proof conversion to a γδ phenotype. However, it is possible that signalling through the transgenic TCR, for example as a result of the stress conditions following viral infection, might induce CD16 upregulation and hence reprogramme the cells to some extent towards the γδ phenotype.

Next, we investigated whether the γδ TCR is functional in the transduced cells. Signalling of the γδ TCR was assessed by looking phosphorylation of Zap70, ERK and Nf-KB at 360s post stimulation in a Phospho-Flow assay **(Figure 4.7)**. When the γδ TCR was crosslinked, significant increase in phosphorylation ERK and NF-KB was detected compared to the unstimulated controls. While Zap-70 showed the same trend, the result was not found significant. This could be due to the time point of evaluation of the phosphorylation, indeed Zap70 is immediately downstream from CD3-ζ and is an expected early event following TCR stimulation. These data give an indication of the ability of the γδ TCR transduced αβT cells to signal through the transgenic TCR. As mentioned in the results section, a strong PhosphoFlow experimental design should have included multiple time points including also earlier time points than the one chosen in this experiment, as ZAP70 was one of the intracellular molecules that was investigated. ZAP-70 is immediately downstream from CD3-ζ, so it would be predicted to be an early signalling event, therefore we hypothesize this could be the reason we did not see a significant increase of phosphorylation. Designing this as a time course experiment, would be more accurate and would allow to observe the contribution of phosphorylation and de-phosphorylation of the investigated signalling molecules over a longer period of time. However, this Phosphoflow protocol has been optimized overtime in the lab and these results, while not complete, still provide an indication of the phosphorylation status of the molecules investigated at 360s post stimulation. We do appreciate however, that optimization of the protocol for these specific conditions is required and a time course experiment will be undoubtedly necessary in the future to confirm and complete these set of results.

After confirming the ability of the G115 γδ TCR transduced αβ T cells to initiate signalling event through the transgenic TCR, the in vitro functionality of G1 15 γδ TCR transduced αβ T cells in terms of cytotoxicity, cytokine production and proliferation towards a γδ T cell sensitive target, Daudi, was investigated. The transgenic G115- γδ TCR was able to redirect αβ T cells cytotoxicity towards a γδ sensitive target (Daudi) in a ^{51}Cr release assay (**Figure 4.8**) and promoted increased cytokine production in αβ T cells G115 γδ TCR transduced αβ T cells against Daudi (**Figure 4.9**). Interestingly G115 γδ TCR transduced αβ T cells produced significant higher level of cytokines compared to the naïve γδ T cell control, showing that the transgenic γδ TCR is using αβ T cell engine to promote a robust cytokine response.

Proliferation mediated by transgenic γδ TCR transduced αβ T in response to Daudi was investigated next. To achieve this, effector cells were labelled with CellTrace violet, and the dilution of the dye was taken as an indication of proliferation.

Untransduced αβ T cells displayed some unspecific proliferation towards Daudi cells and the same proliferation profile was observed in αβ TCR+ γδ TCR- population within the γδ TCR transduced αβ T cell sample. In contrast, the proliferation of the αβ TCR+ γδ TCR+ and αβ TCR- γδ TCR+ populations was greater compared to the untransduced controls cultured with the Daudi cells (**Figure 4.10**). Normally all short-term proliferation assays performed in this work were conducted over 7 days. However, due to unpredictable circumstances this proliferation assay was performed over 12 days. Ideally, we should have repeated this specific experiment, however we have extensive data in the next chapter that demonstrate proliferation of γδ TCR transduced αβ T cells towards Daudi.

In order to investigate whether the activity of G115 γδ TCR transduced αβ T cells is directed by the new TCR, their cytotoxic activity as well as their ability to produce cytokines was assessed by culturing them with target cells that have been treated with Zoledronate (**Figure 4.11**). Allogeneic monocytes were used as target as these cells are not normally engaged by γδ T cells, while they promote γδ T cell engagement by upregulating phosphoantigens after being stimulated with Zoledronate (Roelofs et al., 2009)

Untransduced αβ T cells, untransduced γδ T cells and γδ TCR transduced αβ T cells showed very low or background levels of cytotoxicity toward the allogeneic monocytes that were not treated with Zoledronate. When the effectors were cultured with targets treated with Zoledronate, however, both untransduced γδ T cells and γδ TCR transduced αβ T cells demonstrated a statistically significant increase in ^{51}Cr release in response to ZOL-treated monocytes, compared to their response to untreated targets. While a significant increase was observed also in terms of cytokine production (IL-2 and IFN-γ) when γδ TCR transduced αβ T were co-cultured with monocytes + ZOL compared to untreated monocytes, also untransduced αβ T cells produced IL-2 and IFN-γ in response to the same targets, making the results hard to interpret. This confounding effect once again can be attributed to alloreactivity of the αβ TCR to the allogeneic monocytes.

However, overall, all these results suggest that it is possible to express a transgenic γδ TCR in αβ T cells and that the transgenic TCR is able to re-direct αβ T cells anti-tumour activity towards a γδ T cell sensitive target.

In all the previous results discussed in this chapter, the γδ TCR transduced αβ T cells containing the mix of the three different populations described previously,

were used as effectors. However, moving forward to prevent any potential allogenic reaction caused by the presence of the αβ TCR in the mixed transduced effectors, we developed a protocol to purify the αβ TCR+ γδ TCR- population by negative selection of αβTCR+ populations present in the γδ TCR transduced αβ T cells. The method for selection can be found in the material and methods section. Success of the purification was assessed by flow cytometry (**Figure 4.12**) and purified γδ TCR+αβ TCR- were tested alongside mix γδ TCR transduced αβ T cells in order to assess any reduction in alloreactivity.

Both effectors were co-cultured with monocytes and cytotoxic activity was investigate by a ^{51}Cr release assay (**Figure 4.13**). We did indeed demonstrate that the depletion of αβ TCR+ population eliminated the alloreactivity as cell lysis induced by γδ TCR+αβ TCR- was significantly lower than the lysis prompted by the mixed γδ TCR transduced αβ T cells. This result demonstrated that is possible to purify the γδ TCR+αβ TCR- population within the γδ TCR transduced αβ T cells and that the purified population shows reduced alloreactivity.

Lastly in order to gain insights on the expression of the G115 γδ TCR over time, the expression of the transgene was assessed by flow cytometry, in both undepleted γδ TCR transduced αβ T cells and in purified γδ TCR+ αβ TCR- cells kept in culture with no extra stimulation other than Il-2 addition every other day to keep the cells healthy, on day 6 and 13 post-transduction (**Figure 4.14**). We observed that in both effectors, the transgene started losing its expression overtime towards a more αβ TCR+ phenotype.

The drop that we observe, could be loss of LTR-driven TCR transgene transcriptional activity. Moreover, several studies support the hypothesis that

lymphocyte activation may be a key determinant of transgene expression: Pollok and colleagues transduced primary human T lymphocytes with an MMLV-based retrovirus encoding murine B7-1 and observed that although transgene expression decreased rapidly in the presence of IL-2 in vitro, it was up-regulated upon short-term exposure to plates coated with both anti-CD3 and anti-CD28 monoclonal antibodies. In future works, it would be interesting to investigateG115- γδ TCR expression on αβ T cells upon re-stimulation.

A solution to overcome this could be to use gene editing to knock out the endogenous αβ TCR. One elegant solution might be using CRISPR/Cas9 technology to insert γδ TCR in the TRAC locus. It is previously noted that CAR expression from the TRAC locus is highly efficient. Moreover, there is only one active TRAC locus per cell, hence incomplete editing can still lead to complete deletion in a single cell. This approach would potentially give simultaneously high efficiency expression of the transgenic TCR while knocking-down the endogenous αβTCR. However, one of the major concerns for implementing CRISPR/Cas9 technology for gene therapy is the high frequency (≥50%) of off-target effects (OTEs). These are RNA-guided endonuclease (RGEN) induced mutations at sites other than the intended on-target site (Zhang et al., 2015). Strategies to overcome this limitation include engineered Cas9 variants that exhibit reduced OTE and optimizing guide designs. All these factors need to be taken into consideration in order to design a safe and effective therapy.

5 RESULTS III – Characterization of γδ TCR -TE9 CCRs transduced αβT

5.1 Introduction

Co-stimulation is an essential component of T cell biology and plays a key role in determining the quality of T cell differentiation, proliferation, and memory formation. The aim of this chapter was to co-express on αβT cells, a tumour reactive γδ TCR and a CCR targeting a tumour associated antigen as an alternative approach to deliver antigen specific tumour reactivity as well as provide a safety mechanism to avoid on-target off tumour toxicity.

In the previous chapter we focused on characterising the γδ TCR component of the proposed system and we demonstrated that it was possible to redirect αβ T cells against γδ sensitive cancer cells by expressing a tumour-reactive γδ TCR on αβ T cells.

In this chapter we investigated whether it was possible to co-express a CCR together with a γδ TCR on αβT cells, and we investigated the in vitro activity of γδ TCR – CCR transduced αβ T cells in terms of cytotoxicity, ability to produce cytokines and proliferate in response to specific stimuli, in order to study the contribution of co-stimulation in such a system. While there are studies that have focused on investigating the activity of a CCR in γδ T cells in order to avoid on-target of tumour toxicity (J. Fisher et al., 2017), there is no literature record of studies investigating the contribution of co-stimulation through a CCR in αβ T cells engineered to express a γδ TCR.

5.2 Cloning of retroviral vectors expressing G115 transgenic γδ TCR – TE9 CCRs.

Based on the results in result chapter I, TE9 binder targeting B7-H3 was chosen to be included in a CCR format in order to investigate the γδ TCR – CCR in an αβ T cell model.

The majority of CAR clinical studies to date focus on CAR-T cells engineered with CD28 or 4-1BB co-stimulatory molecules (J.N. et al., 2010; Ramos et al., 2017). Previous studies demonstrated CD28 and 4-1BB molecules confer distinct functionalities to T cells. CD28 co-stimulation has been validated to induce a quicker T cell activation leading to T cell differentiation into cells with an effector memory phenotype. In contrast, 4-1BB induced enhanced persistence and central memory differentiation, showing a more progressive and long-lasting response.

Therefore, CD28 and 41BB were chosen as co-stimulatory endodomains to be included in the CCR structure to be investigated in our in vitro model.

TE9-CD8 stalk-CD8tm-CD28 and TE9-CD8 stalk-CD8tm-4-1BB were ordered as gene block and were incorporated in the SFG gamma-retroviral vector expressing the G115 γδ TCR by restriction cloning, resulting in the following constructs:

- G115- γδ TCR- TE9-CD8 stalk-CD8tm-CD28 (γδ TCR-TE9-28 in short).
- G115- γδ TCR- TE9-CD8 stalk-CD8tm-41BB (γδ TCR-TE9-41BB in short).

The G115 γδ TCR and TE9-CCR sequences were separated by a T2A self-cleaving peptide which allows the equimolar expression of the two constructs as separate proteins encoded from a single open reading frame (ORF) (Szymczak-Workman et al., 2012).

Figure 5.1 Design of G115 γδ TCR – TE9 CCR expressing constructs. The retroviral vector used was the splicing oncoretroviral vector SFG, pseudotyped with an RD114 envelope. TE9-CD8 stalk-CD8tm-CD28 and TE9-CD8 stalk-CD8tm-CD28 were ordered as gene block and were incorporated in the SFG gamma-retroviral vector expressing the G115 γδ TCR by restriction cloning. The sequences between the LTR regions include G115 γδ TCR, T2A self-cleaving peptide and TE9-CCR (with either CD28 or 4-1BB as co-stimulatory endodomain).

5.3 Upregulation of γδ TCR engagement by anti-BTN3A 20.1 monoclonal antibody.

5.3.1 Surface expression of BTN3A in a panel of human cell lines

As discussed in the introduction, Vγ9Vδ2 TCR mediated recognition is a complex mechanism. While there is still a lack of knowledge on the totality of factors that are involved, findings support the role of BTN3A in γδ TCR engagement. Studies have shown that Vγ9Vδ2 T cells can be modulated by anti-BTNA3 antibodies. Specifically, the monoclonal anti- BTN3A antibody (mAb) 20.1 antibody which bind to the extracellular domain of BTN3A molecule has been used to induce TCR activation. The activity of this antibody has been investigated in several studies and had variable results in inducing TCR mediated activation of Vγ9Vδ2 cells (Harly et al., 2012; Palakodeti et al., 2012; Starick et al., 2017)

Daudi, Jurkat WT, Jurkat B7H3 and AML cell lines MV4-11, NOMO-1 and THP-1 were used to investigate the in vitro efficacy of γδ TCR-TE9-28 and γδ TCR-TE9-41BB. While we have previously seen that the γδ TCR engage Daudi cell line, we investigated whether it was possible to induce γδ TCR engagement with the rest

of the cell line panel by stimulating the targets with 20.1 monoclonal anti- BTN3A antibody. In order to investigate the effect of the 20.1 mAb on γδ TCR engagement with our cell lines, firstly the surface expression of BTN3A on Daudi, Jurkat WT, MV4-11, NOMO-1 and THP-1 was determined by flow cytometry through MFI. (Figure 5.2). Cells were stained with a commercially available anti-BTN3A 20.1-PE antibody (orange histogram) following the manufacturer's directions. Cells were stained with an isotype control to detect any unspecific binding (blue histogram) and unstained cells were used as negative control (red histograms). All cell lines show a slight shift in MFI between the isotype control and the anti- BTN3A 20.1 antibody. This shift in MFI is consistent with staining of BTN3A+ cells as per manufacturer's direction.

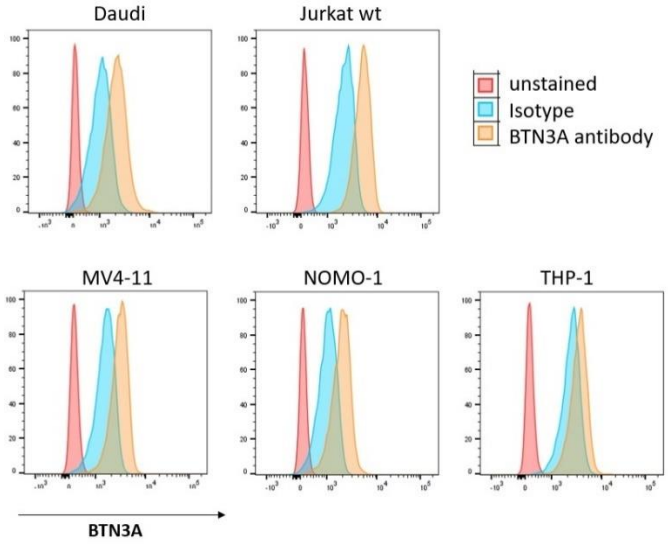

Figure 5.2 Surface expression of BTN3A in a panel of human cell lines. Surface BTN3A expression was assessed through median fluorescence intensity (MFI) by flow cytometry, using an anti-human BTN3A 20.1-PE antibody (orange histograms). Cell stained with an isotype control antibody (blue histogram) and unstained cells were used as control (red histograms). Representative histograms of BTN3A detection on Daudi, Jurkat WT and AML cell lines MV4-11, NOMO-1, and THP-1.

5.3.2 Quantification of IL-2 and IFN-γ production mediated by γδ TCR-transduced αβ T cells in response to 20.1

After assessing the surface expression of BTN3A on our cell line panel, cells were stimulated with 20.1 antibody, and TCR mediated activation of γδ TCR-transduced αβ T cells was assessed by quantification of cytokines production.

In order to achieve this, PBMCs were isolated from healthy donors, and activated αβT cells were transduced on day 4 with retroviral supernatant to express γδ TCR construct. Transduction efficacy was confirmed by flow cytometry, and the αβTCR-γδTCR+ population was purified by αβTCR depletion as explained in chapter 4. Purified γδ TCR transduced αβT cells were used as effectors and untransduced αβT cells were included as control.

Jurkat WT, Daudi, MV411, NOMO-1 and THP-1 cells were treated with 20.1 antibody. In order to do so, cells were pelleted and up to $1x10^8$ cells were resuspended 100 µl of PBS containing 1 µg of antibody following manufacturer's direction. Cells were then incubated for 1 hour at 37°C and post incubation they were wash thoroughly to eliminate any unbound antibody. 20.1 treated target cells were co-cultured with untransduced αβT cells and γδ TCR transduced αβT cells for 18h at 1:1 E:T ratio. Untreated target cells were also co-cultured with the same effectors as control. Effectors were also cultured with no targets to detect any background cytokine release.

Post 18 hours, supernatant was collected, and quantification of IFN-γ and IL-2 was assessed by ELISA following the manufacturer's direction (figure 5.3A).

γδ TCR transduced αβ T cells produced IFN-γ when they were co-cultured with Daudi, MV4-11, NOMO-1, and THP-1 treated with the 20.1 antibody. They

produced respectively 4297±1635, 3379±1696, 2269±1286 and 3052±1646 pg/mL (mean±SD, n=3) while interestingly they did not produce any detectable amount of IFN-γ when they were co-cultured with untreated targets.

The same pattern was observed for IL-2 release, γδ TCR transduced αβT cells produced IL-2 in response to Daudi, MV4-11, NOMO-1 and THP-1 treated with the 20.1 antibody (respectively 2263±1270, 1842±1135, 952±428 and 1184±799 pg/mL) while no IL-2 was produced when they were co-cultured with untreated targets. In previous experiments, Daudi cells showed cytokine production when co-cultured with γδ TCR transduced αβ T cells even in absence of 20.1 treatment, therefore, this is an interesting result.

In contrast, γδ TCR transduced αβT cells did not release any IFN-γ or IL-2 when co-cultured with untreated or 20.1 treated Jurkat WT. We hypothesised that co-stimulation might be required in this instance to see any effect; therefore, we still brought the isogenic cell line forward.

Importantly, while we see a statistically significant upregulation in cytokine production when γδ TCR transduced αβT cells are co-cultured with 20.1 treated targets compared to when they are co-cultured with untreated targets, this upregulation in not seen in untransduced αβ T cells, in fact they did not produce any cytokines in response to treated or untreated targets. Statistical significance between γδ TCR transduced αβT cells co-cultured with 20.1 treated targets and untreated targets, is reported in figure 5.3B.

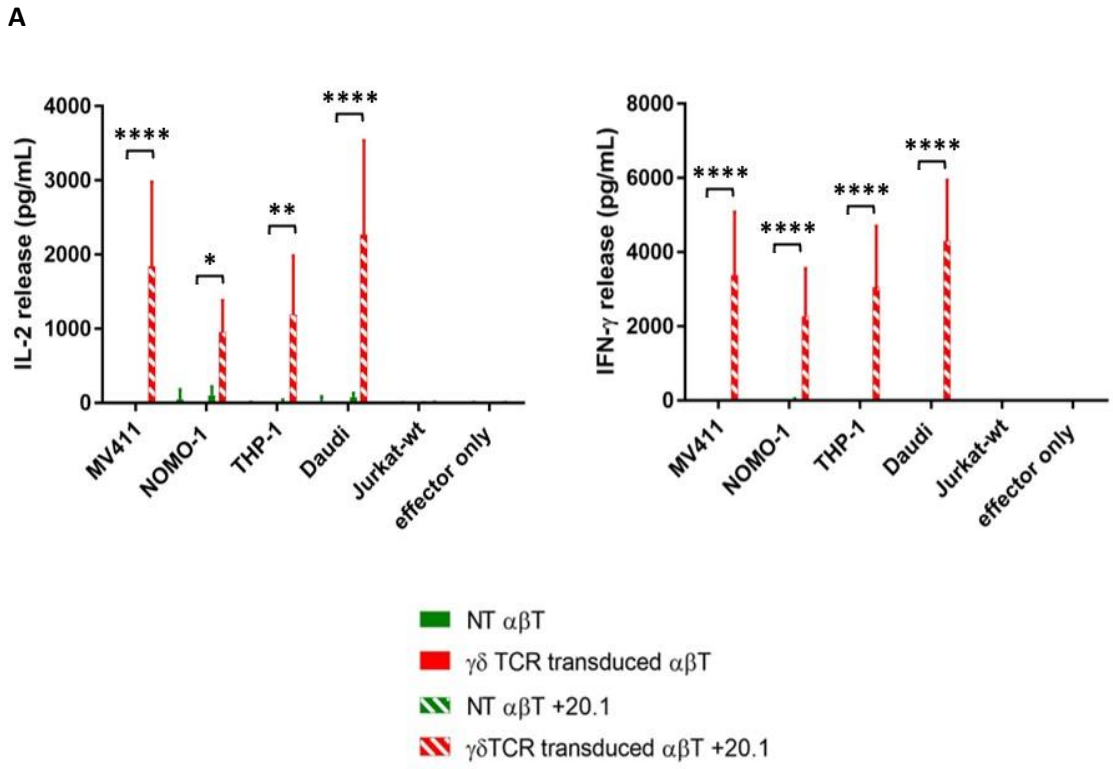

Figure 5.3. Quantification of IL-2 and IFN-γ production mediated by γδ TCR-transduced αβ T cells in response to 20.1. G115 γδ TCR transduced αβ T cells were co-cultured for 18 hours with Daudi, MV411, NOMO-1 and THP-1 cell line untreated or treated with 20.1 antibody or alone at 1:1 E:T ratio. Effectors were also cultured with no targets to detect any background cytokine production. IL-2 and IFN-γ were measured by ELISA from supernatant from the co-culture. (A) Graphs show mean cytokine release ± SD (n=3 independent biological replicates). Statistical analysis was done on γδTCR transduced αβ T cells: 20.1 treated targets vs untreated targets – analysis was performed by 2-way ANOVA, followed by Tukey post hoc analysis: ****p<0.0001, **p<0.01, *p<0.1.

5.4 Characterization of γδ TCR-TE9-28 and γδ TCR-TE9-41BB in vitro

After demonstrating that is possible to use the 20.1 antibody to upregulate γδ TCR engagement, the activity of γδ TCR-TE9-28 and γδ TCR-TE9-41BB transduced cells was investigated in vitro.

Their efficacy in vitro was firstly investigated on isogenic cell lines Jurkat WT and Jurkat B7H3, in order to evaluate responses mediated by the γδ TCR-TE9-28 and

γδ TCR-TE9-41BB in the presence and absence of their cognate antigen when γδ TCR is engaged. Daudi was included as positive control for γδ TCR engagement.

The in vitro activity towards B7H3 positive AML cell line MV411, NOMO-1 and THP-1 was then investigated.

Lastly, the activity against murine isogenic cell line 3T3 WT and 3T3 B7H3 which do not engage the γδ TCR, was investigated in order to assess on-target off-tumour toxicity mediated by γδ TCR-TE9-28 and γδ TCR-TE9-41BB.

The in vitro activity of the γδ TCR-TE9-CCR effectors was studied by assessing their ability to be cytotoxic, produce cytokines and proliferate in response to specific stimuli.

5.4.1 Expression of the transgenic γδ TCR-TE9-28 and γδ TCR-TE9-41BB on primary human αβ T cells.

In order to validate γδ TCR-TE9-28 and γδ TCR-TE9-41BB contribution in vitro, their surface expression on αβ T cells was investigated.

To achieve this, PBMCs were isolated from healthy donors, and activated αβT cells were transduced on day 4 with retroviral supernatant to express γδ TCR, γδ TCR-TE9-28 and γδ TCR-TE9-41BB constructs. Untransduced αβT cells were used as controls. Transduction efficacy was assessed on day 6 by flow cytometry by staining with anti-CD3 BV785, anti-αβTCR-FITC, anti- Vδ2-PE antibodies from Biolegend and using anti- B7-H3-Histag protein and a secondary anti-His-APC antibody to detect the TE9-CCRs.

Figure 5.4A shows representative plots illustrating the gating strategy to identify αβTCR- Vδ2+ and CCR+ populations. Cells were gated on CD3+ after exclusion of doublets and dead cells, as shown previously. Untransduced αβ T cells were positive for αβTCR and negative for γδTCR. In contrast, αβ T cells that were transduced to express the γδ TCR-TE9-28 and γδ TCR-TE9-41BB constructs acquired a distribution of transduced populations which is comparable to the profile of γδ TCR-transduced αβ T cells as described in the previous chapter: the presence of αβTCR+ Vδ2-, αβTCR+ Vδ2+ and αβTCR- Vδ2+ populations were observed. αβTCR- γδTCR+ population was also positive for the TE9-CCR in both γδ TCR-TE9-28 and γδ TCR-TE9-41BB transduced αβ T cells while there was no detection of the CCR in γδ TCR transduced αβ T cells.

Figure 5.4B represent the frequency of the αβTCR- γδTCR+ population (also CCR+ for the TE9-CCR transduced αβ T cells) across multiple experiments (n=5). γδTCR transduced αβ T cells are 33±6% (Mean ± SD) αβTCR- γδTCR+ while γδ TCR-TE9-28 and γδ TCR-TE9-41BB transduced αβ T cells are respectively 15±3% and 14±5%.

The difference in transduction efficiency between the γδTCR transduced αβ T cells and the γδ TCR-TE9-28 and γδ TCR-TE9-41BB transduced αβ T cells was statistically significant, respectively $p=0.0116$ and $p=0.0226$. In contrast, no statistically significant difference was detected in the transduction efficiency between the two γδTCR -TE9 CCR constructs.

As γδ TCR and CCR seem to be equimolarly co-expressed in the αβTCR- γδTCR+ population in γδ TCR-TE9-28 and γδ TCR-TE9-41BB transduced αβ T cells, moving forward only anti-Vδ2 antibody was used to detect the constructs.

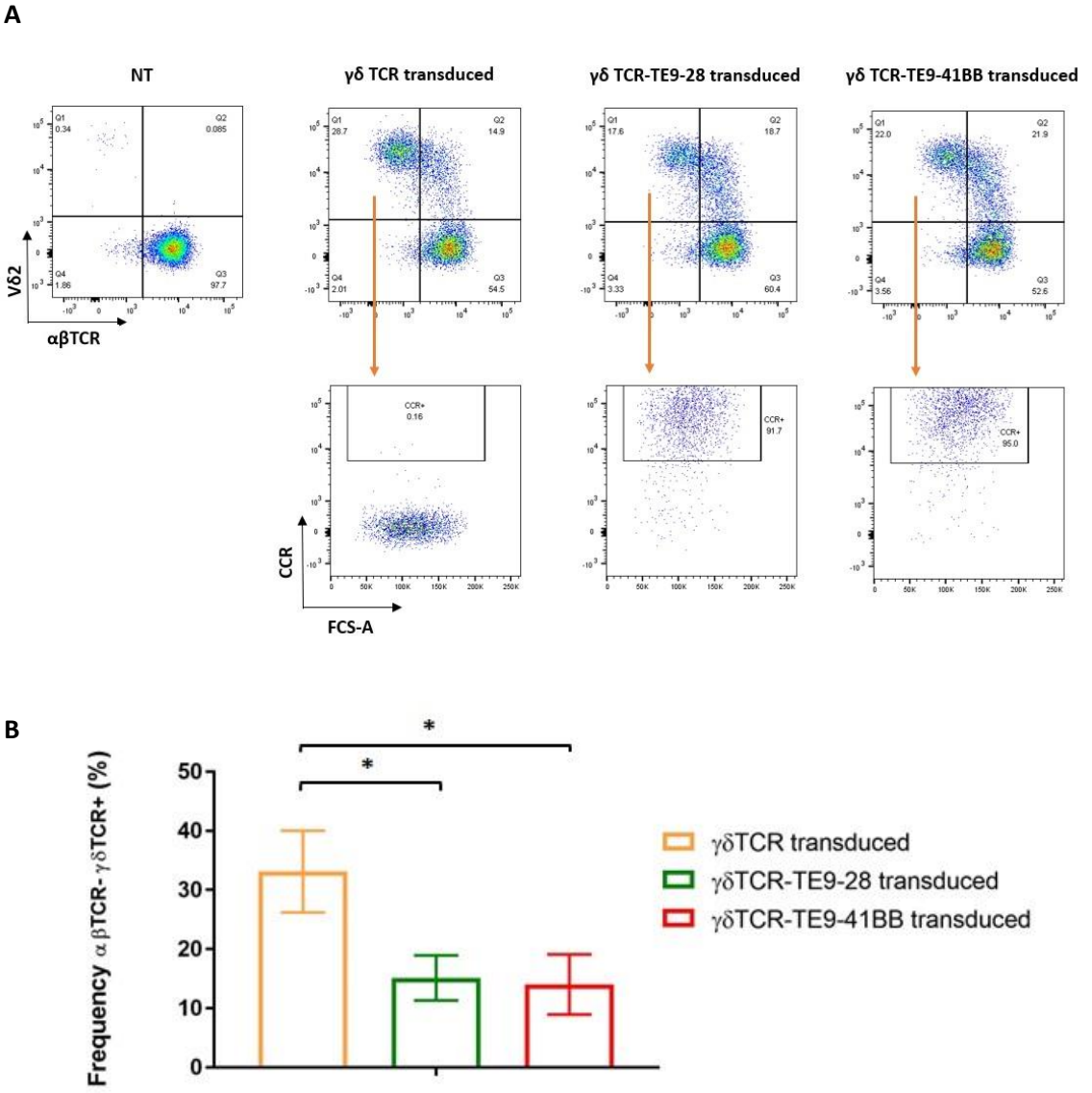

Figure 5.4 Transduction efficacy of G115 γδ TCR-TE9 CCR constructs on primary human αβ T cells. Activated αβ T cells were transduced with retroviral supernatant to express G115 γδ TCR, G115 γδ TCR-TE9-28 and G115 γδ TCR-TE9-41BB constructs on day 4 post isolation. Transduction efficacy was determined by flow cytometry by using anti-CD3 BV785, anti- Vδ2-PE, anti αβ TCR-FITC and anti- B7-H3-His-APC antibodies. (A) Representative plots showing the gating strategy to detect the transduced populations gating on γδ TCR, αβTCR and CCR. Cells were gated on CD3+ after exclusion of doublets and dead cells as shown in previous experiments (data not shown). Untransduced αβ T cells were used as controls. (B) mean expression of αβTCR- γδ TCR+ cell population ± SD (n=5 independent biological replicates). Statistical analysis was performed by One-way ANOVA, followed by Tukey's post hoc analysis: *p<0.1.

After confirming transduction efficacy by flow cytometry on day 6 post PBMCs isolation, as shown in the previous chapter, the αβTCR- γδTCR+ single positive population (in this case also CCR+), was then purified by depletion of a αβTCR+ populations. The purified population was used as effectors in downstream experiments only after successful depletion was confirmed by flow cytometry (data not shown). Check 7-day proliferation + re-stimulation section in the material and methods section for further details and clarification on time points.

After αβTCR- γδTCR+ CCR+ population was purified, cells were then rested for 24 to 48 hours, and functional assays were usually set up on day 9. In all the following experiments, purified effector cells were co-cultured with irradiated targets that were untreated or treated previously with 20.1 antibody, at 1:1 E:T ratio for a total of $2.5x10^5$ cell/well in 0.5 mL of media, and co-cultured for 18 hours at 37C. Post 18h, supernatant was collected for cytokine quantification by ELISA. Collected supernatant was replaced with fresh media and the co-cultures were incubated for further 7 days to evaluate proliferation. After 7 days, co-cultures were re-stimulated: 250 µl of media was replaced by fresh non irradiated, CellTrace violet labelled targets treated or untreated with 20.1 antibody at the same density provided on day 1 of setting up the co-culture.

Co-cultures were then incubated for further 18 hours before supernatant was collected for cytokine quantification by ELISA. The rest of the cells were collected for flow cytometry analysis of proliferation. Cytotoxicity was also analysed by flow cytometry, as the targets were labelled with CellTrace violet it was possible to detect loss of live cells.

The schematic in figure 5.5 represent the overall experimental timeline for all the following experiments in this chapter.

Figure 5.5 experimental timeline from αβTCR depletion to functional assays read-outs. Diagram showing timeline from purification of the γδTCR+ and γδTCR+ CCR+ populations to the read-outs of functional assays: cytokine quantification by ELISA, proliferation, and cytotoxicity detection by flow cytometry.

5.4.2 Surface expression of B7H3 on Daudi cell line

As the Daudi cell line was to be used as a control in the following experiments, the expression of B7H3 on its surface was determined through median fluorescence intensity (MFI) by flow cytometry. Daudi cells were stained with a commercially available anti-human CD276 (B7-H3)-APC antibody from Biolegend, following manufacturer's directions (blue histogram). Unstained cells were used as negative control (red histograms). We observe a similar shift in MFI that was observed when Jurkat WT cells were stained with the same antibody. We confirmed staining specificity with an isotype control also in this instance (data not shown) and

concluded that no significant surface expression of B7-H3 was detected on Daudi cells (MFI=424) (Figure 5.6).

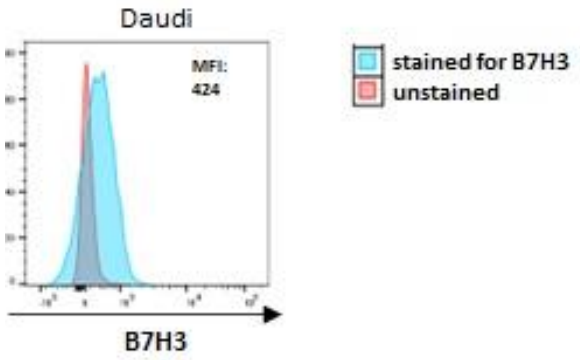

Figure 5.6 Surface expression of B7-H3 on Daudi cell line. Surface B7-H3 expression was assessed through median fluorescence intensity (MFI) by flow cytometry, using anti-human CD276 (B7-H3) – APC antibody (blue histograms). Unstained cells were used as control (red histograms). Representative histograms of B7-H3 detection on Daudi cells.

5.4.3 In vitro activity of γδ TCR-TE9-28 and γδ TCR-TE9-41BB transduced αβ T cells against Jurkat WT, Jurkat B7H3 and Daudi cell line.

As mentioned earlier, the efficacy in vitro was firstly investigated on isogenic cell lines Jurkat WT and Jurkat B7H3, in order to have a clean system to test the activity of γδ TCR-TE9-28 and γδ TCR-TE9-41BB in the presence and absence of their cognate antigen when γδ TCR is engaged. Daudi, which is a highly sensitive to γδ T cells, was included as a positive control for γδ TCR engagement.

5.4.3.1 Quantification of IL-2 and IFN-γ production mediated by γδ TCR-TE9-28 and γδ TCR-TE9-41BB transduced αβ T cells against Jurkat WT, Jurkat B7H3 and Daudi cell line.

Quantification of cytokines post 18 hours

Untransduced αβ T cells and γδ TCR, γδ TCR-TE9-28 and γδ TCR-TE9-41BB transduced αβ T cells were co-cultured with irradiated untreated and 20.1 treated Jurkat WT, Jurkat B7H3 and Daudi cell line for 18 hours at 1:1 ratio at a density of $2.5x10^5$ cell/well in 0.5 mL. Post 18 hours, supernatant was collected, and cytokine quantification was performed by ELISA.

Figure 5.7A shows IL-2 and IFN-γ production mediated by the effector cells when co-cultured with the targets. γδ TCR-TE9-28 transduced αβ T cells released higher levels of IL-2 when co-cultured with untreated and 20.1 treated Jurkat B7H3, producing respectively 983±27 and 1419±278 pg/mL (mean±SD n=3), compared to when they were co-cultured with untreated or 20.1 treated Jurkat WT. The same trend is seen in IFN-γ production: γδ TCR-TE9-28 transduced αβ T cells produced 1135±40 and 1465±301 pg/mL when co-cultured with untreated and 20.1 treated Jurkat B7H3, respectively. The difference in IL-2 and IFN- γ release mediated by γδ TCR-TE9-28 transduced αβ T cells between untreated/20.1 treated Jurkat B7H3 and untreated/20.1 treated Jurkat WT is statistically significant ($p<0.0001$). When comparing cytokine release by γδ TCR-TE9-28 transduced αβ T cells between untreated and 20.1 treated Jurkat B7H3 cells, statistical significance is found only in IL-2 production ($p=0.0014$). These data are consistent with the presence of the CCR conferring antigen dependent co-stimulation leading to cytokine secretion.

Figure 5.7B shows cytokine production mediated by γδ TCR-TE9-28 transduced αβ T cells co-cultured with untreated and 20.1 treated Daudi. All the effectors apart

from untransduced αβ T cells (NT) produced high levels of IL-2 and IFN-γ in response to Daudi. This is expected considering that Daudi is a highly γδ TCR sensitive cell line. The levels of IL-2 produced in response to untreated Daudi are as follows for respectively γδ TCR, γδ TCR-TE9-28 and γδ TCR-TE9-41BB transduced αβ T cells: 8225±2406, 5367±2201, 8928±559 pg/mL; while with 20.1 treated Daudi they produced 8374±2401, 5524±1147, 7289±552 pg/mL. No statistically significant difference was observed between the untreated and 20.1 treated conditions. The same trend was seen for IFN-γ release. γδ TCR, γδ TCR-TE9-28 and γδ TCR-TE9-41BB transduced αβ T cells produced 7362±2083, 5856±1732, 6188±1130 pg/mL respectively against untreated Daudi and 9314±2019, 7646±1413, 9060±1435 pg/mL in response to 20.1 treated Daudi. Again, no statistically significant difference was observed between the untreated and 20.1 treated conditions.

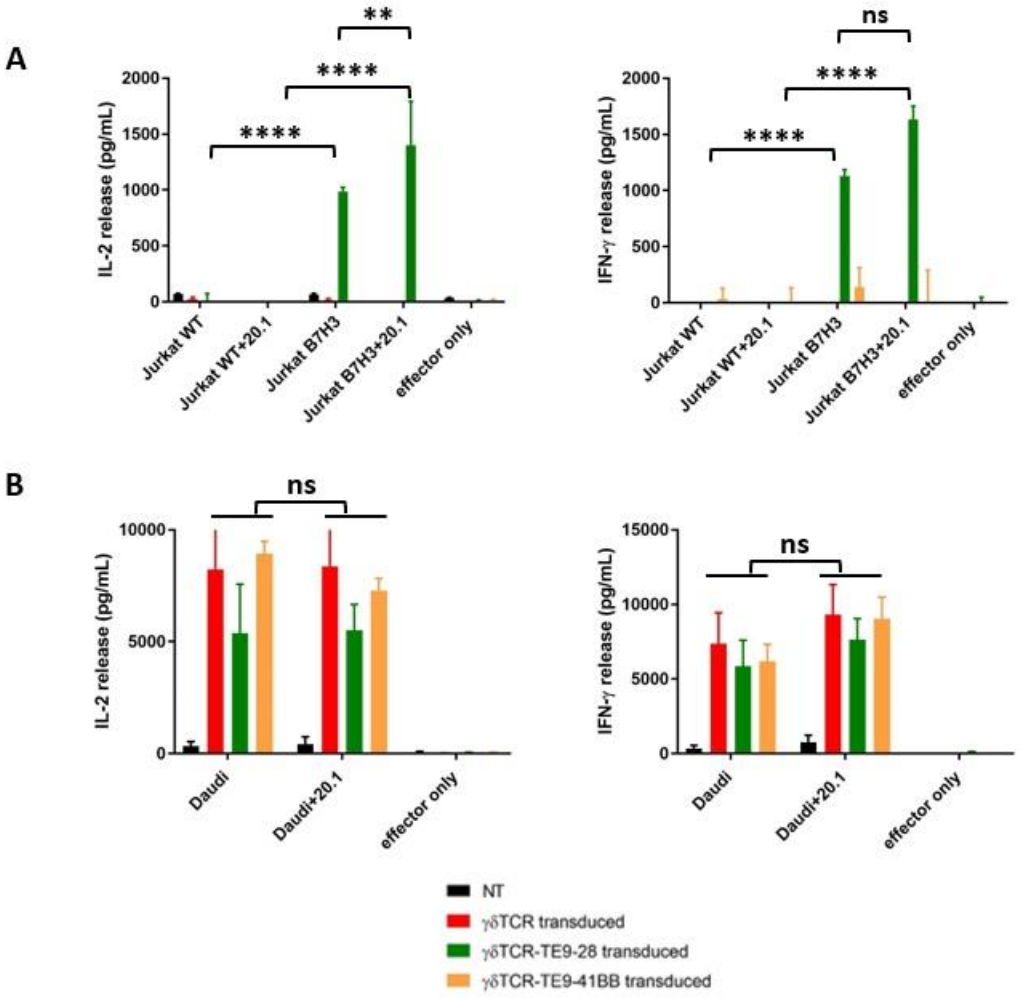

Figure 5.7 Quantification of IL-2 and IFN-γ production mediated by γδ TCR-TE9-28 and γδ TCR-TE9-41BB transduced αβ T cells against Jurkat WT, Jurkat B7H3 and Daudi cell line post 18 hours. Untransduced αβ T cells and αβ T cells transduced with γδ TCR, γδ TCR-TE9-28 and γδ TCR-TE9-41BB were co-cultured for 18 hours with irradiated untreated and 20.1 treated Jurkat WT and Jurkat B7H3 (A) and Daudi (B) or alone at 1:1 E:T ratio.IL-2 and IFN-γ were measured by ELISA. Graphs show mean ± SD (n=3 independent biological replicates). Statistical analysis was performed by 2-way ANOVA, followed by Tukey post hoc analysis : ** p<0.01 ****p<0.0001.

Quantification of cytokines post re-stimulation

In adoptive cell therapy using engineered T cells, long-term responses upon antigen rechallenge are as important as the immediate responses upon antigen recognition. Therefore, we investigated the responses of γδ TCR-TE9-28 and γδ TCR-TE9-41BB transduced αβ T upon rechallenge with B7H3 positive and negative targets.

In order to achieve this, as mentioned previously, after collecting 18 hours supernatant for cytokine quantification seen in the previous section, an amount equivalent to the collected supernatant was replaced by fresh media, and the co-cultures were incubated for 7 days at 37 °C. No IL-2 was provided to the cells when setting up the co-cultures or throughout the 7 days of incubation. Media colour was monitored during the 7 days, and 250µl of old media was replaced with the same volume of fresh media only if needed.

After 7 days, the co-cultures were re-stimulated with non-irradiated targets: 250µl of old media was replaced by the same volume of fresh media containing CellTrace violet labelled untreated and 20.1 treated targets. The same number as the initial seeding density of target cells were added to the co-cultures ($1.25x10^5$ targets/well). They were then incubated for another 18 hours at 37°C. After 18 hours incubation, supernatant was collected to quantify IL-2 and IFN-γ by ELISA. Figure 5.8A shows IL-2 and IFN-γ production when effectors were re-stimulated with untreated and 20.1 treated Jurkat WT and Jurkat B7H3.

γδ TCR-TE9-28 transduced αβ T cells produced IL-2 when co-cultured with Jurkat B7H3 treated with 20.1 (764±80 pg/mL) but not with the untreated targets

($p<0.0001$). In contrast, γδ TCR-TE9-28 transduced αβ T cells produced IFN-γ when co-cultured with both untreated and 20.1 treated Jurkat B7H3; 3028±898 and 3625±175 pg/mL, respectively. However no statistical difference was observed between the two conditions. No cytokines were produced by γδ TCR-TE9-28 transduced αβ T cells when co-cultured with untreated and 20.1 treated Jurkat WT.

Interestingly, γδ TCR-TE9-41BB transduced αβ T cells produced high levels of IFN-γ in an antigen independent manner, in fact they produced over 6000 pg/mL when co-cultured with all the targets independently from the presence of the antigen or 20.1 treatment. No statistically significant difference was detected between all these conditions for the γδ TCR-TE9-41BB transduced cells. Moreover, γδ TCR-TE9-41BB transduced αβ T cells cultured with no target also produced 3828±752 pg/mL indicative of a specific antigen and target independent response of the 41BB CCR in this cellular context.

Figure 5.8B shows IL-2 and IFN-γ production when effectors were re-stimulated with untreated and 20.1 treated Daudi. It is observed again that the presence of the γδ TCR only is sufficient to promote cytokine production in response to the targets whether they were untreated or 20.1 treated. The presence of the CCR does not seem to have any added benefit in this context. IL-2 release range between 4700-8500 pg/ml for γδ TCR, γδ TCR-TE9-28 and γδ TCR-TE9-41BB transduced αβ T cells co-cultured with untreated and 20.1 treated Daudi cells. No statistically significant difference between the treated and untreaded conditions was observed. However, this release is statistically significant compared to the untransduced αβ T cell control.

IFN- γ production follows the same trend, however γδ TCR-TE9-41BB transduced αβ T cells cultured with no targets also produced some level of IFN-γ (3828±752 pg/mL).

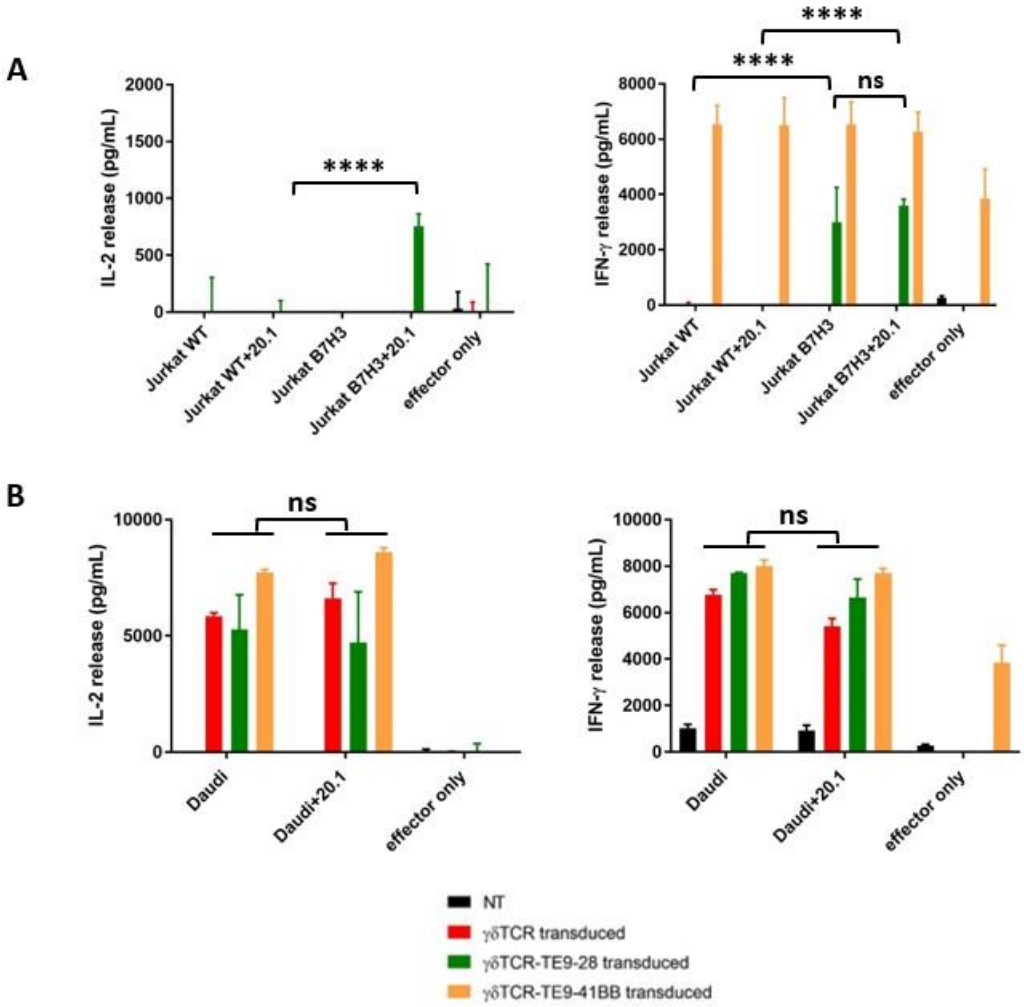

Figure 5.8 Quantification of IL-2 and IFN-γ production mediated by γδ TCR-TE9-28 and γδ TCR-TE9-41BB transduced αβ T cells against Jurkat WT, Jurkat B7H3 and Daudi cell line post antigen re-challenge. After 7 days co-culture, untransduced αβ T cells and αβ T cells transduced with γδ TCR, γδ TCR-TE9-28 and γδ TCR-TE9-41BB were re-stimulated with untreated and 20.1 treated Jurkat WT and Jurkat B7H3 (A) and Daudi (B) or alone at 1:1 E:T ratio. Post 18h, IL-2 and IFN-γ were measured by ELISA. Graphs show mean ± SD (n=3 independent biological replicates). Statistical analysis was performed by 2-way ANOVA, followed by Tukey post hoc analysis : ****p<0.0001.

5.4.3.2 Expansion mediated by γδ TCR-TE9-28 and γδ TCR-TE9-41BB transduced αβ T cells against Jurkat WT, Jurkat B7H3 and Daudi cell lines.

In order to investigate the effect of the co-stimulation in promoting expansion of γδ TCR-TE9-28 and γδ TCR-TE9-41BB transduced αβ T cells in an antigen dependent manner, effectors were co-cultured for 7 days with irradiated untreated and 20.1 treated Jurkat WT, Jurkat B7H3 and Daudi cell lines. As described previously, untransduced αβ T cells, γδ TCR, by γδ TCR-TE9-28 and γδ TCR-TE9-41BB transduced αβ T cells were co-cultured with targets for 7 days and then re-stimulated with targets on day 7. One day later cells were collected, and expansion was analysed by detecting absolute T cell number using Count Bright Absolute Counting Beads. Effectors were also cultured with no target in order to detect any background proliferation.

Figure 5.9A illustrate the gating strategy to detect counting beads and CD3+ cells in a co-culture with Daudi cells. Cells are gated on SSC-A and FCS-A and gated CD3-positive live cells. For Jurkat however, as they also are CD3, the gating was on CD3-pos CellTrace Violet-neg cells as targets were labelled with the dye (not shown).

Figure 5.9B shows absolute cell number of T cells after 7 days co-culture and re-stimulation with Jurkat WT and Jurkat B7H3. As it can be observed in the histogram the cell numbers of γδ TCR-TE9-28 transduced αβ T cells co-culture with untreated and 20.1 treated Jurkat B7H3 are higher compared to the Jurkat WT conditions and the effector only control. The mean absolute cell count ±SD for γδ TCR-TE9-28 transduced αβ T cells co-cultured with untreated and 20.1 treated Jurkat B7H3 are 409637±534721 and 606921±667841 respectively, compared to 27946±9922

and 47812±7268 with untreated and 20.1 treated Jurkat WT. This data is consistent with what was observed in terms of cytokine release. γδ TCR-TE9-41BB transduced αβ T cell numbers also seem higher than γδ TCR transduced αβ T cells control, however that response is antigen independent as comparable cell count can be observed also when the cells are co-cultured with Jurkat WT. Moreover, no statistically significant difference was observed compared to the effector only control.

Figure 5.9C shows absolute cell number of T cells after 7 days co-culture and re-stimulation with Daudi. Consistently with what seen in terms of cytokine production, cell number of γδ TCR, γδ TCR-TE9-28 and γδ TCR-TE9-41BB transduced αβ T cells co-cultured with untreated and 20.1 treated Daudi are all higher compared to the untransduced αβ T cells and effector only control. Overall, the proliferation data shows similar effects of co-stimulation through the CD28 induced by antigen as was observed with cytokine read out. Moreover, the 41BB CCR confers an unexpected high background antigen and target cell-independent activation by 7 days of expansion.

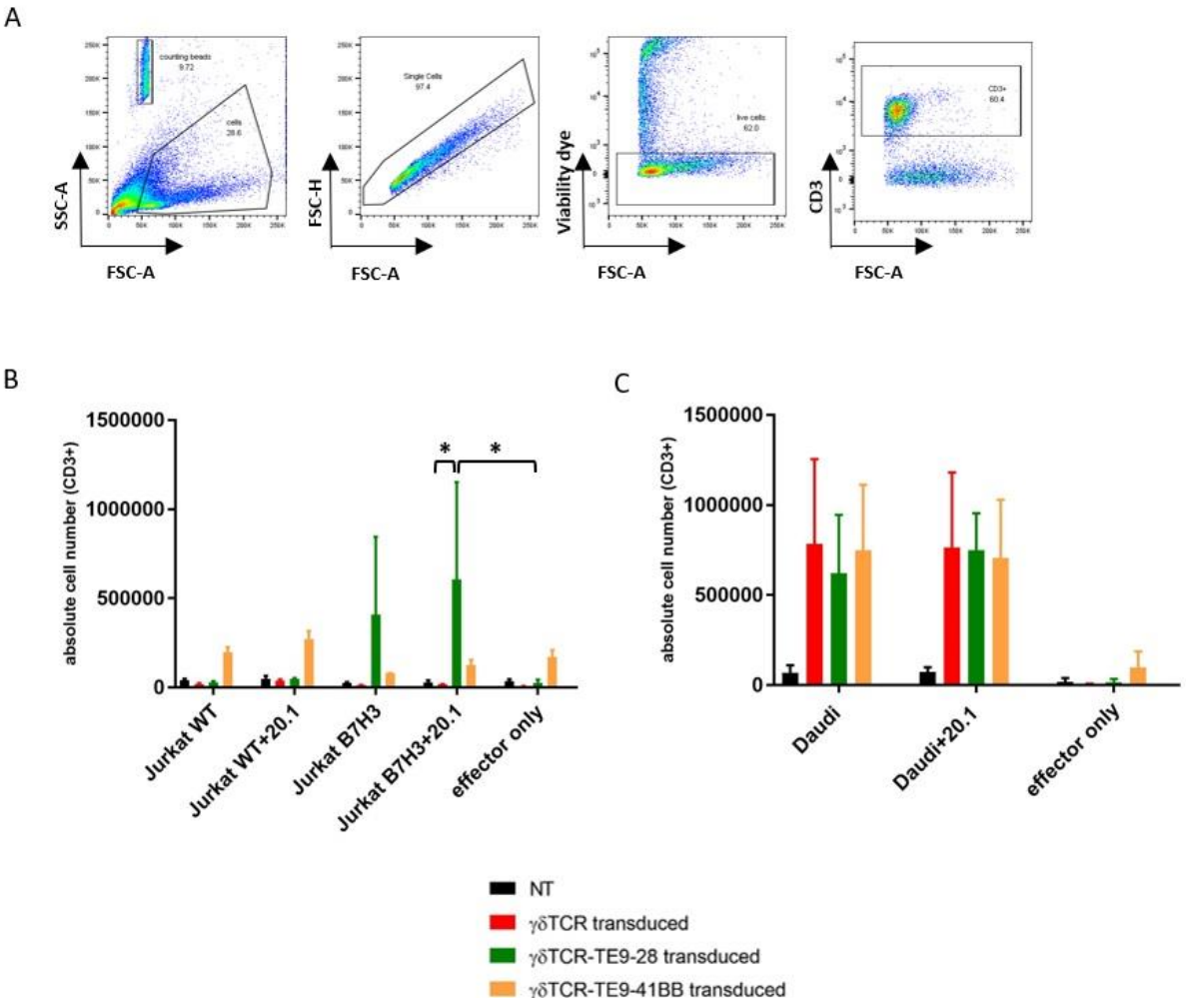

Figure 5.9 Proliferation mediated by γδ TCR-TE9-28 and γδ TCR-TE9-41BB transduced αβ T cells against Jurkat WT, Jurkat B7H3 and Daudi cell line. Untransduced αβ T cells and αβ T cells transduced with γδ TCR, γδ TCR-TE9-28 and γδ TCR-TE9-41BB were co-cultured for 7 days with irradiated untreated and 20.1 treated Jurkat WT and Jurkat B7H3 and Daudi or alone at 1:1 E:T ratio. After 7 days cells effectors were re-stimulated with non-irradiated fresh targets and proliferation was assessed on day 8. (A) Representative gating strategy to identify T cells after exclusion of dead and doublet cells. (B) histograms showing the absolute cell numbers of effectors cells after being co-cultured with Jurkat WT and Jurkat B7H3 and (C) Daudi. n=3 independent biological replicates. Statistical analysis was performed by 2-way ANOVA, followed by Tukey post hoc analysis: * $p<0.1$.

5.4.3.3 Cytotoxicity mediated by γδ TCR-TE9-28 and γδ TCR-TE9-41BB transduced αβ T cells against Jurkat WT, Jurkat B7H3 and Daudi cell lines.

As previously mentioned, when re-stimulating the co-cultures with fresh non-irradiated, untreated and 20.1 treated targets, the cells were labelled with CellTrace violet, therefore post 18 hours, when collecting the cells to detect proliferation, it was also possible to investigate cytotoxic activity of γδ TCR-TE9-28 and γδ TCR-TE9-41BB transduced αβ T cells by detecting loss of live targets by flow cytometry. Count Bright Absolute Counting Beads were used to assess the absolute cell numbers.

Figure 5.10A illustrate the gating strategy to detect loss of Jurkat WT, Jurkat B7H3 and Daudi live cells in one representative donor when co-cultured with untransduced αβ T cells, γδ TCR , γδ TCR-TE9-28 and γδ TCR-TE9-41BB transduced αβ T cells. Cells are gated on SSC-A and FCS-A and gated on the live cells (not shown). Live Daudi cells were then gated on CD3-neg CellTrace violet-pos and Jurkat WT were gated on CD3-pos CellTrace violet-pos while Jurkat B7H3 were gated on CD3-neg (not shown) and then on B7H3-pos CellTrace violet-pos population.

Figure 5.10B shows the absolute cell numbers in these gatings, calculated based on the relative number of counting beads. Counting beads were gated on the SSC-A and FCS-A plot as shown in previous experiment (not shown). Targets were cultured with no effectors as negative control. No statistically significant difference in the loss of untreated and 20.1 treated Jurkat WT was detected when comparing cells co-cultured with untransduced αβ T cells and γδ TCR, γδ TCR-TE9-28 and γδ TCR-TE9-41BB transduced αβ T cells. In contrast when the effectors were co-

cultured with untreated and 20.1 treated Jurkat B7H3, it is possible to observe a drop in the absolute cell number when the target were co-cultured with γδ TCR-TE9-28 and γδ TCR-TE9-41BB transduced αβ T cells compared to the γδ TCR transduced αβ T cells control. The mean absolute cell count ±SD of untreated Jurkat B7H3 when co-cultured with γδ TCR transduced αβ T cells was 206020±8999 compared to 15087±17492 and 7482±6044 when co-cultured with γδ TCR-TE9-28 and γδ TCR-TE9-41BB transduced αβ T cells, respectively. The difference in live cell count is statistically significant ($p<0.0001$ for both comparisons). The same trend was observed for 20.1 treated Jurkat B7H3: while the live cell count when they were co-cultured with γδ TCR transduced αβ T cells was 147912±24117, when they were co-cultured with γδ TCR-TE9-28 and γδ TCR-TE9-41BB transduced αβ T cells, their live cell count dropped to 1627±2172 and 1342±53, respectively. This difference as well was statistically significant ($p=0.0003$ for both comparisons).

Loss of live Daudi cells reflected what was seen in terms of cytokine production and proliferation. Daudi live cell count dropped when both untreated and 20.1 treated targets were co-cultured with γδ TCR transduced αβ T cells; 3913±10 and 3034±122 (untreated and 20.1 treated respectively) compared to19811±3764 and 27005±2149 when they were co-cultured with untransduced αβ T cells ($p<0.0001$). Live target cell count when co-cultured with γδ TCR-TE9-28 and γδ TCR-TE9-41BB transduced αβ T cells was comparable to the cell count when co-cultured with γδ TCR transduced αβ T cells, no statistically significant difference was detected between the conditions.

A

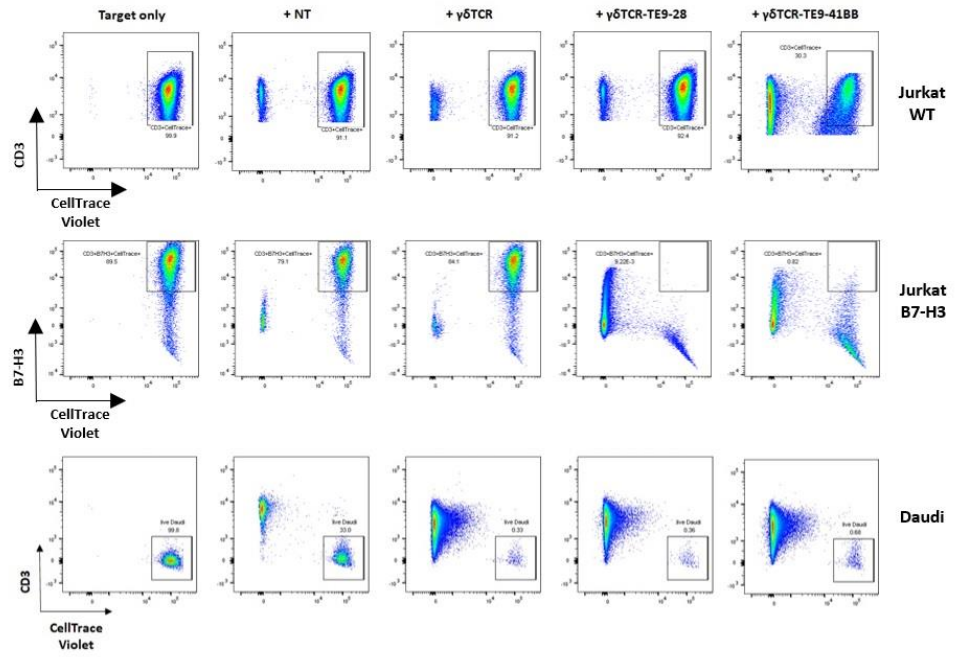
Target only
+ NT
+ γδTCR
+ γδTCR-TE9-28
+ γδTCR-TE9-41BB
Jurkat WT
Jurkat B7-H3
Daudi
CD3
B7-H3
CellTrace Violet

B

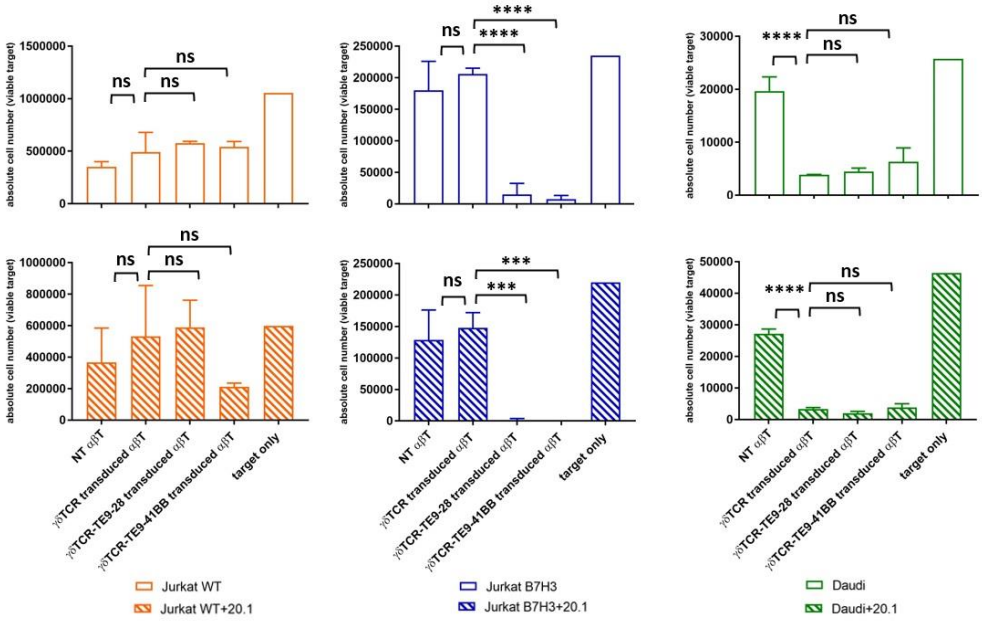
absolute cell number (viable target)
ns
****
***
NT αβT
γδTCR transduced αβT
γδTCR-TE9-28 transduced αβT
γδTCR-TE9-41BB transduced αβT
target only
Jurkat WT
Jurkat WT+20.1
Jurkat B7H3
Jurkat B7H3+20.1
Daudi
Daudi+20.1

Figure 5.10 Cytotoxicity mediated by γδ TCR-TE9-28 and γδ TCR-TE9-41BB transduced αβ T cells against Jurkat WT, Jurkat B7H3 and Daudi cell line. Untransduced αβ T cells and αβ T cells transduced with γδ TCR, γδ TCR-TE9-28 and γδ TCR-TE9-41BB were co-cultured for 7 days with irradiated untreated and 20.1 treated Jurkat WT and Jurkat B7H3 and Daudi or alone at 1:1 E:T ratio. After 7 days cells effectors were re-stimulated with fresh untreated and 20.1 treated targets labelled with CellTrace violet. 18 hours post re-challenge, cells were analysed for loss of live target cells by flow cytometry. (A) Representative gating strategy to identify target cells after exclusion of dead and doublet cells. (B) histograms showing the absolute cell numbers of target cells post co-culture. n=3 independent biological replicates. Statistical analysis was performed by 2-way ANOVA, followed by Tukey post hoc analysis: ****p<0.0001, ***p<0.001.

5.4.4 In vitro activity of γδ TCR-TE9-28 and γδ TCR-TE9-41BB transduced αβ T cells against AML cell lines.

5.4.4.1 Quantification of IL-2 and IFN-γ production mediated by γδ TCR-TE9-28 and γδ TCR-TE9-41BB transduced αβ T cells against AML cell line.

Quantification of cytokines post 18 hours

After investigating antigen dependent efficacy of γδ TCR-TE9-28 and γδ TCR-TE9-41BB transduced αβ T cells using isogenic cell line Jurkat WT and Jurkat B7H3 as proof of concept, their activity towards AML cell lines was investigated next.

In order to achieve this, untransduced αβ T cells and γδ TCR, γδ TCR-TE9-28 and γδ TCR-TE9-41BB transduced αβ T cells were co-cultured with AML cell lines, MV4-11, NOMO-1 and THP-1 for 18 hours at 1:1 ratio at a density of $2.5x10^5$ cell/well in 0.5 mL. Post 18 hours, supernatant was collected and IL-2 and IFN-γ cytokines were quantified by ELISA.

Figure 5.11 shows IL-2 and IFN-γ production mediated by untransduced αβ T cells and γδ TCR, γδ TCR-TE9-28 and γδ TCR-TE9-41BB transduced αβ T when co-cultured with untreated and 20.1 treated MV4-11, NOMO-1, and THP-1 cells.

γδ TCR-TE9-28 transduced αβ T cells appear to release higher levels of IL-2 when co-cultured with untreated and 20.1 treated MV4-11, NOMO-1, and THP-1 cells, compared to the γδ TCR-transduced αβ T cells control. They produced respectively 71±118, 159±137 and 722±465 pg/mL (mean±SD n=3), when co-cultured with untreated targets and 291±162, 104±60 and 1204±449 when co-cultured with 20.1 treated targets.

The difference in IL-2 production between γδ TCR-TE9-28 transduced αβ T cells and the γδ TCR-transduced αβ T cells was not statistically significant for the cells co-cultured with untreated MV4-11 and NOMO-1 cell. In contrast, the difference in cytokine level when co-cultured with 20.1 treated MV4-11 and NOMO-1 were found statistically significant: $p=0.0007$ and $p= 0.0405$, respectively. The difference in IL-2 production between γδ TCR-TE9-28 transduced αβ T cells and γδ TCR-transduced αβ T cells when co-cultured with untreated and 20.1 treated THP-1 cells was also statistically significant, $p<0.0001$ and $p= 0.0141$, respectively. No statistical difference was detected overall when comparing the untreated and 20.1 treated targets conditions.

IFN-γ production followed the same trend for γδ TCR-TE9-28 and γδ TCR-TE9-41BB transduced αβ T cells, by producing higher level of cytokines when compared to the γδ TCR-transduced αβ T cells control. γδ TCR-TE9-28 transduced αβ T cells produced 722±369, 1866±74 and 2800±608 when co-cultured with untreated M4-11, NOMO-1, and THP-1 respectively, and 2681±1480, 3257±492 and 4505±1619 when co-cultured with the 20.1 treated targets. γδ TCR-TE9-41BB transduced αβ T cells produced 1039±540, 1911±209 and 1806± 823 against untreated MV411, NOMO-1 and THP-1 and 3403±1962, 3691±1015 and 4167±2655 against 20.1 treated targets.

The difference in IFN-γ between the untreated and 20.1 treated targets however was not statistically significant for either effector. The difference in IFN-γ production between γδ TCR-TE9-28 transduced αβ T cells and γδ TCR-transduced αβ T cells when co-cultured with untreated and 20.1 treated MV4-11 was also not statistically significant. In contrast, the differences between the two effectors when co-cultured with untreated and 20.1 treated NOMO-1 and THP-1 was found to be statistically significant ($p= 0.0478$ and $p= 0.0093$ for untreated NOMO-1 and $p= 0.0006$ and $p<0.0001$ for untreated and treated THP-1 respectively). The difference in IFN-γ production between γδ TCR-TE9-41BB transduced αβ T cells and the γδ TCR-transduced αβ T cells when co-cultured with untreated MV4-11 was not statistically significant. In contrast differences between the two effectors when co-cultured with 20.1 treated MV4-11 and untreated and 20.1 treated NOMO-1 and THP-1 was found to be statistically significant ($p= 0.0043$ for 20.1 treated MV4-11, $p= 0.0413$ and $p= 0.0016$ for untreated and 20.1 treated NOMO-1 and $p= 0.0285$ and $p<0.0002$ for untreated and treated THP-1). The difference in cytokine release between the two effectors was also not found statistically significant.

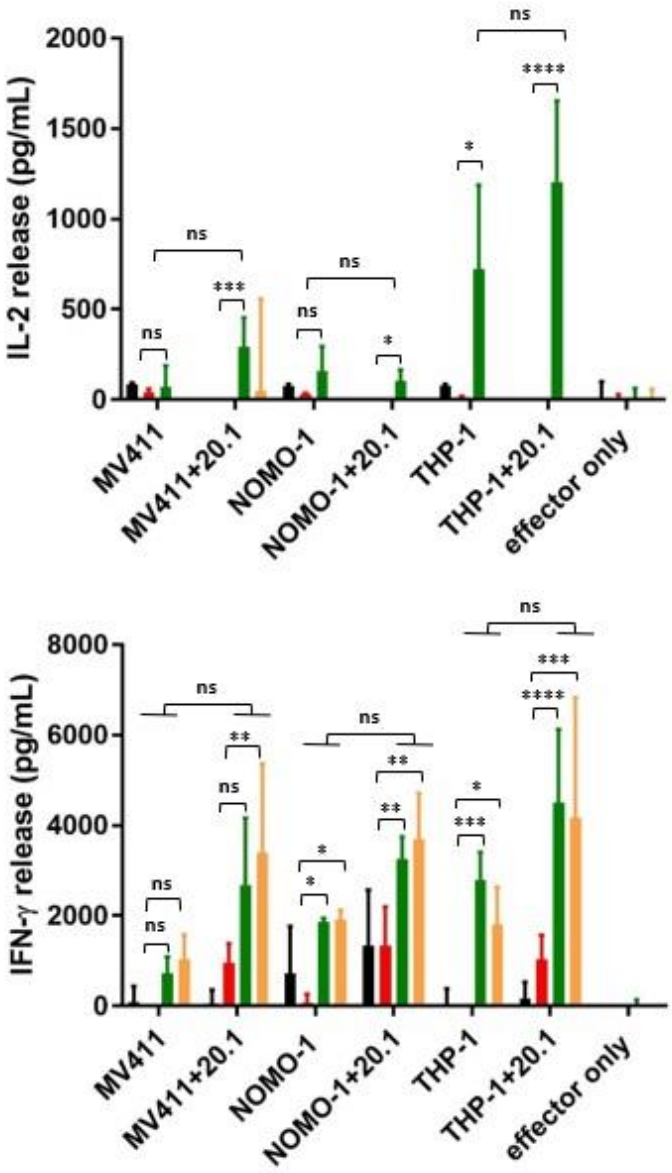

Figure 5.11 Quantification of IL-2 and IFN-γ production mediated by γδ TCR-TE9-28 and γδ TCR-TE9-41BB transduced αβ T cells against AML cell line post 18 hours. Untransduced αβ T cells and αβ T cells transduced with γδ TCR, γδ TCR-TE9-28 and γδ TCR-TE9-41BB were co-cultured for 18 hours with AML cell lines MV4-11, NOMO-1, and THP-1 or alone at 1:1 E:T ratio. IL-2 and IFN-γ were measured by ELISA. Graphs show mean ± SD (n=3 independent biological replicates). Statistical analysis was performed by 2-way ANOVA, followed by Tukey post hoc analysis : *p<0.1, ** p<0.01, ***p<0.001, ****p<0.0001.

Quantification of cytokines post re-stimulation

The responses of γδ TCR-TE9-28 and γδ TCR-TE9-41BB transduced αβ T upon rechallenge with B7H3 positive AML cell lines, were then investigated.

In order to achieve this, as mentioned previously, supernatant was collected from the co-culture after 18 hours incubation post re-challenge with targets, and IL-2 and IFN-γ were quantified by ELISA. Figure 5.12 shows IL-2 and IFN-γ production when effectors were re-stimulated with untreated and 20.1 treated AML cell lines.

γδ TCR-TE9-28 transduced αβ T cells produced low levels of IL-2 when co-cultured with untreated MV4-11, NOMO-1, and THP-1 and with 20.1 treated NOMO-1, however, the release was not statistically significant when compared to γδ TCR transduced αβ T cells against the same target. In contrast, γδ TCR-TE9-28 transduced αβ T cells produced statistically higher levels of IL-2 when co-cultured with 20.1 treated MV4-11 and THP-1, 4285±1436 and 2979±1747 pg/mL when compared to γδ TCR transduced αβ T cells ($p<000.1$). γδ TCR-TE9-41BB transduced αβ T cells also produced higher level of IL-2 when compared to γδ TCR-TE9-28 transduced αβ T cells when they were co-cultured with 20.1 treated MV4-11, 2919±873 pg/mL ($p<0.0001$). Statistical significance was detected between untreated and 20.1 treated MV4-11 and THP-1 when they were co-cultured with γδ TCR-TE9-28 (both target cell lines) and γδ TCR-TE9-41BB (just MV4-11) transduced αβ T cells.

In contrast, γδ TCR-TE9-28 transduced αβ T cells produced higher level of IFN-γ when co-cultured with both untreated and 20.1 treated AML cell lines when compared to γδ TCR transduced αβ T cells ($p<0.0001$). They produced 3487±798,

5247±1055 and 6068±486 pg/mL when co-cultured with untreated MV4-11, NOMO-1, and THP-1 respectively, and 4866.±166, 4258±305 and 6002±572 when co-cultured with the 20.1 treated targets. However no statistical difference was observed between the untreated and 20.1 treated conditions.

γδ TCR-TE9-41BB transduced αβ T cells also produced higher levels of IFN-γ when co-cultured with all the targets compare to γδ TCR-transduced αβ T cells ($p<000.1$) with levels comparable to the release by γδ TCR-TE9-28 transduced αβ T cells. However, γδ TCR-TE9-41BB transduced αβ T cells cultured with no target also produced high level of IFN-γ; 3933±765 pg/mL. While this level of release is still significantly lower than what produced against the untreated and 20.1 treated AML cell lines (7018±466, 7136±265 and 6889±85 with untreated MV4-11, NOMO-1 and THP-1 respectively and 7457±6, 7357±99 and 6889±85 with 20.1 treated targets), the data in consistent with an unexpected phenomenon of tonic signalling and cytokine induction specific to the 41BB containing CCR.

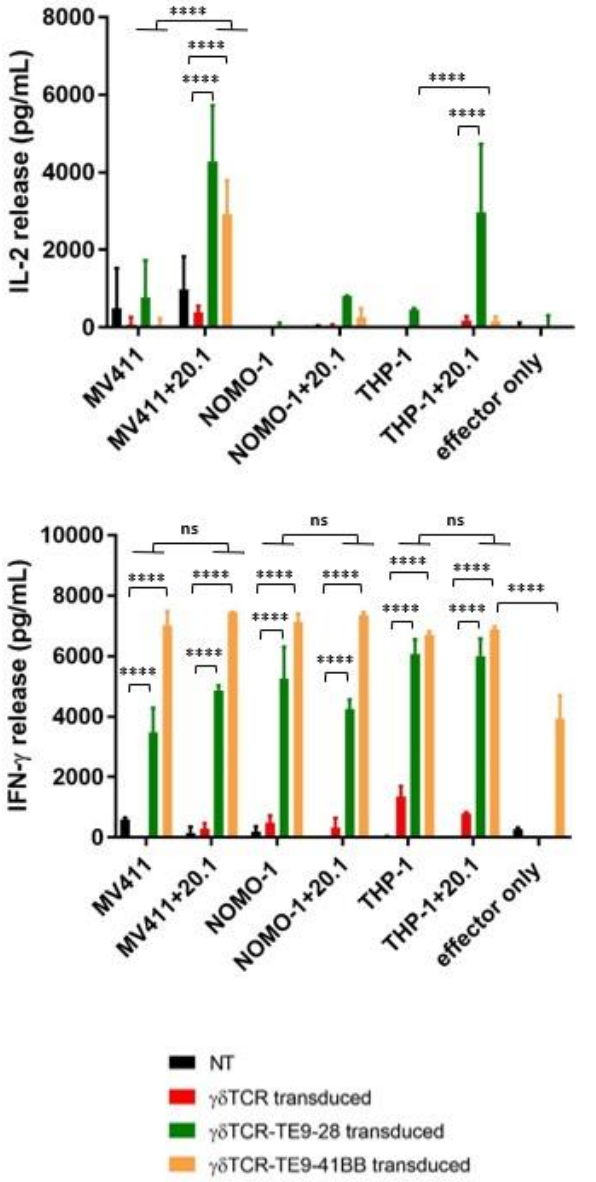

Figure 5.12 Quantification of IL-2 and IFN-γ production mediated by γδ TCR-TE9-28 and γδ TCR-TE9-41BB transduced αβ T cells against AML cell lines post antigen re-challenge. After 7 days co-culture, untransduced αβ T cells and αβ T cells transduced with γδ TCR, γδ TCR-TE9-28 and γδ TCR-TE9-41BB were re-stimulated with untreated and 20.1 treated AML MV4-11, NOMO-1, and THP-1 or alone at 1:1 E:T ratio. Post 18h, IL-2 and IFN-γ were measured by ELISA. Graphs show mean ± SD (n=3 independent biological replicates). Statistical analysis was performed by 2-way ANOVA, followed by Tukey post hoc analysis : ****p<0.0001.

5.4.4.2 Expansion mediated by γδ TCR-TE9-28 and γδ TCR-TE9-41BB transduced αβ T cells against AML cell lines.

In order to investigate the effect of the co-stimulation in promoting expansion of γδ TCR-TE9-28 and γδ TCR-TE9-41BB transduced αβ T cells in response to AML cell lines, effectors were co-cultured for 7 days with untreated and 20.1 treated MV4-11, NOMO-1 and THP-1 cell lines. As described previously, untransduced αβ T cells, γδ TCR, γδ TCR-TE9-28 and γδ TCR-TE9-41BB transduced αβ T cells were co-cultured with targets for 7 days and then re-stimulated with targets on day 7. One day later cells were collected, and expansion was analysed by flow cytometry analysis by detecting absolute T cell number using Count Bright Absolute Counting Beads. Effectors were also cultured with no target in order to detect any background proliferation. Gating strategy to detect counting beads and effector cells has been illustrated previously. Cells were gated on SSC-A and FCS-A and then gated on CD3-pos live cells.

Figure 5.13 shows absolute cell numbers of T cells after 7 days co-culture and re-stimulation with AML cell lines. As can be observed in the histogram, the cell numbers of γδ TCR-TE9-28 transduced αβ T cells co-culture with untreated and 20.1 treated AML cell lines are higher compared to the γδ TCR transduced αβ T cells conditions and the effector only control. The mean absolute cell count ±SD for γδ TCR-TE9-28 transduced αβ T cells co-culture with untreated MV4-11, NOMO-1 and THP-1 are 72039±70852, 204477±213239 and 309217±321848 respectively compared to the γδ TCR transduced αβ T cell count after co-culturing with the same targets, 21086±4607, 28769±9656 and 44556±17442.

The difference in absolute cell number between the two effectors co-cultured with the same targets however shows statistical significance only in the NOMO-1 (p=0.032) and THP-1 (p=0.0006) conditions.

A similar pattern is observed when γδ TCR-TE9-28 transduced αβ T cells are co-cultured with 20.1 treated MV4-11, NOMO-1, and THP-1. Absolute cell count ±SD were 80733±96531, 161462±117920 and 233609±211918 respectively compared to the γδ TCR transduced αβ T cell count after co-culturing with the same targets: 11510±4468, 28056±18136 and 37826±19163. Statistical significance is between the two effectors only when co-cultured with 20.1 treated THP-1 cell (p=0.0006).

γδ TCR-TE9-41BB transduced αβ T cell numbers also seem higher than γδ TCR transduced αβ T cells control when co-cultured with AML targets, however no statistically significant difference was observed between the two effectors. Moreover, γδ TCR-TE9-41BB transduced αβ T cell numbers have a higher absolute cell count when cultured with no targets, compared to the other effectors in the same condition. No statistical difference was observed between the untreated and 20.1 treated conditions.

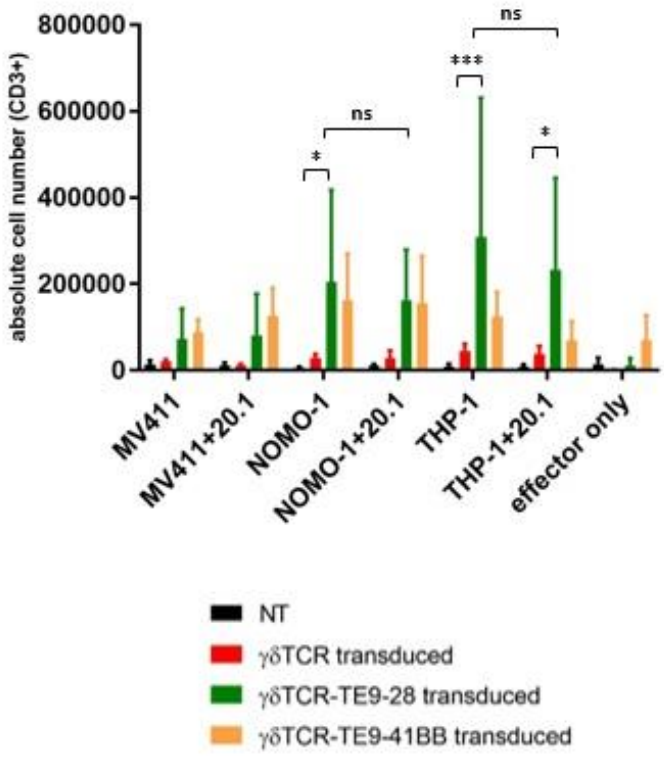

Figure 5.13 Proliferation mediated by γδ TCR-TE9-28 and γδ TCR-TE9-41BB transduced αβ T cells against AML cell lines. Untransduced αβ T cells αβ T cells transduced with γδ TCR, γδ TCR-TE9-28 and γδ TCR-TE9-41BB were co-cultured for 7 days with irradiated untreated and 20.1 treated MV4-11, NOMO-1, and THP-1 or alone at 1:1 E:T ratio. After 7 days cells effectors were re-stimulated with fresh targets and proliferation was assessed on day 8. Histograms showing the absolute cell numbers of effectors cells after being co-cultured with targets, n=3 independent biological replicates. Statistical analysis was performed by 2-way ANOVA, followed by Tukey post hoc analysis: * $p<0.1$, *** $p<0.001$.

5.4.4.3 Phenotyping of effectors cells co-cultured with AML cell lines.

For investigating proliferation, as described in the previous section, absolute cell numbers of T cells were calculated gating on all CD3+ cells as we used purified populations of effectors in these experiments.

However, we wanted to investigate the phenotype of the purified cell population post co-culture with the AML target. Figure 5.14 compares the αβ TCR and γδ TCR populations within the CD3+ cells between effectors right after purification of the single positive αβ TCR-γδ TCR+ population by depletion of αβ TCR+ cells and after these purified effectors have been in co-culture with the AML targets. Cells were gated αβ TCR and Vδ2 after gating on CD3+ cells excluding dead cells and doublets.

Interestingly, γδ TCR transduced αβ T cells, which did not show a significant increase in T cell number in response to targets in the results in the previous section, maintained the αβ TCR-γδ TCR+ phenotype. In contrast, γδ TCR-TE9-28 and γδ TCR-TE9-41BB transduced αβ T cells which have proliferated in response to the targets, present with 3 populations with distinct TCR expression: a αβ TCR+ γδ TCR- population, a αβ TCR+ γδ TCR+ population and a αβ TCR- γδ TCR+. It is possible that the γδ TCR has been downregulated post engagement, however single cell sequencing would be necessary to fully characterize and confirm the identity of the different cell population.

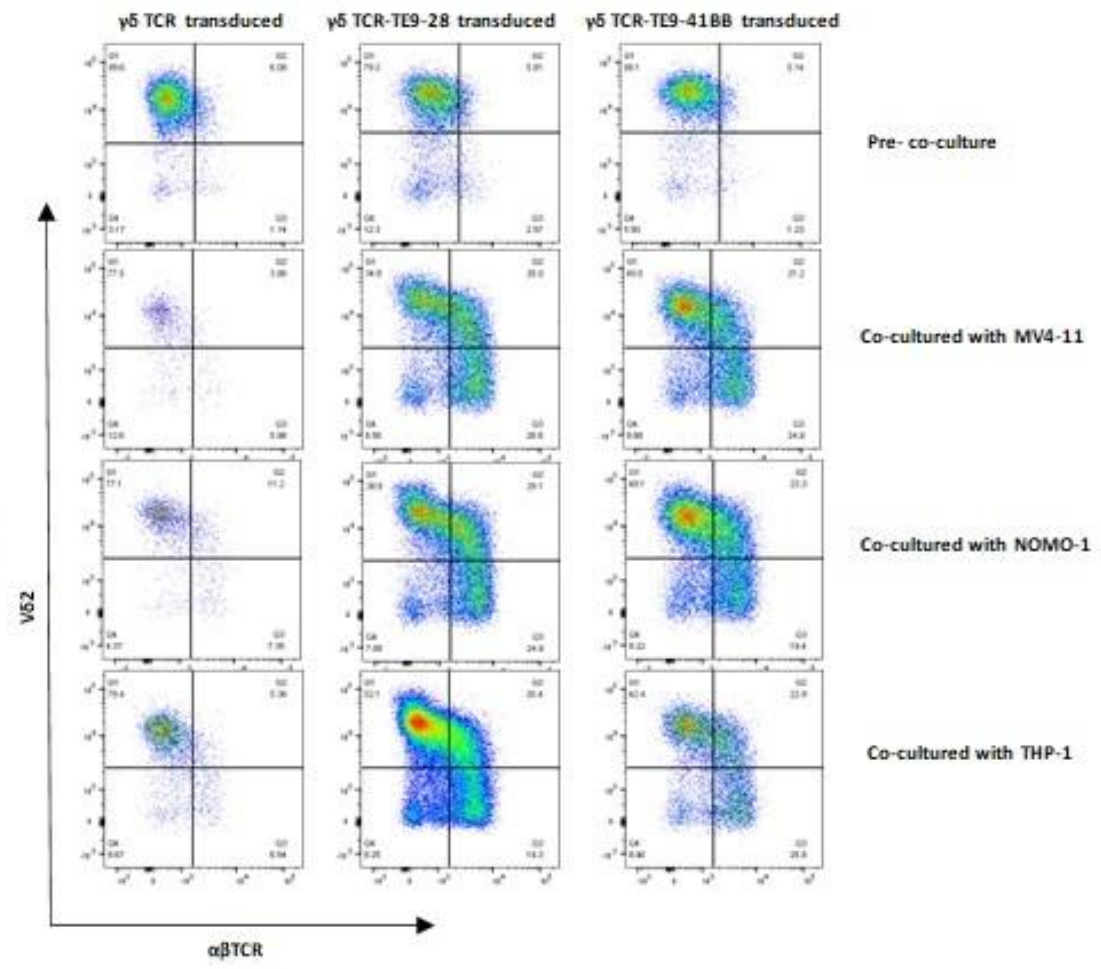

Figure 5.14 Phenotyping of effectors cells co-cultured with AML cell lines. αβ TCR and γδ TCR expression was detected on purified γδ TCR, γδ TCR-TE9-28 and γδ TCR-TE9-41BB αβ T cells before and after the effectors were co-cultured with AML cell lines for 7 days. αβ TCR and γδ TCR populations were detected by flow cytometry using anti- αβ TCR FITC and anti-Vδ2-PE antibodies.

5.4.4.4 Cytotoxicity mediated by γδ TCR-TE9-28 and γδ TCR-TE9-41BB transduced αβ T cells against AML cell lines.

As previously described, when re-stimulating the co-cultures with fresh untreated and 20.1 treated targets, they were labelled with CellTrace violet. Therefore post 18 hours from re-stimulation, when collecting the cells to detect proliferation, it was also possible to investigate cytotoxic activity of γδ TCR-TE9-28 and γδ TCR-TE9-

41BB transduced αβ T cells by detecting loss of live targets by flow cytometry. Count Bright Absolute Counting Beads were used to assess the absolute cell numbers.

Figure 5.15A illustrate the gating strategy to detect loss of live AML cells in one representative donor when co-cultured with untransduced αβ T cells, γδ TCR, γδ TCR-TE9-28 and γδ TCR-TE9-41BB transduced αβ T cells. Cells were gated on live and CD3-neg cells and then gated on CellTrace violet-pos and B7H3-pos population.

Figure 5.15B shows the absolute cell numbers in these gatings, calculated based on the relative number of counting beads. Counting beads were gated on the SSC-A and FCS-A plot as shown in previous experiment (not shown). Targets were cultured with no effectors as negative control.

When the effectors were co-cultured with untreated and 20.1 treated MV411, it is possible to observe a drop in the absolute cell number when the targets were co-cultured with γδ TCR-TE9-28 and γδ TCR-TE9-41BB transduced αβ T cells compared to the γδ TCR transduced αβ T cells control. The mean absolute cell count ±SD of untreated MV4-11 when co-cultured with γδ TCR transduced αβ T cells was 85479±15730 compared to 14239±18801 and 151±85 when co-cultured with γδ TCR-TE9-28 and γδ TCR-TE9-41BB transduced αβ T cells, respectively. The difference in live cell count is statistically significant ($p<0.0001$ for both comparisons). Moreover, no statistical significance was observed in absolute target count between γδ TCR transduced αβ T cells and untransduced αβ T cells.

The same trend was observed for 20.1 treated MV4-11: while the live cell count when they were co-cultured with γδ TCR transduced αβ T cells was 34638±4929,

when they were co-cultured with γδ TCR-TE9-28 and γδ TCR-TE9-41BB transduced αβ T cells, their live cell count dropped to 208±136 and 50±14 respectively. This difference as well was statistically significant (p=0.0180 for γδ TCR-TE9-28 and p= 0.0175 for γδ TCR-TE9-41BB. Again, no statistical significance was observed in absolute target count between γδ TCR transduced αβ T cells and untransduced αβ T cells.

Same behaviour was observed when effectors were co-cultured with untreated and 20.1 treated NOMO-1 cells. The absolute target cell count dropped when the targets were co-cultured with γδ TCR-TE9-28 and γδ TCR-TE9-41BB transduced αβ T cells compared to the γδ TCR transduced αβ T cells control. The mean absolute cell count ±SD of untreated NOMO-1 when co-cultured with γδ TCR transduced αβ T cells was 86543±10105 compared to 13566±16488 and 1841±2301 when co-cultured with γδ TCR-TE9-28 and γδ TCR-TE9-41BB transduced αβ T cells, respectively.

The difference in live cell count is statistically significant (p=0.0002 for γδ TCR-TE9-28 and p<0.0001 for γδ TCR-TE9-41BB), while no statistical significance was observed in absolute target count between γδ TCR transduced αβ T cells and untransduced αβ T cells. The same trend was observed for 20.1 treated NOMO-1: while the live cell count when they were co-cultured with γδ TCR transduced αβ T cells was 55769±14288, when they were co-cultured with γδ TCR-TE9-28 and γδ TCR-TE9-41BB transduced αβ T cells, their live cell count dropped to 2560±3019 and 126±22respectively. This difference as well was statistically significant (p=0.0132 for γδ TCR-TE9-28 and p= 0.0099 for γδ TCR-TE9-41BB. Again, no statistical significance was observed in absolute target count between γδ TCR transduced αβ T cells and untransduced αβ T cells, again demonstrating the

significant effect of co-stimulation to drive sustained cytotoxicity against these targets.

In contrast, analysis of loss of live cells when effectors were co-cultured with THP-1 cells, shows a drop in live cells absolute numbers already when the targets were co-cultured with γδ TCR transduced αβ T cells (22580±2566 untreated THP-1 and 38420±1878220.1 treated THP-1) compared to the untransduced αβ T cell control (81727±3767 untreated THP-1 and 62709±10673 20.1 treated THP-1). The difference in cell count was statistically significant ($p<0.0001$ for untreated NOMO-1 and $p=0.0248$ for 20.1 treated NOMO-1 cells). However, it was still possible to observe a statistically significant drop in the absolute cell number when the targets were co-cultured with γδ TCR-TE9-28 and γδ TCR-TE9-41BB transduced αβ T cells compared to the γδ TCR transduced αβ T cells control. The mean absolute cell count ±SD of untreated THP-1 was 685±267 and 768± 42 when co-cultured with γδ TCR-TE9-28 and γδ TCR-TE9-41BB transduced αβ T cells, respectively. The mean absolute cell count ±SD of 20.1 treated THP-1 was 4176±2146 and 11440±6563 when co-cultured with γδ TCR-TE9-28 and γδ TCR-TE9-41BB transduced αβ T cells, respectively.

The difference in live cell count between targets co-cultured with γδ TCR-TE9-28 and γδ TCR-TE9-41BB transduced αβ T cells compared to γδ TCR transduced αβ T cells was statistically significant ($p=0.0423$ and $p=0.0431$ respectively, for untreated THP-1 cells and $p=0.0029$ and $p= 0.0137$ respectively, for 20.1 treated targets).

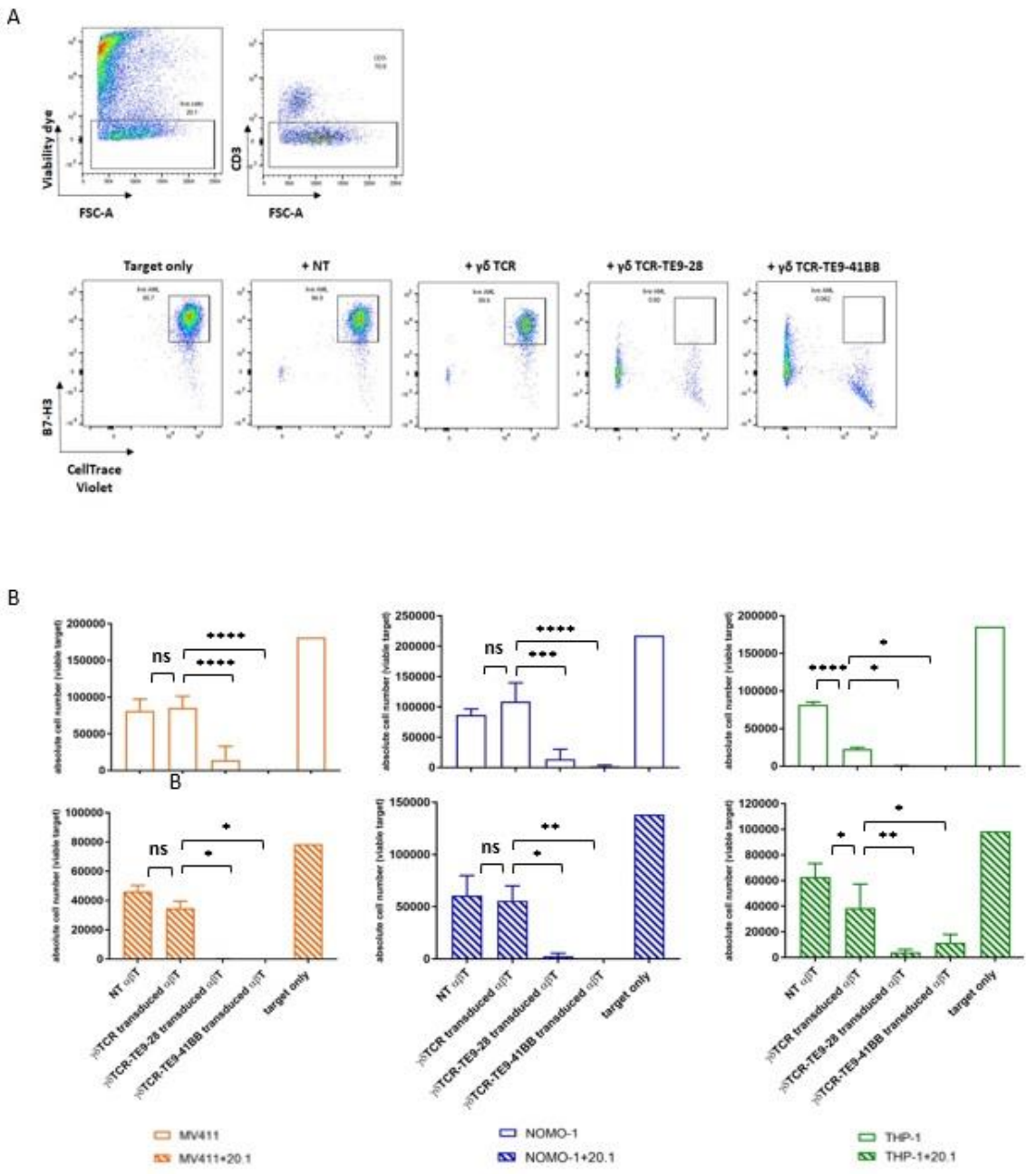

Figure 5.15 Cytotoxicity mediated by γδ TCR-TE9-28 and γδ TCR-TE9-41BB transduced αβ T cells against AML cell lines. Untransduced αβ T cells αβ T cells transduced with γδ TCR, γδ TCR-TE9-28 and γδ TCR-TE9-41BB were co-cultured for 7 days with irradiated untreated and 20.1 MV4-11, NOMO-1, and THP-1 or alone at 1:1 E:T ratio. After 7 days cells effectors were re-stimulated with fresh untreated and 20.1 treated targets labelled with CellTrace violet. 18 hours post re-challenge, cells were analysed for loss of live target cells by flow cytometry. (A) Representative gating strategy to identify target cells after exclusion of dead and doublet cells. (B) histograms showing the absolute cell numbers of target cells post co-culture. n=3 independent biological replicates. Statistical analysis was performed by 2-way ANOVA, followed by Tukey post hoc analysis: *p<0.1, ** p<0.01, ***p<0.001, ****p<0.0001.

5.4.5 In vitro activity of γδ TCR-TE9-28 and γδ TCR-TE9-41BB transduced αβ T cells against 3T3 WT and 3T3-B7H3 cell lines

In order to study the safety of the γδ TCR-TE9 CCR in αβ T cell system, we investigated the in vitro activity of γδ TCR-TE9-28 and γδ TCR-TE9-41BB transduced αβ T cells against 3T3 WT and 3T3-B7H3 cell lines. 3T3 cell line derives from mouse embryonic fibroblasts, therefore they are not able to engage human γδ TCR. In this setting is possible to study the activity of TCR-TE9 CCR in αβ T cells when the γδ TCR is not engaged.

In this section, αβ T cells were also transduced to express the second generation TE9-28-ζ CAR. The intent was to use TE9-28-ζ transduced αβ T cells as positive control for engagement of the cognate antigen, independently from TCR engagement. Transduction efficiency was confirmed by flow cytometry. The following experiments were performed in two biological replicates; therefore, we did not perform any statistical analysis.

5.4.5.1 Generation of 3T3-B7H3 cell line

3T3 WT cells were transduced with γ-retroviral supernatant produced from triple transfection of 293T cells with a oncoretroviral SFG vector encoding for 4IgB7-H3. Transduction efficiency was assessed by flow cytometry by using the commercially available anti-human CD276 (B7-H3)-APC that has been used to stain all the other B7H3+ cell lines. Figure 5.16 shows B7H3 staining of 3T3 WT cells and 3T3 cells post transduction with the 4IgB7-H3 construct. Based on that gating, high B7H3 cells were bulk sorted and used in the following experiments. Due to time limitation,

cells weren't single cell sorted for high expressing clones, however future work but will require generation of stable clones.

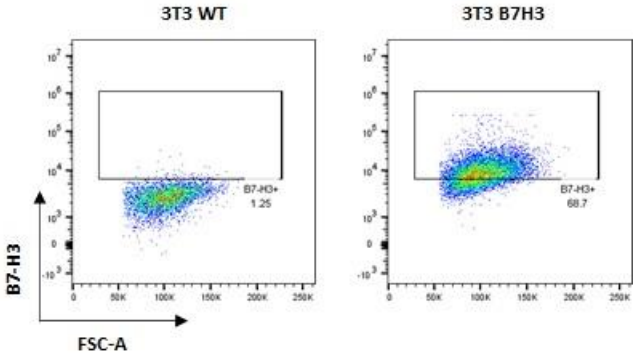

Figure 5.16. Generation of 3T3-B7H3 cell line. 3T3 WT cells were transduced with γ-retroviral supernatant produced from triple transfection of 293T cells with a oncoretroviral SFG vector encoding for 4IgB7-H3. Transduction efficiency was assessed by flow cytometry by using the commercially available anti-human CD276 (B7-H3)-APC. Representative FACS plots gated on B7H3 before and after transduction.

5.4.5.2 Quantification of IL-2 and IFN-γ production mediated by γδ TCR-TE9-28 and γδ TCR-TE9-41BB transduced αβ T cells against 3T3 and 3T3-B7H3.

<u>Quantification of cytokines post 18 hours</u>

Untransduced αβ T cells, γδ TCR, γδ TCR-TE9-28,γδ TCR-TE9-41BB and TE9-28-ζ transduced αβ T cells were co-cultured with 3T3 WT and 3T3 B7H3 cells for 18 hours at 1:1 ratio at a density of $2.5x10^5$ cell/well in 0.5 mL. Post 18 hours, supernatant was collected and IL-2 and IFN-γ cytokines were quantified by ELISA. Figure 5.17 shows IL-2 and IFN-γ production mediated by the effectors when co-cultured with untreated and 20.1 treated 3T3 WT and 3T3 B7H3 cells.

Low level of IL-2 is produced by all effectors (below 200 pg/mL for all of them) and it is not possible to describe any specific trend. In contrast, IFN-γ production looks cleaner: TE9-28-ζ transduced αβ T cells produced higher level of IFN-γ when co-cultured with untreated and 20.1 treated 3T3 B7H3 (1813±1283 and 1569±635 pg/mL respectively), compared to the untreated and 20.1 treated 3T3 WT control (300±303 and -349±388 pg/mL respectively). As this experiment was performed in two biological replicates, it was not possible to detect any statistical significance. Other effectors did not produce any detectable amount of IFN-γ.

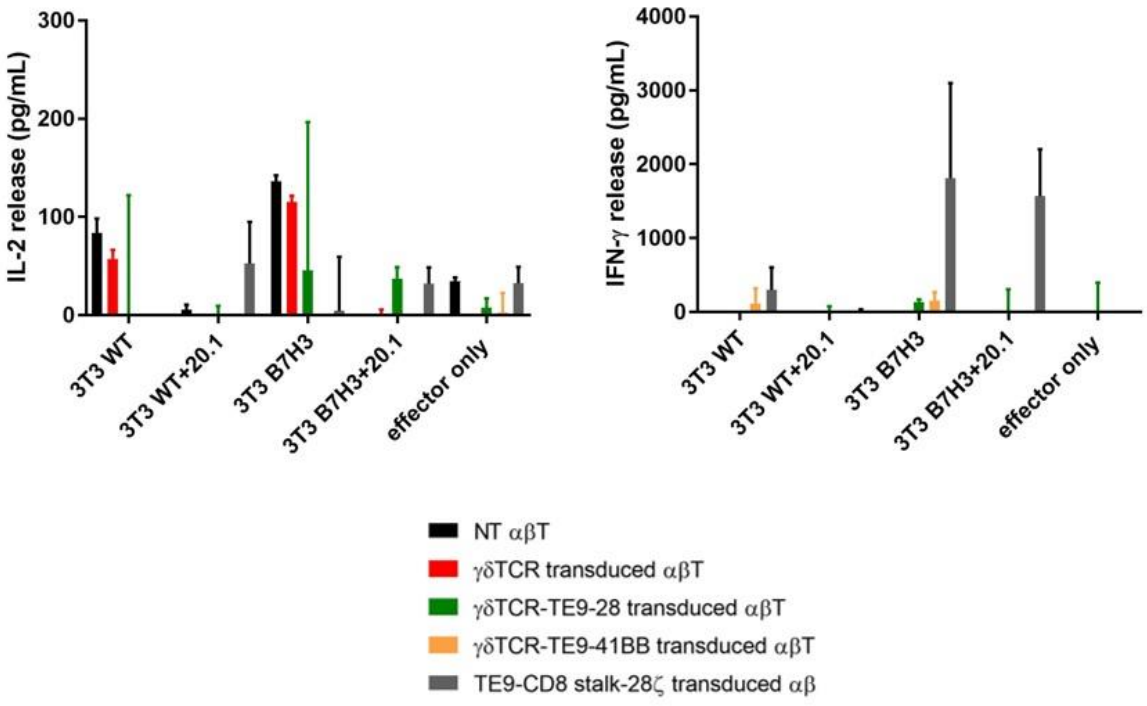

Figure 5.17 Quantification of IL-2 and IFN-γ production mediated by γδ TCR-TE9-28 and γδ TCR-TE9-41BB transduced αβ T cells against 3T3 WT and 3T3 B7H3 cell line post 18 hours. Untransduced αβ T cells and αβ T cells transduced with γδ TCR, γδ TCR-TE9-28, γδ TCR-TE9-41BB and TE9-28-ζ were co-cultured for 18 hours with untreated and 20.1 treated 3T3 WT and 3T3 B7H3 cells or alone at 1:1 E:T ratio. IL-2 and IFN-γ were measured by ELISA. Graphs show mean ± SD (n=2 independent biological replicates). No statistical analysis was performed.

Quantification of cytokines post re-stimulation

Cytokine were quantified by ELISA after re-stimulation of the co-culture with untreated and 20.1 treated 3T3 WT and 3T3 B7H3 cells (Figure 5.18).

IL-2 production by the effectors was not interpretable as seen in the cytokine release post 18 hours. There are some levels of IL-2 production by γδ TCR-TE9-28 transduced αβ T cells and TE9-28-ζ transduced αβ T cells in response to both 3T3 WT and 3T3 B7H3 cells. The level of production is variable between the two donors, and no statistical analysis was performed given the lack of biological replicates. In contrast, TE9-28-ζ transduced αβ T cells appear to produce higher level of IFN-γ when co-cultured with untreated and 20.1 treated 3T3 B7H3 (2033±981 and 1222±241 pg/mL respectively), compared to the untreated and 20.1 treated 3T3 WT control (192±193 and 648±796 pg/mL respectively). No statistical analysis was performed.

γδ TCR-TE9-4-1BB transduced αβ T cells, as seen in the previous experiments produced high levels of IFN-γ independently from the presence of the antigen, in fact IFN-γ production in the range of 7000-8000 pg/mL is observed in response to untreated and 20.1 treated 3T3 WT and 3T3 B7H3 cells. Moreover, the effector produced high levels of IFN-γ (3850±1063) even when cultured with no targets.

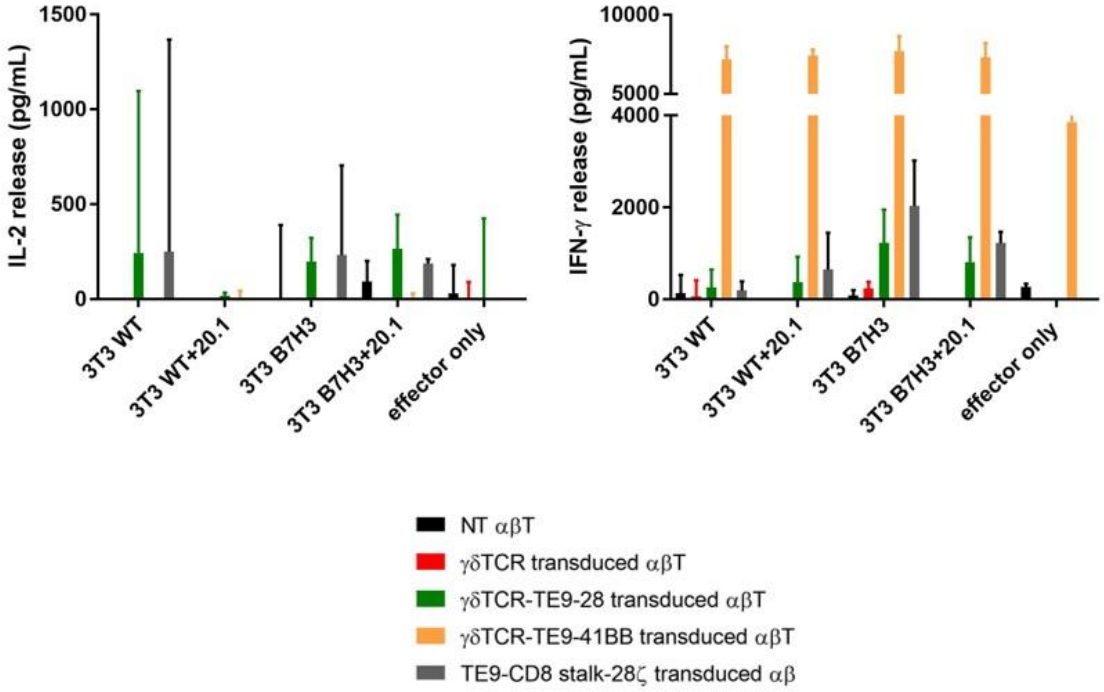

Figure 5.18 Quantification of IL-2 and IFN-γ production mediated by γδ TCR-TE9-28 and γδ TCR-TE9-41BB transduced αβ T cells against 3T3 WT and 3T3 B7H3 cell line post re-challenge. After 7 days co-culture, untransduced αβ T cells and αβ T cells transduced with γδ TCR, γδ TCR-TE9-28 and γδ TCR-TE9-41BB were re-stimulated with untreated and 20.1 treated 3T3 WT and 3T3 B7H3 cells or alone at 1:1 E:T ratio. Post 18h, IL-2 and IFN-γ were measured by ELISA. Graphs show mean ± SD (n=2 independent biological replicates). No statistical analysis was performed.

5.4.5.3 Expansion mediated by γδ TCR-TE9-28 and γδ TCR-TE9-41BB transduced αβ T cells against 3T3 WT and 3T3 B7H3 cell lines.

In order to investigate the expansion mediated by γδ TCR-TE9-28 and γδ TCR-TE9-41BB transduced αβ T cells in response to 3T3 WT and 3T3-B7H3 cell lines, effectors were co-cultured for 7 days with untreated and 20.1 treated targets. Untransduced αβ T cells, γδ TCR, by γδ TCR-TE9-28, γδ TCR-TE9-41BB and TE9-28-ζ transduced αβ T cells were co-cultured with targets for 7 days and then

re-stimulated with targets on day 7. The day after cells were collected and expansion was analysed by flow cytometry analysis by detecting absolute T cell number using Count Bright Absolute Counting Beads. Effectors were also culture with no target in order to detect any background proliferation.

Gating strategy to detect counting beads and effector cells has been illustrated previously. Cells were gated on SSC-A and FCS-A and then gated on CD3-pos live cells. Figure 5.19 shows absolute cell numbers of T cells after 7 days co-culture and re-stimulation with 3T3 and 3T3 B7H3 cell lines. As it can be observed in the histogram the cell numbers of TE9-28-ζ transduced αβ T cells were slightly higher when the effector where co-cultured with untreated and 20.1 treated 3T3 B7H3 (56629±2834 and71855±6582 respectively) compared to the 3T3 WT controls (19119±460 and 24679±876 respectively).

Absolute cell count of γδ TCR-TE9-28 transduced αβ T cells appear to be consistent amount all the conditions. The T cell count of γδ TCR-TE9-41BB transduced αβ T cells, however, is higher than any other effectors, but no difference was observed within the different conditions. The effector absolute cell count when cultured with no-target indicates some degree of proliferation independent from any stimulus. No statistical analysis was performed.

Unfortunately, it was not possible to investigate cytotoxic activity of the effector towards 3T3 WT and 3T3 B7H3, due to a technical mistake.

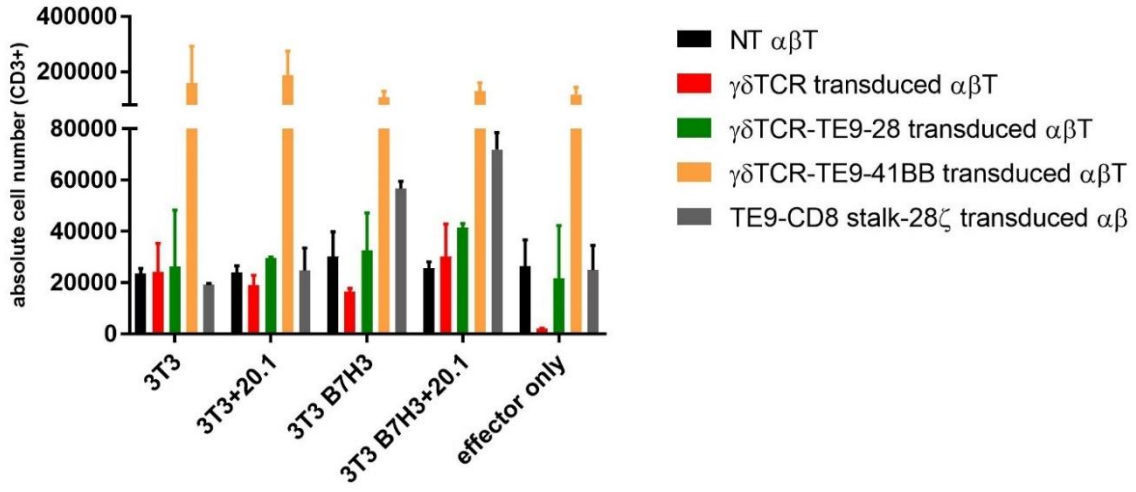

Figure 5.19 Expansion mediated by γδ TCR-TE9-28 and γδ TCR-TE9-41BB transduced αβ T cells against 3T3 WT and 3T3 B7H3. Untransduced αβ T cells αβ T cells transduced with γδ TCR, γδ TCR-TE9-28, γδ TCR-TE9-41BB and TE9-28-ζ were co-cultured for 7 days with irradiated untreated and 20.1 3T3 WT and 3T3 B7H3 or alone at 1:1 E:T ratio. After 7 days cells effectors were re-stimulated with fresh targets and expansion was assessed on day 8. Histograms showing the absolute cell numbers of effectors cells after being co-cultured with targets, n=2 independent biological replicates. No statistical analysis was performed.

5.5 DISCUSSION

The aim of this chapter was to co-express on αβT cells, a tumour reactive γδ TCR and a CCR targeting a tumour associated antigen as an alternative approach to deliver antigen specific tumour reactivity as well as provide a safety mechanism to avoid on-target off tumour toxicity. As mentioned previously, while different studies have focused on investigating the activity of a CCR in γδ T cells in order to avoid on-target of tumour toxicity (Fisher et al., 2017), this is the first time at our knowledge that the contribution of co-stimulation through a CCR is investigated in αβ T cells engineered to express a γδ TCR.

In this chapter we investigated whether it was possible to co-express an anti-B7H3 CCR together with a γδ TCR on αβT cells, and we investigated the in vitro activity of γδ TCR - CCR transduced αβ T cells in terms of cytotoxicity, ability to produce cytokines and proliferate in response to specific stimuli, in order to study the contribution of co-stimulation in such a system.

TE9-CD8 binder-spacer targeting B7-H3 and CD28 or 4-1BB co-stimulatory endodomains were chosen to be included in the CCR component of the proposed system. The binder was chosen based on the results in chapter I, while CD28 and 4-1BB were chosen as prototypic co-stimulatory endodomains as they are widely studies in CAR-T cell based strategies (J.N. et al., 2010; Ramos et al., 2017) with CD28 inducing a quicker T cell activation and 4-1BB promoting a more progressive long lasting response. γδ TCR-TE9-28 and γδ TCR-TE9-41BB constructs were generated by restriction cloning by incorporating TE9-28 and TE9-41BB CCR sequences in the SFG gamma-retroviral vector expressing the G115 γδ TCR.

In the previous chapter the transgenic γδ TCR component of the proposed system was investigated and most of the work was done on a γδ T cell sensitive cell line, Daudi.

In contrast, in this chapter we evaluated the activity of γδ TCR-TE9-28 and γδ TCR-TE9-41BB in a panel of cell lines. Therefore, before testing our constructs, to ensure γδ TCR engagement with the rest of the cell lines, cells were stimulated with the 20.1 monoclonal anti- BTN3A antibody, which bind extracellular domain of BTN3A molecule and has been used to induce TCR activation in previous studies. In order to do this, BTN3A was firstly assessed on target cells Jurkat WT and AML cell lines, MV4-11, NOMO-1, and THP-1. We demonstrated that all the target cell lines expressed BTN3A (**Figure 5.2**), therefore we proceeded to stimulated them with the antibody and investigated the activity mediated by purified γδ TCR-transduced αβ T cells in response to the treatment.

The optimal way to investigated potential γδ TCR activation would have been by assessing upregulation of killing, however the radioactivity laboratory was not available for use during the time frame of this experiments, therefore it was not possible to perform a ^{51}Cr release assay. As an alternative we investigated the cytokine production by γδ TCR-transduced αβ T cells after targets were stimulated with 20.1 (**Figure 5.3**). We found that γδ-TCR transduced αβT cells produced significant higher levels of cytokines when they were co-cultured with the 20.1 treated Daudi, MV4-11, NOMO-1, and THP-1 targets compared to the untreated controls.

The data on Daudi is interesting considering that we have evaluated γδ TCR-transduced αβ T cells on Daudi in previous occasions and the effectors have

produced cytokines even without the need of stimulating the target cells in order to guarantee TCR engagement. Moreover, additional results in this chapter showed that γδ TCR transduced αβ T cells were able to produce cytokines even in response to untreated Daudi. Therefore, we are not aware of why no cytokine production is observed in this instance. We hypothesise that it might have to do with the health state of the cell line in that specific experiment. Interestingly, γδ TCR-transduced αβ T cells did not produced any cytokines against 20.1 treated Jurkat WT, however we hypothesised that some γδ TCR synapses might benefit from co-stimulation interaction to stabilise the synapse, and that co-stimulation might be required in this instance to see any effect.

After confirming that it was possible to upregulate γδTCR engagement using the 20.1 antibody, we proceeded to evaluate the expression of γδ TCR-TE9-28 and γδ TCR-TE9-41BB constructs on transduced αβ T cells and compared to the expression of the γδ TCR construct (**Figure 5.4**).

The transduction profile of γδ TCR-TE9-28 and γδ TCR-TE9-41BB transduced αβ cells was similar to the one of γδ TCR construct, with the exception that the αβ TCR- γδTCR+ population in γδ TCR-TE9-28 and γδ TCR-TE9-41BB transduced αβ T cells were also positive for the CCR. Interestingly the transduction efficiency of the αβ TCR- γδTCR+ population in γδ TCR-TE9-28 and γδ TCR-TE9-41BB transduced αβ T cells was significantly lower compared to the γδ TCR control. Indeed, while γδTCR transduced αβ T cells are 33±6% αβTCR- γδTCR+, γδ TCR-TE9-28 and γδ TCR-TE9-41BB transduced αβ T cells are respectively 15±3% and 14±5%.

The size of the inserts between the LTRs in the retroviral constructs are respectively 1977 bp for the γδTCR construct, 3162 bp for γδ TCR-TE9-41BB and 3159 bp for γδ TCR-TE9-28. The lower transduction efficiency was quite a limiting factor considering that the αβTCR- γδTCR+ were purified by depletion of αβ TCR+ populations before being used in the following experiments. We attempted to overcome this limitation by cloning our constructs into lentiviral format, however for unknown reasons we failed to express the constructs through lentiviral production (data not shown). Therefore, for the scope of the experiments in this chapter we worked with the retroviral constructs. However, a strategy to achieve better transduction efficiency with the bigger constructs needs to be optimized in order for this approach to be feasible at a technical level.

The efficacy in vitro of γδ TCR-TE9-28 and γδ TCR-TE9-41BB transduced αβ T cells was firstly investigated on isogenic cell lines Jurkat WT and Jurkat B7H3, in order to evaluate responses mediated by co-stimulation in presence and absence of their cognate antigen when γδ TCR is engaged. Daudi was included as positive control for γδ TCR engagement, and which is also usefully negative for B7-H3 (**Figure 5.6**). Untreated and 20.1 treated targets were used in all the following experiment, however no striking difference upon treatment as seen in figure 5.3 was detected in any of the experiments. The only difference between the following experiment and the preliminary experiment performed in order to test 20.1 antibody is that the targets in the following experiments were irradiated. It is possible that the irradiation is behind the experimental differences. While we are not fully aware of the mechanism involved, we hypothesis that Irradiation might modulate expression or activation of BTN3A molecules on the cell surface.

In an 18 hours co-culture we found that γδ TCR-TE9-28 transduced αβ T cells were able to mount a response in an antigen dependent manner as they produced IFN-γ and IL2 in response to Jurkat B7H3 but not Jurkat WT. in contrast, as expected, γδ TCR engagement alone was sufficient to drive anti-tumour responses and no added benefit through co-stimulation was detected, consistent with the fact that Daudi are B7H3 negative (**Figure 5.7**).

When cytokines were quantified after restimulation of effectors with targets after 7 days co-culture (**Figure 5.8**), γδ TCR-TE9-28 transduced αβ cells produced cytokines again in an antigen dependent manner. γδ TCR-TE9-41BB transduced αβ cells which activity was not seen in the 18 hours co-culture, after 7 days produced very high level of IFN-γ in an antigen and target independent manner, as the effectors produced high levels of IFN- γ when they were cultured with Jurkat WT, Jurkat B7H3 but also when they were cultured with no targets. This data in consistent with an unexpected phenomenon of tonic signalling and cytokine induction specific to the 41BB containing CCR.

CARs are designed to drive antigen-specific activation upon binding of the scFv to its cognate antigen, however in certain combinations of scFv, hinge, and costimulatory domains, they can also elicit different levels of ligand-independent constitutive signalling, also known as tonic signalling. Antigen-independent signalling is partly caused by high density of CARs on the T cell surface that results in physical interactions between CAR molecules. CARs displaying tonic signalling are associated with accelerated T cell differentiation and exhaustion and impaired antitumor effects.

To our knowledge, no previous study of a non-engaged 41BB CCR has shown this level of specific activation and function after prolonged culturing, therefore, it could have implications in terms of choice of CCR for clinical use since the tonic signalling could result in both exhaustion and toxicity..

Proliferation data was consistent with what was observed in terms of cytokine production; indeed, absolute T count of γδ TCR-TE9-28 transduced αβ T cells increased significantly when they were cultured with Jurkat B7H3 targets compared to Jurkat WT, once again highlighting the role of co-stimulation in the presence of the cognate antigen (**Figure 5.9**). Cytotoxicity on targets was also assessed by flow cytometry and data were consistent with what seen in terms of cytokine production and proliferation (**Figure 5.10**). Results showed significant loss of live Jurkat B7H3 when co-cultured with γδ TCR-TE9-28 transduced αβ T cells compared to γδ TCR transduced αβ T cells while no significant loss of Jurkat WT was detected. Comparable results were seen for γδ TCR-TE9-41BB, however cytotoxicity data cannot inform on any potential tonic signalling.

The in vitro activity of γδ TCR-TE9-28 and γδ TCR-TE9-41BB transduced αβ T cells towards B7H3 positive AML cell line MV411, NOMO-1 and THP-1 was investigated next (**Figure 5.11**). consistent with the previous data, γδ TCR-TE9-28 transduced αβ cells produced higher cytokine levels when co-cultured with AML targets compared to the γδ TCR transduced αβ control with some degree of statistically non-significant variability between untreated and 20.1 treated targets. Interestingly, γδ TCR-TE9-41BB transduced αβT cells produced cytokines towards the AML targets in the 18h co-culture, something that was not observed with the positive control Jurkat B7-H3. This cytokine production was significantly higher than the γδ TCR transduced αβ control.

After re-stimulation (**Figure 5.13**) γδ TCR-TE9-28 produced significant levels of IL-2 only in response to 20.1 treated MV411 and THP-1. In contrast the effector produced significant higher levels of IFN-γ compared to the γδ TCR control when co-cultured with all targets. Once again, γδ TCR-TE9-41BB transduced αβT cells mounted an IFN-γ cytokine response which could not be attributed to the effect of the target cells as the effector alone also produced high level of cytokine.

Proliferation of these effectors co-cultured with the AML targets in some degree reflected what was observed in terms of cytokine release. Indeed, γδ TCR-TE9-28 transduced αβT absolute cell count increased when co-cultured with the AML cell lines. While statistical significance is detected only when co-cultured with untreated NOMO-1 untreated and 20.1 treated THP-1, the same trend is observed on all the other targets.

γδ TCR-TE9-41BB transduced αβ T cells also showed some degree of proliferation when co-cultured with the AML targets, however it was not found to be significant when compared to the cell count of the effector when it was not cultured with any target. For investigating the proliferation, absolute cell numbers of T cells were calculated gating on all CD3+ cells as we used purified populations of effectors in these experiments. However, we wanted to investigate the phenotype of the purified cell population post co-culture with the AML target. Therefore, we compared the αβ TCR and γδ TCR populations within the CD3+ cells between effectors right after purification of the single positive αβ TCR-γδ TCR+ population by depletion of αβ TCR+ cells and after these purified effectors have been in co-culture with the AML targets (**Figure 5.14)**.

Interestingly, γδ TCR transduced αβ T cells, which did not show a significant increase in T cell number in response to targets, maintained a αβ TCR-γδ TCR+ phenotype. In contrast, in γδ TCR-TE9-28 and γδ TCR-TE9-41BB transduced αβ T cells which have proliferated in response to the targets, 3 populations with distinct TCR expression were detected: a αβ TCR+ γδ TCR- population, a αβ TCR+ γδ TCR+ population and a αβ TCR- γδ TCR+.

We are not fully aware of the mechanism behind the selective expression of the endogenous αβ TCR or the transgenic γδ TCR. It is possible that the γδ TCR has been downregulated post engagement, however only single cell sequencing could fully characterize and confirm the identity of the different cell populations. Cytotoxicity data (**Figure 5.15**) demonstrated increased loss of live MV411 and NOMO-1 (untreated and treated with 20.1) when the targets were co-cultured with γδ TCR-TE9-28 and γδ TCR-TE9-41BB transduced αβ T cells compared to the γδ TCR transduced αβ T cells control. In contrast, significant increase in loss of live THP-1 was observed when the cells were cultured with the γδ TCR transduced αβ T cells, showing some cytotoxicity mediated by the γδ TCR only. However, the loss of live THP-1 was even greater when the targets were co-cultured with the γδ TCR-TE9-28 and γδ TCR-TE9-41BB transduced αβ T cells, suggesting added contribution effect of co-stimulation.

Interestingly, stimulation with 20.1 does not sensitise AML cell lines to killing by γδ TCR transduced αβ T cells in the absence of expression of the costimulatory receptor. This can also be seen in terms of cytokine release (**Figure 5.12**). No significant level of cytokines is produced when γδ TCR transduced αβ T cells are co-cultured with 20.1 treated AML cell lines, compared to the untreated control. The same effect was also seen when Jurkat cell lines (**Figure 5.9 and 5.10**).

This is an interesting and surprising result, however as mentioned previously, it is possible that some γδ TCR synapses benefit from co-stimulation interaction in order to stabilise the synapse; Including a truncated CCR control would be interesting to understand this observation.

Overall, these results demonstrated the efficacy γδ TCR-TE9-28 to mount a robust anti-tumour response in vitro in an antigen-dependent manner, with full activation only when the CCR engages the cognate antigen. The data also demonstrated presence of tonic signalling in γδ TCR-TE9-41BB transduced αβ T cells.

Finally, in order to study the on-target off tumour toxicity of γδ TCR-TE9 CCR in αβ T cell, the in vitro activity of γδ TCR-TE9-28 and γδ TCR-TE9-41BB transduced αβ T cells was investigated against murine isogenic cell line 3T3 WT and 3T3 B7H3 after generating them by transducing the WT cell line with 4IgB7H3 construct. 3T3 cells derived from mouse embryonic fibroblasts, therefore, allows to study the activity of TCR-TE9 CCR in αβ T cells when the γδ TCR is not engaged. In this last set of data, αβ T cells were also transduced to express the second generation TE9-28-ζ CAR. The intent was to use TE9-28-ζ transduced αβ T cells as positive control for engagement of the cognate antigen, independently from TCR engagement. In this experiment was performed in two biological replicates therefore, no statistical analysis was performed.

Effectors were co-cultured with 3T3 WT and 3T3 B7H3 and cytokine were detected after 18 hours and post re-stimulation after 7 days of co-culture (**Figure 5.17**). IL-2 production by the effectors is uninterpretable both at 18h and after re-stimulation, no trend can be observed. In contrast, at 18h, TE9-28-ζ transduced αβ T cells produced higher level of IFN-γ when co-cultured with 3T3 B7H3 compared to the

3T3 WT control, while the other effectors did not produce any detectable amount of IFN-γ. After re-stimulation with targets (**Figure 5.18**) TE9-28-ζ transduced αβ T cells appear to produce higher level of IFN-γ when co-cultured with 3T3 B7H3 compared to the 3T3 WT control. In contrast, γδ TCR-TE9-41BB transduced αβ T cells, produced high levels of IFN-γ in an antigen and target independent manner as observed in previous results.

Analysis of absolute T cell count after 7 days co-culture reflects what observed in terms of cytokine production: cell numbers of TE9-28-ζ transduced αβ T cells were higher when the effector where co-cultured with 3T3 B7H3 compared to the 3T3 WT controls. Consistent with the explanation of tonic signalling mediated by 41BB in this CCR format, the T cell count of γδ TCR-TE9-41BB transduced αβ T cells were higher than any other effectors, but no difference was observed within the different conditions. Also, in this set of data no significant different was observed between untreated and 20.1 treated targets.

Overall, the last set of data demonstrated preliminary evidence that the γδ TCR-TE9 CCR system have the potential to avoid on target of tumour toxicity, as no significant activity was detected by the γδ TCR-TE9-28 transduced αβ T cells in response to 3T3 B7H3, suggesting potential safety of the system even in presence of antigen when the TCR is not engaged. In contrast if was shown that the second generation TE9-28- ζ was able to mount a response to 3T3 B7H3 bypassing the TCR. However, more replicates and a cytotoxicity experiment which was not performed in this instance due to a technical mistake, could provide more evidence in order to demonstrate statistically significant avoidance of activation when signal 1 is absent.

6 FINAL DISCUSSION AND CONCLUSIONS

AML accounts for approximately 25% of all leukaemias, making it the most frequent type of myeloid leukaemia. While it is mostly a disease of later adulthood, it is also the second most common form of leukaemia in children. The extensive body of work that has been conducted in the field of AML, led to a better understanding of the molecular heterogenicity of AML as well as the interplay between AML blasts, the hematopoietic niche, and the cells of the immune system for AML development and growth (Isidori et al., 2014; Ladikou et al., 2020). However, despite advances in risk stratification, optimization of chemotherapy regimens, improvement in stem cell transplantation techniques, the prognosis for AML still remains poor, emphasizing the importance to find novel treatment strategies. In the past two decades, we have witnessed important advances in the field of cancer immunotherapy: extensive work has been conducted on CAR T cell-based strategies.

CAR-T cell therapy targeting CD19 in ALL, has demonstrated one of the most promising responses in haematological malignancies. Due to the MHC unrestricted nature of the CAR, CD19 CAR T cells are toxic to CD19+ ALL as well as healthy CD19+ B-cells, leading to B cell aplasia. The success of CAR-T therapy in B-cell malignancies is predicated on the tolerability of the off-target effect. Disruption of normal myelopoiesis, however, is not tolerable, and the fact that most AML-associated surface antigens are also expressed on normal myeloid progenitor cells, is one of the main reasons why CAR T cell-based strategy has not proven as successful in AML.

The overall aim of this project was to explore different targeting strategies based on engineered T cells, to overcome this limitation. In this context, we explored CD33–specific and B7H3–specific CAR T cells as a potential therapy. The functionality in vitro as well as the potential hematopoietic toxicity of this approaches were investigated. Additionally, an alternative approach consisting of αβ T cells engineered to co-express a tumour reactive γδTCR and an AML-targeting chimeric costimulatory receptor (CCR), was also explored. This system aims to offer another degree of safety by separating signal 1 (TCR) and signal 2 (CCR), thus avoiding the potential on-target off-tumour toxicity when one of the signals is not engaged.

CD33 and B7-H3 as target antigen in AML were subject of our study. CD33 is an attractive candidate for AML targeted immunotherapy strategies as it is overexpressed in 90% of leukemic blasts in AML patients and it is not associated to a specific karyotype. The main limitation of this target strategy consists in on-target off-tumour toxicity caused by the presence of the targeted antigen on a wide range of healthy cells including myeloid-committed cells in the bone marrow and circulating monocytes. A wide range of CAR-T cell-based strategies targeting CD33 in clinical trial phases 1 and 2 have demonstrated sustained anti-tumour activity in vitro against AML targets, however, this was often associated with off-target effects in the healthy myeloid compartment (Wang et al., 2015).

Different strategies have been investigated in order to avoid long-term myelosuppression and enhance the viability of anti-CD33 CAR. Among these, Kenderian et al designed a transiently expressed mRNA anti-CD33 CAR to drive transient expression of the CAR in T cells (Kenderian et al., 2015). Moreover, different scFv are likely to have different affinities to CD33, therefore another

strategy to overcome off-tumour toxicity, could be designing a CAR with lower affinity to the antigen. Different settings may necessitate CARs with different affinities (Ghorashian et al., n.d.; Labanieh et al., 2018) and low affinity CAR may be beneficial when the target antigen is expressed at high densities on tumour but at low levels on normal cells.

In contrast, B7-H3 is widely expressed on multiple childhood and adult human cancers including AML, but has limited expression on healthy cells (Majzner et al., n.d.; Modak et al., 2001). B7-H3 is involved in immune cell inhibition and several studies suggest it may provide a novel source of checkpoint inhibition (Leitner et al., 2009; Steinberger et al., 2004). Moreover, B7-H3 has some non-immunological roles in tumorigenesis and while the pathways through which it signal are poorly understood, targeting B7-H3 seems to increase the susceptibility of cancer cells to chemotherapy (Li et al., 2017; P. Zhang et al., 2017). Due to its restricted expression profile on healthy cells and his involvement in checkpoint inhibition, targeting B7-H3 in AML has the potential to improve clinical outcomes of CAR-T cell-based immunotherapy. Several studies have been conducted using anti-B7-H3 CAR T cells and have shown promising results in preclinical in vitro and in vivo models (Lichtman et al., 2021; Liu et al., 2021; Z. Zhang et al., 2020).

In result chapter I, we investigated the in vitro activity of CD33–specific and B7H3–specific CAR T cells as well as the potential hematopoietic toxicity.

To summarize our findings, we generated two second generation anti-CD33-28-ζ CARs and two anti-B7H3-28-ζ CARs containing different stalk/transmembrane region (CH2CH3 or Fc stalk/CD28tm and CD8/CD8tm) and investigated the in vitro activity. The data gathered by the functional assays demonstrated that anti B7-H3

TE9-CD8-28-ζ CAR T cells were able to mount an antitumor response in terms of cytotoxicity, ability to produce cytokines and proliferate in an antigen-dependent manner. In contrast, anti-CD33 CAR T cells and TE9-Fc-28-ζ CAR T cells demonstrated suboptimal activity towards some of the targets. While we are not aware of the exact mechanisms behind the lack of activity of these constructs we speculated on potential reasons.

TE9-Fc-28-ζ CAR T cells did not show any anti-tumour response to neither positive control Jurkat B7-H3 or AML cell lines. Therefore, we hypothesised that lack of accessibility of the TE9 binder to the recognition epitope on B7H3 due to length and spatial orientation of the Fc stalk could be one of the factors involved in lack of activity of TE9-Fc-28-ζ CAR T cells. To date, we do not have information available on the binding site or sites for TE9, therefore while the Fc stalk is more flexible than the CD8 spacer, it does not necessarily guarantee better chances of antigen engagement as antigenic dimensions, stalk length and epitope location, are all involved in the formation of a functional immune synapse.

In contrast, anti-CD33 CARs demonstrated tumour reactivity towards positive control SUP-T1 CD33, while they were suboptimal against AML targets. In this instance we hypothesised that the difference in antigen density on AML cell lines compared to the positive control SUP-T1 CD33 might be the reason for lack of response to AML cell lines by the T cells . While antigen density testing was not performed, MFI of CD33 on the target cells was used as indication of differences in CD33 expression, given that the same number of cells were stained with the same amount of antibody. Based on this assumption, we observed that antigen density in SUP-T1 CD33 was greater than antigen density on AML cell lines.

Majzner et al. have demonstrated that CD19 CAR activity is dependent upon antigen density and insufficient reactivity against cells with low antigen density has been shown as an important cause of CAR resistance in other studies (Majzner et al., 2020). The authors demonstrated that the CAR construct in axicabtagene ciloleucel (CD19-CD28ζ) outperforms that in tisagenlecleucel (CD19-4-1BBζ) against antigen-low tumours. Inclusion of ITAMs in the CD19-4-1BBζ CAR in order to enhance signal strength and/or replacement of the CD8 hinge-transmembrane (H/T) region with a CD28-H/T is shown to lowers the threshold for CAR reactivity and lead to the formation of a more stable and efficient immunologic synapse. These results highlight the importance of precise CAR design to tune the threshold for antigen recognition based on antigen density.

Another hypothesis for lack of killing of AML cell lines by CD33-Fc-28ζ and CD33-CD8-28ζ T cells consist in the expression of different CD33 isoforms on SUP-T1 CD33 and AML cell lines. The same anti-CD33 scFv is likely to have different affinities for different isoforms. By producing a soluble CD33 scFv-protein and testing binding to both SUP-T1 CD33 and AML cell lines, would allow to confirm this hypothesis, however, as generating an optimal CD33 CAR was beyond the scope of the thesis, we did not investigate further. Overall, these findings strengthen the knowledge that fine tuning of the CAR structure is crucial to drive anti-tumour responses toward a specific tumour target. All the components within a CAR structure play a crucial role in allowing the formation of a correct immunological synapse.

Based on these results, TE9-Fc-28-ζ CAR T cells were brought forward in order to investigate the potential hematopoietic toxicity, which is one on the main limitations of current strategies targeting AML. Functional assays demonstrated lack of toxicity

of these effectors towards healthy monocytes, as well as lack of toxicity towards normal hematopoietic progenitors present in cord blood by performing a colony formation assay. Overall, these results showed that B7H3 has the potential to be a suitable candidate for AML targeted therapies. As previously mentioned, this set of results lack the validation in an in vivo model, however, this work has been discussed and is in the plans for the future to test TE9-CD8-28-ζ CAR T cells in NSG mice engrafted with NOMO-1. For translation to the clinic in AML, it would be important also to demonstrate superiority of TE9-CD8-28-ζ versus other candidate CAR approaches for AML. Most investigators are evaluating myeloid specific targets that have high potential for myeloid toxicity; and hence the approaches are being viewed as a bridge to transplant. The B7H3 approach is one of few innovative technologies that could potentially overcome this limitation but extensive studies in humanised mouse models would be required, beyond the scope of this thesis.

Zhang et al. performed a large-scale screening of the expression of B7-H3 using TCGA data and IHC and found homogeneous overexpression of B7-H3 only in a small percentage of samples of liver, breast, cervical, and bladder cancers and SSCC, whereas its expression in other cancer types was highly heterogeneous. Different studies have also reported variable expression patterns of B7-H3 in patients with AML (Z. Zhang et al., 2020). Although B7-H3 represents a promising target, expression heterogeneity and variation have to be carefully considered in translating B7-H3-targeted CAR-T cell therapy into clinical practice and it is suggested that it may be necessary to examine the B7-H3 expression status in surgical specimens before starting targeted therapy. A good alternative could be developing dual-targeting approaches combining B7-H3 with a second AML surface antigen (Guéry et al., 2013; Lichtman et al., 2021).

While in chapter I we demonstrated that is possible to avoid toxicity by choosing a target antigen that has a better expression profile compared to the antigens currently targeted, also B7H3 is expressed in some degree in some healthy tissues. Therefore, the proposed system aims to offer another degree of safety by separating signal 1 (TCR) and signal 2 (CCR), thus avoiding the potential on-target off-tumour toxicity when the TCR is not engaged. B7-H3 was used as target antigen in this system as proof of concept and because it is the antigen of interest in our study. Ideally the γδ TCR + CCR in αβT system could be applied to any other target antigen, in fact it would be even more relevant when the antigen is expressed with less of a restricted profile on heathy cells as well, such is the case for CD33 for example.

The basic structure of CARs used in αβT cell engineering comprised of a CD3-ζ signalling endodomain and an antibody based ectodomain which allows CAR-T cells to simultaneously bypass MHC-restriction and to specifically target a tumour antigen through their ScFv. As mentioned previously, this can lead to on-target off-tumour toxicity due to the CAR reacting to their cognate antigen present on healthy cells. Using γδ T cells has the potential to overcome this limitation; as γδ TCRs are not MHC-restricted and detect moieties associated with cellular stress, it is possible to design a CAR that only comprises of one or multiple co-stimulatory endodomain allowing to discriminate between an antigen positive healthy cell and an antigen positive tumour cell. This approach has been described by Fisher et al. in the context of neuroblastoma (Fisher et al., 2017). An anti-GD2-DAP10 CAR was expressed in Vγ9Vδ2+ T cells and it was demonstrated that pro-inflammatory cytokine response was dependent on activation of both receptors. Moreover, the authors demonstrated killing of GD2+ neuroblastoma cell lines by the anti-GD2-

DAP10 CAR, while GD2+ cell lines which did not engage Vγ9Vδ2 TCR were untouched.

This system offers the potential for a safer immunotherapy by overcoming on-target off-tumour effect and allowing to target a broader target selection. However, while αβ T cells have been used extensively and shown their potential to mediate tumour responses and to persist long term to prevent recurrence, γδ T has no proven track record in adoptive transfer for long term disease control. In our approach we hypothesised that αβ T cells might be a better chassis to carry a γδ TCR by combining long term expansion and engraftment capacity of αβ T with lack of GVHD and capacity of co-expression with CCR that is associated with γδ T cells.

The ultimate goal of chapter II and III was to validate an alternative approach consisting of αβ T cells engineered to co-express a γδTCR and an AML-targeting CCR; this is the first time that the contribution of co-stimulation through a CCR is investigated in αβ T cells engineered to express a γδ TCR.

In results chapter II, the γδ TCR component of the proposed system was investigated, and we demonstrated that it was possible to express a prototypic transgenic G115 γδ TCR in αβ T cells and that the transgenic TCR was functional and was able to re-direct αβ T cells anti-tumour activity towards a γδ T cell sensitive target (Daudi). Interestingly, when αβ T cells were transduced with the G115 γδ TCR, a peculiar distribution of transduced populations was observed by flow cytometry. Three populations with different TCR expression profile were detected: a population negative for αβ TCR and negative for γδ TCR, a population positive for both αβ and γδ TCRs and a population negative for αβ TCR and positive for γδ TCR.

This same distribution and the ability of redirecting αβT cells with a γδ TCR was observed also in a study by Marcu Malina et al. The authors use γ9δ2TCR to redirect αβT cells selectively against tumour cells as an alternative to overcome limitations of the more conventional transfer of tumour-specific αβTCR, such as MHC restriction and risk to mediate self-reactivity after pairing with endogenous α or βTCR chains. The authors have shown that the γ9δ2TCR was able to efficiently reprogram both CD4+ and CD8+ αβT cells against a broad panel of cancer cells while ignoring normal cells (Marcu-Malina et al., 2011).

As previously mentioned, we are unaware of the mechanism behind the downregulation of the endogenous TCR and upregulation of the transgenic TCR. Competition due to greater numbers of the transduced TCR components or greater affinity of γδ TCR for CD3 assembly, or combination of both, or an effect of transgenic TCR to diminish expression of one or both chains of the αβ TCR, could all be plausible mechanism of action. In addition, while we proceeded on the assumption that the population negative for αβ TCR and positive for γδ TCR were αβ T cells that downregulated their endogenous TCR based on the circumstantial evidence that they were positive for either CD4 or CD8, sequencing of the cells to demonstrate functional rearrangements of the αβ TCR and lack of rearrangements of the γδ TCR would be required, to confirm the identity of such population.

We additionally demonstrated that by purifying the αβ TCR- γδ TCR+ by depleting αβ TCR+ population with bead magnetic separation, it was possible to reduce alloreactivity of the effectors towards targets. Additionally, in both purified αβ TCR- γδ TCR+ and mixed γδ TCR transduced αβT cells, we observed that the transgene started losing its expression overtime towards a more αβ TCR+ phenotype.

The drop that we observe, could be attributed to loss of LTR-driven TCR transgene transcriptional activity. Moreover, several studies support the hypothesis that lymphocyte activation may be a key determinant of transgene expression: Pollok and colleagues transduced primary human T lymphocytes with an MMLV-based retrovirus encoding murine B7-1 and observed that although the transgene expression decreased rapidly in the presence of IL-2 in vitro, it was up-regulated upon short-term exposure to plates coated with both anti-CD3 and anti-CD28 monoclonal antibodies. In future works, it would be interesting to investigate G115-γδ TCR expression on the very same cells upon re-stimulation.

We discussed that CRISPR/Cas9 based gene editing, to knock out the endogenous αβ TCR and insert γδ TCR in the TRAC locus might prevent the loss of the transgene. It has been previously demonstrated that CAR expression from the TRAC locus is highly efficient. Moreover, there is only one active TRAC locus per cell, hence incomplete editing can still lead to complete deletion in a single cell. This approach would potentially give simultaneously high efficiency expression of the transgenic TCR while knocking-down the endogenous αβTCR. However, one of the major concerns for implementing CRISPR/Cas9 technology for gene therapy is the high frequency (≥50%) of off-target effects, which consist in RNA-guided endonuclease induced mutations at sites other than the intended on-target site (Zhang et al., 2015). While strategies such as engineering Cas9 variants that exhibit reduced off-target effects and optimizing guide designs, are currently investigated to overcome these limitations, all these factors need to be taken into consideration to design a safe and effective therapy.

After demonstrating the possibility to redirect αβT cells anti-tumour specificity through a transgenic γδ TCR, in result chapter III we focused on bringing all the

components together. Based on the findings in results chapter I, we decided to include the TE9-CD8stalk binder in a CCR format and co-express on αβT cells with a tumour reactive γδ TCR. Contribution of CCR has been studied in other settings, such as CCR in γδ T cells or CCR in αβT cells expressing another CAR. Katsarou et al investigated a CCR-based strategy to improve relapse rate in patients with haematological cancers, which is thought to be partially caused by both low antigen density and reduced persistence of CAR T cells. They developed an anti-CD38 CCR to provide intracellular signalling to support anti-CD19 CAR T cell activation and observed increased cytotoxicity tumour cells in vitro and in vivo, even against tumour cells with very low antigen density. This was associated with improved CAR T cell persistence. These results suggest that implementing CCR based strategies may improve clinical outcomes for patients receiving CAR T cell treatments (Katsarou et al., 2021).

In our project, the novelty consists in studying the contribution of co-stimulation in αβT cells engineered to express a tumour reactive γδ TCR. CD28 and 4-1BB were chosen as co-stimulatory endodomain based on the extensive body of work that have been done on these two co-stimulatory molecules.

We demonstrated by flow cytometry expression on αβ T cells of γδ TCR-TE9-28 and γδ TCR-TE9-41BB constructs: their transduction profile in terms of differential TCR expression, was comparable to the one of the γδ TCR construct, with the addition that the αβ TCR- γδ TCR+ population in γδ TCR-TE9-28 and γδ TCR-TE9-41BB transduced αβ T cells was also positive for the TE9 CCR. Interestingly, while the transduction profile was comparable within the constructs, transduction efficiencies of the γδ TCR-TE9-28 and γδ TCR-TE9-41BB constructs were significantly lower than the single γδ TCR construct, which was quite a limiting

technical factor, due to the lack of optimal number of effectors to work with after purifying the αβ TCR- γδ TCR+ population.

A better delivery system or a protocol to achieve higher viral titre need to be optimized in order to achieve better transduction efficiencies. We are not fully aware of the mechanism behind the reduction in transduction efficiencies, however it is possible that the size or the insert plays a role. Switching to a lentiviral backbone would most likely be the simplest solution to achieve the required high transduction efficiencies of the larger construct. This was originally attempted but for unknown reasons we failed to express the constructs through a lentiviral system. Alternatively, as mentioned previously, gene editing using CRISPR/Cas9 technology to insert the γδ TCR + CCR in the TRAC locus could achieve high efficiency of expression of the γδ TCR + CCR construct while simultaneously knocking-out the endogenous αβ TCR. Again, it is important to be mindful of the risks mentioned earlier regarding this system. The approach would require flanking of the gene of interest with homology regions for homologous recombination, and simultaneous cutting of the target locus with introduction of double stranded DNA into the cells. Several approaches could be employed to achieve these ends and an initial aim of the PhD was to evaluate AAV transduction with Cas9 following electroporation. However, technical challenges in AAV production preventing this being actualised.

Overall, the results in chapter II and III demonstrated the ability of γδ TCR-TE9-28 transduced αβ T cells to mount a robust anti-tumour response in vitro in an antigen dependent manner when co-cultured with AML cell lines and B7H3-Jurkat, with full activation only when the CCR engage the cognate antigen. The data interestingly also demonstrated presence of tonic signalling in γδ TCR-TE9-41BB transduced

αβ T cells. Indeed, γδ TCR-TE9-41BB T cells expanded and induced cytokine release in an antigen and target independent manner after prolonged culturing.

Antigen-independent tonic signalling by CARs depends on a combination of factors and can increase differentiation and exhaustion of T cells, limiting their potency. High levels of tonic signalling have been reported in CARs targeting c-Met (5D5 scFv), mesothelin (SS1 scFv), and GD2 (14g2a scFv) (Gomes-Silva et al., 2017).

The expression system, including the promoter and the vector used to express the CAR, as well as the design of the scFv and the hinge contributes to tonic signalling. scFv prone to aggregation may drive tonic signalling at lower CAR densities, while certain combinations of scFv and hinges can facilitate CAR flexibility, increasing the chances of spontaneous activation.

Studies show that incorporating 4-1BB co-stimulation in CARs may enable T cells to resist functional exhaustion; Gomes-Silva et al demontrsated that tonic CAR-derived 4-1BB signalling can produce toxicity in T cells via continuous TRAF2-dependent activation of the NF-kB pathway and augmented Fas-dependent cell death. They show that this mechanism was amplified in a non-self-inactivating gammaretroviral vector through positive feedback on the LTR promoter, enhancing even more CAR expression and tonic signalling. Changing the expression system to a self-inactivating lentiviral vector improved T-cell expansion and anti-tumour function (Gomes-Silva et al., 2017). Another study shows that replacing CD28 with 4-1BB co-stimulation reversed exhaustion in GD2 CAR T cells (Long et al., 2015). Potential ramifications of tonic 4-1BB signalling in CAR T cells, however, remain unclear.

To our knowledge, no previous study of a non-engaged 41BB CCR has shown this level of specific activation and function after prolonged culturing, therefore, it could have implications in terms of choice of CCR for clinical use since the tonic signalling could result in both exhaustion and toxicity.

In addition, we observed preliminary evidence that the γδ TCR-TE9 CCR system have the potential to avoid on target of tumour toxicity, as no significant activity was detected by the γδ TCR-TE9-28 transduced αβ T cells in response to the murine cell line 3T3 B7H3, suggesting potential safety of the system even in presence of antigen when the TCR is not engaged. To support the difference in toxicity, it was shown that the second generation TE9-28- ζ was able to mount a response to 3T3 B7H3 bypassing the TCR. Cytotoxicity assay and more biological replicates to assess cytokine production and T cell expansion are required to complete this set of data and confirm our findings, as we cannot draw any final conclusion just based on what is observed in this experiment.

On-target off-tumour toxicity is one of the major limitations in current AML immunotherapy strategies; the ability to differentiate between a specific antigen on tumour and on healthy cells proposed in our system, not only reduce toxicity of one specific strategy but has the potential of making previously overlooked antigens available for targeting.

In conclusion, we have identified two novel approaches to the therapeutic targeting of AML based on the B7H3 antigen that have the potential to overcome limitations of current strategies. Our findings can be used as preliminary data to investigate further these two approaches side by side in therapeutic models to allow prioritisation of an approach for clinical translation.

7 BIBLIOGRAPHY

Acuto, O., Bartolo, V. Di, & Michel, F. (2008). Tailoring T-cell receptor signals by proximal negative feedback mechanisms. In *Nature Reviews Immunology*. https://doi.org/10.1038/nri2397

Ahmadi, M., King, J. W., Xue, S. A., Voisine, C., Holler, A., Wright, G. P., Waxman, J., Morris, E., & Stauss, H. J. (2011). CD3 limits the efficacy of TCR gene therapy in vivo. *Blood*, *118*(13), 3528–3537. https://doi.org/10.1182/blood-2011-04-346338

Aifantis, I., Raetz, E., & Buonamici, S. (2008). Molecular pathogenesis of T-cell leukaemia and lymphoma. In *Nature Reviews Immunology*. https://doi.org/10.1038/nri2304

Allison, T. J., Winter, C. C., Fournie, J. J., Bonneville, M., & Garboczi, D. N. (2001). Structure of a human gammadelta T-cell antigen receptor. *Nature*, *411*(6839), 820–824. https://doi.org/10.1038/35081115

Anelli, L., Pasciolla, C., Zagaria, A., Specchia, G., & Albano, F. (2017). Monosomal karyotype in myeloid neoplasias: a literature review. *OncoTargets and Therapy*, *10*, 2163. https://doi.org/10.2147/OTT.S133937

Antony, P. A., & Restifo, N. P. (2005). CD4+CD25+ T regulatory cells, immunotherapy of cancer, and interleukin-2. In *Journal of Immunotherapy*. https://doi.org/10.1097/01.cji.0000155049.26787.45

Appelbaum, F. R., Gundacker, H., Head, D. R., Slovak, M. L., Willman, C. L., Godwin, J. E., Anderson, J. E., & Petersdorf, S. H. (2006). Age and acute myeloid leukemia. *Blood*, *107*(9), 3481–3485.

https://doi.org/10.1182/BLOOD-2005-09-3724

Arber, D. A., Orazi, A., Hasserjian, R., Thiele, J., Borowitz, M. J., Le Beau, M. M., Bloomfield, C. D., Cazzola, M., & Vardiman, J. W. (2016a). *Review Series THE UPDATED WHO CLASSIFICATION OF HEMATOLOGICAL MALIGNANCIES The 2016 revision to the World Health Organization classification of myeloid neoplasms and acute leukemia*. https://doi.org/10.1182/blood-2016-03-643544

Arber, D. A., Orazi, A., Hasserjian, R., Thiele, J., Borowitz, M. J., Le Beau, M. M., Bloomfield, C. D., Cazzola, M., & Vardiman, J. W. (2016b). The 2016 revision to the World Health Organization classification of myeloid neoplasms and acute leukemia. *Blood*, *127*(20), 2391–2405. https://doi.org/10.1182/BLOOD-2016-03-643544

Asslan, R., Pradines, A., Pratx, C., Allal, C., Favre, G., & Le Gaillard, F. (1999). Epidermal growth factor stimulates 3-hydroxy-3-methylglutaryl-coenzyme A reductase expression via the ErbB-2 pathway in human breast adenocarcinoma cells. *Biochemical and Biophysical Research Communications*, *260*(3), 699–706. https://doi.org/10.1006/BBRC.1999.0945

Austin, R., Smyth, M. J., & Lane, S. W. (2016). Harnessing the immune system in acute myeloid leukaemia. *Critical Reviews in Oncology/Hematology*, *103*, 62–77. https://doi.org/10.1016/J.CRITREVONC.2016.04.020

Bach, F. H., Bach, M. L., & Sondel, P. M. (1976). Differential function of major histocompatibility complex antigens in T-lymphocyte activation. *Nature*. https://doi.org/10.1038/259273a0

Baniyash, M. (2004). TCR ζ-chain downregulation: Curtailing an excessive

inflammatory immune response. In *Nature Reviews Immunology*. https://doi.org/10.1038/nri1434

Beatty, G. L., & Gladney, W. L. (2015). Immune escape mechanisms as a guide for cancer immunotherapy. In *Clinical Cancer Research* (Vol. 21, Issue 4, pp. 687–692). https://doi.org/10.1158/1078-0432.CCR-14-1860

Belmant, C., Decise, D., & Fournié, J. J. (2006). Phosphoantigens and aminobisphosphonates: New leads targeting γδ T lymphocytes for cancer immunotherapy. *Drug Discovery Today: Therapeutic Strategies*, *3*(1), 17–23. https://doi.org/10.1016/J.DDSTR.2006.02.001

Benzaïd, I., Mönkkönen, H., Bonnelye, E., Mönkkönen, J., & Clézardin, P. (2012). In vivo phosphoantigen levels in bisphosphonate-treated human breast tumors trigger Vγ9Vδ2 T-cell antitumor cytotoxicity through ICAM-1 engagement. *Clinical Cancer Research*, *18*(22), 6249–6259. https://doi.org/10.1158/1078-0432.CCR-12-0918

Bevan, M. J. (1976). Cross-priming for a secondary cytotoxic response to minor h antigens with H-2 congenic cells which do not cross-react in the cytotoxic assay*. *Journal of Experimental Medicine*. https://doi.org/10.1084/jem.143.5.1283

Blattman, J. N., Antia, R., Sourdive, D. J. D., Wang, X., Kaech, S. M., Murali-Krishna, K., Altman, J. D., & Ahmed, R. (2002). Estimating the precursor frequency of naive antigen-specific CD8 T cells. *Journal of Experimental Medicine*. https://doi.org/10.1084/jem.20001021

Boissel, L., Betancur, M., Wels, W. S., Tuncer, H., & Klingemann, H. (2009). Transfection with mRNA for CD19 specific chimeric antigen receptor restores

NK cell mediated killing of CLL cells. *Leukemia Research*, *33*(9), 1255–1259. https://doi.org/10.1016/j.leukres.2008.11.024

Brennan, P. J., Brigl, M., & Brenner, M. B. (2013). Invariant natural killer T cells: An innate activation scheme linked to diverse effector functions. In *Nature Reviews Immunology*. https://doi.org/10.1038/nri3369

Bridgeman, J. S., Hawkins, R. E., Bagley, S., Blaylock, M., Holland, M., & Gilham, D. E. (2010). The Optimal Antigen Response of Chimeric Antigen Receptors Harboring the CD3ζ Transmembrane Domain Is Dependent upon Incorporation of the Receptor into the Endogenous TCR/CD3 Complex. *The Journal of Immunology*. https://doi.org/10.4049/jimmunol.0901766

Brocker, T., & Karjalainen, K. (1995). Signals through T cell receptor-ζ chain alone are insufficient to prime resting T lymphocytes. *Journal of Experimental Medicine*. https://doi.org/10.1084/jem.181.5.1653

Büchner, T., Berdel, W. E., Haferlach, C., Haferlach, T., Schnittger, S., Müller-Tidow, C., Braess, J., Spiekermann, K., Kienast, J., Staib, P., Grüneisen, A., Kern, W., Reichle, A., Maschmeyer, G., Aul, C., Lengfelder, E., Sauerland, M. C., Heinecke, A., Wörmann, B., & Hiddemann, W. (2009). Age-related risk profile and chemotherapy dose response in acute myeloid leukemia: a study by the German Acute Myeloid Leukemia Cooperative Group. *Journal of Clinical Oncology : Official Journal of the American Society of Clinical Oncology*, *27*(1), 61–69. https://doi.org/10.1200/JCO.2007.15.4245

Cabillic, F., Toutirais, O., Lavoué, V., De La Pintière, C. T., Daniel, P., Rioux-Leclerc, N., Turlin, B., Mönkkönen, H., Mönkkönen, J., Boudjema, K., Catros, V., & Bouet-Toussaint, F. (2010). Aminobisphosphonate-pretreated dendritic

cells trigger successful Vγ9Vδ2 T cell amplification for immunotherapy in advanced cancer patients. *Cancer Immunology, Immunotherapy*, *59*(11), 1611–1619. https://doi.org/10.1007/s00262-010-0887-0

Cameron, B. J., Gerry, A. B., Dukes, J., Harper, J. V., Kannan, V., Bianchi, F. C., Grand, F., Brewer, J. E., Gupta, M., Plesa, G., Bossi, G., Vuidepot, A., Powlesland, A. S., Legg, A., Adams, K. J., Bennett, A. D., Pumphrey, N. J., Williams, D. D., Binder-Scholl, G., … Jakobsen, B. K. (2013). Identification of a titin-derived HLA-A1-presented peptide as a cross-reactive target for engineered MAGE A3-directed T cells. *Science Translational Medicine*, *5*(197). https://doi.org/10.1126/scitranslmed.3006034

Campbell, J. J., Murphy, K. E., Kunkel, E. J., Brightling, C. E., Soler, D., Shen, Z., Boisvert, J., Greenberg, H. B., Vierra, M. A., Goodman, S. B., Genovese, M. C., Wardlaw, A. J., Butcher, E. C., & Wu, L. (2001). CCR7 Expression and Memory T Cell Diversity in Humans. *The Journal of Immunology*. https://doi.org/10.4049/jimmunol.166.2.877

Cantor, H., & Boyse, E. A. (1977). Regulation of Cellular and Humoral Immune Responses by T-cell Subclasses. *Cold Spring Harbor Symposia on Quantitative Biology*. https://doi.org/10.1101/sqb.1977.041.01.006

Capsomidis, A., Benthall, G., Van Acker, H. H., Fisher, J., Kramer, A. M., Abeln, Z., Majani, Y., Gileadi, T., Wallace, R., Gustafsson, K., Flutter, B., & Anderson, J. (2018). Chimeric Antigen Receptor-Engineered Human Gamma Delta T Cells: Enhanced Cytotoxicity with Retention of Cross Presentation. *Molecular Therapy*, *26*(2), 354–365. https://doi.org/10.1016/J.YMTHE.2017.12.001

Castaigne, S., Pautas, C., Terré, C., Raffoux, E., Bordessoule, D., Bastie, J. N., Legrand, O., Thomas, X., Turlure, P., Reman, O., De Revel, T., Gastaud, L., De Gunzburg, N., Contentin, N., Henry, E., Marolleau, J. P., Aljijakli, A., Rousselot, P., Fenaux, P., … Dombret, H. (2012). Effect of gemtuzumab ozogamicin on survival of adult patients with de-novo acute myeloid leukaemia (ALFA-0701): a randomised, open-label, phase 3 study. *Lancet (London, England)*, *379*(9825), 1508–1516. https://doi.org/10.1016/S0140-6736(12)60485-1

Cheng, M., Chen, Y., Xiao, W., Sun, R., & Tian, Z. (2013). NK cell-based immunotherapy for malignant diseases. In *Cellular and Molecular Immunology* (Vol. 10, Issue 3, pp. 230–252). https://doi.org/10.1038/cmi.2013.10

Cheson, B. D., Bennett, J. M., Kopecky, K. J., Büchner, T., Willman, C. L., Estey, E. H., Schiffer, C. A., Doehner, H., Tallman, M. S., Lister, T. A., LoCocco, F., Willemze, R., Biondi, A., Hiddemann, W., Larson, R. A., Löwenberg, B., Sanz, M. A., Head, D. R., Ohno, R., & Bloomfield, C. D. (2003). Revised recommendations of the International Working Group for Diagnosis, Standardization of Response Criteria, Treatment Outcomes, and Reporting Standards for Therapeutic Trials in Acute Myeloid Leukemia. *Journal of Clinical Oncology : Official Journal of the American Society of Clinical Oncology*, *21*(24), 4642–4649. https://doi.org/10.1200/JCO.2003.04.036

Cohen, C. J., Zhao, Y., Zheng, Z., Rosenberg, S. A., & Morgan, R. A. (2006). Enhanced antitumor activity of murine-human hybrid T-cell receptor (TCR) in human lymphocytes is associated with improved pairing and TCR/CD3

stability. *Cancer Research*, *66*(17), 8878–8886. https://doi.org/10.1158/0008-5472.CAN-06-1450

Contor, H., & Boyse, E. A. (1975). Functional subclasses of T lymphocytes bearing different Ly antigens. I. The generation of functionally distinct T cell subclasses is a differentiative process independent of antigen. *Journal of Experimental Medicine*. https://doi.org/10.1084/jem.141.6.1376

Cornelissen, J. J., Van Putten, W. L. J., Verdonck, L. F., Theobald, M., Jacky, E., Daenen, S. M. G., Van Marwijk Kooy, M., Wijermans, P., Schouten, H., Huijgens, P. C., Van Der Lelie, H., Fey, M., Ferrant, A., Maertens, J., Gratwohl, A., & Lowenberg, B. (2007). Results of a HOVON/SAKK donor versus no-donor analysis of myeloablative HLA-identical sibling stem cell transplantation in first remission acute myeloid leukemia in young and middle-aged adults: benefits for whom? *Blood*, *109*(9), 3658–3666. https://doi.org/10.1182/BLOOD-2006-06-025627

Davis, J. L., Theoret, M. R., Zheng, Z., Lamers, C. H. J., Rosenberg, S. A., & Morgan, R. A. (2010). Development of human anti-murine T-cell receptor antibodies in both responding and nonresponding patients enrolled in TCR gene therapy trials. *Clinical Cancer Research*. https://doi.org/10.1158/1078-0432.CCR-10-1280

Davis, M. M., & Bjorkman, P. J. (1988). T-cell antigen receptor genes and T-cell recognition. In *Nature*. https://doi.org/10.1038/334395a0

Davis, S. J., & van der Merwe, P. A. (2006). The kinetic-segregation model: TCR triggering and beyond. In *Nature Immunology*. https://doi.org/10.1038/ni1369

De Kouchkovsky, I., & Abdul-Hay, M. (2016). ‘Acute myeloid leukemia: a

comprehensive review and 2016 update’ *Blood Cancer Journal*, *6*, 441. https://doi.org/10.1038/bcj.2016.50

de Witte, M. A., Bendle, G. M., van den Boom, M. D., Coccoris, M., Schell, T. D., Tevethia, S. S., van Tinteren, H., Mesman, E. M., Song, J.-Y., & Schumacher, T. N. M. (2008). TCR gene therapy of spontaneous prostate carcinoma requires in vivo T cell activation. *Journal of Immunology (Baltimore, Md. : 1950)*, *181*(4), 2563–2571. https://doi.org/181/4/2563 [pii]

Dembic, Z., Haas, W., Weiss, S., McCubrey, J., Kiefer, H., von Boehmer, H., & Steinmetz, M. (1986). Transfer of specificity by murine alpha and beta T-cell receptor genes. *Nature*.

Deschler, B., & Lübbert, M. (2006). Acute myeloid leukemia: epidemiology and etiology. *Cancer*, *107*(9), 2099–2107. https://doi.org/10.1002/CNCR.22233

Dimova, T., Brouwer, M., Gosselin, F., Tassignon, J., Leo, O., Donner, C., Marchant, A., & Vermijlen, D. (2015). Effector Vγ9Vδ2 T cells dominate the human fetal γδ T-cell repertoire. *Proceedings of the National Academy of Sciences of the United States of America*, *112*(6), E556–E565. https://doi.org/10.1073/PNAS.1412058112

Dobosz, P., & Dzieciątkowski, T. (2019). The Intriguing History of Cancer Immunotherapy. *Frontiers in Immunology*, *10*. https://doi.org/10.3389/FIMMU.2019.02965

Dobrowolska, H., Gill, K. Z., Serban, G., Ivan, E., Li, Q., Qiao, P., Suciu-Foca, N., Savage, D., Alobeid, B., Bhagat, G., & Colovai, A. I. (2013). Expression of immune inhibitory receptor ILT3 in acute myeloid leukemia with monocytic differentiation. *Cytometry. Part B, Clinical Cytometry*, *84*(1), 21–29.

https://doi.org/10.1002/CYTO.B.21050

Döhner, H., Estey, E., Grimwade, D., Amadori, S., Appelbaum, F. R., Büchner, T., Dombret, H., Ebert, B. L., Fenaux, P., Larson, R. A., Levine, R. L., Lo-Coco, F., Naoe, T., Niederwieser, D., Ossenkoppele, G. J., Sanz, M., Sierra, J., Tallman, M. S., Tien, H. F., … Bloomfield, C. D. (2017). Diagnosis and management of AML in adults: 2017 ELN recommendations from an international expert panel. *Blood*, *129*(4), 424–447. https://doi.org/10.1182/BLOOD-2016-08-733196

Dörrie, J., Krug, C., Hofmann, C., Müller, I., Wellner, V., Knippertz, I., Schierer, S., Thomas, S., Zipperer, E., Printz, D., Fritsch, G., Schuler, G., Schaft, N., & Geyeregger, R. (2014a). Human adenovirus-specific γ/δ and CD8+ T cells generated by T-cell receptor transfection to treat adenovirus infection after allogeneic stem cell transplantation. *PLoS ONE*, *9*(10). https://doi.org/10.1371/journal.pone.0109944

Dörrie, J., Krug, C., Hofmann, C., Müller, I., Wellner, V., Knippertz, I., Schierer, S., Thomas, S., Zipperer, E., Printz, D., Fritsch, G., Schuler, G., Schaft, N., & Geyeregger, R. (2014b). Human adenovirus-specific γ/δ and CD8+ T cells generated by T-cell receptor transfection to treat adenovirus infection after allogeneic stem cell transplantation. *PLoS ONE*, *9*(10). https://doi.org/10.1371/JOURNAL.PONE.0109944

Doyle, C., & Strominger, J. L. (1987). Interaction between CD4 and class II MHC molecules mediates cell adhesion. *Nature*. https://doi.org/10.1038/330256a0

Dudley, M. E., Wunderlich, J. R., Robbins, P. F., Yang, J. C., Hwu, P., Schwartzentruber, D. J., Topalian, S. L., Sherry, R., Restifo, N. P., Hubicki,

A. M., Robinson, M. R., Raffeld, M., Duray, P., Seipp, C. A., Rogers-Freezer, L., Morton, K. E., Mavroukakis, S. A., White, D. E., & Rosenberg, S. A. (2002). Cancer regression and autoimmunity in patients after clonal repopulation with antitumor lymphocytes. *Science*. https://doi.org/10.1126/science.1076514

Dudley, M. E., Yang, J. C., Sherry, R., Hughes, M. S., Royal, R., Kammula, U., Robbins, P. F., Huang, J. P., Citrin, D. E., Leitman, S. F., Wunderlich, J., Restifo, N. P., Thomasian, A., Downey, S. G., Smith, F. O., Klapper, J., Morton, K., Laurencot, C., White, D. E., & Rosenberg, S. A. (2008). Adoptive cell therapy for patients with metastatic melanoma: Evaluation of intensive myeloablative chemoradiation preparative regimens. *Journal of Clinical Oncology*. https://doi.org/10.1200/JCO.2008.16.5449

Dummer, W., Niethammer, A. G., Baccala, R., Lawson, B. R., Wagner, N., Reisfeld, R. A., & Theofilopoulos, A. N. (2002). T cell homeostatic proliferation elicits effective antitumor autoimmunity. *Journal of Clinical Investigation*. https://doi.org/10.1172/JCI0215175

Dustin, M. L., Chakraborty, A. K., & Shaw, A. S. (2010). Understanding the structure and function of the immunological synapse. In *Cold Spring Harbor perspectives in biology*. https://doi.org/10.1101/cshperspect.a002311

Ehninger, A., Kramer, M., Röllig, C., Thiede, C., Bornhäuser, M., Von Bonin, M., Wermke, M., Feldmann, A., Bachmann, M., Ehninger, G., & Oelschlägel, U. (2014). Distribution and levels of cell surface expression of CD33 and CD123 in acute myeloid leukemia. *Blood Cancer Journal*, *4*(6). https://doi.org/10.1038/BCJ.2014.39

Estey, E., & Döhner, H. (2006). Acute myeloid leukaemia. *Lancet (London, England)*, *368*(9550), 1894–1907. https://doi.org/10.1016/S0140-6736(06)69780-8

Fahl, S. P., Coffey, F., & Wiest, D. L. (2014). Origins of γδ T Cell Effector Subsets: A Riddle Wrapped in an Enigma. *The Journal of Immunology*, *193*(9), 4289–4294. https://doi.org/10.4049/jimmunol.1401813

Finney, H. M., Akbar, A. N., & Lawson, A. D. G. (2004). Activation of Resting Human Primary T Cells with Chimeric Receptors: Costimulation from CD28, Inducible Costimulator, CD134, and CD137 in Series with Signals from the TCRζ Chain. *The Journal of Immunology*. https://doi.org/10.4049/jimmunol.172.1.104

Fisher, J., Abramowski, P., Wisidagamage Don, N. D., Flutter, B., Capsomidis, A., Cheung, G. W. K., Gustafsson, K., & Anderson, J. (2017). Avoidance of On-Target Off-Tumor Activation Using a Co-stimulation-Only Chimeric Antigen Receptor. *Molecular Therapy*, *25*(5), 1234–1247. https://doi.org/10.1016/J.YMTHE.2017.03.002

Fisher, J. P. H., Flutter, B., Wesemann, F., Frosch, J., Rossig, C., Gustafsson, K., & Anderson, J. (2016). Effective combination treatment of GD2-expressing neuroblastoma and Ewing's sarcomausing anti-GD2 ch14.18/CHO antibody with Vγ9Vδ2+γδT cells. *OncoImmunology*, *5*(1). https://doi.org/10.1080/2162402X.2015.1025194

Fisher, J. P. H., Heuijerjans, J., Yan, M., Gustafsson, K., & Anderson, J. (2014). γδ T cells for cancer immunotherapy: A systematic review of clinical trials. *OncoImmunology*, *3*(1). https://doi.org/10.4161/ONCI.27572

Fisher, J. P. H., Yan, M., Heuijerjans, J., Carter, L., Abolhassani, A., Frosch, J., Wallace, R., Flutter, B., Capsomidis, A., Hubank, M., Klein, N., Callard, R., Gustafsson, K., & Anderson, J. (2014a). Neuroblastoma killing properties of Vδ2 and Vδ2-negative γδT cells following expansion by artificial antigen-presenting cells. *Clinical Cancer Research*, *20*(22), 5720–5732. https://doi.org/10.1158/1078-0432.CCR-13-3464

Fisher, J. P. H., Yan, M., Heuijerjans, J., Carter, L., Abolhassani, A., Frosch, J., Wallace, R., Flutter, B., Capsomidis, A., Hubank, M., Klein, N., Callard, R., Gustafsson, K., & Anderson, J. (2014b). Neuroblastoma killing properties of V-delta 2 and V-delta2 negative gamma delta T cells following expansion by artificial antigen presenting cells. *Clinical Cancer Research : An Official Journal of the American Association for Cancer Research*, *20*(22), 5720. https://doi.org/10.1158/1078-0432.CCR-13-3464

Fong, C. to, & Brodeur, G. M. (1987). Down's syndrome and leukemia: epidemiology, genetics, cytogenetics and mechanisms of leukemogenesis. *Cancer Genetics and Cytogenetics*, *28*(1), 55–76. https://doi.org/10.1016/0165-4608(87)90354-2

Forman, D., Stockton, D., Møller, H., Quinn, M., Babb, P., De Angelis, R., & Micheli, A. (2003). Cancer prevalence in the UK: results from the EUROPREVAL study. *Annals of Oncology : Official Journal of the European Society for Medical Oncology*, *14*(4), 648–654. https://doi.org/10.1093/ANNONC/MDG169

Foulds, K. E., Zenewicz, L. A., Shedlock, D. J., Jiang, J., Troy, A. E., & Shen, H. (2002). Cutting Edge: CD4 and CD8 T Cells Are Intrinsically Different in

Their Proliferative Responses. *The Journal of Immunology*. https://doi.org/10.4049/jimmunol.168.4.1528

Friedrich, M., Henn, A., Raum, T., Bajtus, M., Matthes, K., Hendrich, L., Wahl, J., Hoffmann, P., Kischel, R., Kvesic, M., Slootstra, J. W., Baeuerle, P. A., Kufer, P., & Rattel, B. (2014). Preclinical characterization of AMG 330, a CD3/CD33- bispecific T-cell-engaging antibody with potential for treatment of acute myelogenous leukemia. *Molecular Cancer Therapeutics*, *13*(6), 1549–1557. https://doi.org/10.1158/1535-7163.MCT-13-0956

Gammaitoni, L., Giraudo, L., MacAgno, M., Leuci, V., Mesiano, G., Rotolo, R., Sassi, F., Sanlorenzo, M., Zaccagna, A., Pisacane, A., Senetta, R., Cangemi, M., Cattaneo, G., Martin, V., Coha, V., Gallo, S., Pignochino, Y., Sapino, A., Grignani, G., … Sangiolo, D. (2017). Cytokine-induced killer cells kill chemo-surviving melanoma cancer stem cells. *Clinical Cancer Research*, *23*(9), 2277–2288. https://doi.org/10.1158/1078-0432.CCR-16-1524

Garcillán, B., Marin, A. V. M., Jiménez-Reinoso, A., Briones, A. C., Muñoz-Ruiz, M., García-León, M. J., Gil, J., Allende, L. M., Martínez-Naves, E., Toribio, M. L., & Regueiro, J. R. (2015). γδ T Lymphocytes in the Diagnosis of Human T Cell Receptor Immunodeficiencies. *Frontiers in Immunology*, *6*(JAN). https://doi.org/10.3389/FIMMU.2015.00020

Garrido, F., Aptsiauri, N., Doorduijn, E. M., Garcia Lora, A. M., & van Hall, T. (2016). The urgent need to recover MHC class I in cancers for effective immunotherapy. *Current Opinion in Immunology*, *39*, 44–51. https://doi.org/10.1016/j.coi.2015.12.007

Gattinoni, L., Finkelstein, S. E., Klebanoff, C. A., Antony, P. A., Palmer, D. C.,

Spiess, P. J., Hwang, L. N., Yu, Z., Wrzesinski, C., Heimann, D. M., Surh, C. D., Rosenberg, S. A., & Restifo, N. P. (2005). Removal of homeostatic cytokine sinks by lymphodepletion enhances the efficacy of adoptively transferred tumor-specific CD8+ T cells. *Journal of Experimental Medicine*. https://doi.org/10.1084/jem.20050732

Gentles, A. J., Newman, A. M., Liu, C. L., Bratman, S. V., Feng, W., Kim, D., Nair, V. S., Xu, Y., Khuong, A., Hoang, C. D., Diehn, M., West, R. B., Plevritis, S. K., & Alizadeh, A. A. (2015). The prognostic landscape of genes and infiltrating immune cells across human cancers. *Nature Medicine*, *21*(8), 938–945. https://doi.org/10.1038/NM.3909

Geppert, T. D., & Lipsky, P. E. (1985). Antigen presentation by interferon-gamma-treated endothelial cells and fibroblasts: differential ability to function as antigen-presenting cells despite comparable Ia expression. *Journal of Immunology (Baltimore, Md. : 1950)*.

Germain, R. N. (2002). T-cell development and the CD4–CD8 lineage decision. *Nature Reviews Immunology 2002 2:5*, *2*(5), 309–322. https://doi.org/10.1038/nri798

Gerstung, M., Papaemmanuil, E., Martincorena, I., Bullinger, L., Gaidzik, V. I., Paschka, P., Heuser, M., Thol, F., Bolli, N., Ganly, P., Ganser, A., McDermott, U., Döhner, K., Schlenk, R. F., Döhner, H., & Campbell, P. J. (2017). Precision oncology for acute myeloid leukemia using a knowledge bank approach. *Nature Genetics*, *49*(3), 332–340. https://doi.org/10.1038/NG.3756

Gertner-Dardenne, J., Castellano, R., Mamessier, E., Garbit, S., Kochbati, E.,

Etienne, A., Charbonnier, A., Collette, Y., Vey, N., & Olive, D. (2012). Human V 9V 2 T Cells Specifically Recognize and Kill Acute Myeloid Leukemic Blasts. *The Journal of Immunology*, *188*(9), 4701–4708. https://doi.org/10.4049/jimmunol.1103710

Gertner-Dardenne, Julie, Bonnafous, C., Bezombes, C., Capietto, A. H., Scaglione, V., Ingoure, S., Cendron, D., Gross, E., Lepage, J. F., Quillet-Mary, A., Ysebaert, L., Laurent, G., Sicard, H., & Fournié, J. J. (2009). Bromohydrin pyrophosphate enhances antibody-dependent cell-mediated cytotoxicity induced by therapeutic antibodies. *Blood*, *113*(20), 4875–4884. https://doi.org/10.1182/BLOOD-2008-08-172296

Gill, S., Tasian, S. K., Ruella, M., Shestova, O., Li, Y., Porter, D. L., Carroll, M., Danet-Desnoyers, G., Scholler, J., Grupp, S. A., June, C. H., & Kalos, M. (2014). Preclinical targeting of human acute myeloid leukemia and myeloablation using chimeric antigen receptor-modified T cells. *Blood*, *123*(15), 2343–2354. https://doi.org/10.1182/BLOOD-2013-09-529537

Gramer, M. J., Van Den Bremer, E. T. J., Van Kampen, M. D., Kundu, A., Kopfmann, P., Etter, E., Stinehelfer, D., Long, J., Lannom, T., Noordergraaf, E. H., Gerritsen, J., Labrijn, A. F., Schuurman, J., Van Berkel, P. H. C., & Parren, P. W. (2013). Production of stable bispecific IgG1 by controlled Fab-arm exchange: Scalability from bench to large-scale manufacturing by application of standard approaches. *MAbs*, *5*(6), 962–973. https://doi.org/10.4161/MABS.26233

Greaves, M., & Maley, C. C. (2012). Clonal evolution in cancer. In *Nature*. https://doi.org/10.1038/nature10762

Gründer, C., Van Dorp, S., Hol, S., Drent, E., Straetemans, T., Heijhuurs, S., Scholten, K., Scheper, W., Sebestyen, Z., Martens, A., Strong, R., & Kuball, J. (2012). γ9 and δ2CDR3 domains regulate functional avidity of T cells harboring γ9δ2TCRs. *Blood*, *120*(26), 5153–5162. https://doi.org/10.1182/blood-2012-05-432427

Guery, T., Roumier, C., Berthon, C., Renneville, A., Preudhomme, C., & Quesnel, B. (2015). B7-H3 protein expression in acute myeloid leukemia. *Cancer Medicine*, *4*(12), 1879–1883. https://doi.org/10.1002/CAM4.522

Guest, R. D., Hawkins, R. E., Kirillova, N., Cheadle, E. J., Arnold, J., O'Neill, A., Irlam, J., Chester, K. A., Kemshead, J. T., Shaw, D. M., Embleton, M. J., Stern, P. L., & Gilham, D. E. (2005). The role of extracellular spacer regions in the optimal design of chimeric immune receptors: Evaluation of four different scFvs and antigens. *Journal of Immunotherapy*. https://doi.org/10.1097/01.cji.0000161397.96582.59

Harly, C., Guillaume, Y., Nedellec, S., Peigné, C. M., Mönkkönen, H., Mönkkönen, J., Li, J., Kuball, J., Adams, E. J., Netzer, S., Déchanet-Merville, J., Léger, A., Herrmann, T., Breathnach, R., Olive, D., Bonneville, M., & Scotet, E. (2012). Key implication of CD277/butyrophilin-3 (BTN3A) in cellular stress sensing by a major human γδ T-cell subset. *Blood*, *120*(11), 2269. https://doi.org/10.1182/BLOOD-2012-05-430470

Harrer, D. C., Simon, B., Fujii, S. ichiro, Shimizu, K., Uslu, U., Schuler, G., Gerer, K. F., Hoyer, S., Dörrie, J., & Schaft, N. (2017). RNA-transfection of γ/δ T cells with a chimeric antigen receptor or an α/β T-cell receptor: A safer alternative to genetically engineered α/β T cells for the immunotherapy of

melanoma. *BMC Cancer*, *17*(1). https://doi.org/10.1186/s12885-017-3539-3

Heusel, J. W., Wesselschmidt, R. L., Shresta, S., Russell, J. H., & Ley, T. J. (1994). Cytotoxic lymphocytes require granzyme B for the rapid induction of DNA fragmentation and apoptosis in allogeneic target cells. *Cell*. https://doi.org/10.1016/0092-8674(94)90376-X

Hiasa, A., Nishikawa, H., Hirayama, M., Kitano, S., Okamoto, S., Chono, H., Yu, S. S., Mineno, J., Tanaka, Y., Minato, N., Kato, I., & Shiku, H. (2009). Rapid alphabeta TCR-mediated responses in gammadelta T cells transduced with cancer-specific TCR genes. *Gene Therapy*, *16*(5), 620–628. https://doi.org/10.1038/GT.2009.6

Himoudi, N., Morgenstern, D. A., Yan, M., Vernay, B., Saraiva, L., Wu, Y., Cohen, C. J., Gustafsson, K., & Anderson, J. (2012). Human γδ T Lymphocytes Are Licensed for Professional Antigen Presentation by Interaction with Opsonized Target Cells. *The Journal of Immunology*, *188*(4), 1708–1716. https://doi.org/10.4049/JIMMUNOL.1102654

Hombach, A., Heuser, C., Gerken, M., Fischer, B., Lewalter, K., Diehl, V., Pohl, C., & Abken, H. (2000). T cell activation by recombinant FcεRI γ-chain immune receptors: An extracellular spacer domain impairs antigen-dependent T cell activation but not antigen recognition. *Gene Therapy*. https://doi.org/10.1038/sj.gt.3301195

Hombach, A., Hombach, A. A., & Abken, H. (2010). Adoptive immunotherapy with genetically engineered T cells: Modification of the IgG1 Fc spacer domain in the extracellular moiety of chimeric antigen receptors avoids off-target activation and unintended initiation of an innate immune response. *Gene*

Therapy. https://doi.org/10.1038/gt.2010.91

Huang, A. Y. C., Golumbek, P., Ahmadzadeh, M., Jaffee, E., Pardoll, D., & Levitsky, H. (1994). Role of bone marrow-derived cells in presenting MHC class I-restricted tumor antigens. *Science*. https://doi.org/10.1126/science.7513904

Hudecek, M., Sommermeyer, D., Kosasih, P. L., Silva-Benedict, A., Liu, L., Rader, C., Jensen, M. C., & Riddell, S. R. (2015). The nonsignaling extracellular spacer domain of chimeric antigen receptors is decisive for in vivo antitumor activity. *Cancer Immunology Research*, *3*(2), 125–135. https://doi.org/10.1158/2326-6066.CIR-14-0127

Huehls, A. M., Coupet, T. A., & Sentman, C. L. (2015). Bispecific T-cell engagers for cancer immunotherapy. *Immunology and Cell Biology*, *93*(3), 290–296. https://doi.org/10.1038/ICB.2014.93

Isidori, A., Salvestrini, V., Ciciarello, M., Loscocco, F., Visani, G., Parisi, S., Lecciso, M., Ocadlikova, D., Rossi, L., Gabucci, E., Clissa, C., & Curti, A. (2014). The role of the immunosuppressive microenvironment in acute myeloid leukemia development and treatment. *Expert Review of Hematology*, *7*(6), 807–818. https://doi.org/10.1586/17474086.2014.958464

J.N., K., M.E., D., M., S.-S., W.H., W., J.E., J., D.-A.N., N., I., M., M., R., S.A., F., R.A., M., & S.A., R. (2010). A phase I clinical trial of treatment of B-cell malignancies with autologous anti-CD19-CAR-transduced T cells. *Blood*, *116*(21). http://www.embase.com/search/results?subaction=viewrecord&from=export&id=L70775744%0Ahttp://abstracts.hematologylibrary.org/cgi/content/abstra

ct/116/21/2865?maxtoshow=&hits=60&RESULTFORMAT=&searchid=1&FIRSTINDEX=1080&displaysectionid=Poster+Session&fdate=

Jenkins, M. R., & Griffiths, G. M. (2010). The synapse and cytolytic machinery of cytotoxic T cells. In *Current Opinion in Immunology*. https://doi.org/10.1016/j.coi.2010.02.008

Jorritsma, A., Gomez-Eerland, R., Dokter, M., Van De Kasteele, W., Zoet, Y. M., Doxiadis, I. I. N., Rufer, N., Romero, P., Morgan, R. A., Schumacher, T. N. M., & Haanen, J. B. A. G. (2007). Selecting highly affine and well-expressed TCRs for gene therapy of melanoma. *Blood*, *110*(10), 3564–3572. https://doi.org/10.1182/blood-2007-02-075010

Karunakaran, M. M., Willcox, C. R., Salim, M., Paletta, D., Fichtner, A. S., Noll, A., Starick, L., Nöhren, A., Begley, C. R., Berwick, K. A., Chaleil, R. A. G., Pitard, V., Déchanet-Merville, J., Bates, P. A., Kimmel, B., Knowles, T. J., Kunzmann, V., Walter, L., Jeeves, M., … Herrmann, T. (2020). Butyrophilin-2A1 Directly Binds Germline-Encoded Regions of the Vγ9Vδ2 TCR and Is Essential for Phosphoantigen Sensing. *Immunity*, *52*(3), 487-498.e6. https://doi.org/10.1016/J.IMMUNI.2020.02.014

Kenderian, S. S., Ruella, M., Shestova, O., Klichinsky, M., Aikawa, V., Morrissette, J. J. D., Scholler, J., Song, D., Porter, D. L., Carroll, M., June, C. H., & Gill, S. (2015). CD33-specific chimeric antigen receptor T cells exhibit potent preclinical activity against human acute myeloid leukemia. *Leukemia*, *29*(8), 1637–1647. https://doi.org/10.1038/LEU.2015.52

Kronenberg, M. (2014). When Less Is More: T Lymphocyte Populations with Restricted Antigen Receptor Diversity. *The Journal of Immunology*.

https://doi.org/10.4049/jimmunol.1401491

Krug, U., Büchner, T., Berdel, W. E., & Müller-Tidow, C. (2011). The Treatment of Elderly Patients With Acute Myeloid Leukemia. *Deutsches Ärzteblatt International*, *108*(51–52), 863. https://doi.org/10.3238/ARZTEBL.2011.0863

Krupka, C., Kufer, P., Kischel, R., Zugmaier, G., Bögeholz, J., Köhnke, T., Lichtenegger, F. S., Schneider, S., Metzeler, K. H., Fiegl, M., Spiekermann, K., Baeuerle, P. A., Hiddemann, W., Riethmüller, G., & Subklewe, M. (2014). CD33 target validation and sustained depletion of AML blasts in long-term cultures by the bispecific T-cell-engaging antibody AMG 330. *Blood*, *123*(3), 356–365. https://doi.org/10.1182/BLOOD-2013-08-523548

Lachowiez, C., Konopleva, M., Kadia, T. M., Daver, N., Loghavi, S., Wang, S. A., Adeoti, M., Pierce, S. A., Takahashi, K., Short, N. J., Sasaki, K., Borthakur, G., Issa, G. C., Wierda, W. G., Pemmaraju, N., Montalban Bravo, G., Ferrajoli, A., Jain, N., Masarova, L., … Dinardo, C. D. (2020). Interim Analysis of the Phase 1b/2 Study of the BCL-2 Inhibitor Venetoclax in Combination with Standard Intensive AML Induction/Consolidation Therapy with FLAG-IDA in Patients with Newly Diagnosed or Relapsed/Refractory AML. *Blood*, *136*(Supplement 1), 18–20. https://doi.org/10.1182/BLOOD-2020-134300

Ladikou, E. E., Sivaloganathan, H., Pepper, A., & Chevassut, T. (2020). Acute Myeloid Leukaemia in Its Niche: the Bone Marrow Microenvironment in Acute Myeloid Leukaemia. *Current Oncology Reports*, *22*(3). https://doi.org/10.1007/S11912-020-0885-0

Lamers, C. H. J., Sleijfer, S., Vulto, A. G., Kruit, W. H. J., Kliffen, M., Debets, R.,

Gratama, J. W., Stoter, G., & Oosterwijk, E. (2006). Treatment of metastatic renal cell carcinoma with autologous T-lymphocytes genetically retargeted against carbonic anhydrase IX: first clinical experience. In *Journal of clinical oncology : official journal of the American Society of Clinical Oncology* (Vol. 24, Issue 13). https://doi.org/10.1200/JCO.2006.05.9964

Landsverk, O. J. B., Bakke, O., & Gregers, T. F. (2009). MHC II and the endocytic pathway: Regulation by invariant chain. In *Scandinavian Journal of Immunology*. https://doi.org/10.1111/j.1365-3083.2009.02301.x

Lee, K. H., Dinner, A. R., Tu, C., Campi, G., Raychaudhuri, S., Varma, R., Sims, T. N., Burack, W. R., Wu, H., Wang, J., Kanagawa, O., Markiewicz, M., Allen, P. M., Dustin, M. L., Chakraborty, A. K., & Shaw, A. S. (2003). The Immunological Synapse Balances T Cell Receptor Signaling and Degradation. *Science*. https://doi.org/10.1126/science.1086507

Lefranc, M. (2001). Nomenclature of the human T cell receptor genes. *Current Protocols in Immunology*, *Appendix 1*(1). https://doi.org/10.1002/0471142735.IMA01OS40

Legut, M., Dolton, G., Mian, A. A., Ottmann, O. G., & Sewell, A. K. (2018). CRISPR-mediated TCR replacement generates superior anticancer transgenic t cells. *Blood*, *131*(3), 311–322. https://doi.org/10.1182/blood-2017-05-787598

Linette, G. P., Stadtmauer, E. A., Maus, M. V., Rapoport, A. P., Levine, B. L., Emery, L., Litzky, L., Bagg, A., Carreno, B. M., Cimino, P. J., Binder-Scholl, G. K., Smethurst, D. P., Gerry, A. B., Pumphrey, N. J., Bennett, A. D., Brewer, J. E., Dukes, J., Harper, J., Tayton-Martin, H. K., … June, C. H.

(2013). Cardiovascular toxicity and titin cross-reactivity of affinity-enhanced T cells in myeloma and melanoma. *Blood*, *122*(6), 863–871. https://doi.org/10.1182/blood-2013-03-490565

Lo-Coco, F., Cimino, G., Breccia, M., Noguera, N. I., Diverio, D., Finolezzi, E., Pogliani, E. M., Di Bona, E., Micalizzi, C., Kropp, M., Venditti, A., Tafuri, A., & Mandelli, F. (2004). Gemtuzumab ozogamicin (Mylotarg) as a single agent for molecularly relapsed acute promyelocytic leukemia. *Blood*, *104*(7), 1995–1999. https://doi.org/10.1182/blood-2004-04-1550

Löhning, M., Hegazy, A. N., Pinschewer, D. D., Busse, D., Lang, K. S., Höfer, T., Radbruch, A., Zinkernagel, R. M., & Hengartner, H. (2008). Long-lived virus-reactive memory T cells generated from purified cytokine-secreting T helper type 1 and type 2 effectors. *The Journal of Experimental Medicine*, *205*(1), 53–61. https://doi.org/10.1084/JEM.20071855

Malissen, B., & Bongrand, P. (2015). Early T Cell Activation: Integrating Biochemical, Structural, and Biophysical Cues. *Annual Review of Immunology*. https://doi.org/10.1146/annurev-immunol-032414-112158

Marcu-Malina, V., Heijhuurs, S., Van Buuren, M., Hartkamp, L., Strand, S., Sebestyen, Z., Scholten, K., Martens, A., & Kuball, J. (2011). Redirecting αβT cells against cancer cells by transfer of a broadly tumor-reactive γδT-cell receptor. *Blood*, *118*(1), 50–59. https://doi.org/10.1182/BLOOD-2010-12-325993

Mardiros, A., Dos Santos, C., McDonald, T., Brown, C. E., Wang, X., Budde, L. E., Hoffman, L., Aguilar, B., Chang, W. C., Bretzlaff, W., Chang, B., Jonnalagadda, M., Starr, R., Ostberg, J. R., Jensen, M. C., Bhatia, R., &

Forman, S. J. (2013). T cells expressing CD123-specific chimeric antigen receptors exhibit specific cytolytic effector functions and antitumor effects against human acute myeloid leukemia. *Blood*, *122*(18), 3138–3148. https://doi.org/10.1182/BLOOD-2012-12-474056

Martens, J. H. A., & Stunnenberg, H. G. (2010). The molecular signature of oncofusion proteins in acute myeloid leukemia. *FEBS Letters*, *584*(12), 2662–2669. https://doi.org/10.1016/J.FEBSLET.2010.04.002

Mckeithan, T. W. (1995). Kinetic proofreading in T-cell receptor signal transduction. *Proceedings of the National Academy of Sciences of the United States of America*. https://doi.org/10.1073/pnas.92.11.5042

Medeiros, B. C., Othus, M., Fang, M., Roulston, D., & Appelbaum, F. R. (2010). Prognostic impact of monosomal karyotype in young adult and elderly acute myeloid leukemia: the Southwest Oncology Group (SWOG) experience. *Blood*, *116*(13), 2224–2228. https://doi.org/10.1182/BLOOD-2010-02-270330

Monks, C. R. F., Freiberg, B. A., Kupfer, H., Sciaky, N., & Kupfer, A. (1998). Three-dimensional segregation of supramolecular activation clusters in T cells. *Nature*. https://doi.org/10.1038/25764

Morgan, R. A., Dudley, M. E., Wunderlich, J. R., Hughes, M. S., Yang, J. C., Sherry, R. M., Royal, R. E., Topalian, S. L., Kammula, U. S., Restifo, N. P., Zheng, Z., Nahvi, A., de Vries, C. R., Rogers-Freezer, L. J., Mavroukakis, S. A., & Rosenberg, S. A. (2006). Cancer Regression in Patients After Transfer of Genetically Engineered Lymphocytes. *Science*, *314*(5796), 126–129. https://doi.org/10.1126/science.1129003

Morgan, Richard A., Yang, J. C., Kitano, M., Dudley, M. E., Laurencot, C. M., &

Rosenberg, S. A. (2010). Case report of a serious adverse event following the administration of t cells transduced with a chimeric antigen receptor recognizing ERBB2. *Molecular Therapy*, *18*(4), 843–851. https://doi.org/10.1038/mt.2010.24

Morita, C. T., Beckman, E. M., Bukowski, J. F., Tanaka, Y., Band, H., Bloom, B. R., Golan, D. E., & Brenner, M. B. (1995). Direct presentation of nonpeptide prenyl pyrophosphate antigens to human γδ T cells. *Immunity*, *3*(4), 495–507. https://doi.org/10.1016/1074-7613(95)90178-7

Moritz, D., & Groner, B. (1995). A spacer region between the single chain antibody-and the CDS ζ-chain domain of chimeric T cell receptor components is required for efficient ligand binding and signaling activity. *Gene Therapy*.

Mrózek, K., Heinonen, K., & Bloomfield, C. D. (2001). Clinical importance of cytogenetics in acute myeloid leukaemia. *Best Practice & Research Clinical Haematology*, *14*(1), 19–47. https://doi.org/10.1053/BEHA.2000.0114

Naito, T., Tanaka, H., Naoe, Y., & Taniuchi, I. (2011). Transcriptional control of T-cell development. *International Immunology*. https://doi.org/10.1093/intimm/dxr078

Naito, Y., Saito, K., Shiiba, K., Ohuchi, A., Saigenji, K., Nagura, H., & Ohtani, H. (1998). CD8+ T cells infiltrated within cancer cell nests as a prognostic factor in human colorectal cancer. *Cancer Research*.

Nedellec, S., Sabourin, C., Bonneville, M., & Scotet, E. (2010). NKG2D Costimulates Human V 9V 2 T Cell Antitumor Cytotoxicity through Protein Kinase C -Dependent Modulation of Early TCR-Induced Calcium and

Transduction Signals. *The Journal of Immunology*, *185*(1), 55–63. https://doi.org/10.4049/jimmunol.1000373

Neefjes, J., Jongsma, M. L. M., Paul, P., & Bakke, O. (2011). Towards a systems understanding of MHC class i and MHC class II antigen presentation. In *Nature Reviews Immunology*. https://doi.org/10.1038/nri3084

Niktoreh, N., Lerius, B., Zimmermann, M., Gruhn, B., Escherich, G., Bourquin, J. P., Dworzak, M., Sramkova, L., Rossig, C., Creutzig, U., Reinhardt, D., & Rasche, M. (2019). Gemtuzumab ozogamicin in children with relapsed or refractory acute myeloid leukemia: a report by Berlin-Frankfurt-Münster study group. *Haematologica*, *104*(1), 120–127. https://doi.org/10.3324/HAEMATOL.2018.191841

Norment, A. M., Salter, R. D., Parham, P., Engelhard, V. H., & Littman, D. R. (1988). Cell-cell adhesion mediated by CD8 and MHC class I molecules. *Nature*. https://doi.org/10.1038/336079a0

Palakodeti, A., Sandstrom, A., Sundaresan, L., Harly, C., Nedellec, S., Olive, D., Scotet, E., Bonneville, M., & Adams, E. J. (2012). The Molecular Basis for Modulation of Human Vγ9Vδ2 T Cell Responses by CD277/Butyrophilin-3 (BTN3A)-specific Antibodies. *The Journal of Biological Chemistry*, *287*(39), 32780. https://doi.org/10.1074/JBC.M112.384354

Papaioannou, D., Brazier, J., & Paisley, S. (2013). Systematic searching and selection of health state utility values from the literature. *Value in Health : The Journal of the International Society for Pharmacoeconomics and Outcomes Research*, *16*(4), 686–695. https://doi.org/10.1016/J.JVAL.2013.02.017

Parker, C. M., Groh, V., Band, H., Porcelli, S. A., Morita, C., Fabbi, M., Glass, D., Strominger, J. L., & Brenner, M. B. (1990). Evidence for extrathymic changes in the T cell receptor gamma/delta repertoire. *The Journal of Experimental Medicine*, *171*(5), 1597–1612. https://doi.org/10.1084/JEM.171.5.1597

Pauza, C. D., & Cairo, C. (2015). Evolution and function of the TCR Vgamma9 chain repertoire: It's good to be public. *Cellular Immunology*, *296*(1), 22–30. https://doi.org/10.1016/J.CELLIMM.2015.02.010

Philip, B., Kokalaki, E., Mekkaoui, L., Thomas, S., Straathof, K., Flutter, B., Marin, V., Marafioti, T., Chakraverty, R., Linch, D., Quezada, S. A., Peggs, K. S., & Pule, M. (2014). A highly compact epitope-based marker/suicide gene for easier and safer T-cell therapy. *Blood*, *124*(8), 1277–1287. https://doi.org/10.1182/BLOOD-2014-01-545020

Picarda, E., Ohaegbulam, K. C., & Zang, X. (2016). Molecular Pathways: Targeting B7-H3 (CD276) for Human Cancer Immunotherapy. *Clinical Cancer Research : An Official Journal of the American Association for Cancer Research*, *22*(14), 3425–3431. https://doi.org/10.1158/1078-0432.CCR-15-2428

Pickart, C. M., & Eddins, M. J. (2004). Ubiquitin: Structures, functions, mechanisms. In *Biochimica et Biophysica Acta - Molecular Cell Research*. https://doi.org/10.1016/j.bbamcr.2004.09.019

Pötzsch, C., Voigtländer, T., & Lübbert, M. (2002). p53 Germline mutation in a patient with Li-Fraumeni Syndrome and three metachronous malignancies. *Journal of Cancer Research and Clinical Oncology*, *128*(8), 456–460. https://doi.org/10.1007/S00432-002-0360-3

Poupot, M., & Fournié, J.-J. (2004). Non-peptide antigens activating human Vgamma9/Vdelta2 T lymphocytes. *Immunology Letters*, *95*(2), 129–138. https://doi.org/10.1016/j.imlet.2004.06.013

Preston, D. L., Kusumi, S., Tomonaga, M., Izumi, S., Ron, E., Kuramoto, A., Kamada, N., Dohy, H., Matsui, T., Nonaka, H., Thompson, D. E., Soda, M., & Mabuchi, K. (1994). Cancer incidence in atomic bomb survivors. Part III: Leukemia, lymphoma and multiple myeloma, 1950-1987. *Radiation Research*, *137*(2 SUPPL.). https://doi.org/10.2307/3578893

Qureshi, O. S., Zheng, Y., Nakamura, K., Attridge, K., Manzotti, C., Schmidt, E. M., Baker, J., Jeffery, L. E., Kaur, S., Briggs, Z., Hou, T. Z., Futter, C. E., Anderson, G., Walker, L. S. K., & Sansom, D. M. (2011). Trans-endocytosis of CD80 and CD86: A molecular basis for the cell-extrinsic function of CTLA-4. *Science*. https://doi.org/10.1126/science.1202947

Rabinowitz, J. D., Beeson, C., Wülfing, C., Tate, K., Allen, P. M., Davis, M. M., & McConnell, H. M. (1996). Altered T cell receptor ligands trigger a subset of early T cell signals. *Immunity*. https://doi.org/10.1016/S1074-7613(00)80489-6

Raffaghello, L., Prigione, I., Airoldi, I., Camoriano, M., Morandi, F., Bocca, P., Gambini, C., Ferrone, S., & Pistoia, V. (2005). Mechanisms of immune evasion of human neuroblastoma. *Cancer Letters*, *228*(1–2), 155–161. https://doi.org/10.1016/J.CANLET.2004.11.064

Rajvanshi, P., Shulman, H. M., Sievers, E. L., & McDonald, G. B. (2002). Hepatic sinusoidal obstruction after gemtuzumab ozogamicin (Mylotarg) therapy. *Blood*, *99*(7), 2310–2314. https://doi.org/10.1182/BLOOD.V99.7.2310

Ramos, C. A., Ballard, B., Zhang, H., Dakhova, O., Gee, A. P., Mei, Z., Bilgi, M., Wu, M. F., Liu, H., Grilley, B., Bollard, C. M., Chang, B. H., Rooney, C. M., Brenner, M. K., Heslop, H. E., Dotti, G., & Savoldo, B. (2017). Clinical and immunological responses after CD30-specific chimeric antigen receptor-redirected lymphocytes. *The Journal of Clinical Investigation*, *127*(9), 3462–3471. https://doi.org/10.1172/JCI94306

Raphael, I., Nalawade, S., Eagar, T. N., & Forsthuber, T. G. (2015). T cell subsets and their signature cytokines in autoimmune and inflammatory diseases. In *Cytokine*. https://doi.org/10.1016/j.cyto.2014.09.011

Restifo, N. P., & Gattinoni, L. (2013). Lineage relationship of effector and memory T cells. In *Current Opinion in Immunology*. https://doi.org/10.1016/j.coi.2013.09.003

Ries, L., Harkins, D., Krapcho, M., Mariotto, A., Miller, B., Feuer, E., Clegg, L., Eisner, M., Horner, M.-J., Howlader, N., Hayat, M., Hankey, B., & Edwards, B. (2006). SEER Cancer Statistics Review, 1975-2003. *Public Health Faculty Publications*. https://scholarworks.gsu.edu/iph_facpub/132

Rigau, M., Ostrouska, S., Fulford, T. S., Johnson, D. N., Woods, K., Ruan, Z., McWilliam, H. E. G., Hudson, C., Tutuka, C., Wheatley, A. K., Kent, S. J., Villadangos, J. A., Pal, B., Kurts, C., Simmonds, J., Pelzing, M., Nash, A. D., Hammet, A., Verhagen, A. M., … Uldrich, A. P. (2020). Butyrophilin 2A1 is essential for phosphoantigen reactivity by γδ T cells. *Science (New York, N.Y.)*, *367*(6478). https://doi.org/10.1126/SCIENCE.AAY5516

Rischer, M., Pscherer, S., Duwe, S., Vormoor, J., Jürgens, H., & Rossig, C. (2004). Human gammadelta T cells as mediators of chimaeric-receptor

redirected anti-tumour immunity. *British Journal of Haematology*, *126*(4), 583–592. https://doi.org/10.1111/J.1365-2141.2004.05077.X

Roelofs, A. J., Jauhiainen, M., Mönkkönen, H., Rogers, M. J., Mönkkönen, J., & Thompson, K. (2009). Peripheral blood monocytes are responsible for γδ T cell activation induced by zoledronic acid through accumulation of IPP/DMAPP. *British Journal of Haematology*, *144*(2), 245. https://doi.org/10.1111/J.1365-2141.2008.07435.X

Romieu-Mourez, R., François, M., Boivin, M.-N., Stagg, J., & Galipeau, J. (2007). Regulation of MHC Class II Expression and Antigen Processing in Murine and Human Mesenchymal Stromal Cells by IFN-γ, TGF-β, and Cell Density. *The Journal of Immunology*. https://doi.org/10.4049/jimmunol.179.3.1549

Rowe, J. M., & Löwenberg, B. (2013). Gemtuzumab ozogamicin in acute myeloid leukemia: a remarkable saga about an active drug. *Blood*, *121*(24), 4838–4841. https://doi.org/10.1182/BLOOD-2013-03-490482

Rudolph, M. G., Stanfield, R. L., & Wilson, I. A. (2006). HOW TCRS BIND MHCS, PEPTIDES, AND CORECEPTORS. *Annual Review of Immunology*. https://doi.org/10.1146/annurev.immunol.23.021704.115658

Ruella, M., & Kalos, M. (2014). Adoptive immunotherapy for cancer. *Immunological Reviews*, *257*(1), 14–38. https://doi.org/10.1111/imr.12136

Ruella, M., & Maus, M. V. (2016). Catch me if you can: Leukemia Escape after CD19-Directed T Cell Immunotherapies. *Computational and Structural Biotechnology Journal*, *14*, 357–362. https://doi.org/10.1016/J.CSBJ.2016.09.003

Russano, A. M., Agea, E., Corazzi, L., Postle, A. D., De Libero, G., Porcelli, S., de Benedictis, F. M., & Spinozzi, F. (2006). Recognition of pollen-derived phosphatidyl-ethanolamine by human CD1d-restricted gamma delta T cells. *The Journal of Allergy and Clinical Immunology*, *117*(5), 1178–1184. https://doi.org/10.1016/J.JACI.2006.01.001

Sadelain, M., Brentjens, R., & Rivière, I. (2013). The basic principles of chimeric antigen receptor design. In *Cancer Discovery*. https://doi.org/10.1158/2159-8290.CD-12-0548

Sakaguchi, S., Sakaguchi, N., Asano, M., Itoh, M., & Toda, M. (1995). Immunologic self-tolerance maintained by activated T cells expressing IL-2 receptor alpha-chains (CD25). Breakdown of a single mechanism of self-tolerance causes various autoimmune diseases. *Journal of Immunology (Baltimore, Md. : 1950)*.

Sallusto, F., Geginat, J., & Lanzavecchia, A. (2004). C entral M emory and E ffector M emory T C ell S ubsets : Function, Generation, and Maintenance . *Annual Review of Immunology*. https://doi.org/10.1146/annurev.immunol.22.012703.104702

Sandstrom, A., Peigné, C. M., Léger, A., Crooks, J., Konczak, F., Gesnel, M. C., Breathnach, R., Bonneville, M., Scotet, E., & Adams, E. J. (2014). The intracellular B30.2 domain of butyrophilin 3A1 binds phosphoantigens to mediate activation of human Vγ9Vδ2T Cells. *Immunity*, *40*(4), 490–500. https://doi.org/10.1016/j.immuni.2014.03.003

Savitz, D. A., & Andrews, K. W. (1997). Review of epidemiologic evidence on benzene and lymphatic and hematopoietic cancers. *American Journal of*

Industrial Medicine, *31*(3), 287–295. https://doi.org/10.1002/(SICI)1097-0274(199703)31:3<287::AID-AJIM4>3.0.CO;2-V

Savoldo, B., Ramos, C. A., Liu, E., Mims, M. P., Keating, M. J., Carrum, G., Kamble, R. T., Bollard, C. M., Gee, A. P., Mei, Z., Liu, H., Grilley, B., Rooney, C. M., Heslop, H. E., Brenner, M. K., & Dotti, G. (2011). CD28 costimulation improves expansion and persistence of chimeric antigen receptor-modified T cells in lymphoma patients. *Journal of Clinical Investigation*. https://doi.org/10.1172/JCI46110

Schatz, D. G., Oettinger, M. A., & Schlissel, M. S. (1992). V(D)J recombination: Molecular biology and regulation. In *Annual Review of Immunology*. https://doi.org/10.1146/annurev.iy.10.040192.002043

Schreiber, R. D., Old, L. J., & Smyth, M. J. (2011). Cancer immunoediting: Integrating immunity's roles in cancer suppression and promotion. In *Science*. https://doi.org/10.1126/science.1203486

Scimone, M. L., Aifantis, I., Apostolou, I., Von Boehmer, H., & Von Andrian, U. H. (2006). A multistep adhesion cascade for lymphoid progenitor cell homing to the thymus. *Proceedings of the National Academy of Sciences of the United States of America*. https://doi.org/10.1073/pnas.0602024103

Sewell, A. K. (2012). Why must T cells be cross-reactive? In *Nature Reviews Immunology*. https://doi.org/10.1038/nri3279

Shankaran, V., Ikeda, H., Bruce, A. T., White, J. M., Swanson, P. E., Old, L. J., & Schreiber, R. D. (2001). IFNγ, and lymphocytes prevent primary tumour development and shape tumour immunogenicity. *Nature*. https://doi.org/10.1038/35074122

Shinkai, Y., Rathbun, 0Gary, Lam, K. P., Oltz, E. M., Stewart, V., Mendelsohn, M., Charron, J., Datta, M., Young, F., Stall, A. M., & Alt, F. W. (1992). RAG-2-deficient mice lack mature lymphocytes owing to inability to initiate V(D)J rearrangement. *Cell*. https://doi.org/10.1016/0092-8674(92)90029-C

Sievers, E. L., Larson, R. A., Stadtmauer, E. A., Estey, E., Löwenberg, B., Dombret, H., Karanes, C., Theobald, M., Bennett, J. M., Sherman, M. L., Berger, M. S., Eten, C. B., Loken, M. R., Van Dongen, J. J. M., Bernstein, I. D., & Appelbaum, F. R. (2001). Efficacy and safety of gemtuzumab ozogamicin in patients with CD33-positive acute myeloid leukemia in first relapse. *Journal of Clinical Oncology*, *19*(13), 3244–3254. https://doi.org/10.1200/JCO.2001.19.13.3244

Sigal, L. J., Crotty, S., Andino, R., & Rock, K. L. (1999). Cytotoxic T-cell immunity to virus-infected non-haematopoietic cells requires presentation of exogenous antigen. *Nature*. https://doi.org/10.1038/18038

Sill, H., Olipitz, W., Zebisch, A., Schulz, E., & Wölfler, A. (2011). Therapy-related myeloid neoplasms: pathobiology and clinical characteristics. *British Journal of Pharmacology*, *162*(4), 792–805. https://doi.org/10.1111/J.1476-5381.2010.01100.X

Silva-Santos, B., Serre, K., & Norell, H. (2015). γδ T cells in cancer. *Nature Reviews. Immunology*, *15*(11), 683–691. https://doi.org/10.1038/NRI3904

Silva-Santos, B., & Strid, J. (2018). Working in “NK Mode”: Natural Killer Group 2 Member D and Natural Cytotoxicity Receptors in Stress-Surveillance by γδ T Cells. *Frontiers in Immunology*, *9*(APR). https://doi.org/10.3389/FIMMU.2018.00851

Smith-Garvin, J., & Koretzky, G. (2009). T cell activation. *Annual Review of Immunology*, *27*, 591–619. https://doi.org/10.1146/annurev.immunol.021908.132706.T

Spada, F. M., Grant, E. P., Peters, P. J., Sugita, M., Melián, A., Leslie, D. S., Lee, H. K., Van Donselaar, E., Hanson, D. A., Krensky, A. M., Majdic, O., Porcelli, S. A., Morita, C. T., & Brenner, M. B. (2000). Self-recognition of CD1 by gamma/delta T cells: implications for innate immunity. *The Journal of Experimental Medicine*, *191*(6), 937–948. https://doi.org/10.1084/JEM.191.6.937

Starick, L., Riano, F., Karunakaran, M. M., Kunzmann, V., Li, J., Kreiss, M., Amslinger, S., Scotet, E., Olive, D., De Libero, G., & Herrmann, T. (2017). Butyrophilin 3A (BTN3A, CD277)-specific antibody 20.1 differentially activates Vγ9Vδ2 TCR clonotypes and interferes with phosphoantigen activation. *European Journal of Immunology*, *47*(6), 982–992. https://doi.org/10.1002/EJI.201646818

Stasi, R., Del Poeta, G., Masi, M., Tribalto, M., Venditti, A., Papa, G., Nicoletti, B., Vernole, P., Tedeschi, B., Delaroche, I., Mingarelli, R., & Dallapiccola, B. (1993). Incidence of chromosome abnormalities and clinical significance of karyotype in de novo acute myeloid leukemia. *Cancer Genetics and Cytogenetics*, *67*(1), 28–34. https://doi.org/10.1016/0165-4608(93)90040-S

Stein, E. M., DiNardo, C. D., Fathi, A. T., Mims, A. S., Pratz, K. W., Savona, M. R., Stein, A. S., Stone, R. M., Winer, E. S., Seet, C. S., Döhner, H., Pollyea, D. A., McCloskey, J. K., Odenike, O., Löwenberg, B., Ossenkoppele, G. J., Patel, P. A., Roshal, M., Frattini, M. G., … Tallman, M. S. (2021). Ivosidenib

or enasidenib combined with intensive chemotherapy in patients with newly diagnosed AML: a phase 1 study. *Blood*, *137*(13), 1792–1803. https://doi.org/10.1182/BLOOD.2020007233

Stone, R. M., Mandrekar, S. J., Sanford, B. L., Laumann, K., Geyer, S., Bloomfield, C. D., Thiede, C., Prior, T. W., Döhner, K., Marcucci, G., Lo-Coco, F., Klisovic, R. B., Wei, A., Sierra, J., Sanz, M. A., Brandwein, J. M., de Witte, T., Niederwieser, D., Appelbaum, F. R., … Döhner, H. (2017). Midostaurin plus Chemotherapy for Acute Myeloid Leukemia with a FLT3 Mutation . *New England Journal of Medicine*, *377*(5), 454–464. https://doi.org/10.1056/NEJMOA1614359/SUPPL_FILE/NEJMOA1614359_DISCLOSURES.PDF

Sutton, V. R., Davis, J. E., Cancilla, M., Johnstone, R. W., Ruefli, A. A., Sedelies, K., Browne, K. A., & Trapani, J. A. (2000). Initiation of apoptosis by granzyme B requires direct cleavage of Bid, but not direct granzyme B-mediated caspase activation. *Journal of Experimental Medicine*. https://doi.org/10.1084/jem.192.10.1403

Szotkowski, T., Rohon, P., Zapletalova, J., Sicova, K., Hubacek, J., & Indrak, K. (2010). Secondary acute myeloid leukemia - a single center experience. *Neoplasma*, *57*(2), 170–178. https://doi.org/10.4149/NEO_2010_02_170

Taksin, A. L., Legrand, O., Raffoux, E., de Revel, T., Thomas, X., Contentin, N., Bouabdallah, R., Pautas, C., Turlure, P., Reman, O., Gardin, C., Varet, B., de Botton, S., Pousset, F., Farhat, H., Chevret, S., Dombret, H., & Castaigne, S. (2007). High efficacy and safety profile of fractionated doses of Mylotarg as induction therapy in patients with relapsed acute myeloblastic

leukemia: a prospective study of the alfa group. *Leukemia*, *21*(1), 66–71. https://doi.org/10.1038/SJ.LEU.2404434

Tammana, S., Huang, X., Wong, M., Milone, M. C., Ma, L., Levine, B. L., June, C. H., Wagner, J. E., Blazar, B. R., & Zhou, X. (2010). 4-1BB and CD28 signaling plays a synergistic role in redirecting umbilical cord blood t cells against b-cell malignancies. *Human Gene Therapy*. https://doi.org/10.1089/hum.2009.122

Tanchot, C., Lemonnier, F. A., Pérarnau, B., Freitas, A. A., & Rocha, B. (1997). Differential requirements for survival and proliferation of CD8 naive or memory T cells. *Science*. https://doi.org/10.1126/science.276.5321.2057

Van Der Merwe, P. A., & Dushek, O. (2010). Mechanisms for T cell receptor triggering. *Nature Reviews Immunology 2011 11:1*, *11*(1), 47–55. https://doi.org/10.1038/nri2887

Van Der Merwe, P. A., & Dushek, O. (2011). Mechanisms for T cell receptor triggering. In *Nature Reviews Immunology*. https://doi.org/10.1038/nri2887

van der Veken, L. T., Coccoris, M., Swart, E., Falkenburg, J. H. F., Schumacher, T. N., & Heemskerk, M. H. M. (2009). Alpha beta T cell receptor transfer to gamma delta T cells generates functional effector cells without mixed TCR dimers in vivo. *Journal of Immunology (Baltimore, Md. : 1950)*, *182*(1), 164–170. https://doi.org/10.4049/JIMMUNOL.182.1.164

Van Der Veken, L. T., Hagedoorn, R. S., Van Loenen, M. M., Willemze, R., Falkenburg, J. H. F., & Heemskerk, M. H. M. (2006). Alphabeta T-cell receptor engineered gammadelta T cells mediate effective antileukemic reactivity. *Cancer Research*, *66*(6), 3331–3337. https://doi.org/10.1158/0008-

5472.CAN-05-4190

van Loenen, M. M., de Boer, R., Amir, A. L., Hagedoorn, R. S., Volbeda, G. L., Willemze, R., van Rood, J. J., Falkenburg, J. H. F., & Heemskerk, M. H. M. (2010). Mixed T cell receptor dimers harbor potentially harmful neoreactivity. *Proceedings of the National Academy of Sciences*, *107*(24), 10972–10977. https://doi.org/10.1073/pnas.1005802107

Vardiman, J. W., Harris, N. L., & Brunning, R. D. (2002). The World Health Organization (WHO) classification of the myeloid neoplasms. *Blood*, *100*(7), 2292–2302. https://doi.org/10.1182/BLOOD-2002-04-1199

Varma, R., Campi, G., Yokosuka, T., Saito, T., & Dustin, M. L. (2006). T Cell Receptor-Proximal Signals Are Sustained in Peripheral Microclusters and Terminated in the Central Supramolecular Activation Cluster. *Immunity*. https://doi.org/10.1016/j.immuni.2006.04.010

Vavassori, S., Kumar, A., Wan, G. S., Ramanjaneyulu, G. S., Cavallari, M., El Daker, S., Beddoe, T., Theodossis, A., Williams, N. K., Gostick, E., Price, D. A., Soudamini, D. U., Voon, K. K., Olivo, M., Rossjohn, J., Mori, L., & De Libero, G. (2013). Butyrophilin 3A1 binds phosphorylated antigens and stimulates human γδ T cells. *Nature Immunology*, *14*(9), 908–916. https://doi.org/10.1038/ni.2665

von Boehmer, H., & Fehling, H. J. (1997). STRUCTURE AND FUNCTION OF THE PRE-T CELL RECEPTOR. *Annual Review of Immunology*. https://doi.org/10.1146/annurev.immunol.15.1.433

von Boehmer, H., Teh, H. S., & Kisielow, P. (1989). The thymus selects the useful, neglects the useless and destroys the harmful. *Immunology Today*.

https://doi.org/10.1016/0167-5699(89)90307-1

Wan, Y. Y., & Flavell, R. A. (2009). How diverse-CD4 effector T cells and their functions. In *Journal of Molecular Cell Biology*. https://doi.org/10.1093/jmcb/mjp001

Willemze, R., Suciu, S., Meloni, G., Labar, B., Marie, J. P., Halkes, C. J. M., Muus, P., Mistrik, M., Amadori, S., Specchia, G., Fabbiano, F., Nobile, F., Sborgia, M., Camera, A., Selleslag, D. L. D., Lefreѐre, F., Magro, D., Sica, S., Cantore, N., … De Witte, T. (2014). High-dose cytarabine in induction treatment improves the outcome of adult patients younger than age 46 years with acute myeloid leukemia: results of the EORTC-GIMEMA AML-12 trial. *J. Clin. Oncol.*, *32*(3), 219–228. https://doi.org/10.1200/jco.2013.51.8571

Williams, M. A., & Bevan, M. J. (2007). Effector and Memory CTL Differentiation. *Annual Review of Immunology*. https://doi.org/10.1146/annurev.immunol.25.022106.141548

Xu, C., Gagnon, E., Call, M. E., Schnell, J. R., Schwieters, C. D., Carman, C. V., Chou, J. J., & Wucherpfennig, K. W. (2008). Regulation of T Cell Receptor Activation by Dynamic Membrane Binding of the CD3ε Cytoplasmic Tyrosine-Based Motif. *Cell*. https://doi.org/10.1016/j.cell.2008.09.044

Yang, S., Cohen, C. J., Peng, P. D., Zhao, Y., Cassard, L., Yu, Z., Zheng, Z., Jones, S., Restifo, N. P., Rosenberg, S. A., & Morgan, R. A. (2008). Development of optimal bicistronic lentiviral vectors facilitates high-level TCR gene expression and robust tumor cell recognition. *Gene Therapy 2008 15:21*, *15*(21), 1411–1423. https://doi.org/10.1038/gt.2008.90

Yewdell, J. W., & Haeryfar, S. M. M. (2005). UNDERSTANDING

PRESENTATION OF VIRAL ANTIGENS TO CD8 + T CELLS IN VIVO: The Key to Rational Vaccine Design . *Annual Review of Immunology*. https://doi.org/10.1146/annurev.immunol.23.021704.115702

Youngblood, B., Hale, J. S., & Ahmed, R. (2013). T-cell memory differentiation: Insights from transcriptional signatures and epigenetics. *Immunology*. https://doi.org/10.1111/imm.12074

Zhang, Z., Jiang, C., Liu, Z., Yang, M., Tang, X., Wang, Y., Zheng, M., Huang, J., Zhong, K., Zhao, S., Tang, M., Zhou, T., Yang, H., Guo, G., Zhou, L., Xu, J., & Tong, A. (2020). B7-H3-Targeted CAR-T Cells Exhibit Potent Antitumor Effects on Hematologic and Solid Tumors. *Molecular Therapy Oncolytics*, *17*, 180. https://doi.org/10.1016/J.OMTO.2020.03.019

Zhong, X. S., Matsushita, M., Plotkin, J., Riviere, I., & Sadelain, M. (2010). Chimeric antigen receptors combining 4-1BB and CD28 signaling domains augment PI 3 kinase/AKT/Bcl-X L activation and CD8 T cell-mediated tumor eradication. *Molecular Therapy*. https://doi.org/10.1038/mt.2009.210